Synthesis, Evaluation and Immobilisation of Anion Sensors Based on the 4-amino-1,8-naphthalimide Fluorophore

A thesis submitted for fulfilment of the degree of

Doctor of Philosophy

Andrew J. Blok

BTech (Forens&AnalytChem), BSc (Hons)

Flinders UNIVERSITY

Faculty of Science and Engineering

School of Chemical and Physical Sciences

November 2013

Declaration

"I certify this thesis does not incorporate, without acknowledgement, any material previously submitted for a degree or diploma in any university; and that to the best of my knowledge and belief it does not contain any material previously published or written by another, except where due reference is made in the text".

Andrew J. Blok

_____ on _____

Acknowledgements

It has been a long journey to get to this point and there have been several people whom have assisted with the research which has gone into this thesis along the way. First off, I would like to thank my supervisor Associate Professor Claire Lenehan for her friendship, guidance and understanding over the years and for never giving up on me. I'd like to thank Associate Professor Martin Johnston for all of his advice and for never grumbling about the mysterious yellow stains all over the lab. Finally I'd like to thank Dr Fred Pfeffer at Deakin University for all the helpful hints he provided with regards to the synthesis and evaluation of the sensors, despite the often long time between project updates.

Thanks to Simon for reading my thesis and his advice over the years. Treat yourself. To Taryn and Bek thanks for ensuring I never blew up the lab and also making the lab an enjoyable place to be even when things weren't going my way. Thanks for introducing me to the taste. Thanks to Jess, Eric and all the other inhabitants of the Organic Corridor over the years for the good times, the bad times and something in between.

To Oh Dark One and Rachel it was a pleasure to be a temporary inhabitant in your office over the years, to the point where at one stage I was the only one in it. Thanks to all the people in our research group over the years who have made our group meetings entertaining and filling (mmmm cake). Thanks to Kez for putting up with my grumbles over the Uni years (I can't believe I have known you the entire time and we haven't killed each other…. Yet).

To my dad, Adam and my sisters Tracy and Karen thanks for all your love and support over the years. I would like to dedicate this thesis to the memory of my mum, Elizabeth who passed away in February 2012. Even when she was sick, she was always ardent in her support of my research and I hope that wherever she is now, she knows I have followed it through to the end and am ready to set off on the next big adventure!

Summary

Molecules based on the 4-amino-1,8-naphthalimide fluorophore combined with powerful urea and thiourea recognition units have been shown to be excellent sensors for anions including dihydrogen phosphate, acetate and fluoride. The majority of the literature with regards to these particular sensors however reports solution phase sensing. This thesis details the synthesis of a series of sensors based on the combination of the 4-amino-1,8-naphthalimide fluorophore and a urea recognition unit, incorporating a terminal double bond at the imide position. This terminal double bond can then be used to immobilise the sensors onto a silica surface, broadening the potential applications of this sensing technology.

The synthesis of eight different sensors each containing the 4-amino-1,8-naphthalimide fluorophore and a urea or thiourea recognition group is described. The fluorophore and the recognition group are connected covalently *via* a spacer molecule, with the use of three different spacer molecules investigated; 2-aminobenzylamine, 4-aminobenzylamine and 3-aminobenzylamine. Previous literature reports had indicated that small changes in the sensor molecule influenced the properties of the sensors towards different anions. Several changes to the recognition group were also investigated (urea *vs*. thiourea, addition of a chloro group on the phenyl ring attached to the recognition group, introduction of triethoxysilyl groups to enable a different method of immobilisation).

The use of microwave irradiation as an alternative to conventional heating methods was also trialled for the synthesis of three of the sensors. Reaction time was decreased, whilst in some cases purity and yield were also improved. In one step the reaction time was reduced from fourty-eight hours to sixty minutes, whilst in another a product was able to be purified using recrystallisation, whereas column chromatography was usually required when using conventional heating techniques.

After successful synthesis of the sensors, their ability to sense anions (dihydrogen phosphate, acetate, fluoride and bromide) was monitored in the solution phase using

both fluorescence spectrophotometry and ^{1}H NMR spectroscopy. Strong interactions were observed upon addition of both dihydrogen phosphate and acetate to a solution of sensor in DMSO, with quenching of the fluorescent emission signal observed and also significant downfield shifts for the resonances assigned to the urea protons of each sensor in the ^{1}H NMR spectrum. Significant shifts were also observed for the 4-amino NH proton resonance dependant on the sensor being evaluated. Little quenching or changes in the ^{1}H NMR spectrum were observed upon addition of bromide to a solution of sensor. The most interesting results were obtained upon the addition of fluoride, with a colour change from yellow to red as greater amounts of fluoride were added due to deprotonation of the 4-amino NH proton. Again significant changes were noted in the ^{1}H NMR spectrum of each sensor.

Finally after establishing the sensors were suitable for the detection of anions, immobilisation onto a silica surface was investigated. Initially the terminal double bond included in the sensor design was used to covalently attach the sensor to a hydride modified silica gel using hydrosilation chemistry. Definitive spectroscopic characterisation of the surface was hard to obtain, however deprotonation of the 4-amino NH proton by addition of fluoride to the surface was observed, suggesting successful attachment. Alternative immobilisation methods including building the sensor onto a 3-aminopropyl functionalised silica surface and by condensing triethoxysilyl groups (introduced in three of the sensors as part of the recognition unit) onto mesoporous silica were also investigated, proving that immobilisation of the sensors onto a silica surface is viable and may be an alternative to solution phase sensing.

Table of Contents

List of Figures

List of Tables

List of Schemes

Abbreviations and Symbols

Abbreviation, Symbol or Unit	Explanation
°C	Degrees Celsius
^{13}C	Carbon-13
^{19}F	Fluorine-19
^{1}H	Proton (Hydrogen-1)
^{29}Si	Silicon-29
Å	Angstrom
AcO^-	Acetate
ADP	Adenosine diphosphate
AMP	Adenosine monophosphate
API	Atmospheric Pressure Ionization
AR	Analytical Reagent
ATP	Adenosine 5'-triphosphate
ATR	Attenuated total reflectance
Br^-	Bromide
bs	Broad singlet
cf.	Compared with
CE	Capillary Electrophoresis
CH_3COO^-	Acetate
Cl^-	Chloride
cm	Centimetre
cm^{-1}	Wavenumbers
cm^3	Cubic centimetres
CO_3^{2-}	Carbonate
COSY	Correlation Spectroscopy
CP-MAS	Cross Polarisation – Magic Angle Spinning
CPTS	3-chloropropyltrimethoxysilane
C-TAB	Cetyl Trimethyl Ammonium Bromide
d	Doublet
dATP	Deoxyadenosine triphosphate
DMF	Dimethylformamide
DMSO	Dimethyl sulfoxide
DMSO-d_6	Deuterated dimethyl sulfoxide
dq	Doublet of quartets
dt	Doublet of triplets
EPA	Environmental Protection Authority
ESI	Electrospray Ionisation
EtOH	Ethanol
F^-	Fluoride
FDA	Food and Drug Administration
FTIR	Fourier Transform Infrared Spectroscopy
g	Grams
G	Guest

GR	**Guaranteed Reagent**
h	Hours
H	Host
Hz	Hertz
H_2O	Water
$H_2PO_4^-$	Dihydrogen Phosphate
HCO_3^-	Bicarbonate
HDMS	High Definition Mass Spectrometry
HF_2^-	Bifluoride
HG	Host-Guest complex
HMBC	Heteronuclear Multiple-Bond Correlation
HMQC	Heteronuclear Multiple-Quantum Correlation
HOMO	Highest Occupied Molecular Orbital
HPLC	High Performance Liquid Chromatography
HPMA	2-hydroxypropyl methacrylate
HPO_4^{2-}	Monohydrogen Phosphate
HSO_4^-	Hydrogen Sulfate
I	Intensity
i.e.	*id est* (that is)
I_0	Initial Intensity
IC	Ion Chromatography
ICT	Internal Charge Transfer
K	Binding constant
K^+	Potassium Ion
KBr	Potassium Bromide
kHz	Kilohertz
$kJ.mol^{-1}$	Kilojoule/mol
lb	Line broadening
Lit.	Literature
λmax	Maximum wavelength
Log	Logarithmic
m	Multiplet
m.p.	Melting point
m/z	Mass to charge ratio
MAS	Magic Angle Spinning
Me	Methyl
MeCN	Acetonitrile
mg/mL	Milligram
μg/mL	Micrograms per millilitre
mg/mL	Milligrams per millilitre
MHz	Megahertz
min	Minutes
mL	Millilitres
μL	Microlitres
mM	Millimolar
μm	Micrometre
mm	Millimetre
$mol.L^{-1}$	Moles per litre

ms	Milliseconds
μs	Microseconds
MW	Microwave
N	Newtons
N/A	Not available
nm	Nanometre
NMR	Nuclear Magnetic Resonance
NO_2	Nitrogen Dioxide
NO_3^-	Nitrate
ODTMA	Octadecyltrimethyl ammonium bromide
PET	Photoinduced Electron Transfer
Ph	Phenyl
ppm	Parts Per Million
PTFE	Polytetrafluoroethylene
q	Quartet
quin	Quintet
rt	Room temperature
s	Singlet
Sec	Seconds
t	Triplet
TEA	Triethylamine
THF	Tetrahydrofuran
TLC	Thin Layer Chromatography
TSPM	3-(trimethoxysilyl)propyl methacrylate
USA	United States of America
UV-Visible	Ultraviolet-Visible
v/v%	Volume/Volume
W	Watts
ZnSe	Zinc Selenide
ZrO_2	Zirconium Dioxide

Summary of Host Molecules

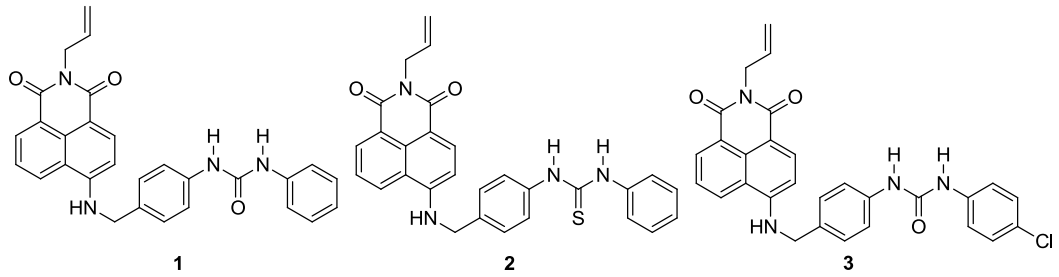

1 2 3

***N*-Allyl-4-(4-(*N*-phenylureido)benzylamino)-1,8-naphthalimide (1)**

***N*-Allyl-4-(4-(*N*-phenylthioureido)benzylamino)-1,8-naphthalimide (2)**

***N*-Allyl-4-(4-(*N*-chlorophenylureido)benzylamino)-1,8-naphthalimide (3)**

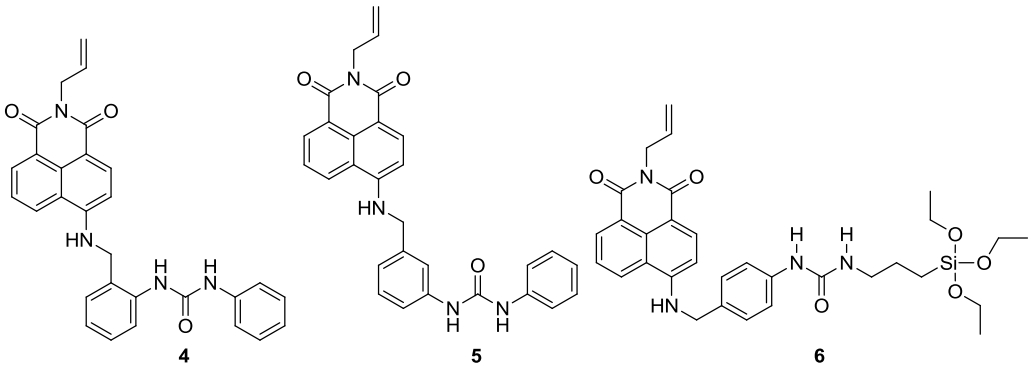

4 5 6

***N*-Allyl-4-(2-(*N*-phenylureido)benzylamino)-1,8-naphthalimide (4)**

***N*-Allyl-4-(3-(*N*-phenylureido)benzylamino)-1,8-naphthalimide (5)**

***N*-Allyl-4-(4-(*N*-3-(triethoxysilyl)propylureido)benzylamino)-1,8-naphthalimide (6)**

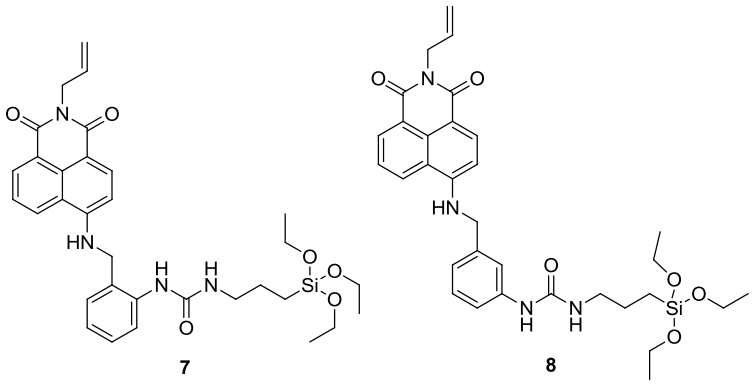

7 8

***N*-Allyl-4-(2-(*N*-3-(triethoxysilyl)propylureido)benzylamino)-1,8-naphthalimide (7)**

***N*-Allyl-4-(3-(*N*-3-(triethoxysilyl)propylureido)benzylamino)-1,8-naphthalimide (8)**

Chapter 1

INTRODUCTION

1.1 Overview

Anions, chemical species in which the number of electrons exceed the number of protons, are ubiquitous in nature [1]. For example, 70-75% of all substrates and co-factors engaged in biological processes are anions [2]. Anions also form part of the make-up of amino acids, neurotransmitters and nucleic acids [3]. Environmentally high concentrations of anions such as phosphate have been linked to the process of eutrophication in waterways, whilst the production of pertechnetate during the reprocessing of nuclear fuel is also of great concern [4]. The metabolites of nitrate when released into the environment have also been linked to the process of carcinogenesis [4]. The fluoride anion is associated with nerve gases, the analysis of drinking water and the refinement of uranium used in nuclear weapons manufacture [5]. Anions are also of importance in defence and forensic science where the analysis of explosives is performed [6]. As a result the detection and monitoring of anionic species is of great interest as their use is widespread and there exists important industrial, biological, medicinal and environmental applications [7].

Supramolecular chemistry exploits intermolecular interactions between molecules to form molecular assemblies [8]. Commonly termed host – guest chemistry, intermolecular interactions such as hydrogen bonding can allow discrimination of one molecule/ion from another [8]. Chemical sensing using supramolecular chemistry offers the opportunity for highly selective, sensitive analyte specific detection [9]. The fields of supramolecular chemistry and anion sensing are described in this chapter, followed by a detailed literature review of anion sensing using a urea or thiourea recognition group. Emphasis is given to sensors that use the 4-amino-1,8-naphthalimide as their signalling unit. Common methods used in the immobilisation of organic molecules onto a solid support surface are also discussed.

1.2 Traditional anion detection methods

Capillary electrophoresis (CE) [10-13], ion chromatography (IC) [14-17], and electrochemical methods [18-20] are most commonly used for the detection of anions. Whilst each method is well-established and many EPA and FDA methods have been developed using them, they do have some downfalls. Electrochemical detection can be

subject to electrode fouling, which negatively impacts on quantitation [21]. Conductivity detection, commonly used in CE and IC, can suffer from interference due to background electrical noise, as well as from high background signals from buffers [22]. As a result conductivity often has poor limits of detection (mM) and is unsuitable for dilute samples [22]. Alternate IC and CE detection methods use UV-visible and fluorescence spectrophotometries [22]. However, as many common anions do not have a suitable chromophore or fluorophore which would allow for their easy detection, CE and IC coupled with these detection methods may suffer from poor sensitivity. Molecules or ions which do not have a suitable chromophore for analysis by UV-Visible or fluorescence spectrophotometries can be detected indirectly whereby the analytes of interest are detected by their lack of absorbance as opposed to the amount they absorb [22, 23]. Indirect detection is generally performed by adding a strongly adsorbing ion (probe) into the background electrolyte used in the analysis [22, 23]. During analysis the probe will be displaced by other ions in solution which are of the same charge and thus the absorbance of the probe will decrease which can then be taken as detection of the previously undetectable species [22, 23]. The use of indirect detection in CE leads to skewed peak shapes due to the difference in electrophoretic mobility between the analyte and the probe [24, 25]. This poor peak shape makes accurate quantitation difficult. It is also possible that the probe may interact with other species in the background electrolyte and may form insoluble precipitates which are a further hindrance to analysis [26], as well as the possibility of the probe absorbing onto the capillary wall.

An alternative approach for the detection of anion species is to use fluorescence spectrophotometry to analyse a compound which interacts with an anion *via* intramolecular interactions such as hydrogen bonding or direct chemical reaction. Fluorescence is a process where electromagnetic light is absorbed by atoms or molecules giving rise to an excited state of that atom or molecule [27]. They then return back to the ground state with subsequent emission of photons at a wavelength longer than the original wavelength of excitation [27]. Fluorescence detection possesses sensitivity that is three orders of magnitude greater and works over a greater linear range than UV-Visible absorption detection methods [27]. These benefits of fluorescence detection are however tempered by the fact that very few molecules

are able to undergo the process of fluorescence (particularly in comparison to UV-Visible absorption) [27]. The majority of molecules which are able to undergo fluorescence emission upon absorption of electromagnetic radiation will contain an aromatic ring or rings (there are certain examples of aliphatic/alicyclic compounds which also undergo fluorescence but they are far out-numbered by compounds containing aromatic rings or at the least conjugated double bonds) [27].

It is the aim of this research to develop fluorescent supramolecular anion sensors that are permanently immobilised onto a solid surface. These will allow for direct and potentially selective detection of target ions *via* fluorescence spectrophotometry. The use of fluorescence detection should allow for lower limits of detection compared to the use of conductivity and electrochemical detection.

1.3 Supramolecular Chemistry

Supramolecular Chemistry has been defined by one of its founding fathers Jean-Marie Lehn, as the "chemistry of molecular assemblies and of the intermolecular bond" [8]. Put simply it can be seen as chemistry involving a host and a guest molecule (Figure 1), with the host (red semi-circle) and the guest (blue ball) binding through non-covalent interactions. To successfully form a host-guest complex, the host needs convergent binding sites, and the guest divergent binding sites, whilst for selective use as a sensor the host has to have the ability to discriminate between different guests [8].

Figure 1: Generalised structure of a host-guest interaction, with the host indicated by the red semi-circle and the guest by the blue circle.

The history of supramolecular anion sensing can be traced back to 1968 and the discovery of katapinands (**9-11**) by Park and Simmonds at DuPont de Nemours Company in 1967 [28]. This paper was only preceded by Pedersen's landmark work with dibenzo(18)crown-6 (**12**) [29], which has been described as the beginning of

modern supramolecular chemistry [8]. Park and Simmonds discovered that the katapinands were able to bind halides within their marcobicyclic cavity when the ring head nitrogen atoms were protonated [28]. However despite this early initial work in the area of supramolecular anion chemistry, limited research on anion interaction was undertaken in the area until the 1980's, well after the development of the supramolecular chemistry of cationic and neutral guests [8].

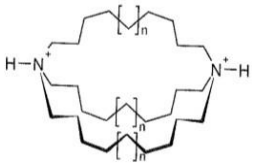

9 n=0, **10** n=1, **11** n=2

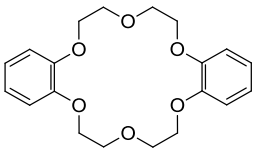

12

There are many reasons why anion supramolecular chemistry was slow to develop, even though rules regarding preorganisation, complementarity and solvation that apply to cation and neutral supramolecular chemistry are similar. Reasons for this delay include:

i) Anions are larger in comparison to cations, thus they require a much larger cavity to which they can bind. For example fluoride, one of the smallest anions, has an ionic radius (1.33 Å) similar to that of potassium (1.38 Å)[8, 30].

ii) Anions have greater free energies of solvation in comparison to cations, thus the design of the anion host must allow the host-anion interaction to be more competitive than the solvent-anion interaction. As an example in water, fluoride has a free energy of solvation of -456 $kJ.mol^{-1}$, whereas potassium has a free energy of solvation of -295 $kJ.mol^{-1}$ [8].

iii) Even the simplest inorganic anions exist in many shapes and geometries which makes it hard to design simple hosts which will be able to sense numerous anions [8, 30]. Halide ions are spherical, whilst the phosphate anion is tetrahedral and nitrate anion planar.

iv) The geometry of an anion can change dependant on the pH environment the anion exists in [8, 30]. Potential changes in pH and their effect on anion geometry present further problems in host design as the host may not be fully protonated over the pH region where the anion of choice is in the desired form. Figure 2 shows a speciation diagram for phosphate [31]. It can be seen that as

the pH of the solution is altered that phosphate exists in many forms, predominantly taking the form of dihydrogen phosphate at mildly acidic pH (pH 3.5 to 6), whilst in the form of phosphate at highly basic pH (pH >13).

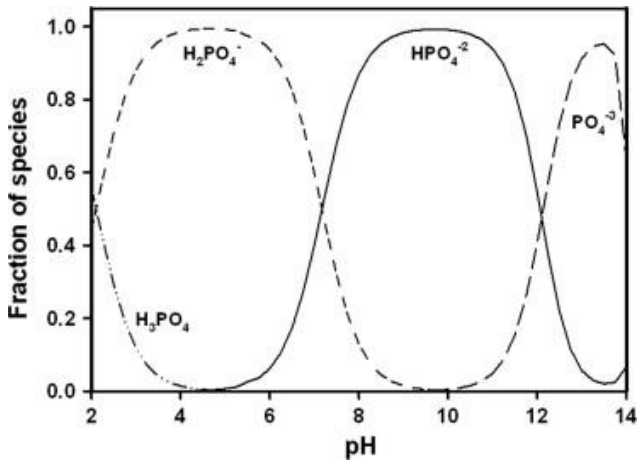

Figure 2: Speciation diagram for Phosphate.

Taken from Kang and co-workers [31].

v) Anions often bind by comparatively weak-forces such as hydrogen-bonding and Van der Waals forces [8].

In the case of the katapinands, the first recognised anion supramolecular sensor, the host is not preorganised. When the anion binds inside the katapinand cavity, the molecule undergoes a conformational change (Figure 3). This binding occurs in much the same way as crown ethers bind cations in aqueous solution. It has been shown that it is the bicylic nature of the katapinand system which is responsible for the binding of the anion and the anion itself is not responsible for any of the organisation [8].

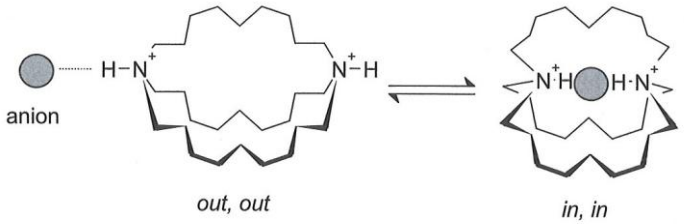

Figure 3: Conformational change in a katapinand on binding of an anion.

Image reproduced from Steed and Atwood [8].

As well as allowing for preorganisation, there needs to be complementarity between the host and guest. It would therefore seem logical that a neutral or especially a positively charged host would be suitable to bind an anionic guest. Electrostatic interactions however are non-directional and thus any anion in solution would be attracted to a cationic host on an electrostatic basis. In this way there would be a competition for the host between the desired anionic guest and any other anions in the solution. Whilst this problem is still evident when using a neutral host as there is still a charge difference between it and the negatively charged anion, neutral hosts are generally the preferred motif on which to design a supramolecular anion sensor [8]. The major advantage of a neutral host is that it is not charged and therefore depending on the geometry (i.e. size and fit for a particular anion) and type of binding site (hydrogen bonding) they can be highly selective for particular anions. The use of a neutral host also circumvents another issue with charged hosts, in that to make a positively charged host there must be a negative counter anion and the existence of this counter anion, will affect the binding of the target anion. Therefore a binding constant obtained for an anion-host complex in the case of a positively charged host, is the ratio of the affinity for one anion over the other rather than the actual affinity of the host to the guest [8].

In nature there exists a number of highly selective systems for anions, which serve as good models for the design of synthetic supramolecular anion sensors. In cellular systems anions are transported through the cell membrane predominantly by proteins [32]. This is a result of the anion interacting with the N-H group on the protein backbone through hydrogen bonding interactions [32]. For example, the amino acid arginine (Figure 4) has a guanidine group which facilitates anion transfer *via* hydrogen bonding [8]. In cellular systems the guanidine group can become protonated and form two sets of hydrogen bonds with important biological anions such as carboxylates, phosphates and sulfates (an example with phosphate is shown in Figure 4) [8].

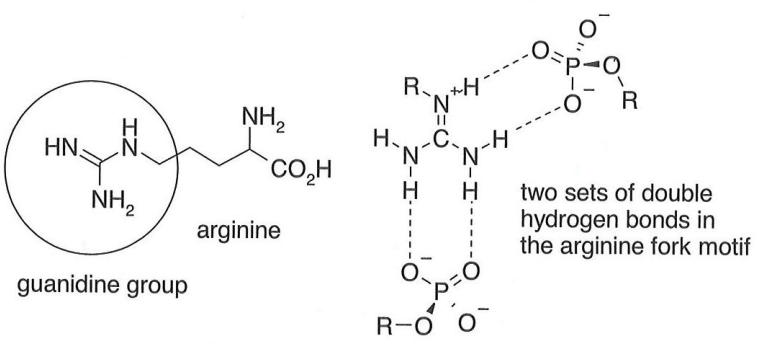

Figure 4: Structure of the amino acid residue Arginine. The guanidinium group is circled and then it is highlighted how an anion is able to form two hydrogen bonds with the protonated guanidinium moiety.

This image was reproduced from Steed and Atwood [8].

Taking inspiration from nature by using N-H groups in an effort to ensure interaction with an anion, the first synthesised neutral supramolecular anion sensor was reported by Pascal and co-workers [33]. They employed a cage structure with N-H groups directed toward the centre of the molecule **13**. Analysis by ^{1}H and ^{19}F NMR spectroscopy suggested that fluoride interacted with the sensor *via* hydrogen bonding, however it was not clear whether fluoride was encapsulated in the sensor [33]. Since the synthesis of **13**, numerous molecules have been proposed as supramolecular hosts for a range of anionic guests. Specific hosts with relevance to this research will be discussed in Section 1.3.3.

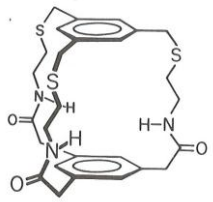

13

1.3.1 Building an Anion Sensor

In order to create a sensor the design of the supramolecular host needs to incorporate a binding site (receptor) along with a signalling subunit [34]. It is the signalling subunit which changes an ordinary host molecule into a sensor molecule. A host can bind a guest, but if we are unable to readily and easily observe a change upon binding the use of the host as a sensor for that guest is futile. It is possible to complex a host with a guest, grow crystals of it and then obtain X-ray crystallographic data of the crystals to

show that the guest has been included in the host, but this technique would not provide real time information. The formation of a host-guest complex can be monitored in real time by NMR spectroscopy, adding aliquots of guest to host and then monitoring changes in the NMR spectrum as greater amounts of guest are added. This technique however suffers from poor sensitivity [35] in comparison to other methods and also is difficult to be made portable and potentially taken out of the lab to real-world situations. One of the more common techniques which has been used to show the recognition of anionic guests is the monitoring of changes in fluorescence emission [36, 37]. Fluorescence spectrophotometry has much better sensitivity than NMR spectroscopy [35] which in turn allows lower host and guest concentrations to be used, allowing the determination of binding constants over a larger range. Therefore the use of a fluorophore as the signalling subunit has become well established and as described in Section 1.2, will be used in this research.

The use of a signalling subunit and binding site (receptor) in tandem is usually achieved in one of two ways; i) the binding site can be part of or directly attached to the signalling unit (as shown in Figure 5) or the signalling unit and receptor are connected using a covalent spacer as shown in Figure 6 [32, 34]. In the first approach (Figure 5) the binding site is integrated within the signalling site [34]. Recognition of an anion at the binding site will result in changes in the absorption spectrum and depending on the signalling unit used also changes in the emission spectrum [34]. In the second approach (Figure 6) the binding site and signalling subunit are joined through covalent bonds (spacer moiety), thus both sites are electronically independent of each other [34]. In the case of a colourimetric sensor, the change at the receptor is usually communicated to the signalling unit through conjugation with an aromatic compound [34]. Fluorescent sensors however are typically designed with the binding site and signalling unit joined covalently by a short aliphatic spacer, allowing for the process of photoinduced electron transfer (PET) to occur [34]. The separation imparted between the receptor and fluorophore by the spacer ensures that no ground state π-π^* or n-π^* interactions can occur [34]. When the anion is bound at the receptor site and the interaction is monitored by fluorescence spectrophotometry, the emission spectrum of the signalling subunit will change considerably, along with little to no change in the absorption spectrum [34, 38].

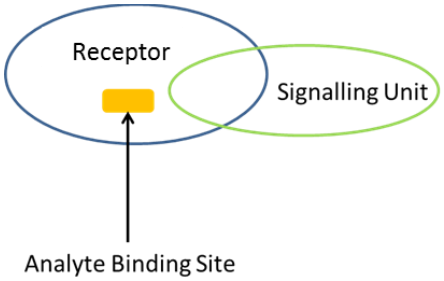

Figure 5: A sensor containing the binding site integrated within the signalling unit.

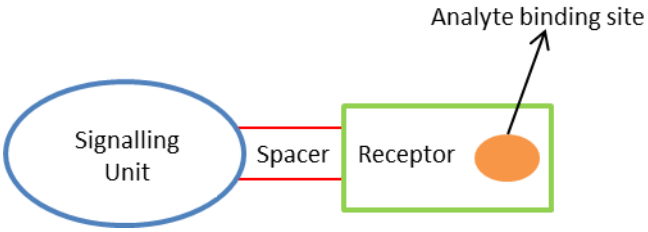

Figure 6: A sensor containing a fluorophore and receptor joined using a covalent spacer [39].

Two variations of the process of photoinduced electron transfer are depicted in Figure 7 [40]. As depicted in Figure 7 upon absorption of light by the chromophore, an electron is elevated to a higher energy orbital, resulting in an excited state molecule. This molecule can act as either a strong oxidising agent or a strong reducing agent [40]. Oxidative electron transfer results when an electron is transferred out from the high energy orbital to an electron poor quencher. Alternatively, an electron rich quencher can donate an electron to the molecule (reductive electron transfer). The process that occurs is dependent on the species interacting with the host. Both processes involve the transfer of electrons after excitation of a molecule upon absorbance of light, hence the name photoinduced electron transfer. A third process, termed energy transfer, involves energy from the excited state chromophore being transferred directly to the quencher [40].

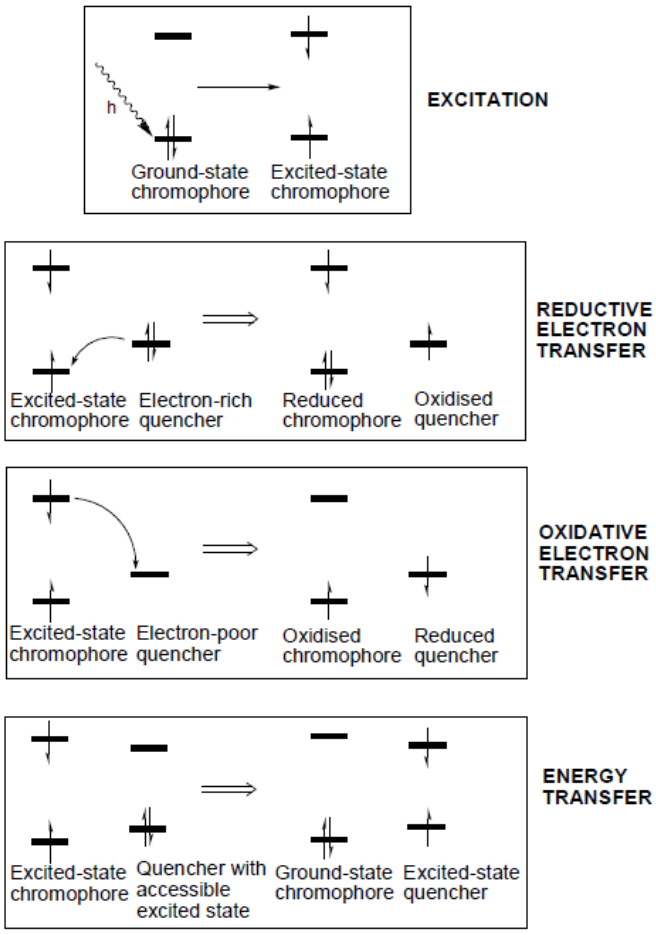

Figure 7: Mechanisms for fluorescence quenching.

Image taken from Ward [40].

Gunnlaugsson and co-workers [3] have proposed that the binding of an anion to **14** at the thiourea receptor site (*via* hydrogen bonding) alters the reduction potential of the receptor. Upon binding, the reduction potential of the receptor-anion complex is increased which leads to a greater rate of PET between the HOMO of the receptor and the excited state of the anthracene signalling moiety. This results in the fluorescent emission of the anthracene moiety being quenched or "switched off". This behaviour is the reverse of what is seen for cations where the fluorescent emission is observed to be "switched on" [3].

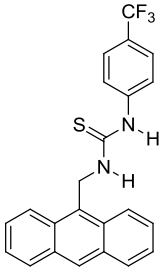

14

1.3.2 Choosing the recognition subunit

There are many examples of recognition groups which have been used for the analysis of anions. The guanidine group, described earlier in Section 1.3, is just one example of a suitable binding site for an anion sensor (providing the ability to hydrogen bond with the one anion). As was shown in Figure 4, the guanidinium group (the protonated form of guanidine) was able to form a number of hydrogen bonds with two phosphate anions. Other commonly used binding sites include those based on secondary amide (can donate a single hydrogen bond like guanidine), pyrrole, indole, triazole, hydroxyl, pyridinium, metal and Lewis acid groups [30, 32, 41, 42]. Recent research has suggested phosphoric triamide and thiophosphoric triamide based receptors could also be useful to provide hydrogen bonding interactions with anions [43].

Urea and thiourea moieties are commonly used in many supramolecular anion sensing molecules. Unlike an amide receptor which can provide a single hydrogen bond, urea and thiourea groups provide two parallel hydrogen bonds [32]. Subsequently they are good receptors for y-shaped anions such as carboxylate and other inorganic oxoanions (see Figure 8(a)) [4, 32]. The two N-H bonds are also able to chelate spherical anions such as the halides (see Figure 8(b)) [32]. The urea and thiourea group have found particularly high appeal as a receptor group as they are easily incorporated into a sensor through the reaction of a primary amine with an isocyanate or isothiocyanate [32]. It has been noted that thiourea receptors will generally bind anions with a greater affinity than a urea receptor [30]. This is due to the greater acidity of the thioureido NH protons in comparison to urea protons [30] (pk_a 21.1 for thiourea versus 26.9 for urea in DMSO [44]), which leads to stronger hydrogen bonding between the NH group and the anion [30].

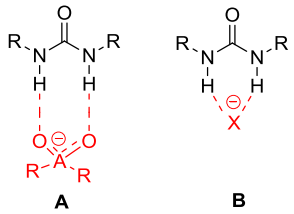

Figure 8: (a) A urea functional group interacting with an oxo-anion, (b) urea functional group interacting with a spherical anion [32].

Similar interactions are observed for the thiourea functional group.

The anion binding properties of urea and its use in supramolecular chemistry was first noted by Wilcox and co-workers who, in 1992, synthesised the urea containing compound **15** [45]. They demonstrated that **15** interacts with a range of phosphonates, sulfates and carboxylates when prepared in dichloromethane. The proposed binding interaction is shown in Figure 9 [45]. Benzoate was shown to form the strongest complex with the sensor, with log *K*=4.43 [45].

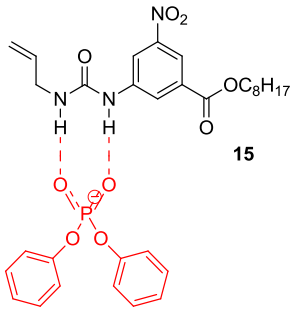

Figure 9: Urea containing compound 15 (shown in black) interacting with a phosphonate anion (shown in red) [45].

Due to their excellent anion binding properties, urea and thiourea recognition groups will be incorporated into the sensors synthesised in this research.

1.3.3 Choosing the signalling subunit

To make a sensor where the response upon anion detection will be a change in fluorescence, a fluorophore is required as the signalling subunit. As discussed briefly in Section 1.2 in order for a molecule to undergo the process of fluorescence, the molecule typically needs to be aromatic in nature [27]. Therefore several polycyclic aromatic hydrocarbons including anthracene (**16**), naphthalene (**17**) and pyrene (**18**) have found use as the signalling subunit in anion sensors (discussed in Sections 1.3.3.1-1.3.3.3 below).

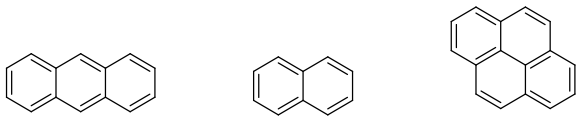

16 **17** **18**

1.3.3.1 Anthracene (16) based anion sensors

Anthracene (**16**) is one of the most commonly used signalling subunits in anion sensors [38]. The chemistry to functionalise the anthracene molecule is well established and the fluorescent properties of anthracene derivatives are well-known [38].

Anthracene has been combined with urea and thiourea moieties by many researchers to create anion sensors with some examples reviewed by Martìnez-Máñez and Sancenón [38] and Gunnlaugsson and co-workers [39]. The molecules synthesised by Gunnlaugsson **14** (Section 1.3.1), **19** and **20** are excellent examples of this [3]. All of these molecules exhibit a thiourea binding site coupled with an anthracene signalling subunit connected covalently *via* a methylene spacer.

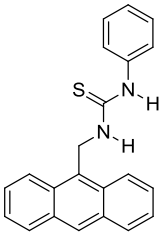

19

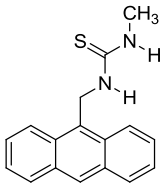

20

Hosts **14**, **19** and **20** were designed for the detection of fluoride, acetate and dihydrogen phosphate [3]. All three molecules were found using NMR spectroscopy to have a 1:1 anion interaction, with the binding occurring due to hydrogen bond interactions between the thiourea subunit and the anion. They were also shown to display ideal behaviour for a fluorescent sensor, that is only the fluorescence emission was quenched upon anion recognition (there was no change in the UV-Vis absorption spectrum) [3].

The excited state of the sensor molecules was investigated by fluorescence spectrophotometry titration of the molecules with various anions. To a solution of **14** in DMSO, the acetate anion was added (tetrabutylammonium salt) and as the concentration of the anion increased, it was determined that the anthracene emission at 419 nm, was quenched by approximately 70% (i.e. "*switched off*") (after addition of 32 mM acetate). Similar titrations were undertaken with dihydrogen phosphate (50% quenching at 419 nm) and fluoride (90% quenching at 443 nm, Figure 10), whilst little

change was seen in the emission spectrum when the **14** was titrated with either chloride or bromide [3].

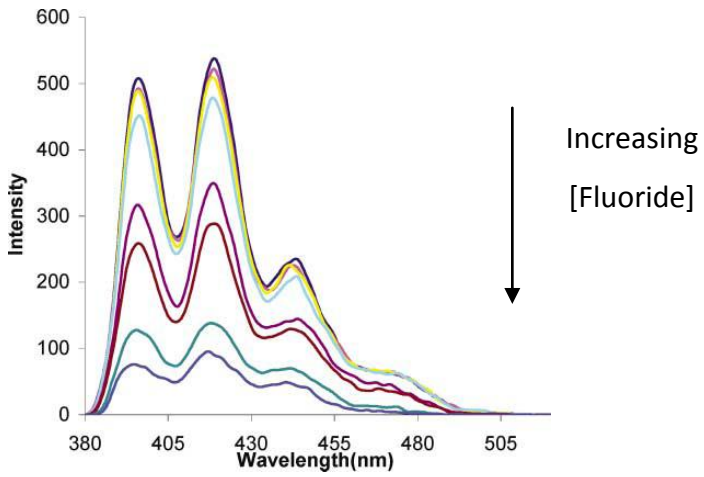

Figure 10: Fluorescence spectrum (λ_{ex}=370 nm) of host 14 in DMSO upon addition of tetrabutylammonium fluoride (0→32mM) [3].

The aforementioned results, and Figure 11, show that using this type of sensor molecule there is potential for selectivity as the different anions have a different interaction with **14**. Gunnlaugsson and co-workers propose that this different interaction is due to the different abilities each anion has to form a complex with the host molecule [3]. For example fluoride is a small spherical anion which has a high charge density and thus can easily hydrogen bond to the receptor, whereas chloride and bromide which are much larger and have lower charge densities are unable to bond strongly to the receptor. Similarly acetate is able to form stronger linear directed hydrogen bonds to the thiourea receptor than dihydrogen phosphate explaining the 20% difference in the fluorescence emission signal [3].

Results for sensors **14**, **19** and **20** are summarised in Table 1. As can be seen addition of the electron withdrawing trifluoromethyl group in sensor **14** leads to increased binding constants compared to the similar sensor **19** without the trifluoromethyl group. Sensor **20** which had no phenyl group attached to the urea recognition group produced lower quenching for acetate, dihydrogen phosphate and fluoride. These results suggest small changes to the sensor molecules can have a big effect on their anion binding abilities.

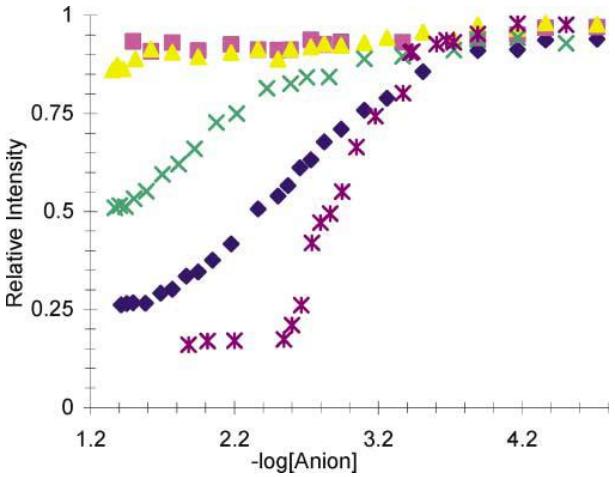

Figure 11: Graph showing the relative intensity of the fluorescence emission spectrum at 419 nm of host 14 in DMSO, versus the log of anion concentration upon addition of tetrabutylammonium acetate (♦), tetrabutylammonium dihydrogen phosphate (×), tetrabutylammonium fluoride (*), tetrabutylammonium chloride (▲) and tetrabutylammonium bromide (■) [3].

Table 1: Comparison of Hosts 14, 19 and 20 and their interaction with various anions (0 to 32 mM anion added) [3].

Host	19		14		20	
Anion	%Quench	log *K*	%Quench	log *K*	%Quench	log *K*
AcO^-	73	2.15	75	2.33	43	1.75
$H_2PO_4^-$	46	1.82	50	2.05	38	2.05
F^-	64	2.9	90	3.35	55	2.37
Cl^-	8	n/a	7	n/a	12	n/a
Br^-	7	n/a	12	n/a	14	n/a

Anthracene signalling subunits whilst well utilised (many examples in [38, 39]) do have some inherent problems. Sensors based on the anthracene molecule and its derivatives show emission close to the ultra-violet region, meaning that matrix interferences in real-life samples can become an issue [38]. Therefore alternative polyaromatic hydrocarbons such as naphthalene (**17**) have been investigated.

1.3.3.2 Naphthalene based sensors

Naphthalene (**17**), like anthracene (**16**), has excellent fluorescence properties and has also found common use as a signalling subunit in combination with the thiourea or urea recognition unit with many examples reviewed in [38, 39]. As an example highlighting how small changes to the sensor molecule can affect the sensing

observed, Qian and Liu synthesised sensors **21** and **22** which differ in the number of hydroxymethyl groups attached to the thiourea receptor [46].

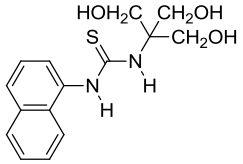

21

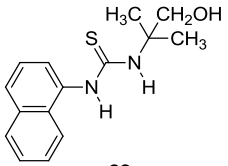

22

The fluorescent sensing ability of host **21** was tested in an 80% methanol/20% water solution with various anions added as their sodium salts. When host **21** was not in the presence of an anion, the fluorescent signal was very weak, however upon addition of specific anions the fluorescence emission could be "*switched on*" (the reverse of what was seen for anthracene) [46].

Table 2 summarises the fluorescent enhancement observed for a variety of different anions added to hosts **21** and **22**. It can been seen quite markedly from the results in Table 2 that the change in the number of hydroxymethyl groups has quite an impact on the fluorescent enhancement obtained [46]. For example host **21** (with three hydroxymethyl groups) sees the fluorescence emission enhanced 14.7 times upon addition of carbonate, whilst host **22** (with only one hydroxymethyl group) see enhancement of only 2.5 times upon addition of the same anion

Table 2: Fluorescent enhancement seen in host molecules 21 and 22 upon addition of various anions in 100 times excess in methanol [46].

	I/I_0	
Anion	**Host 21**	**Host 22**
CO_3^{2-}	14.7	2.5
HPO_4^{2-}	6.5	2.5
HCO_3^-	2.2	1.4
CH_3COO^-	3.8	1.0
$H_2PO_4^{2-}$	3.1	1.0
NO_3^-	1.5	1.0
HSO_4^-	1.0	1.5

Where I is the fluorescence intensity of the compounds after addition of anions, and I_o is the fluorescence intensity of the free compound.

Similarly to anthracene (**16**), naphthalene (**17**) based sensors do have their inherent problems for use as sensors in biological applications. This is primarily due to the fact that **17** and molecules containing **17** emit at a short wavelength (372 nm for **21** and 425 nm for **22**), leading to the potential for background auto-fluorescence and light scattering which will effect results obtained by the sensor [39].

1.3.3.3 Pyrene (18) based sensors

Pyrene (**18**) is another highly fluorescent polycylic aromatic hydrocarbon that has found application as a signalling subunit in the development of chemical sensors for various anions (again various examples are reviewed in [38, 39]). As an example Kanekiyo and co-workers [47] produced the pyrene based fluorescent sensor molecule **23** and a polycation **24** which were used in tandem for the detection of the biologically important anionic molecule adenosine 5'-triphosphate (ATP) (this time with the developed sensor not involving urea or thiourea groups). Sensor **23** assembles onto **24** in the presence of ATP. This is due to the electostatic interaction that occurs between ATP and the polycation. Subsequently an ester linkage is formed between the boronate group in the pyrene based sensor and the diol group in ATP (Figure 12). The formation of the complex produces an inherent change in fluorescence properties including formation of an excimer band which can then be detected using fluorescence spectophotometry. From increases in excimer emission intensity it was shown that as ATP concentration increased so did the amount of aggregated sensor. It was found that ATP could be detected amongst related compounds such as ADP, AMP and dATP with a detection limit of 0.1μm using the developed system [47].

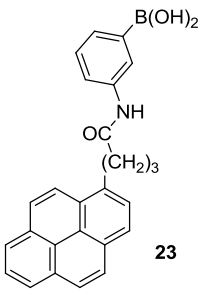

23

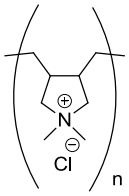

24

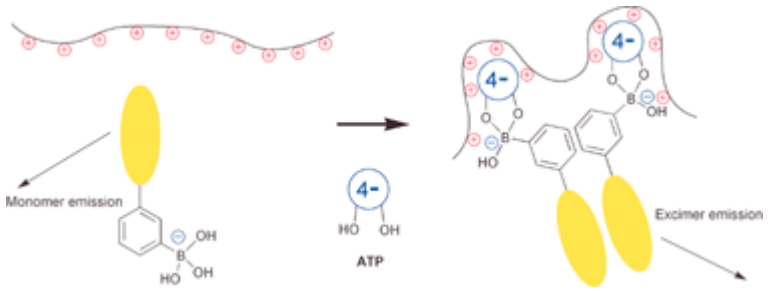

Figure 12: Stylised mechanism for the involvement of ATP in the aggregation of 23 and 24. 23 is represented by the yellow oval with boronate group, whilst the polycation 24 is represented by the positively charged surface. Image reproduced from Kanekiyo and co-workers [47].

1.3.4 Naphthalimide based sensors

In addition to the polyaromatic hydrocarbons already described, the naphthalimide motif (Figure 13) has also been a common component in the design of fluorescent anion sensing molecules (many examples reviewed in [34, 38, 39]) and is the motif which will be used in this research. The fluorescent and colorimetric properties of the fluorophore can be altered by varying the kind of substituents and their position on the naphthalimide ring structure, with the most common sites substituted those denoted as R_1 (the 4-position) or R_2 (the 3-postion) on Figure 13 [34]. A molecule based on the 4-nitro-1,8-naphthalimide fluorophore (R_1=NO_2 R_2=H) will have a high energy excited state due to the electron withdrawing nature of both the imide functionality and the nitro group, with a broad absorption maximum at 360 nm with subsequent emission at a longer wavelength than anthracene or naphthalene [34]. Reduction of the nitro group to an amine (R_1=NH_2, R_2=H) however results in different properties and leads to a "push-pull" internal charge transfer (ICT) excited state due to the electron withdrawing nature of the imide functionality and the now electron donating nature of the amine group [34]. This leads to broad absorption and emission bands, with two emission bands generally observed at 450 and 550 nm when the emission spectrum is collected in water [34]. The absorption and emission bands and the quantum yield of the compound have been observed to be greatly affected by the choice of solvent that the analysis is undertaken in [34]. Generally the quantum yield will be high (approaching unity) in organic solvents, whilst much lower in water [34].

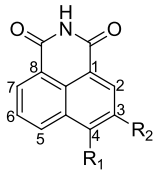

Figure 13: Generalised structure of 1,8-naphthalimide, where R_1 is the substituent at the 4-position and R_2 a substituent at the 3-position. For 1,8-naphthalimide, R_1=R_2=H.

Niu and co-workers have shown in **25** that it is possible to add a carbon chain with a terminal double bond to the naphthalimide structure, allowing future immobilisation of the sensor to a surface [48]. They used **25** for the sensing of nitrofurantoin (a zwitterionic molecule with antibiotic properties) [48]. Addition of the double bond allowed for the copolymerisation of **25** onto a silanised glass surface. The detection limit of the sensor for nitrofurantoin using a PTFE flow cell and bifurcated optical fibre with detection by fluorescence spectrophotometry was 4.8×10^{-7} mol.L^{-1}[48]. Analysis was undertaken successfully on both pharmaceutical preparations and urine samples [48], showing that sensors based on this fluorophore have found important practical applications.

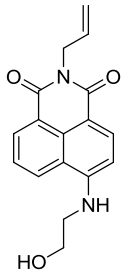

25

1.3.4.1 4-amino-1,8-naphthalimide (26)

In particular, it is the 4-amino-1,8-naphthalimide fluorophore (**26**) which has found particular use in the area of anion sensing as evidenced by the wealth of examples reviewed by Duke *et al.* [34].

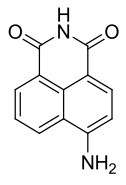

26

Gunnlaugsson, Pfeffer and co-workers have undertaken a considerable amount of research with regards to 4-amino-1,8-naphthalimide based anion sensors, with the examples outlined in [49-53], being of particular relevance to this research. Hence the findings in [49-53] will be presented in detail, followed by a brief overview of selected other 4-amino-1,8-naphthalimide based anion sensors which also contain a urea or thiourea recognition group.

Host molecules **27** and **28** were developed in 2003 [51]. The synthesis of **27** and **28** was based on a series of anthracene based PET chemosensors reported by Gunnlaugsson *et al*. [3] (discussed in Section 1.3.3.1). The issue of the short emission wavelength of anthracene (and naphthalene as well) prohibiting potential biological applications is removed as the 4-amino-1,8-naphthalimide fluorophore has a much longer emission wavelength (540-550nm) and is therefore not subject to interference commonly observed in complex matrices [39]. The fluorophore also has a high quantum yield, high-photo stability and strong absorption in the visible region [39, 48]. The use of naphthalimide has also been advantageous as there is potential for it to be used as a colourimetric sensor as well as a fluorescent sensor. This opportunity arises from the existence of an internal charge transfer excited state (briefly discussed in Section 1.3.4) in the ground state which means the colour of the compound can be modulated *via* hydrogen bonding or *via* deprotonation of the 4-amino moiety [51]. Using UV-Visible spectrophotometry both highly coloured compounds **27** and **28** were found to have λ_{max} of 444 nm [51]. This band was assigned to the internal charge transfer excited state [51]. Excitation at this wavelength yielded a strong emission in the green region [51]. Addition of fluoride, acetate and dihydrogen phosphate caused a substantial decrease in emission intensity, with fluoride resulting in the greatest level of quenching [51]. The fluorescence quenching was reported to be due to PET between the thiourea moiety and the naphthalimide moiety [51]. It was further shown that the quenching was reversible as addition of methanol to a solution containing a complex of **27** or **28** with an anion resulted in fluorescence emission being switched back on as the hydrogen bonding interactions were disrupted [51].

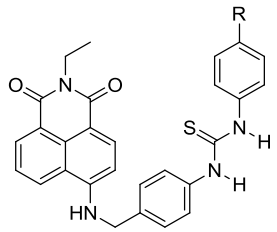

R=H (**27**), CF_3 (**28**)

Quenching of the fluorescence emission of **27** upon the addition of acetate and dihydrogen phosphate was less than that of fluoride, whilst addition of larger halide anions such as chloride and bromide did not change the emission spectrum of the host at all. The addition of the trifluoromethyl group in **28** resulted in greater binding between the anion and host molecule (binding constants in Table 3). This was due to the increased acidity of the thiourea protons, due to the electron withdrawing nature of trifluoromethyl group. Anion sensing was also shown using ^{1}H NMR spectroscopy and it was found that binding for both hosts was 1:1 for dihydrogen phosphate and 1:2 for fluoride. It was also possible to view the 1:2 binding of fluoride visually as after addition of 2-2.5 equivalents of fluoride to the host, the solution underwent a marked colour change from light yellow to deep purple, highlighting the potential of naphthalimide sensors to be used a colourimetric sensors (briefly discussed in Section 1.3.4). It was established that the colour change was due to interaction of fluoride with the 4-amino moiety and subsequent deprotonation of the amino moiety due to the highly basic nature of fluoride. Using UV-visible spectroscopy changes were also seen in the spectrum of the host when hydroxide (another highly basic anion) was added. The deprotonation hypothesis for the observed colour change was proven through the synthesis of a reference compound without the ability to undergo PET [51].

Table 3: Binding constants (log β) for the interaction of 27 and 28 with various anions as determined by fluorescence spectrophotometry [51].

Anion	27	28
Fluoride	3.8	4.4
Acetate	3.9	4.0
Dihydrogen Phosphate	2.9	3.7

Pfeffer and co-workers further refined the sensor design in synthesising **29** [49]. Sensor **29** was designed to try and overcome the rigidity of the *para*-substituted aromatic spacer in **27** and **28**. It was hoped that by removing the structural rigidity that an anion would be able to cooperatively bind with all three amino groups (two thiourea in the recognition group and the 4-amino NH moiety). This was achieved by reacting the imide with ethylenediamine, resulting in an ethyl spacer rather than the rigid phenyl group used in **27** and **28**. Proton NMR spectroscopy was used to monitor the binding of various anions (acetate, dihydrogen phosphate, fluoride, bromide and iodide) by **29**. Of the halide anions, only fluoride exhibited any effect on the NMR spectrum with the 4-amino N-H resonance broadened until it disappeared altogether after 0.5 equivalents of fluoride had been added. This disappearance was coupled with a colour change from yellow/green to deep red/purple. Upon addition of 2.0 equivalents of fluoride, a triplet in the NMR spectrum at 16.00 ppm was apparent. This was assigned to the formation of the bifluoride anion (HF_2^-), providing further evidence that fluoride deprotonates the 4-amino NH proton [49].

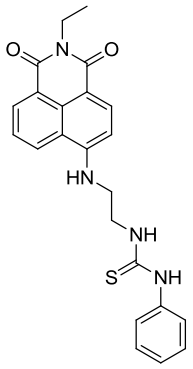

29

Large changes were observed when monitoring the thiourea resonances by ^{1}H NMR spectroscopy upon addition of acetate to **29**, indicating there is strong bonding between the acetate anion and the thiourea receptor. Little change was observed in the resonances of the naphthalimide protons and the 4-amino NH moiety, indicating the introduction of a more flexible spacer had little effect in allowing those protons to have a role in the binding of acetate. Binding was again found to be 1:1, with log K = 3.6. Addition of the tetrahedral dihydrogen phosphate anion to **29** resulted in a downfield shift for the resonances assigned to the thiourea protons, again indicating strong binding between the thiourea receptor and dihydrogen phosphate (binding

stoichiometry was 1:1, with log *K*= 3.4). A large downfield shift was observed for the 4-amino N-H proton indicating that this proton is involved in the binding. Unlike **27** and **28**, when using **29** no luminescent changes were observed upon addition of anions, even though there were significant changes in the ^{1}H NMR spectrum. This is thought to be due to the spacer used in the new sensor, and the fact it is not an electron-rich aromatic spacer, therefore reducing PET quenching efficiency [49].

In 2006, Pfeffer and co-workers reported the synthesis of **30** and **31**. The principle design difference is that in place of the ethylenediamine (used in **29**) or 4-aminobenzylamine (used in **27** or **28**) spacers, 2-aminobenzylamine is used. The use of 2-aminobenzylamine overcomes the issues discovered with **29** in that it brings the electron donor and electron acceptor into closer contact and gives the thiourea recognition group greater aromatic character [50].

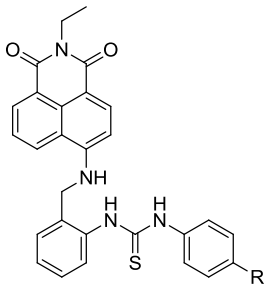

R=H (**30**) or R=F (**31**)

Interactions between **30** and **31** and the anions acetate, dihydrogen phosphate, fluoride and bromide were initially monitored using ^{1}H NMR spectroscopy. As seen with **27**-**29**, little difference was detected upon the addition of bromide. The 4- amino N-H signal was broadened after the addition of only small quantities of fluoride, disappearing completely upon addition of just 0.6 equivalents. As observed with **29**, this change in the ^{1}H NMR spectrum was accompanied by a visual change in the solution of **30** and **31** from fluorescent yellow/green to deep red/purple. A triplet at 16.00 ppm after addition of 2.5 equivalents of fluoride was added to both **30** and **31** was again assigned as due to the bifluoride anion. Therefore as seen previously fluoride is able to deprotonate the N-H naphthalic proton [50].

Addition of acetate again resulted in significant changes, with large downfield shifts observed for the two thiourea proton resonances. This was indicative once again of

strong binding between the acetate anion and thiourea receptor. Only small changes were observed for the resonances assigned to the naphthalic N-H proton or any of the naphthalimide ring protons of **30** and **31**. This was despite the introduction of the more flexible aromatic spacer. Binding was again observed as 1:1 with log *K*= 2.8 for **30** and 3.4 for **31**. This was less than that observed for the interaction between **29** and acetate – possibly due to the bulkiness of the aromatic spacer as opposed to the ethyl spacer [50].

Addition of the tetrahedral dihydrogen phosphate to **30** and **31** also produced changes in the ^{1}H NMR spectrum. Again significant changes were evident for the thiourea protons, however the naphthalimide N-H resonance was also observed to completely disappear after addition of three equivalents of dihydrogen phosphate. This indicated the 4-amino NH proton did play a role in the binding. A 1:1 binding stoichiometry was evident for the interaction between the thiourea protons and **30** or **31**. Binding between **30** and **31** and the 4-amino NH proton was observed as 1:2 host:guest. Binding constants were determined using low temperature studies for both acetate and dihydrogen phosphate using **31**, with log *K*= 3.2 for acetate and 3.9 for dihydrogen phosphate, showing a reversal in what had previously been observed (binding constant for acetate usually higher than dihydrogen phosphate) indicating it is possible to modify the host to preferentially bind different guests [50].

Using fluorescence spectrophotometry it was determined that fluorescence emission was quenched upon addition of anion (up to five equivalents) to **30** and **31** to varying degrees. Using **30**, fluorescence emission was quenched 31% for acetate and only 6.5% for dihydrogen phosphate, whereas for **31**, fluorescence emission was quenched 59% for acetate and 36 % for dihydrogen phosphate. The increased quenching observed for addition of anions to **31** is due to the increased electron deficient character of the thiourea receptor in comparison to **30** as a result of the addition of the highly electronegative fluoro group. It was also shown that even though the 4-amino proton plays a role in binding, no role was observed for it in fluorescent quenching. This was the first known case where it has been demonstrated that binding by the two binding sites cooperatively has been accompanied by fluorescent quenching [50].

Finally sensors **32**-**36** were also prepared by Gunnlaugsson and co-workers, this time with hydrazine monohydrate introduced to link the signalling unit and recognition group (4-aminobenzylamine in **27** and **28**, ethylenediamine in **29** and 2-aminobenzylamine in **30** and **31**) [52, 53]. Sensors **32** and **33** were reported in 2005 with colourimetric changes observed upon addition of acetate, dihydrogen phosphate and fluoride to a solution of the host in DMSO [53]. Higher concentrations of fluoride also resulted in deprotonation of the 4-amino NH proton (shown using ^{1}H NMR spectroscopy and changes in the UV-Visible spectrum) [53]. It was found that addition of a hydrogen-bonding solvent did not reverse the colour change observed and hence there was potential for **32** and **33** to operate as sensors in aqueous solutions (log *K* was determined for **32** in a 1:1 (v/v) EtOH-H_2O solution with log *K*=3.4 for acetate, 2.2 for dihydrogen phosphate and 1.0 for fluoride) [53]. Sensors **34**-**36** were reported in 2008 with colour changes occurring upon addition of dihydrogen phosphate, acetate and fluoride to solutions of the sensors in DMSO [52]. Unlike with **32** and **33** however these colour changes were able to be reversed upon addition of a hydrogen bonding solvent and hence were not suitable as sensors in aqueous solutions [52].

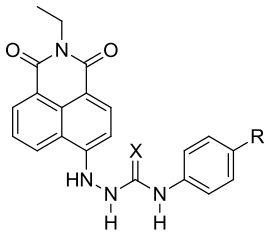

32 R=CH_3, X=S
33 R=CF_3, X=S
34 R=H, X=O
35 R=CH_3, X=O
36 R=CF_3, X=O

Many of the steps used in the synthesis of sensors **27**-**36**, will be used in the synthesis of the sensors in this research. Several other sensors **37**-**41**, involving the use of a 4-amino-1,8-naphthalimide signalling moiety in combination with a urea or thiourea recognition have also been proposed [54-56].

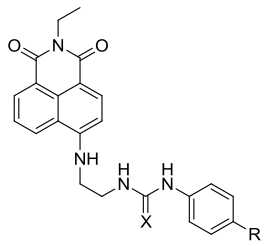

37 X=S, R=H, **38** X=S, R=CF_3
39 X=O, R=CF_3

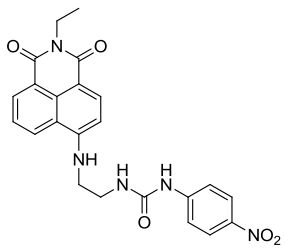

40

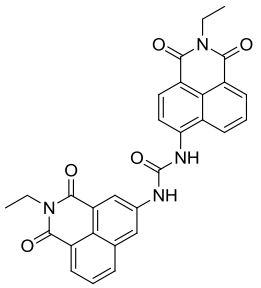

41

Sensors **37-39** were developed by Gunnlaugsson and Duke [54] with **37** and **38** showing excellent selectivity for the fluoride anion. Fluorescence emission was almost completely quenched upon addition of 80 equivalents of fluoride for **37** and **38**, whereas it was only quenched 20% upon addition of fluoride to **39**. This change in quenching behaviour is due to the change from a thiourea recognition group to a less acidic urea recognition group. Quenching of less than 20% was observed for interactions between acetate and dihydrogen phosphate and **37** and **38** with even smaller changes observed for bromide and chloride. The structurally similar compound **40** was synthesised by Bao and co-workers and evaluated for its interaction with anions (fluoride, acetate, chloride, bromide, iodide, hydrogen sulphate, perchlorate and nitrate) using UV-Vis and fluorescence spectrophotometries and ^{1}H NMR spectroscopy [55]. Sensor **40** was shown to be able selectively bind acetate and fluoride over the other anions with a colour change from greenish yellow to bright yellow and significant fluorescence quenching observed [55].

Esteban-Gomez and co-workers reported the synthesis of **41** with two naphthalimide signalling units joined by a urea recognition group [56]. Sensor **41** acted as a colourimetric sensor for the anions hydroxide, fluoride, acetate and dihydrogen phosphate when added to a solution of **41** in DMSO [56]. All four anions were found to be able to deprotonate one of the urea protons and produce a colour change from yellow to red [56]. The highly basic fluoride and hydroxide ions could then further deprotonate the second urea proton, with a colour change from red to blue [56]. In this sense the properties **41** displays are more acid-base chemistry rather than supramolecular [56].

Finally Veale and co-workers have synthesised sensor **42** which is structurally similar to **28** [57]. Instead of the chemistry to include the recognition group being undertaken at the 4-amino position of the naphthalimide ring structure, the spacer and recognition group are attached at the imide position [57]. As with **28**, no changes were observed in the absorption spectrum of **42** upon addition of acetate, dihydrogen phosphate or bromide (in DMSO), whereas a significant colour change was observed upon addition of fluoride [57]. Quenching of the fluorescence emission was once again observed upon addition of dihydrogen phosphate, acetate and fluoride with binding constants of log *K* = 4.2, 3.5 and 4.7 respectively at low concentrations when binding was 1:1 (similar to results observed for **28** with log *K*=4.0, 3.7 and 4.4 respectively)[57]. For **42** at higher concentrations, 1:2 binding was observed for acetate and fluoride with log *K* = 6.2 and 4.9 for the second interaction respectively [57]. The synthesis of **42** and its evaluation show that the sensing was bidirectional and quenching of the fluorescence emission could occur upon anion binding with the recognition group when attached at either the imide position or 4-amino position [57].

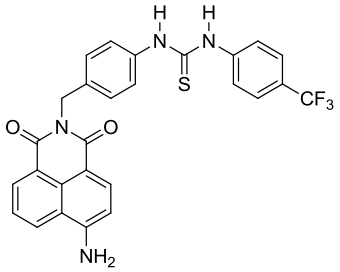

42

As can be seen above there are numerous examples where the 4-amino-1,8-naphthalimide fluorophore and a thiourea or urea recognition group have been used for the successful sensing of various anions. Many other examples as well as other sensors for anions based on the 4-amino-1,8-naphthalimide fluorophore without a urea or thiourea recognition group are reviewed extensively by Duke *et al* [34]. As well as use in anion sensing the 4-amino-1,8-naphthalimide fluorophore has also found extensive use in the area of cation sensing [58-67].

Although the focus of this literature review and research is on anion sensors which use a 4-amino-1,8-naphthalimide signalling subunit and a thiourea or urea recognition group it would be remiss to not mention that recently the 3-amino-1,8-naphthalimide signalling subunit has been combined with a urea recognition group for the sensing of

anions [68]. Duke and Gunnlaugsson reported the synthesis of **43** in 2011 (preliminary results were presented in the review of 1,8-naphthalimide based anion sensors [34]) with results showing that the addition of fluoride to **43** in DMSO caused significant changes in both the absorption and emission spectrum, likely due to deprotonation of the urea receptor group [68]. Finally in addition to use in sensing, molecules based on the 1,8-naphthalimide fluorophore (and sometimes including urea or thiourea groups) have been investigated for their anti-cancer properties. As this is well outside the scope of this research, readers are referred to [69] for a review of recent advances in this area.

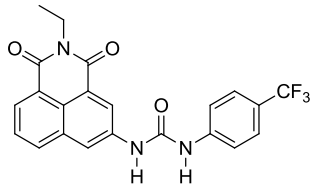

43

1.4 Immobilisation strategies

As detailed in Section 1.3.4, most literature reports on 4-amino-1,8-naphthalimide-based anion sensors only report solution-phase applications. Niu *et al.* [48] demonstrated that a carbon chain with a terminal double bond can be introduced at the imide site (Scheme 1) and the resulting sensor incorporated into a hydroxypropyl methacrylate polymer membrane. UV-irradiation was used to copolymerise the membrane onto a propyl methacrylate functionalised glass surface. Covalent immobilisation of the molecular sensor onto a glass substrate was found to prevent the fluorescent sensor leaching from the surface. The magnitude of fluorescence emission exhibited by the polymer membrane before addition of the analyte, the zwitterioinic molecule nitrofurantoin (interaction shown in Figure 14), was regenerated by simply passing Britton-Robinson buffer (A universal pH indicator consisting of a mixture of phosphoric acid, acetic acid and boric acid, with the pH adjusted through the addition of sodium hydroxide [48, 70]) through the flow cell device, cleaning the sensing medium between samples. When used in a flow cell device, the membrane was found to have a lifetime of at least two months, however no experimental data was provided to support this claim. Similarly, data relating to how many samples can be analysed before sensor degradation was not presented.

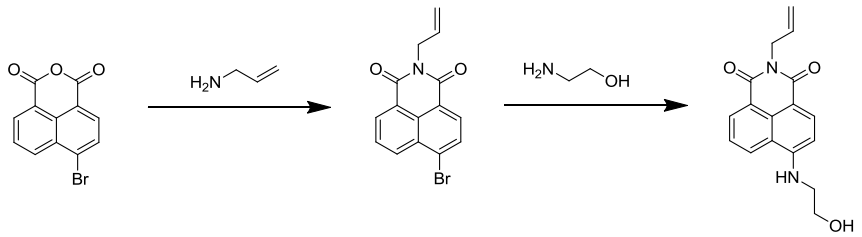

44 45 25

Scheme 1: Synthesis of *N*-Allyl-4-(N-2'-hydroxyethyl)amino-1,8-naphthalimide (25) by Niu and co-workers [48].

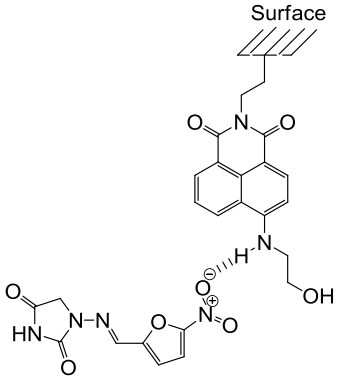

Figure 14: Nitrofurantoin interacting with surface immobilised *N*-Allyl-4-(N-2'-hydroxyethyl)amino-1,8-naphthalimide (25).

Immobilisation of the sensor onto a solid surface increases the ease of use of the sensor, as the sensor becomes more easily portable and can be taken to the field. Also by immobilising the sensor onto a solid surface we create meaningful opportunities for sensor regeneration. Whilst some solvents can be readily removed to yield the solid sensor in a solution-phase scenario, solvents such as DMSO (which was used to evaluate most of the sensors described above) are difficult to remove due to their high boiling points and low vapour pressure. Additionally, the anion can remain bound to the sensor molecule and a series of washings is often required to fully regenerate the sensor. Each step results in loss of product, further decreasing the recovery. These difficulties with regeneration of the sensor can be overcome by immobilising the sensor onto a solid support. Further to this the immobilisation is also beneficial as sensors on solid supports can be easily integrated into automated systems (and potentially regenerated using the automated system) [48, 71-75].

In the past the most common form of immobilisation with fluorescent sensors has been to include it in a polymer matrix and then deposit the polymer onto an optical fibre or other surface for use as a sensor [9]. Inclusion into a polymer however does have some issues, particularly with relation to the sensor existing homogeneously within the polymer and also the potential for the fluorescent probe to leach from the polymer [9]. Despite it being relatively straight forward to include a fluorescent sensor in a polymer matrix, both of these issues have prevented the common inclusion of polymer bound fluorescent sensors into commercial instruments [9].

Covalent immobilisation presents an alternative to just "including" a sensor in a polymer matrix, providing much greater stability and therefore increasing the life and reproducibility of the sensor [9]. Sensors have been covalently immobilised onto polymeric materials by either ensuring the polymer has functional groups which will react with the sensor molecule or by co-polymerising the sensor with a polymer [9]. One example of this highlighted in the literature is a fluorescent sensor of potassium ions, **46** synthesised by He *et al*. [59].

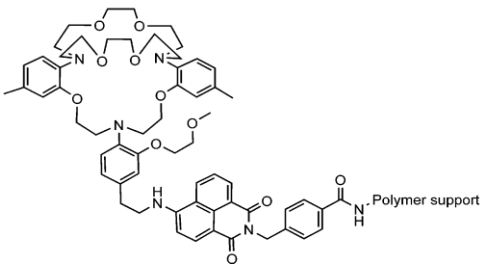

46

Sensor **46** is able to analyse for K^+ in blood using a cryptand binding site and a naphthalimide fluorophore, with the sensor covalently immobilised onto 3-amino-2-hydroxyl-propyl-cellulose [59]. This sensor has gone on to be commercially used by Roche [59]. Other examples of sensors covalently immobilised onto a polymer support can be found in [9].

Sol-gel processes have also been used to covalently immobilise fluorescent sensors to a surface with several examples in [9]. One such example is sensor **47** produced by Ayadim and co-workers [76] who took an aminopropyl silica gel and grafted anthracene onto it. Sensor **47** was observed to operate as a pH probe with the amine

group able to be protonated in the presence of acid resulting in an increase in fluorescence emission from the anthracene moiety [76].

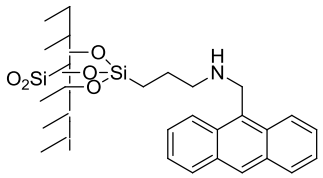

47

Meosporous silica is another commonly used substance for surface immobilisation with several examples reported in [9]. The work of Seo and co-workers [77] saw a 1,8-diaminonaphthalene reacted with 3-(triethoxysilyl)propyl isocyanate to form sensor **48** containing naphthalene as the fluorophore, urea as the receptor and a silanol group bonded to ethoxy groups. The ethoxy groups could then by hydrolysed and condensed onto a silica or mesoporous silica surface to form siloxane linkages between the sensor and surface [77]. The sensor bound on mesoporous silica was found to be responsive to addition of the fluoride anion with a decrease in fluorescence emission observed (little change was observed upon addition of chloride, bromide, iodide or hydrogen sulphate) [77]. It was found that the sensing medium produced when mesoporous silica was used rather than silica gel, resulted in an eight times increase in sensitivity of **48** towards fluoride [77].

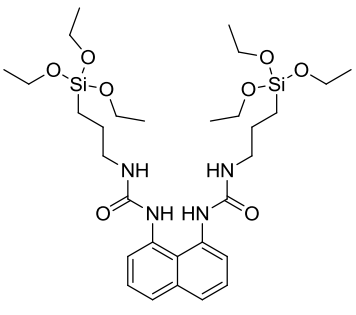

48

Another common method to covalently immobilise fluorescent sensors to a surface is to use a surface such as silicon oxide (glass, silicon, quartz) [9]. By confining the chemical sensing to a surface long term stability is obtained as the sensor cannot be easily removed from the surface, and also a faster response is obtained as all of the receptors on the surface are exposed to the surface-liquid interface [9]. Several examples are reviewed by Basabe-Desmonts *et al*. [9].

With a view to creating sensor which could be used in flow cell devices or in chromatography, the use of a silica surface was investigated. Silica is one of the most commonly used surfaces for sensor immobilisation. Examples already discussed above include mesoporous silica [77-79] and silica gel [77], whilst microscope slides [74], silicon wafers and silicon oxide [72] and fused silica [80, 81] have also been used. Silica is a mechanically stable surface with high thermal resistance [82]. It is resistant to organic solvents and thus can be easily washed using a vast range of organic solvents – ideal for regeneration [82]. In addition, silica can be reacted with a variety of silylation agents which allows the immobilisation of many different types of compounds[82]. Attachment is generally considered easier on a silica surface, than on organic polymeric supports due to simpler surface activation [82]. Silica also has a very high specific surface area and a constant composition, which enables easy analysis of results obtained using a sensor immobilised onto such a surface [82].

Silanisation is a commonly used technique for the direct immobilisation of organic molecules onto silica and is the preferred method used by manufacturers for the preparation of chemically bonded silica based stationary phases for HPLC [81]. In this process a trifunctional organosilane is reacted with surface silanols which crosslink to form the final bonded phase as shown in Scheme 2 [81].

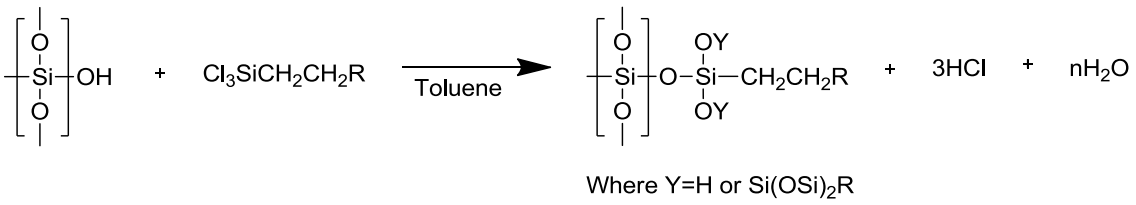

Scheme 2: General scheme for the organosilisation process. Where n=1-3 and Y=H or $Si(OSi)_2R$ depending on the extent that cross linking occurs [13].

Alternatively, a two-step process of silanisation to form a hydride terminated surface (depicted in Scheme 3) followed by hydrosilation (depicted in Scheme 4) can be used to immobilise compounds onto silica based stationary phases. These processes have been used previously in particular with capillaries for open tubular capillary electrochromatography [81].

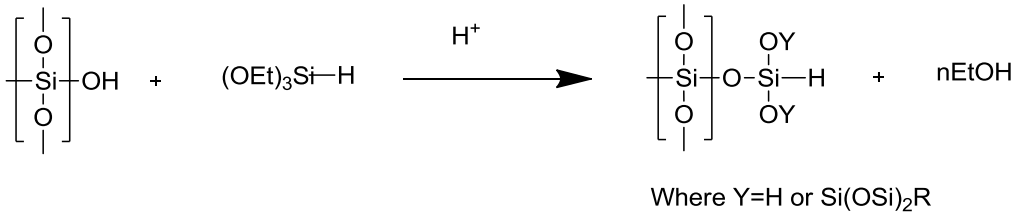

Scheme 3: General scheme for the silanisation process. Where n=1-3 and Y=H or $Si(OSi)_2R$ depending on the extent that cross linking occurs. The typical acid source used is hydrochloric acid.

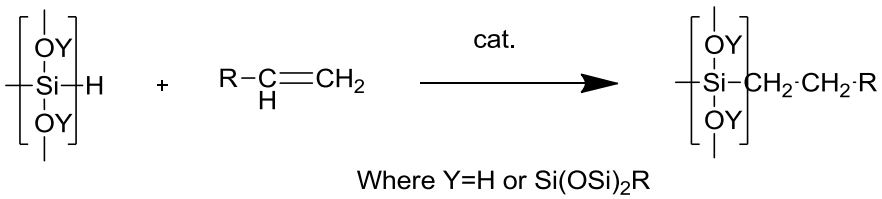

Scheme 4: General scheme for the hydrosilation process. Where Y=H or $Si(OSi)_2R$ depending on the extent that cross linking occurs. The catalysts commonly used include metal complexes such as hexachloroplatinic acid or free radical initiators such as tert-butyl peroxide.

1.5 Proposal

This project aims to develop a series of fluorescent anion sensors based on the 4-amino-1,8-napthalamide moiety, with a view to immobilisation of the sensors on to silica. A proven, high yielding synthetic route to produce naphthalimide based anion sensors for fluoride, dihydrogen phosphate and acetate, established by Gunnlaugsson and co-workers (reviewed in Section 1.3.4.1), forms the basis of the initial synthetic chemistry work in this project.

This project can be further broken down into a series of secondary aims in order to allow accomplishment of the overall aim. The specific stages are:

i. *Synthesis and characterisation of anion sensors*

ii. *Evaluation of anion sensors*

iii. *Immobilisation of sensor on to a surface*

The synthesis of the anion sensors **1**-**5** will be attempted according to the pathway outlined in Scheme 5.

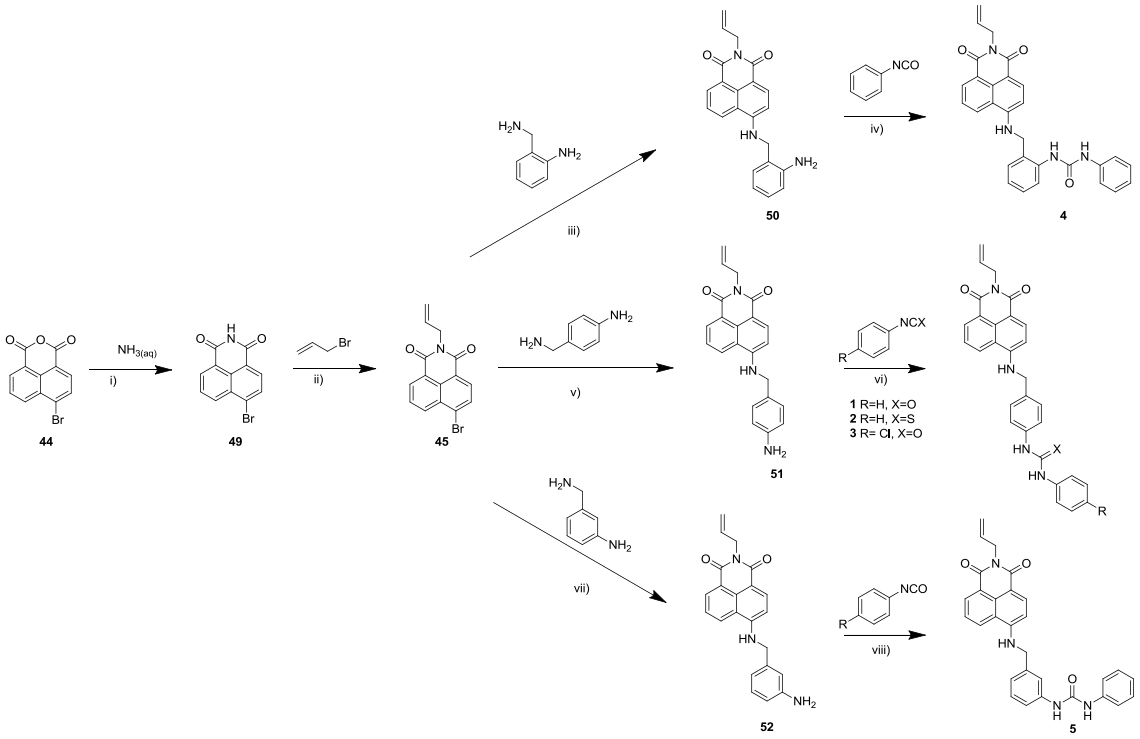

Scheme 5: Proposed synthetic pathway for the synthesis of sensors based on the 4-bromo-1,8-naphthalimide fluorophore.

1.5.1 Step (i) Synthesis and Characterisation of Anion Sensors

The synthesis of sensors based on the 4-amino-1,8-naphthalimide can be broken down into three steps. In the first step, 4-bromo-1,8-naphthalic anhydride (**44**), will be alkylated with allyl bromide, providing the route for future immobilisation. In the second step, a spacer molecule will be added, so that in the final step, the recognition unit can be linked covalently to the signalling unit.

Forming N-allyl-4-bromo-1,8-napthahlimide (45)

Step (i) will be to convert the chosen starting material 4-bromo-1,8-naphthalic anhydride (**44**) to 4-bromo-1,8-naphthalimide (**49**)**.** There are various literature methods [83-85] which have been utilised to accomplish the conversion of the anhydride to the imide. Plakidin and Vostrava reacted **44** with acetamide to form the imide with the reaction undertaken in methanol at 130°C for a period of 18 hours (yield of 87%)[83]. Karishin and Kustol reacted **44** with 16% aqueous ammonia solution for a period of thirty minutes between 60-90^{o}C to obtain the imide in 98% yield [84]. Whilst Peng *et al*, react **44** with formamide and then irradiate the mixture with 400 W

microwaves for two minutes, obtaining the product after recrystallisation in 87% yield [85].

Following on from the synthesis of **49**, *N*-alkylation of the imide to form **45** will be performed to introduce an allyl group. Introduction of an allyl group will allow subsequent immobilisation of the molecule on to a silica surface *via* hydrosilation chemistry as described in Section 1.4. A literature review found several methods for the *N*-alkylation of imides [86-92].

Anwar and co-workers used a two-step synthesis reacting succinimide with propargyl bromide to form *N*-propargyl succinimide [86]. Succinimide was reacted with sodium hydride to remove the imide proton prior to addition of propargyl bromide, producing the product in 87 % yield after work-up and column chromatography [86]. Similarly, McElhinney and Marsden added 5-bromopent-1-ene to succinimide, forming the product in 98% yield [89]. Alkylation reactions have also been undertaken using anhydrous potassium carbonate as the base (instead of sodium hydride) [87, 92]. Khan, Marson and Porter reacted succinimide with methyl iodide and bromobenzene under reflux for four hours to introduce methyl and benzyl groups at the imide position in yields greater than 90% [92]. They also reported the reaction of succinimide with propargyl bromide [87]. Although none of the above reactions used allyl bromide, it was hypothesised that similar conditions would be able to yield the required product *N*-allyl-4-bromo-1,8-naphthalimide (**45**).

Introducing the 4-amino NH group and the spacer

Upon successful alkylation of the imide to produce **45**, the next step is to introduce the 4-amino moiety and spacer in molecules **50**-**52** *via* a nucleophilic aromatic substitution reaction. Reactions for similar molecules to **45** with 4-aminobenzylamine and 2-aminobenzylamine have been previously reported [50, 51].

The initial approach towards the synthesis of *N*-allyl-4-(2-aminobenzylamine)-1,8-naphthalimide (**50**) will be based on a method to produce a similar molecule (the same molecule with an ethyl group in place of the allyl group) published by Pfeffer and co-workers [50]. The aminobenzylamine was placed into a sealed tube with *N*-ethyl-4-

bromo-naphthalimide at 130^{o}C for 12 hours, achieving the desired product in 86% yield.

Approaches to produce *N*-allyl-4-(4-aminobenzylamine)-1,8-naphthalimide (**51**) will be based on previous work by Gunnlaugsson and co-workers [51] who produced *N*-ethyl-4-(4-aminobenzylamine)-1,8-naphthalimide from *N*-ethyl-4-bromo-1,8-naphthalimide (the only difference between this and **45** being an ethyl group at the imide position as opposed to an allyl group). This reaction involved heating the reaction mixture in a sealed tube overnight [51]. *N*-ethyl-4-(4-aminobenzylamine)-1,8-naphthalimide was also synthesised by Parkesh, Lee and also Gunnlaugsson [66] in a much shorter time (thirty minutes) by heating *N*-ethyl-4-bromo-1,8-naphthalimide to near its melting temperature and stirring for 10 minutes under an argon atmosphere before addition of 4-aminobenzylamine.

Finally the synthesis of *N*-allyl-4-(3-aminobenzylamine)-1,8-naphthalimide (**52**) will be achieved based on the methods described above for **50** and **51**. To our knowledge no research has been published where 3-aminobenzylamine has been reacted with the 4-amino-1,8-naphthalimide fluorophore.

Introducing the recognition group

Finally, the recognition group will be added to the aminonaphthalimides **50**-**52** to form sensors **1**-**5**, based on the work described in Section 1.3.4.1. In many of these references an isocyanate or isothiocyanate is reacted with an amine group to create the urea or thiourea recognition group [49-53].

Initial approaches selected to enable the synthesis of **1**-**3** will focus on previous work by Gunnlaugsson and co-workers [51]. In Gunnlaugsson's work, *N*-ethyl-(4-(4-aminobenzylamine)-1,8-naphthalimide (similar to **51**) was reacted with either phenyl isothiocyanate or tetrafluoromethyl phenyl isothiocyanate in dry chloroform stirring overnight. The first approach to synthesise **4** will focus on the work of Pfeffer and co-workers who took *N*-ethyl-(4-(2-aminobenzylamine)-1,8-naphthalimide and reacted with phenyl isothiocyanate or 4-fluoro phenyl isothiocyanate to form the requisite

product by stirring in DMF overnight [50]. The synthesis of **5** will be based on methods used to synthesise **1**-**4** and also the work of Ali and co-workers [52] where acetonitrile was used as the solvent for a reaction between an amine and an isocyanate.

All of the above reactions outlined involve the use of conventional heating techniques. In addition to these methods, microwave irradiation will be trialled for the synthesis of **1**-**5**. It has been shown that many synthetic reactions can be undertaken using microwave assisted procedures, often within significantly shorter timeframes and with increased yield [93, 94].

1.5.2 Step (ii) Evaluation of synthesised sensors

Evaluation of the newly designed chemical sensors will be conducted using fluorescence spectrophotometry and ^{1}H NMR spectroscopy. These evaluation studies will be undertaken in solution with the sensors evaluated for their response to various anions as their tetrabutylammonium salts.

The use of fluorescence spectrophotometry will enable the magnitude of the optical response of the sensors to be determined upon their interaction with one of the target anions. Initially spectral data will be captured in the absence of anions, followed by binding studies where known amounts of anion will be added to ascertain the degree of enhancement of quenching that is seen when the sensor molecule detects the anion.

Proton NMR spectroscopy will also be used to undertake binding studies. The use of the urea recognition group enables the use of NMR spectroscopy to monitor any changes upon interaction with anions. By addition of known amounts of anion to a solution of the sensor it is possible to obtain titration curves which can then be used to determine binding strength.

1.5.3 Step (iii) Immobilisation of sensor on to a silica surface

The initial surface targeted for surface immobilisation will be silica gel, which also has the advantage that it can be packed into columns or capillaries for use with other devices. A terminal double bond has been incorporated into the sensor design to

enable immobilisation onto silica *via* hydrosiliation chemistry as described in Section 1.4.

To produce a silica hydride surface suitable for hydrosilation chemistry, silica gel will be modified using a method adapted from that of Gubbuk and co-workers who introduced chloro groups onto the silica surface [95]. Activated silica was suspended in refluxing toluene to which 3-chloropropyltrimethoxysilane (CPTS) was added, producing the chloro functionalised surface after three days. In this research, the method will be repeated with triethoxysilane in place of CPTS.

The sensor will be reacted with hydride modified silica surface with thought to the methods of Gubbuk *et al.* [95] and Pesek and Matyska [96]. Hydride modified silica will be added to the sensor (1:1 ratio), suspended in anhydrous toluene and refluxed for three days. Approximately twelve drops of the 10 mM Spier's Catalyst solution will be added to the refluxing mixture.

1.6 Conclusion

An overview of the development of anion supramolecular chemistry has been presented, along with discussion of the different signaling units and recognition groups required for fluorescent anion sensors. A number of different immobilisation strategies were also briefly outlined. A number of target molecules and how to synthesise them were defined along with details with regards to their evaluation and how to immobilise them onto silica. In Chapter 2, experimental details for the synthetic procedures undertaken will be detailed, with a description of the synthesis by conventional heating in Chapter 3 and microwave irradiation in Chapter 4. The sensors will be evaluated for their response to various anions by ^{1}H NMR spectroscopy and fluorescence spectrophotometry in Chapter 5. The immobilisation of the synthesised sensors will be detailed in Chapter 6.

Chapter 2

EXPERIMENTAL

2.1 General Laboratory Exercises

All reactions undertaken using conventional heating methods were carried out in flame dried glassware under an atmosphere of dry nitrogen. Reactions undertaken using microwave irradiation were undertaken in a glass walled microwave tube (10 mL) sealed with a septa. Unless otherwise specified, all chemicals were used as received from the supplier with most chemicals obtained from Sigma Aldrich (A detailed list of all chemicals used is provided in Appendix A). Acetone (GR for analysis), acetonitrile (liquid chromatography grade), chloroform (GR for analysis) and methanol (GR for analysis) were obtained from Merck (Damstadt, Germany). Ethanol (Absolute, AR Grade) was obtained from Merck Pty. Ltd. (Victoria, Australia). Triethoxysilane was obtained from Advanced Molecular Technologies, Pty. Ltd (Clayton, Victoria, Australia). Phenyl isothiocyanate was obtained from both Koch-Light Laboratories (Colnbrook-Bicks, England) (puriss) and Acros Organics (Belgium) (98%). Hexane, ethyl acetate, ethanol were generally purchased in bulk and distilled before use. THF was distilled from sodium benzopheneone ketyl immediately before use. Anhydrous acetonitrile, anhydrous ethanol and anhydrous chloroform were purified according to established literature methods [97]. In some cases (specified in text) phenyl isocyanate and phenyl isothiocyanate were purified using Kugelrohr distillation before use.

Solid reagents used in the synthesis and immobilisation experiments (Chapters 3,4 and 6) were weighed out on a K0040 A&D Company Limited (Japan) balance. Solutions for experiments in Chapter 5 were made using “A” grade volumetric glassware and using Gilson Pipetman micropipettes (2 - 20 µl, 20 - 200 µl, 100 - 1000 µl, 1 – 5 mL, 1 – 10 mL). Solid reagents used in Job plot and titration experiments were weighed out on a Mettler Toledo New Classic MS Balance, Model No. MS204S/01.

Chromatographic columns were run using one of two methods. Davisil silica gel (LC60Å, 40-63 µm) was used with a mobile phase mixture of 50:50 hexane:ethyl acetate, for chromatographic separations involved in the synthesis of *N*-allyl-4-bromo-1,8-naphthalimide. Chromatographic separations of reactions with isocyanates/isothiocyanates, involved the use of aluminium oxide (activated, neutral, activity degree 1, Scharlu Chemie SA, Spain) with a mobile phase of 100% chloroform.

Thin layer chromatography (TLC) was performed on pre-coated sheets of Merck silica gel 60 or pre-coated sheets of Merck aluminium oxide 60 and visualised under UV light (254 nm).

Microwave reactions were conducted using a CEM Discover-S microwave system (CEM Corporation, North Carolina, USA) controlled by Synergy Software V1.32. All experiments were run utilising the supplied "conventional method" where only the temperature and time selections were able to be modified. In this mode, the system runs the sample using the conditions that are the most direct to energize the sample. As conditions were different for each sample, these are detailed for each molecule synthesised in Section 2.5. All samples were run in 10 mL Pyrex glass vials sealed with septa. Unless specified samples were simply placed in the tube and not stirred during the irradiation.

2.2 Characterisation of synthesised compounds

2.2.1 Nuclear Magnetic Resonance Spectroscopy

NMR spectroscopy samples were dissolved in DMSO-d_6 (D99.9%) purchased from Cambridge Isotope Laboratories Inc (MA,USA). Spectra were recorded on a Bruker Avance III 400 spectrometer at 400 MHz (^{1}H) and 100 MHz (^{13}C) and a Bruker Avance III 600 spectrometer at 600 MHz (^{1}H) and 150 MHz (^{13}C). Spectra on the 400 MHz instrument were recorded at 26^{o}C, whilst those on the 600 MHz instrument were recorded at 20^{o}C. Chemical shifts (δ) are reported in parts per million (ppm) and are referenced to the central resonance of the residual DMSO-d_6 signal at 2.50 ppm for ^{1}H NMR spectroscopy and 39.52 ppm for ^{13}C. Spin multiplicities are indicated by: s, singlet; bs, broad singlet; d, doublet; t, triplet; q, quartet; quin, quintet; m, multiplet; dd, doublet of doublets; dt, doublet of triplets and dq, doublet of quartets. Peaks were assigned with the aid of homonuclear (^{1}H-^{1}H) correlation spectroscopy (COSY) and heteronuclear (^{1}H-^{13}C) correlation spectroscopy (HMQC and HMBC) when required. As the ^{1}H and ^{13}C NMR spectroscopy data is the same for compounds produced by both conventional heating and microwave irradiation methods, only one lot of data is reported in this thesis.

2.2.2 Mass Spectrometry/Accurate Mass Analysis

Electrospray mass spectral data was obtained using a Micromass Quattro Micro API (Waters, Manchester, UK), High Performance Triple Quadrupole Mass Spectrometer fitted with an Electrospray Ionisation (ESI) probe. Samples were prepared as 1mg/mL samples in DMF and then diluted to 10 μg/mL in acetonitrile.

Accurate mass analysis was performed using a Waters Synapt HDMS, with positive ion with lockspray electrospray ionisation. Spectral data was acquired in the range m/z 100 to 1000. Stock solutions of samples were prepared at a concentration of 1 mg/mL in DMF, with working solutions prepared by dissolution in 0.5 mM sodium formate solution. Raffinose was used as the lock mass signal, m/z 503.1612 in negative ion mode and m/z 527.1588 for the sodium adduct in positive ion mode.

2.2.3 Other Characterisation

ATR-FTIR spectra were recorded on a PerkinElmer Spectrum 400 equipped with a zinc selenide (ZnSe) ATR crystal. The samples analysed were placed directly onto the crystal and appropriate force (typically around 130 N) was applied to obtain the spectrum. Experiments were performed with a resolution of 4.00 cm^{-1} over a range of 4000-650 cm^{-1} with 4 scans per run. As the ATR-FTIR spectroscopy data is the same for compounds produced by both conventional heating and microwave irradiation methods, only one lot of data is reported in this thesis.

Melting points were obtained on a Sanyo Gallenkamp Variable Heater (Cat No. MPD350.BM3.5).

2.3 Characterisation of Immobilised Compounds

ATR-FTIR characterisation of immobilised compounds was undertaken using the method outlined in Section 2.2.3.

$^{13}C(^{1}H)$ cross-polarisation coupled to magic angle spinning (CP-MAS) and $^{29}Si(^{1}H)$ cross-polarisation coupled to magic angle spinning (CP-MAS) spectroscopy experiments were performed on a Bruker 400 MHz Avance III UltraSheild NMR Spectrometer using

Bruker MAS II with rotors (ZrO_2; diameter: 4mm (Wilmad Labglass)), which contained approximately 200 mg of the desired sample.

The experimental details for the ^{13}C-(^{1}H)CP-MAS NMR spectroscopy experiments were as follows: ^{13}C, 100.6 MHz; spinning rate 5-14 kHz (varied between samples); variable amplitude (ramp) contact time 2 ms; 90° ^{1}H transmitter pulse length, 2.9 µs; acquisition time 34 ms; repetition time, 4 sec; lb =50, with tppm15 decoupling during acquisition. The number of scans was varied for each sample, with each sample run until an acceptable signal to noise ratio was obtained.

The experimental details for the ^{29}Si –(^{1}H)CP-MAS NMR spectroscopy experiments were as follows: ^{29}Si, 79.5 MHz; spinning rate 5 kHz; variable amplitude (ramp) contact time 2 ms; 90° ^{1}H transmitter pulse length, 2.6 µs; acquisition time 20 ms; repetition time, 3 sec; lb =50, with tppm15 decoupling during acquisition. The number of scans was varied for each sample, with each run until an acceptable signal to noise ratio was obtained.

2.4 Evaluation of Synthesised Sensors

2.4.1 UV-Visible Spectrophotometry

UV-Visible absorption data was recorded on a Varian Cary 50 Scan UV-Visible Spectrophotometer (Varian Inc, Melbourne, Australia) using a quartz cell (path length 1 cm). Baseline correction was activated and the spectrophotometer was operated in dual beam mode. Data was collected over the range 600 nm – 250 nm at a scan rate of 600 nm min^{-1}, with a data interval of 1.00 nm and scan time of 0.1000 sec. Both host and guest samples were prepared in “A” grade volumetric glassware in DMSO (Sigma Aldrich, 99.9+%, anhydrous). Host and guest solutions were made up initially as a concentration of 1 mg/mL (ie 10 mg in 10 mL) and diluted to 1.0 x 10^{-4} M). The unadulterated solvent was used to baseline the instrument. Solutions for Job plot experiments were made up as per Table 4. The absorbance of each solution at 265 nm was used to create the Job plot which was graphed as the difference in absorbance (predicted versus observed) versus the mole fraction of guest ([G]/[H]+[G]). The

predicted absorbance was calculated from the concentration of the host and guest and the extinction coefficient for each host and guest.

Table 4: Details of solutions made for Job plot experiments.

	Volume of solution added (mLs)								
Host	8	7	6	5	4	3	2	1	0
Guest	0	1	2	3	4	5	6	7	8
DMSO	2	2	2	2	2	2	2	2	2

2.4.2 ^{1}H NMR SpectroscopyTitrations

All ^{1}H NMR spectroscopy titration experiments were performed on a Bruker Avance III 600 spectrometer at 600 MHz. Samples were prepared in DMSO-d_6 (purchased from Cambridge Isotope Laboratories Inc (MA,USA)) with 0.5% water added (herein referred to as hydrated DMSO-d_6). Water was added to DMSO-d_6 as per Gale [98, 99] in order to account for water absorbed from the atmosphere by the highly hygroscopic DMSO. The idea being that the water from the atmosphere will be small in comparison and thus reduce errors between titrations. All spectra were recorded at 20^{o}C. The host solution was initially prepared as 0.01 M in hydrated DMSO-d_6. This host solution was then split into two lots (2 mL each), 2 mL for the titration experiment and 2 mL to make up the guest solution for the titration. An appropriate mass of guest was added to the 2 mL of host, in such a way that when 10 μL of that solution was added to the titration solution, approximately 0.1 equivalents of guest would be added. The preparation of the guest solution in host ensured that the host concentration was kept constant throughout the titration. Over the course of the titration up to ten equivalents of guest were added (representative data in Table 5). Binding constants were calculated using equation 7 (Chapter 5 and Appendix B) and non-linear regression analysis in Microsoft Excel. The chemical shift of each of the two urea protons was followed for the course of the titration, with the chemical shift values obtained for each being used in equation 7. The uncertainty in the binding constant was calculated using a solver stat macro from Chapter 12 of Excel for Chemists [100].

2.4.3 Fluorescence Spectrophotometry Titrations

Fluorescence emission data was recorded on a Varian Cary Eclipse Fluorescence Spectrophotometer (Varian Inc, Melbourne, Australia) using a glass cell (path length 1

Table 5: Addition of guest to host, amount of equivalents added per addition of guest for ^{1}H NMR spectroscopy experiments.

Titration #	Volume of Guest (μL)	Moles of Guest Added	Volume of Host (μL)	Moles of Host	Concentration Guest (M)	Concentration Host (M)	Equivalents Added
1	0	0.00	2000	2.00×10^{-5}	0.00	0.01	0.00
2	10	2.00×10^{-6}	2010	2.01×10^{-5}	9.95×10^{-4}	0.01	0.10
3	30	6.00×10^{-6}	2030	2.03×10^{-5}	2.96×10^{-3}	0.01	0.30
4	50	1.00×10^{-5}	2050	2.05×10^{-5}	4.88×10^{-3}	0.01	0.49
5	70	1.40×10^{-5}	2070	2.07×10^{-5}	6.76×10^{-3}	0.01	0.68
6	80	1.60×10^{-5}	2080	2.08×10^{-5}	7.69×10^{-3}	0.01	0.77
7	90	1.80×10^{-5}	2090	2.09×10^{-5}	8.61×10^{-3}	0.01	0.86
8	100	2.00×10^{-5}	2100	2.10×10^{-5}	9.52×10^{-3}	0.01	0.95
9	110	2.20×10^{-5}	2110	2.11×10^{-5}	1.04×10^{-2}	0.01	1.04
10	120	2.40×10^{-5}	2120	2.12×10^{-5}	1.13×10^{-2}	0.01	1.13
11	150	3.00×10^{-5}	2150	2.15×10^{-5}	1.40×10^{-2}	0.01	1.40
12	200	4.00×10^{-5}	2200	2.20×10^{-5}	1.82×10^{-2}	0.01	1.82
13	300	6.00×10^{-5}	2300	2.30×10^{-5}	2.61×10^{-2}	0.01	2.61
14	400	8.00×10^{-5}	2400	2.40×10^{-5}	3.33×10^{-2}	0.01	3.33
15	500	1.00×10^{-4}	2500	2.50×10^{-5}	4.00×10^{-2}	0.01	4.00
16	700	1.40×10^{-4}	2700	2.70×10^{-5}	5.19×10^{-2}	0.01	5.19
17	1000	2.00×10^{-4}	3000	3.00×10^{-5}	6.67×10^{-2}	0.01	6.67
18	1500	3.00×10^{-4}	3500	3.50×10^{-5}	8.57×10^{-2}	0.01	8.57
19	2000	4.00×10^{-4}	4000	4.00×10^{-5}	1.00×10^{-1}	0.01	10.00

cm). The excitation wavelength was optimised for each sensor depending on its optical properties using the prescan option on the Varian software and are summarised in Table 6. Emission spectra were recorded from 510 nm – 700 nm with the emission slit = 5mm and excitation slit = 5 mm. The host solution was prepared in 10 mL "A" grade volumetric glassware in DMSO (Sigma Aldrich, 99.9+%, anhydrous) with 0.5% water added (herein called hydrated DMSO). The addition of 0.5% water was to enable results to be compared with the ^{1}H NMR spectroscopy titration experiments. For all sensors, 10.0 mg of the sensor was dissolved in 10 mL of hydrated DMSO. This solution was split into two 5 mL aliquots, with an amount of guest added to one aliquot such that when 10.0 μL of the guest solution was added to the host, approximately 0.1 equivalents of guest were added. Over the course of a titration up to twenty equivalents of the guest solution in host were added to the other 5 mL aliquot of host (representative data is included in Table 7). At the end of the titration, methanol was added to the complexed solution in amounts from 10 μL to 15000 μL. Fluorescence emission quenching was calculated for each host-guest complex using equation 7 (Chapter 5). The maximum intensity of the emission spectrum obtained upon addition of each aliquot of guest added to the host-guest complex was used. Binding constants were calculated using equation 7 (Chapter 5) and non-linear regression analysis in Microsoft Excel. Again the maximum intensity attained for each experiment was used to calculate the change in fluorescence emission over the course of the titration. The uncertainty in the binding constant was calculated using a solver stat macro from Chapter 12 of Excel for Chemists [100]. Sensor 2 was unable to be reproduced after its initial synthesis and hence was not submitted to analysis by fluorescence spectrophotometry.

Table 6: Wavelengths utilised for fluorescence spectrophotometry titration experiments.

Sensor	λ_{ex} (nm)	λ_{em} (nm)
1	503.93	531.94
3	504.02	530.00
4	503.93	528.05
5	501.94	527.01
6	504.02	531.02
7	500.00	528.95
8	501.96	528.41

Table 7: Addition of guest to host, amount of equivalents added per addition of guest for fluorescence spectrophotometry experiments.

Titration #	Volume of Guest (μL)	Moles of Guest Added	Volume of Host (μL)	Moles of Host	Concentration of Guest (M)	Concentration of Host (M)	Equivalents Added
1	0	0.00	5000	1.05×10^{-5}	0.00	2.10×10^{-3}	0.00
2	10	1.05×10^{-6}	5010	1.05×10^{-5}	2.09×10^{-4}	2.10×10^{-3}	0.10
3	30	3.15×10^{-6}	5030	1.06×10^{-5}	6.26×10^{-4}	2.10×10^{-3}	0.30
4	50	5.25×10^{-6}	5050	1.06×10^{-5}	1.04×10^{-3}	2.10×10^{-3}	0.50
5	70	7.34×10^{-6}	5070	1.06×10^{-5}	1.45×10^{-3}	2.10×10^{-3}	0.69
6	80	8.39×10^{-6}	5080	1.07×10^{-5}	1.65×10^{-3}	2.10×10^{-3}	0.79
7	90	9.44×10^{-6}	5090	1.07×10^{-5}	1.86×10^{-3}	2.10×10^{-3}	0.88
8	100	1.05×10^{-5}	5100	1.07×10^{-5}	2.06×10^{-3}	2.10×10^{-3}	0.98
9	110	1.15×10^{-5}	5110	1.07×10^{-5}	2.26×10^{-3}	2.10×10^{-3}	1.08
10	120	1.26×10^{-5}	5120	1.07×10^{-5}	2.46×10^{-3}	2.10×10^{-3}	1.17
11	130	1.36×10^{-5}	5130	1.08×10^{-5}	2.66×10^{-3}	2.10×10^{-3}	1.27
12	150	1.57×10^{-5}	5150	1.08×10^{-5}	3.06×10^{-3}	2.10×10^{-3}	1.46
13	200	2.10×10^{-5}	5200	1.09×10^{-5}	4.04×10^{-3}	2.10×10^{-3}	1.92
14	300	3.15×10^{-5}	5300	1.11×10^{-5}	5.94×10^{-3}	2.10×10^{-3}	2.83
15	400	4.20×10^{-5}	5400	1.13×10^{-5}	7.77×10^{-3}	2.10×10^{-3}	3.70
16	500	5.25×10^{-5}	5500	1.15×10^{-5}	9.54×10^{-3}	2.10×10^{-3}	4.55
17	700	7.34×10^{-5}	5700	1.20×10^{-5}	1.29×10^{-2}	2.10×10^{-3}	6.14
18	1000	1.05×10^{-4}	6000	1.26×10^{-5}	1.75×10^{-2}	2.10×10^{-3}	8.33
19	1500	1.57×10^{-4}	6500	1.36×10^{-5}	2.42×10^{-2}	2.10×10^{-3}	11.54
20	2000	2.10×10^{-4}	7000	1.47×10^{-5}	3.00×10^{-2}	2.10×10^{-3}	14.29
21	2750	2.89×10^{-4}	7750	1.63×10^{-5}	3.72×10^{-2}	2.10×10^{-3}	17.74
22	3500	3.67×10^{-4}	8500	1.78×10^{-5}	4.32×10^{-2}	2.10×10^{-3}	20.59

2.5 Synthetic Procedures

4-Bromo-1,8-naphthalimide (49)

Synthesis of **49** was undertaken according to the previous method by Karishin and Kustol [84].

Synthesis by Conventional Heating

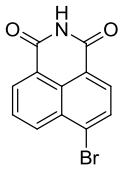

4-Bromo-1,8-naphthalic anhydride (**44**) (0.250g, 9.02×10^{-4} mol), was stirred in 15.5% v/v aqueous ammonia solution (7.0 mL) at 75°C. After 30 minutes the reaction was removed from the heat and water added (3.0 mL) to afford a precipitate. The product was collected using a Hirsch funnel yielding 0.203g (81%) of a pale beige powder 4-bromo-1,8-naphthalimide (**49**)**.**

Synthesis by Microwave Irradiation

Microwave irradiation techniques were not investigated for this synthesis.

Characterisation

***^{1}H NMR* (400 MHz, DMSO-d_6):** δ 11.753 (bs, 1H), 8.501-8.472 (m, 2H), 8.230 (d, *J*=7.8 Hz, 1H), 8.153 (d, *J*=7.8 Hz, 1H), 7.969-7.929 (m, 1H).

***^{13}C NMR:* (100 MHz, DMSO-d_6):** δ 163.58, 132.57, 131.24, 130.81, 130.19, 130.04, 129.55, 129.11, 128.66, 123.22, 122.45.

FTIR(ATR) (υ max solid/cm^{-1}): 3161, 3047, 2851, 1670, 1586, 1500, 1457, 1422, 1400, 1367, 1343, 1330, 1266, 1211, 1187, 1110, 1084, 1040, 958, 855, 838, 779, 749.

Melting Point: 306.8°C-308.6°C.

***N*-Allyl-4-bromo-1,8-naphthalimide (45)**

Synthesis of **45** was undertaken according to the previous method by Niu *et al*.[48].

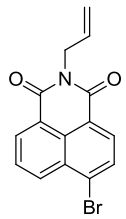

Synthesis by Conventional Heating Methods

4-Bromo-1,8-naphthalic anhydride (2.031g, 0.0073 mol) (**44**), was stirred in absolute ethanol (45 mL). Allylamine (591 μL, 0.0079 mol) was immediately added to the stirred solution and refluxed. After two hours, the reaction was removed from the heat, and the product, **45**, precipitated upon standing. The product was collected using a Hirsch funnel yielding 2.18g (94%) of **45** as a pale white powder.

Synthesis by Microwave Irradiation

4-Bromo-1,8-naphthalic anhydride (0.051g, 1.84×10^{-4} mol) (**44**), absolute ethanol (1.5 mL) and allylamine (30.4 μL, 4.05×10^{-4} mol) were added to a glass walled tube (10 mL), stirred and irradiated for two minutes at 70°C. After cooling to 50°C, the contents of the tube were stirred and irradiated for a further two minutes. This process was repeated a further two times, resulting in a total irradiation time of eight minutes. The product precipitated out upon cooling. The product was collected using a Hirsch funnel yielding 0.051g (87%) of **45** as a pale white powder.

Characterisation

^{1}H NMR (600 MHz, DMSO-d_6): δ 8.607-8.579 (m, 2H) 8.357 (d, *J*=7.8 Hz, 1H), 8.246 (d, *J*=7.8 Hz, 1H), 8.038-8.012 (m, 1H), 5.968-5.904 (m, 1H), 5.166 (dq, *J*=1.2 Hz, 15.8 Hz, 1H), 5.123 (dq, *J*=1.2 Hz, 10.4 Hz, 1H) 4.654 (dt, *J*=1.2 Hz, 5.2 Hz, 2H).

^{13}C NMR (100 MHz, DMSO-d_6): δ 162.54, 162.49, 132.68, 132.57, 131.63, 131.35, 131.01, 129.79, 129.22, 128.79, 128.30, 122.62, 121.84, 116.50, 41.86.

FTIR(ATR) (υ max solid/cm^{-1}): 3071, 2029, 1887, 1698, 1659, 1588, 1571, 1503, 1459, 1425, 1403, 1370, 1345, 1323, 1233, 1193, 1103, 1084, 1047, 1019, 1002, 950, 931, 899, 845, 796, 777, 751, 734, 716, 692.

Melting Point: 143.2°C-145.1°C (Lit. 142 °C -144 °C [48]).

***N*-Allyl-4-(4-aminobenzylamine)-1,8-naphthalimide (51)**

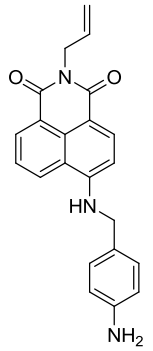

Synthesis by Conventional Heating Methods

N-Allyl-4-bromo-1,8-naphthalimide (**45,** 1.020 g, 3.23×10^{-3} mol), was stirred at 110°C. After ten minutes 4-aminobenzylamine (2.1 mL, 1.85×10^{-2} mol) was added and stirring continued at 110°C. After one hour, the reaction was removed from the heat and water was added to afford the product. The product was collected using a Hirsch Funnel and recrystallised from ethanol yielding 0.839 g (73 %) of **51** as a bright yellow powder.

Synthesis by Microwave Irradiation

N-Allyl-4-bromo-1,8-naphthalimide (**45**, 0.050g, 1.58×10^{-4} mol) and 4-aminobenzylamine (0.179 mL, 0.00158 mol) were added to a glass vial, capped and irradiated at 105°C. After four minutes, the reaction was cooled to 50°C, removed from the microwave reactor and water was added to afford the product. The product was collected using a Hirsch Funnel and recrystallised from ethanol yielding 0.038g (68%) of **51** as a bright yellow powder.

Characterisation

***^{1}H NMR* (600 MHz, DMSO-d_6)**: δ 8.760 (d, *J*=8.4 Hz, 1H), 8.437 (d, *J*=7.2 Hz, 1H), 8.382 (t, *J*=6.0 Hz, 1H), 8.180 (d, *J*=8.4 Hz, 1H), 7.717-7.691 (m, 1H), 7.055 (d, *J*=8.4 Hz, 2H), 6.710 (d, *J*=9.0 Hz, 1H), 6.506 (d, *J*= 8.4 Hz, 2H), 5.936-5.873 (m, 1H), 5.081-5.074 (m, 1H), 5.055 (dq, *J*= 1.2 Hz, 10.4 Hz, 1H), 4.988 (s, 2H), 4.609 (dt, *J*= 1.2 Hz, 5.2 Hz, 2H), 4.453 (d, *J*=6.0 Hz, 2H).

***^{13}C NMR* (100 MHz, DMSO-d_6)**: 163.42, 162.52, 150.60, 147.73, 134.06, 132.29, 130.67, 129.41, 128.63, 127.93, 124.86, 124.28, 121.73, 120.23, 115.92, 113.90, 107.51, 104.52, 45.80, 41.27.

FTIR(ATR) (υ max solid/cm^{-1}): 3387, 1683, 1673, 1634, 1615, 1575, 1542, 1515, 1449, 1417, 1391, 1365, 1333, 1287, 1241, 1172, 1107, 985, 944, 907, 820, 804, 758, 668.

Accurate Mass Analysis:

Calculated mass for $C_{22}H_{20}N_3O_2$=358.1500, observed mass = 358.1552.

Calculated mass for $C_{22}H_{19}N_3O_2Na$=380.1375, observed mass = 380.1376.

Melting Point: 182.5°C-185.4°C.

***N*-Allyl-4-(2-aminobenzylamine)-1,8-naphthalimide (50)**

Synthesis by Conventional Heating Methods

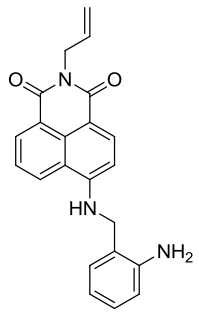

N-Allyl-4-bromo-1,8-naphthalimide (**45**, 0.516 g, 1.44×10^{-3} mol), was stirred at 110°C. After ten minutes 2-aminobenzylamine (1.105 g, 9.04×10^{-3} mol) was added with stirring continued at 110°C. After forty-eight hours, the reaction was removed from the heat and water added to afford the product. The product was collected using a Hirsch Funnel and recrystallised from ethanol yielding 0.367 g (63 %) of **50** as a yellow powder.

Synthesis by Microwave Irradiation

N-Allyl-4-bromo-1,8-naphthalimide (**45**, 0.050 g, 1.58×10^{-4} mol) and 2-aminobenzylamine (0.221 g, 0.0018 mol) were added to a glass vial, capped and irradiated at 105°C. After sixty minutes, the reaction was cooled to 50°C, removed from the microwave reactor and water added to afford the product. The product was collected using a Hirsch Funnel and recrystallised from ethanol yielding 0.0248 g (44 %) of **50** as a yellow powder.

Characterisation

***^{1}H NMR* (600 MHz, DMSO-d_6):** δ 8.765 (d, *J*=8.4 Hz, 1H), 8.456 (d, *J*=7.2 Hz, 1H), 8.346 (t, *J*=6.0 Hz, 1H), 8.195 (d, *J*=8.4 Hz, 1H), 7.749-7.723 (m, 1H), 7.007 (d, *J*=7.8 Hz, 1H), 6.954 (t, *J*=7.8 Hz, 1H), 6.670 (d, *J*=7.8 Hz, 1H), 6.614 (d, *J*=8.4 Hz, 1H), 6.477 (t, *J*=7.8 Hz, 1H), 5.940-5.877 (m, 1H), 5.142 (s, 2H), 5.084-5.078 (m, 1H), 5.058 (dq, *J*= 1.2 Hz, 10.4 Hz, 1H), 4.614 (dt, *J*=1.2 Hz, 5.2 Hz , 2H), 4.451 (d, *J*= 6.0 Hz, 2H).

***^{13}C NMR* (100 MHz, DMSO-d_6):** δ 163.43, 162.54, 150.74, 146.16, 134.11, 133.27, 130.76, 129.43, 128.57, 127.61, 127.19, 124.47, 121.85, 120.32, 120.27, 115.99, 115.91, 115.02, 107.77, 104.58, 43.28, 41.28.

FTIR(ATR) (υ max solid/cm^{-1}): 3365, 1681, 1639, 1614, 1576, 1543, 1496, 1457, 1418, 1391, 1368, 1339, 1295, 1246, 1171, 1106, 1064, 980, 936, 904, 823, 772, 753.

Accurate Mass Analysis

Calculated mass for $C_{22}H_{20}N_3O_2$=358.1500, observed mass = 358.1553.

Calculated mass for $C_{22}H_{19}N_3O_2Na$=380.1375, observed mass = 380.1376.

Melting Point: 177.0°C-179.5°C.

***N*-Allyl-4-(3-aminobenzylamine)-1,8-naphthalimide (52)**

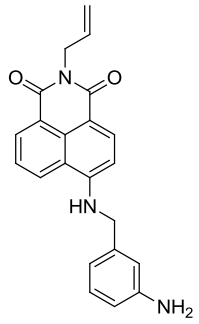

Synthesis by Conventional Heating Methods

N-Allyl-4-bromo-1,8-naphthalimide (**45**, 0.512g, 0.0014 mol), was stirred at 110^{o}C. After ten minutes 3-aminobenzylamine (0.79 mL, 0.007 mol) was added and stirring continued at 110^{o}C. After three hours, the reaction was removed from the heat and water was added to afford the product. The product was collected using a Hirsch Funnel and recrystallised from ethanol yielding 0.452g (78%) of **52** as a bright yellow powder.

Synthesis by Microwave Irradiation

N-Allyl-4-bromo-1,8-naphthalimide (**45**, 0.202g, 6.39x10^{-4} mol) and 3-aminobenzylamine (0.72 mL, 0.0064 mol) were added to a glass vial, capped and irradiated at 105^{o}C. After four minutes, the reaction was cooled to 50^{o}C, removed from the microwave reactor and stirred. The vial was then irradiated for a further four minutes at 105^{o}C, cooled and water was added to afford the product. The product was collected using a Hirsch Funnel and recrystallised from ethanol yielding 0.162 g (71%) of **52** as a bright yellow powder.

Characterisation

***^{1}H NMR* (600 MHz, DMSO-d_6):** δ 8.779 (d, *J*=8.4 Hz, 1H), 8.481 (t, *J*=6.0 Hz, 1H), 8.450 (d, *J*=7.2 Hz, 1H), 8.177 (d, *J*=8.4 Hz, 1H), 7.743-7.716 (m, 1H), 6.963 (t, *J*=7.8 Hz, 1H), 6.633 (d, *J*=8.4 Hz, 1H), 6.553 (s, 1H), 6.520 (d, *J*=7.8 Hz, 1H), 6.413 (d, *J*=7.8 Hz, 1H), 5.938-5.874 (m, 1H), 5.083-5.075 (m, 1H), 5.068-5.049 (m, 3H), 4.612 (dt, *J*= 1.2 Hz, 5.2 Hz, 2H), 4.510 (d, *J*=6.0 Hz, 2H).

***^{13}C NMR* (150 MHz, DMSO-d_6):** δ 163.50, 162.60 150.79, 148.95, 138.96, 134.19, 133.30, 130.86, 129.50, 129.08, 128.71, 124.53, 121.87, 120.30, 115.94, 114.19, 112.68, 111.74, 107.71, 104.67, 146.16, 41.34.

FTIR(ATR) (υ max solid/cm^{-1}): 3365, 1671, 1604, 1573, 1537, 1463, 1386, 1365, 1338, 1294, 1243, 1189, 1111, 994, 927, 822, 755, 771, 694.

Accurate Mass Analysis

Calculated mass for $C_{22}H_{20}N_3O_2$=358.1500, observed mass = 358.1552.

Calculated mass for $C_{22}H_{19}N_3O_2Na$=380.1375, observed mass = 380.1374.

Melting Point: 181.9^{o}C- 183.9^{o}C.

***N*-Allyl-4-(4-(*N*-phenylureido)benzylamino)-1,8-naphthalimide (1)**

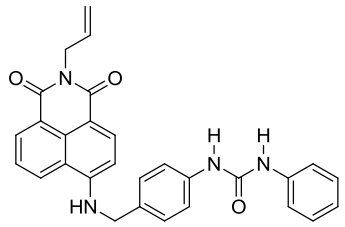

Synthesis by Conventional Heating Method

N-Allyl-4-(4-aminobenzylamine)-1,8-naphthalimide (**51**), (0.203 g, 5.68×10^{-4} mol) was dissolved in DMF (6 mL) and stirred at room temperature. Phenyl isocyanate (92.6 μL, 8.52×10^{-4} mol) and TEA (6 drops) were added to the stirred solution. After 24 hours, water was added to the reaction to afford 0.254g (94%) of the product **1** as a bright yellow powder.

Synthesis by Microwave Irradiation Method

N-Allyl-4-(4-aminobenzylamine)-1,8-naphthalimide (**51**), (0.051 g, 1.43×10^{-4} mol) was dissolved in DMF (1.5mL) in a glass walled microwave tube. Phenyl isocyanate (23.2 μL, 2.13×10^{-4} mol) and TEA (2 drops) were added to the tube with irradiation at 40°C for 2 minutes. Water was added to the reaction, with the solid material collected using a Hirsch funnel. Recrystallisation from methanol yielded 0.037g (54%) of **1** as a bright yellow powder.

Characterisation

***^{1}H NMR* (600 MHz, DMSO-d_6):** δ 8.777 (d, *J*=8.4 Hz, 1H), 8.670 (bs, 1H), 8.650 (bs, 1H), 8.489 (t, *J*=6.0 Hz, 1H), 8.451 (d, *J*=7.2 Hz, 1H), 8.183 (d, *J*=8.4 Hz, 1H), 7.746-7.720 (m, 1H), 7.429-7.402 (m, 4H), 7.314 (d, *J*=8.4 Hz, 2H), 7.270-7.244 (m, 2H), 6.960-6.935 (m, 1H), 6.699 (d, *J*=8.4 Hz, 1H), 5.926-5.880 (m, 1H), 5.082-5.072 (m, 1H), 5.065-5.042 (m, 1H), 4.612-4.595 (m, 4H).

***^{13}C NMR* (100 MHz, DMSO-d_6):** δ 163.43, 162.54, 152.49, 150.51, 139.66, 138.61, 134.07, 133.24, 131.54, 130.77, 129.23, 128.73, 128.63, 127.49, 124.48, 121.83, 121.76, 120.31, 118.38, 118.14, 115.92, 107.86, 104.61, 45.56, 41.26.

FTIR(ATR) (υ max solid/cm^{-1}): 3399, 3296, 1684, 1635, 1576, 1542, 1498, 1442, 1417, 1388, 1367, 1339, 1313, 1233, 1111, 1025, 935, 835, 774, 693.

Accurate Mass Analysis

Calculated mass for $C_{29}H_{25}N_4O_3$=477.1927, observed mass = 477.1929.

Calculated mass for $C_{29}H_{24}N_4O_3Na$=499.1746, observed mass = 499.1748.

Melting Point: 221.6°C-223.7°C.

***N*-Allyl-4-(4-(*N*-phenylthioureido)benzylamino)-1,8-naphthalimide (2)**

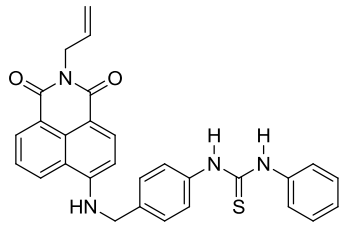

Synthesis by Conventional Heating Method

N-Allyl-4-(4-aminobenzylamine)-1,8-naphthalimide (**51**), (0.199 g, 5.57×10^{-4} mol) was dissolved in DMF (6 mL) and stirred at room temperature. Phenyl isothiocyanate (134.0 μL, 1.12×10^{-3} mol) and TEA (6 drops) were added to the stirred solution. After 24 hours, water was added to the reaction to afford 0.268 g (70.5%) of the product **2** as a bright yellow powder.

Synthesis by Microwave Irradiation Method

This compound was not successfully synthesised using microwave irradiation methods.

Characterisation

***^{1}H NMR* (400 MHz, DMSO-d_6):** δ 9.815 (bs, 2H), 8.775 (d, *J*=8.4 Hz, 1H), 8.507 (t, *J*=6.0 Hz, 1H), 8.453 (d, *J*=7.2 Hz, 1H), 8.186 (d, *J*=8.4 Hz, 1H), 7.758-7.718 (m, 1H), 7.469-7.436 (m, 4H), 7.373-7.286 (m,4H), 7.123-7.086 (m, 1H), 6.707 (d, *J*=8.4 Hz, 1H), 5.954-5.856 (m, 1H), 5.092-5.080 (m, 1H), 5.066-5.037 (m, 1H), 4.633 (d, *J*=6.0 Hz, 2H), 4.618-4.607 (m, 2H).

***^{13}C NMR* (100 MHz, DMSO-d_6):** δ 179.58, 163.42, 162.51, 150.47, 139.43, 138.35, 134.42, 134.05, 133.23, 130.29, 129.42, 128.59, 128.39, 126.99, 124.48, 124.36, 123.83, 123.56, 121.83, 120.29, 115.90, 107.96, 104.58, 45.49, 41.25.

FTIR, accurate mass analysis and a melting point were not determined for this compound as the product was unable to be reproduced after its initial synthesis. All of the material previously obtained had been used in other experiments.

***N*-Allyl-4-(4-(*N*-4-chlorophenylureido)benzylamino)-1,8-naphthalimide (3)**

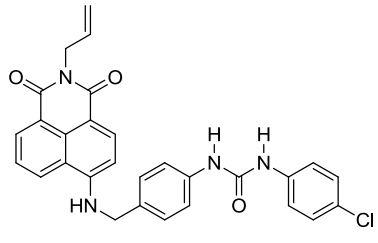

Synthesis by Conventional Heating Method

N-Allyl-4-(4-aminobenzylamine)-1,8-naphthalimide (**51**), (0.111g, 2.17×10^{-4} mol) was dissolved in DMF (3 mL) and stirred at room temperature. 4-chloro-phenyl isocyanate (53.7 μL, 4.20×10^{-4} mol) and TEA (3 drops) were added to the stirred solution. After 24 hours, water was added to the reaction to afford the product, **3**. Reaction yielded 0.129 g (81.3%) of the product **3** as a bright yellow powder.

Synthesis by Microwave Irradiation Method

This compound was not successfully synthesised using microwave irradiation methods.

Characterisation

***^{1}H NMR* (600 MHz, DMSO-d_6):** δ 8.796-8.775 (m, 2H), 8.706 (s, 1H) 8.488 (t, *J*=6.0 Hz, 1H), 8.450 (d, *J*=7.2 Hz, 1H), 8.181 (d, *J*= 8.4 Hz, 1H), 7.745-7.719 (m, 1H), 7.449 (d, *J*=9.0 Hz, 2H), 7.398 (d, *J*=8.4 Hz, 2H), 7.330-7.296 (m, 3H), 6.694 (d, *J*=8.4 Hz, 1H), 5.926-5.880 (m, 1H), 5.082-5.072 (m, 1H), 5.065-5.042 (m, 1H) 4.604-4.596 (m, 4H).

***^{13}C NMR* (150 MHz, DMSO-d_6):** δ 163.48, 162.60, 152.45, 150.56, 138.76, 138.48, 134.16, 133.28, 131.86, 130.87, 130.34, 129.48, 128.68, 127.54, 125.44, 124.57, 121.88, 120.30, 119.84, 118.52, 116.23, 107.88, 104.68, 45.55, 41.33.

FTIR(ATR) (υ max solid/cm^{-1}): 3381, 3298, 1687, 1638, 1590, 1575, 1545, 1492, 1451, 1415, 1391, 1368, 1336, 1299, 1239, 1179, 1140, 1092, 1011, 983, 937, 820, 771, 759, 662.

Accurate Mass Analysis

Calculated mass for $C_{29}H_{24}ClN_4O_3$=511.1537, observed mass = 511.1537.

Calculated mass for $C_{29}H_{23}ClN_4O_3Na$=533.1356, observed mass = 533.1358.

Melting Point: 263.9°C-265.8°C.

***N*-Allyl-4-(2-(*N*-phenylureido)benzylamino)-1,8-naphthalimide (4)**

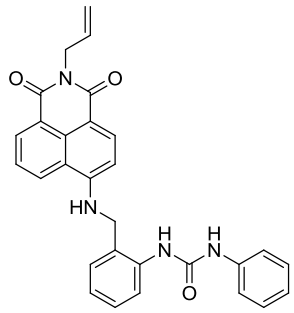

Synthesis by Conventional Heating

N-Allyl-4-(2-aminobenzylamine)-1,8-naphthalimide (**51**) (0.102g, 2.85×10^{-4}mol) was heated under reflux in anhydrous acetonitrile. Phenyl isocyanate (46.5 μL, 4.28×10^{-4}mol) was added and heating continued. After eighteen hours, the reaction was removed from the heat with the product settling upon standing as 0.072g (53%) of **4** as a bright yellow powder.

Synthesis by Microwave Irradiation

N-Allyl-4-(2-aminobenzylamine)-1,8-naphtalimide (**50**) (0.103 g, 2.16×10^{-4} mol) was dissolved in anhydrous acetonitrile (2 mL) in a microwave reaction tube. Phenyl isocyanate (70μL, 6.41×10^{-4} mol) was added and the tube submitted to microwave irradiation at 70°C for 3 lots of 2 minutes. Water was added to precipitate the product, which was then filtered *in vacuo* and washed with ice cold water. Recrystallisation from methanol yielded 0.103 g (75 %) of a bright yellow powder *N*-allyl-4-(2-(*N*-phenylureido)benzylamino)-1,8-naphthalimide (**4**).

Characterisation

^{1}H NMR (600 MHz, DMSO-d_6): 9.011 (s, 1H), 8.791 (d, *J*=8.4 Hz, 1H), 8.462 (d, *J*=7.2 Hz, 1H), 8.396 (t, J=6.0, 1H), 8.256 (s, 1H), 8.193 (d, *J*=8.4 Hz, 1H), 7.754-7.728 (m, 1H), 7.691 (d, *J*=7.8 Hz, 1H), 7.470 (d, *J*=8.4 Hz, 2H), 7.292-7.266 (m, 2H), 7.235 (d, *J*=8.4 Hz, 2H), 7.052-7.027 (m, 1H), 6.976-6.951 (m, 1H), 6.597 (d, *J*=8.4 Hz, 1H), 5.939-5.875 (m, 1H), 5.086-5.078 (m, 1H), 5.071-5.047 (m, 1H), 4.632 (d, *J*=6.0 Hz, 2H), 4.618-4.609 (m, 2H).

***^{13}C NMR* (100 MHz, DMSO-d_6):** δ 163.46, 162.59, 153.12, 150.60, 139.85, 136.73, 134.13, 133.24, 130.87, 129.71, 129.42, 128.80, 128.69, 127.35, 126.77, 124.63, 123.91, 123.70, 121.90, 121.80, 120.33, 118.18, 115.94, 108.19, 104.71, 42.91, 41.31.

FTIR(ATR) (υ max solid/cm^{-1}): 3285, 1684, 1645, 1615, 1593, 1558, 1497, 1379, 1337, 1246, 1187, 1109, 917, 836, 775, 757, 693.

Accurate Mass Analysis

Calculated mass for $C_{29}H_{25}N_4O_3$=477.1927, observed mass = 477.1926.

Calculated mass for $C_{29}H_{24}N_4O_3Na$=499.1746, observed mass = 499.1747.

Melting Point: 251.8°C-252.8°C.

***N*-Allyl-4-(3-(*N*-phenylureido)benzylamino)-1,8-naphthalimde (5)**

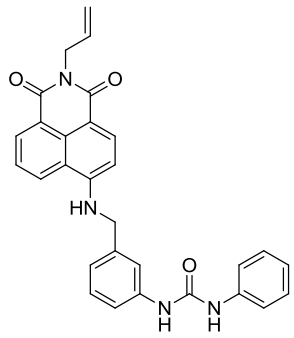

Synthesis by conventional heating

N-Allyl-4-(3-aminobenzylamine)-1,8-naphthalimide (**52**) (0.202g, 5.65×10^{-4}mol) was heated under reflux in anhydrous acetonitrile. Phenyl isocyanate (92.1 μL, 8.48×10^{-4}mol) was added and heating continued. After three hours, the reaction was removed from the heat with the product settling upon standing. The product was collected using a Hirsch funnel and recrystallised from methanol yielding 0.232g (86%) of **5** as a bright yellow powder.

Synthesis by microwave irradiation

N-Allyl-4-(3-aminobenzylamine)-1,8-naphtalimide (**52**) (0.102 g, 2.14×10^{-4} mol) was dissolved in anhydrous acetonitrile (2 mL) in a microwave reaction tube. Phenyl isocyanate (70μL, 6.41×10^{-4} mol) was added and the tube submitted to microwave irradiation at 70°C for 3 lots of 2 minutes. Water was added to precipitate the product, which was then filtered *in vacuo* and washed with ice cold water. Recrystallisation from methanol yielded 0.094 g (69 %) of a bright yellow powder *N*-allyl-4-(3-(*N*-phenylureido)benzylamino)-1,8-naphthalimide (**5**).

Characterisation

***^{1}H NMR:* (600 MHz, DMSO-d_6):** δ 8.803 (d, *J*=8.4 Hz, 1H), 8.754 (s, 1H), 8.662 (s, 1H), 8.558 (t, *J*= 6.0 Hz, 1H), 8.463 (d, *J*=7.2 Hz, 1H), 8.188 (d, *J*=8.4 Hz, 1H), 7.767-7.741 (m, 1H), 7.432 (s, 1H), 7.410-7.385 (m, 3H), 7.259-7.233 (m, 3H), 7.006 (d, *J*=7.8 Hz, 1H), 6.940 (t, *J*=7.2 Hz, 1H), 6.665 (d, *J*=8.4 Hz, 1H), 5.926-5.871 (m, 1H), 5.078-5.047 (m, 2H), 4.645 (d, *J*=6.0 Hz, 2H), 4.618-4.606 (m, 2H).

***^{13}C NMR* (100 MHz, DMSO-d_6):** δ 163.44, 162.56, 152.44, 150.54, 140.00, 139.61, 139.13, 134.11, 133.25, 130.83, 129.44, 129.02, 128.76, 128.60, 124.57, 121.89, 121.82, 120.39, 120.30, 118.14, 116.85, 116.20, 115.93, 107.98, 104.63, 45.97, 41.30

FTIR(ATR) (υ max solid/cm^{-1}): 3323, 1686, 1633, 1575, 1542, 1490, 1146, 1421, 1389, 1369, 1332, 1297, 1242, 1140, 1110, 989, 936, 817, 772, 757, 692.

Accurate Mass Analysis

Calculated mass for $C_{29}H_{25}N_4O_3$=477.1927, observed mass = 477.1931.

Calculated mass for $C_{29}H_{24}N_4O_3Na$=499.1746, observed mass = 499.1747.

Melting Point: 186.4°C-188.6°C.

***N*-Allyl-4-(4-(*N*-3-(triethoxysilyl)propylureido)benzylamino)-1,8-naphthalimide (6)**

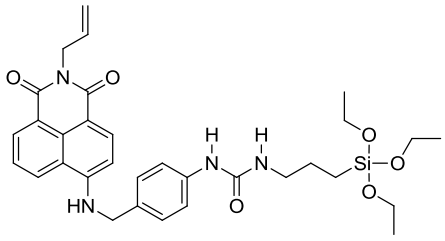

Synthesis by conventional heating

N-Allyl-4-(4-aminobenzylamine)-1,8-naphthalimide (**51**) (0.496g 1.39x10^{-3} mol), was added to anhydrous THF (35 mL) and stirred under a nitrogen atmosphere. In a separate vial, 3-(triethoxysilyl)propyl isocyanate (800 μL 3.23x10^{-3} mol) was added to anhydrous THF (20 mL) and stirred. The resulting mixture was immediately added to the naphthalimide solution and heated under reflux with stirring under a nitrogen atmosphere for 2 days. The resultant mixture was allowed to cool to room temperature under nitrogen and then THF was removed *in vacuo.* The resultant yellow waxy solid was recrystallised from methanol, resulting in 0.326g (38.9%) of bright yellow crystals of *N*-allyl-(4-(4-(*N*-3-(triethoxysilyl)propylureido)benzylamino)-1,8-naphthalimide (**6**).

Synthesis by microwave irradiation

The synthesis of this compound was not attempted using microwave irradiation methods.

Characterisation

***^{1}H NMR:* (600 MHz, DMSO-d_6):** δ 8.765 (d, *J*=8.4 Hz, 1H), 8.457 – 8.444 (m, 2H), 8.369 (s, 1H), 8.172 (d, *J*=8.4 Hz, 1H), 7.736-7.710 (m, 1H), 7.322 (d, *J*=8.4 Hz, 2H), 7.244 (d, J=8.4 Hz), 6.682 (d, *J*=8.4 Hz,1H), 6.122 (t, *J*=5.4 Hz 1H), 5.933-5.870 (m, 1H), 5.086-5.067 (m, 1H), 5.066-5.037 (m, 1H) 4.610-4.602 (m, 2H), 4.559 (d, *J*=6.0 Hz, 2H), 3.730 (q, *J*=6.8 Hz, 6H), 3.019 (q, *J*=6.2 Hz, 2H), 1.445 (quin, *J*=7.8 Hz, 2H), 1.130 (t, *J*=6.8 Hz, 9H), 0.545-0.518 (m, 2H).

^{13}C NMR (150 MHz, DMSO-d_6): δ 163.50, 162.59, 155.18, 150.58, 139.57, 134.15, 133.28, 130.85, 130.55, 130.42, 129.48, 128.71, 127.41, 124.54, 121.86, 120.33, 117.76, 115.94, 107.80, 104.66, 57.73, 45.57, 41.75, 41.33, 30.74, 23.37, 18.25, 7.25.

FTIR(ATR) (υ max solid/cm^{-1}): 3377, 3320, 2973, 2928, 2884, 1688, 1634, 1574, 1543, 1451, 1414, 1392, 1368, 1336, 1298, 1243, 1191, 1166, 1101, 1077, 936, 757.

Accurate Mass Analysis

Calculated mass for $C_{32}H_{40}N_4O_6SiNa$=627.2615, observed mass = 627.2614.

Melting Point: 206.1°C-207.3°C.

***N*-Allyl-4-(2-(*N*-3-(triethoxysilyl)propylureido)benzylamino)-1,8-naphthalimide (7)**

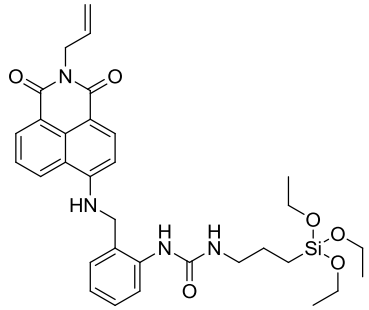

Synthesis by conventional heating

N-Allyl-4-(2-aminobenzylamine)-1,8-naphthalimide (**50**) (0.103g, 2.89×10^{-4} mol), was added to anhydrous THF (7 mL) and stirred under nitrogen. In a separate vial, 3-(triethoxysilyl)propyl isocyanate (200 μL 8.08×10^{-4} mol) was added to anhydrous THF (4 mL) and stirred. The resulting mixture was immediately added to the naphthalimide solution and heated under reflux with stirring under a nitrogen atmosphere for ninety-six hours. The resultant mixture was allowed to cool to room temperature and then THF was removed *in vacuo*. The resultant yellow waxy solid was recrystallised from methanol, resulting in 0.033g (19%) of bright yellow crystals of *N*-allyl-(4-(2-(*N*-3-(triethoxysilyl)propylureido)benzylamino)-1,8-naphthalimide (**7**).

Synthesis by microwave irradiation

Synthesis was not attempted by microwave irradiation for this compound.

Characterisation

***^{1}H NMR:* (600 MHz, DMSO-d_6):** δ 8.767(d, *J*=8.4 Hz, 1H), 8.461 (d, *J*=7.2 Hz, 1H), 8.376 (t, *J*=6.0 Hz, 1H), 8.178 (d, *J*=8.4 Hz, 1H), 7.949 (s, 1H), 7.755-7.728 (m, 1H), 7.617 (d, *J*=7.8 Hz, 1H), 7.199-7.175 (m, 2H), 6.975-6.950 (m, 1H), 6.557 (d, *J*=8.4 Hz, 1H), 6.534 (t, *J*=5.6 Hz, 1H), 5.936-5.873 (m, 1H), 5.084-5.073 (m, 1H), 5.069-5.043 (m, 1H), 4.616-4.607 (m, 2H), 4.556 (d, *J*=6.0 Hz, 2H) 3.723 (q, *J*=6.8 Hz, 6H), 3.078 (q, *J*=6.2 Hz, 2H), 1.491 (quin, *J*=7.8 Hz 2H), 1.119 (t, *J*=6.8 Hz, 9H), 0.581-0.553 (m, 2H).

***^{13}C NMR:* (100 MHz, DMSO-d_6):** δ 163.44, 162.57, 155.76, 150.60, 137.59, 134.11, 133.24, 130.81, 129.41, 129.07, 128.63, 127.23, 126.70, 124.57, 123.15, 121.89, 120.27, 115.92, 108.11, 104.50, 57.70, 48.60, 42.94, 41.98, 41.30, 23.39, 18.20, 7.29.

FTIR(ATR) (υ max solid/cm^{-1}): 3319, 1684, 1642, 1581, 1542, 1378, 1337, 1288, 1244, 1083, 920, 771, 757.

Accurate Mass Analysis

Calculated mass for $C_{32}H_{40}N_4O_6SiNa$=627.2615, observed mass = 627.2615.

Melting Point: 195.0°C-198.1°C.

***N*-Allyl-4-(3-(*N*-3-(triethoxysilyl)propylureido)benzylamino)-1,8-naphthalimide (8)**

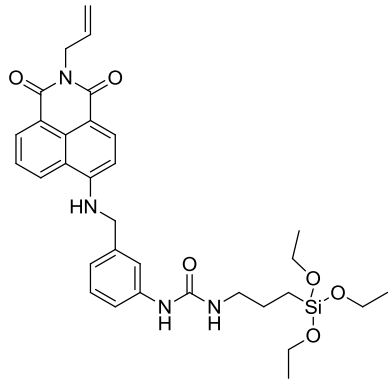

Synthesis by conventional heating:

N-Allyl-4-(3-aminobenzylamine)-1,8-naphthalimide (**52**) (0.106g, 2.97×10^{-4} mol), was added to anhydrous THF (7 mL) and stirred under nitrogen. In a separate vial, 3-(triethoxysilyl)propyl isocyanate (200 μL, 8.08×10^{-4} mol) was added to anhydrous THF (4 mL) and stirred. The resulting mixture was immediately added to the naphthalimide solution and heated under reflux with stirring under a nitrogen atmosphere for fourty-eight hours. The resultant mixture was allowed to cool to room temperature and then THF was removed *in vacuo*. The resultant yellow waxy solid was recrystallised from methanol, resulting in 0.054g (30%) of bright yellow crystals of *N*-allyl-(4-(3-(*N*-3-(triethoxysilyl)propylureido)benzylamino)-1,8-naphthalimide (**8**).

Synthesis by microwave irradiation:

Synthesis was not attempted by microwave irradiation for this compound.

Characterisation:

***^{1}H NMR*(600 MHz, DMSO-d_6):** δ 8.783 (d, *J*=8.4 Hz, 1H), 8.528 (t, *J*=6.0 Hz, 1H), 8.456 (d, *J*=7.2 Hz, 1H), 8.381 (s, 1H), 8.173 (d, *J*=8.4 Hz, 1H), 7.754-7.728 (m, 1H), 7.351 (s, 1H), 7.297 (d, *J*=7.8 Hz, 1H), 7.174 (t, *J*=7.8 Hz, 1H), 6.918 (d, *J*=7.2 Hz, 1H), 6.631 (d, *J*=8.4 Hz, 1H), 6.080 (t, *J*=5.4 Hz, 1H), 5.926-5.880 (m, 1H), 5.084-5.069 (m, 1H), 5.066-5.042 (m, 1H) 4.612-4.604 (m, 4H), 3.717 (q, *J*=6.8 Hz, 6H), 2.997 (q, *J*=6.2 Hz, 2H), 1.424 (quin, *J*=7.8 Hz, 2H), 1.117 (t, *J*=6.8 Hz, 9H), 0.525-0.497 (m, 2H).

^{13}C NMR (150 MHz, DMSO-d_6): δ 163.48, 162.58, 155.11, 150.60, 140.92, 138.93, 134.16, 133.27, 130.87, 129.48, 128.89, 128.66, 124.60, 121.90, 120.31, 119.47, 116.29, 115.93, 115.55, 107.92, 104.65, 57.72, 46.03, 41.71, 41.33, 23.34, 18.24, 7.23.

FTIR(ATR) (υ max solid/cm^{-1}): 3353, 2974, 1688, 1634, 1572, 1454, 1490, 1449, 1416, 1390, 1366, 1333, 1297, 1243, 1190, 1165, 1074, 947, 756, 700.

Accurate Mass Analysis

Calculated mass for $C_{32}H_{40}N_4O_6SiNa$=627.2615, observed mass = 627.2615.

Melting Point: 194.1°C-195.2°C.

2.6 Immobilisation Procedures

Spectral data in relation to the immobilisation procedures is presented with the discussion of the surfaces in Chapter 6.

2.6.1 Approach 1 – Hydrosilation via the terminal double bond

2.6.1.1 Formation of hydride modified silica (53)

Silica gel (1.0 g) was reacted with triethoxysilane (304.4 μL, 0.0017 mol) in toluene (5 mL) under reflux conditions. After seventy-two hours the reaction was removed from the heat and the silica allowed to settle out. The solid material was collected using a Hirsch funnel, washed with toluene and dried under reduced pressure. Hydride modified silica (**53**) was stored in the oven until use (not kept for more than two weeks).

2.6.1.2 Immobilisation of 1 or 2 onto hydride modified silica (54-55)

Hydride modified silica gel (0.5 g) **53** was reacted with *N*-allyl-4-(4-(*N*-phenylureido)benzylamino)-1,8-naphthalimide (**1**) (0.5 g, 0.001 mol) in toluene (2 mL) under reflux conditions. Spier's Catalyst (10 mM platinic chloride in isopropanol, twelve drops) was added to the solution. After seventy-two hours the reaction was removed from the heat and the silica allowed to settle out. The silica was collected with a Hirsch funnel and washed with toluene until no unreacted sensor could be observed. The recovered sensor modified silica **54** was then washed further with acetone, again until no unreacted sensor could be observed. The same method was repeated with **2** to form **55**.

2.6.2 Approach 2- Build the sensor on aminopropyl silica

2.6.2.1 Reaction of 4-amino-1,8-naphthalic anhydride (44) with 3-Aminopropyl functionalised silica to form 56

3-Aminopropyl functionalised silica (0.089g) was added to 4-bromo-1,8-naphthalic anhydride (**44**) (0.202g, 7.29×10^{-4} mol) suspended in ethanol (3 mL) in a sealed glass tube and irradiated in the microwave at 70^{o}C for two minutes. The sample was cooled

to 50°C, taken out and stirred and then irradiated for a further two minutes at 70°C. This cycle was repeated a further two times for a total irradiation time of eight minutes. After the last lot of cooling to 50°C, the solid material was collected using a Hirsch funnel and washed with ethanol to remove unreacted anhydride. After no more anhydride was detected (no precipitate forms) the collected material was washed with acetone, yielding **56** as light brown (beige) powder.

2.6.2.2 Reaction of 56 with 4-aminobenzylamine to form 57

Modified silica **56** (0.5 g) was placed in a microwave tube, covered in excess 4-aminobenzylamine and irradiated at 105°C for two minutes. The reaction was then cooled to 50°C, taken out of the microwave reactor, stirred and then irradiated at 105°C for a further two minutes. This cycle was continued such that the total irradiation time was six minutes. The solid material was collected using a Hirsch funnel and was washed with acetone (soxhlet extraction) until the acetone was seen to run colourless. This yielded a brightly yellow coloured silica gel **57**.

2.6.2.3 Reaction of 57 with phenyl isocyanate to form 58

Modified silica **57** was placed in a microwave tube (0.5 g) and suspended in acetonitrile (2 mL) Phenyl isocyanate (100 μL was added) and the tube irradiated at 70°C. After two minutes the tube was cooled to 50°C, taken out and stirred. This cycle was repeated such that the total irradiation time was six minutes. The solid silica was collected using a Hirsch funnel and washed with acetone (soxhlet extraction), until the acetone was seen to run colourless. This yielded a brightly yellow coloured silica gel **58**. The same reaction was also reported using DMF with an irradiation temperature of 40°C, also yielding **58**.

2.6.3 Approach 3 – Siloxane linkage through triethoxy groups

2.6.3.1 Formation of mesoporous silica

Mesoporous silica was synthesised using the procedure published by Seo *et al.*[77]. Cetyl trimethylammonium bromide (C-TAB) was substituted for octadecyl

trimethylammonium bromide (odTMA) due to availability issues and the mesoporous silica was allowed to form over 120 hours.

A mixture of tetraethylorthosilicate (0.65 mLs), 37% v/v hydrochloric acid (71.0 mL), C—TAB (0.75 g) and distilled water (180 mL) were heated at 80^{o}C for 120 hours. The solid particles were collected using a Hirsch funnel and washed with water. The mesoporous silica was then heated at 600^{o}C for five hours to remove residual C-TAB. Mesoporous silica was kept at approximately 200^{o}C until use.

2.6.3.2 Immobilisation of 6-8 onto mesoporous silica (59-61)

Mesoporous silica (0.100 g) and a sensor containing a triethoxysilyl group (**6**, **7**, or **8**, 0.100 g) were dissolved in DMSO (10 mL) and heated under reflux for 24 hours. The solid material was collected using a Hirsch funnel and initially washed with DMSO to remove unreacted sensor. After drying, the sensor was soxhlet extracted in acetone until no more sensor was observed to be removed from the silica (i.e. the acetone was colourless). (**6** immobilised onto mesoporous silica is **59**, **7** is **60** and **8** is **61**).

Chapter 3

SYNTHESIS – CONVENTIONAL HEATING

3.1 Synthesis of Fluorescent Anion Sensors

As detailed in Chapter 1, it has been well established in the literature [34, 38, 39, 49-53, 57] that molecules based on the 4-amino-1,8-naphthalimide fluorophore in combination with powerful anion binding recognition groups, are potent sensors for the dihydrogen phosphate, acetate and fluoride anions. In the design of an appropriate sensor, the fluorophore (signalling subunit) and the anion binding site (receptor) are connected *via* covalent bonds through a spacer such that the fluorescent properties of the signalling subunit can undergo a change in emission intensity. When an anion is bound at the binding site this is usually a decrease creating an "on-off" sensor or occasionally an increase creating an "off-on" sensor (Figure 15) [38]. In these particular sensors, the observed decrease in fluorescence emission results from photoinduced electron transfer (PET) from the receptor to the fluorophore (Section 1.3.1). The binding of the anion increases the reduction potential of the receptor, leading to a greater rate of PET between the HOMO of the receptor and the excited state of the naphthalimide moiety (depicted in Figure 16). Therefore the fluorescent emission of the naphthalimide moiety is quenched or "switched off" [3].

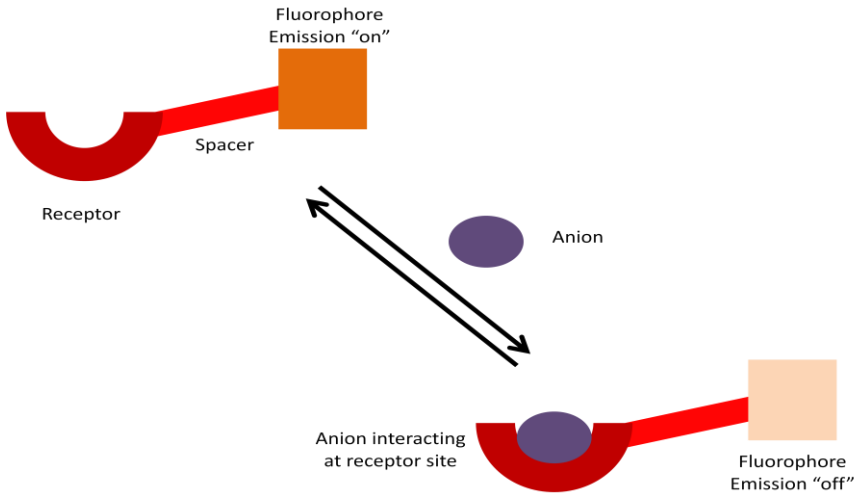

Figure 15: Generalised structure of a sensor based on the fluorophore - spacer - receptor concept. When the anion interacts at the receptor site, the fluorophore emission is switched off.

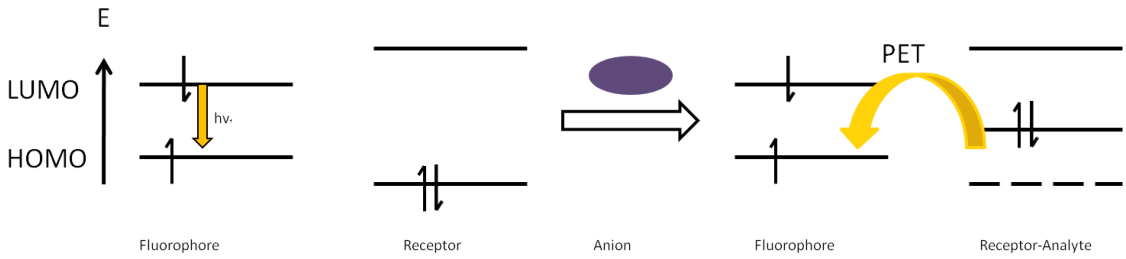

Figure 16: Molecular orbital energy diagrams showing the relative energetic dispositions of the orbitals of the fluorophore and the receptor both before and after interaction with an anionic species.

This chapter focuses on the synthesis of a series of anion sensors based on the 4-amino-1,8-naphthalimide fluorophore using urea and thiourea receptors. The sensors were designed to contain a terminal double bond at the imide moiety, to allow immobilisation onto silica using hydrosilation chemistry (Figure 17). This immobilisation process is detailed in Chapter 6.

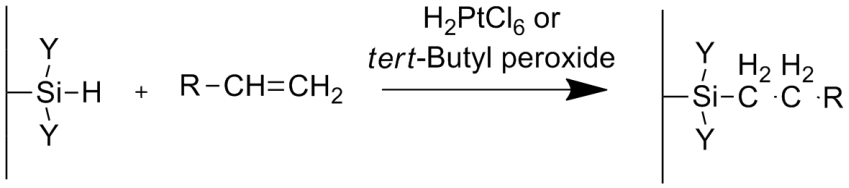

Figure 17: General scheme for the hydrosilation process, where R represents the naphthalimide sensor and Y represents either H or OH depending on the extent of conversion of the silica.

Scheme 6 shows the overall synthetic pathway utilised for the synthesis of 4-amino-1,8-naphthalimide based anion sensors which are able to be surface immobilised. Initially 4-bromo-1,8-naphthalic anhydride (**44**) was reacted with allylamine, forming the imide **45** and introducing the terminal double bond to enable surface immobilisation. In the next step, **45** was reacted with either 2-, 3- or 4-aminobenzylamine, introducing the spacer molecule, providing the covalent link between fluorophore and receptor. Finally, the amino-substituted naphthalimide was reacted with various isocyanates/isothiocyanates to form the anion sensor. A detailed discussion of the results and observations of the methods employed follows.

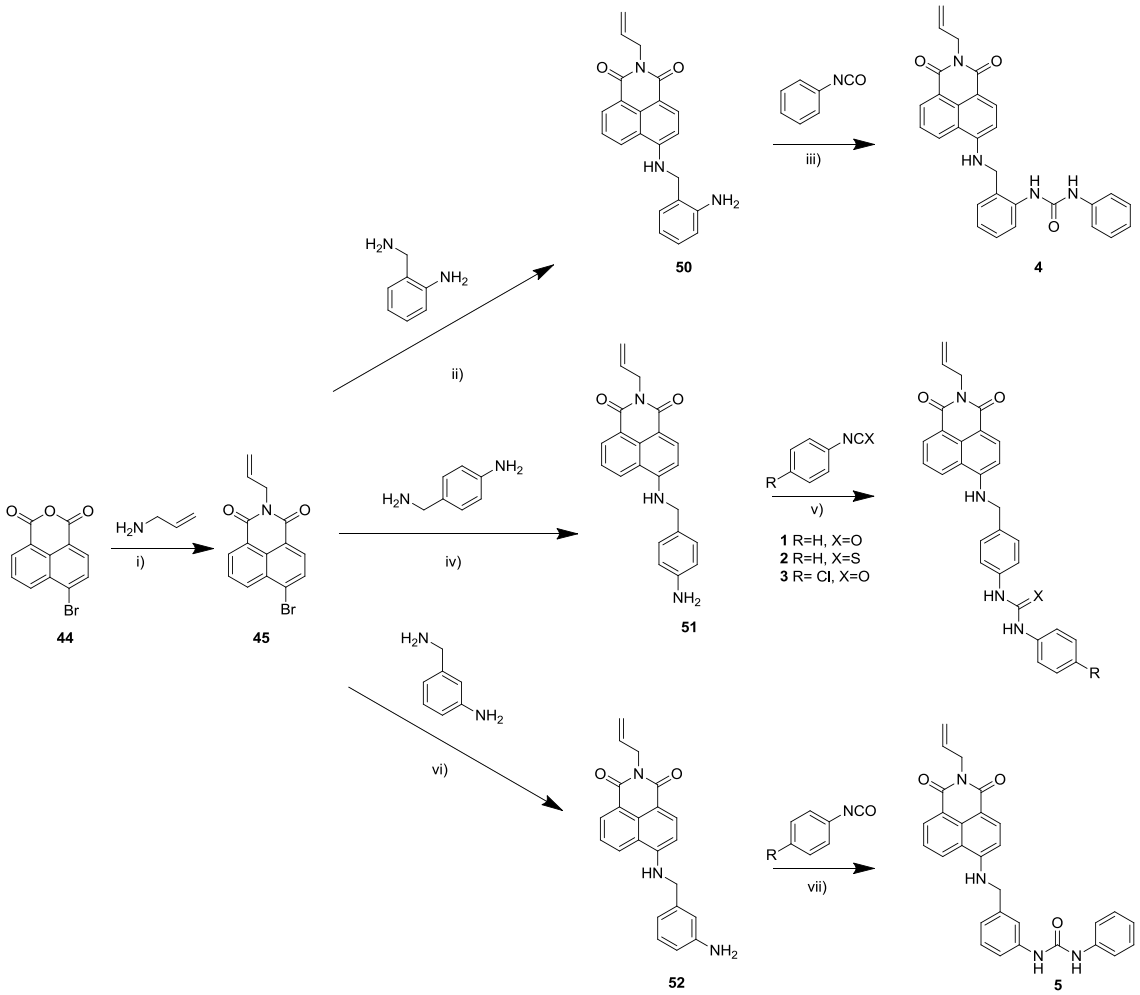

Scheme 6: Synthetic pathway for the synthesis of sensors based on the 4-bromo-1,8-naphthalimide fluorophore.

i) EtOH, reflux, 3h, 94% ii) neat, 110°C, 48h, 63% iii) MeCN, reflux, 15h, 54% iv) neat, 110°C, 2h, 72% v) DMF, TEA, r.t, 15-84h, 1=94%, 2=71%, 3=81% vi) neat, 110°C, 3h, 78% vii) MeCN, reflux, 3h, 86%.

3.2 Synthesis of *N*-allyl-4-bromo-1,8-naphthalimide (45)

Initial experiments focused on the synthesis of *N*-allyl-4-bromo-1,8-naphthalimide, (**45**). A multi-step procedure was employed where the bromo anhydride, **44**, was converted to 4-bromo-1,8-naphthalimide (**49**) and then alkylated with allyl bromide to form **45**.

Scheme 7 illustrates the first step in this process where, 4-bromo-1,8-naphthalic anhydride (**44**) was treated with aqueous ammonia (approx. 15.5 v/v%) at reflux using a previously established method [84] (Scheme 7). The product was collected using a Hirsch funnel, with **49** obtained in good yield (81%) as a pale brown powder.

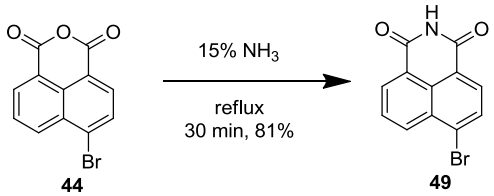

44 **49**

Scheme 7: Synthesis of 4-bromo-1,8-naphthalimide (49).

Analysis of the product using ^{1}H NMR spectroscopy, confirmed the conversion of the anhydride to the imide, with the resonance of the characteristic N-H proton apparent as a broad singlet at 11.71 ppm. The naphthalimide proton resonances were identified as a multiplet (two doublets overlapping) accounting for two protons at 8.55 pm, doublets accounting for one proton each at 8.23 and 8.16 ppm and a further multiplet accounting for one proton at 7.95 ppm. The proton resonance at 7.95 ppm was originally assigned as a triplet, however the two protons which contribute to this coupling do not couple equally to it. Further proton NMR spectroscopy experiments were undertaken to determine the exact multiplicity (dt, dq etc.), however the required resolution was not available and henceforth this proton resonance will be referred to as a multiplet. Carbon NMR spectroscopy showed a downfield shift of the resonance of the carbonyl moiety in **44** from 160.6 ppm to 163.5 ppm in **49**, consistent with conversion from a cyclic anhydride to a cyclic imide. FTIR also confirmed the successful formation of **49**, with the peaks assigned to the anhydride carbonyl in the starting material at 1770.6 cm^{-1} (asymmetric CO stretch) and 1729.6 cm^{-1} (symmetric CO stretch) absent from the FTIR spectrum of **49**. Furthermore the FTIR spectrum of **49** exhibited a significant new peak at 1669.5 cm^{-1}, characteristic of the carbonyl within the cyclic imide functional group. This reaction (Scheme 7), being both robust and high yielding (consistently >75%) was used for all further syntheses of 4-bromo-1,8-naphthalimide (**49**).

Subsequent alkylation of **49** was attempted using allyl bromide (as depicted in Scheme 8). As identified in Section 1.5.1 several methodologies have been employed for the alkylation of different imides by other researchers. Although none of the reactions used allyl bromide as the alkylation agent, it was hypothesised that similar conditions would be able to be used to successfully synthesise *N*-allyl-4-bromo-1,8-naphthalimide (**45**) (see Scheme 8).

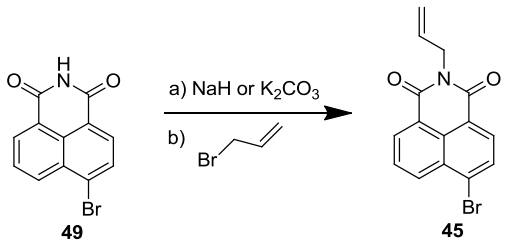

Scheme 8: Synthesis of *N*-allyl-4-bromo-1,8-naphthalimide (45).

Initially a stoichiometric equivalent mixture of potassium carbonate, allyl bromide and **49** were dissolved in anhydrous acetone and heated under reflux for six hours. Over the reaction time, no change from **49** was observed *via* TLC. Proton NMR spectroscopy analysis of the crude reaction mixture demonstrated the absence of the imide proton, observed in ^{1}H NMR spectrum of **49** at 11.72 ppm. Additionally three new clusters of signals were observed at 5.9, 5.1 and 4.6 ppm. These can all be attributed to the incorporation of the allyl group at the imide position. The multiplet at 5.9 ppm represents the single proton on the central allyl carbon; the two doublets of quartets at approximately 5.1 ppm were attributed to the two protons on the terminal carbon and finally the doublet of triplets at 4.6 ppm, accounts for the final two allyl protons. Assuming 100% purity, the recovered material only accounted for a 13% yield and it was shown *via* ^{1}H NMR spectroscopy that the material was not pure. Due to the impure and limited amount of material obtained from the reaction, this method was abandoned and the use of sodium hydride as the base was investigated [86].

Addition of one equivalent of sodium hydride to a DMF solution of **49** resulted in a colour change from beige to pink, indicating formation of the imide anion. After the addition of 1.6 equivalents of allyl bromide to the reaction mixture, reversal of the colour change was observed. This observation was supported by TLC results which showed the formation of a new compound. Analysis by ^{1}H NMR spectroscopy of the crude product showed a mixture of *N*-allyl-4-bromo-1,8-naphthalimide (**45**) and 4-bromo-1,8-naphthalimide (**49**). Integration from ^{1}H NMR spectroscopy suggested that the majority (67%) of the material was the starting material, **49**. Purification was carried out on a subsample of the material by column chromatography to give the desired product. Analysis by ^{1}H NMR spectroscopy confirmed the imide proton was no longer present at 11.9 ppm with ^{13}C NMR showing three extra carbon signals

(compared to **49**) at 132.68 ppm (the central allyl carbon), 116.50 ppm (the terminal carbon) and 41.86 ppm (the final allyl carbon) representing the three carbons present in the newly added allyl group.

In the second synthesis attempt, in order to improve the purity of the reaction products, sodium hydride was added at 0^{o}C and stirred for 15 minutes before addition of allyl bromide. Column chromatography yielded 7.7% of **45**. In an attempt to improve this poor yield, the amount of base was increased to three equivalents resulting in the formation of a bright mustard yellow coloured mixture. TLC indicated all starting material had been consumed and a pure material had formed. Analysis of the material by ^{1}H NMR spectroscopy confirmed the material as *N*-allyl-4-bromo-1,8-naphthlimide (**45**), obtained with high purity in 74% yield. Despite numerous attempts, this result was unable to be replicated and further improvements to the method were required.

Several variations of the method were trialled including those with use of increased equivalents of sodium hydride, different solvents and different temperatures. However a reproducible and high yielding method for the synthesis of **45** was not obtained. Chromatography, whilst successful in purifying the product, gave low yields and was a complicated and time consuming process. Consequently, alternative synthetic methods were explored.

Investigations in the literature found that a terminal allyl group had been introduced to **44** previously, utilising a one-step method involving reflux conditions with allylamine in ethanol [48, 101]. A similar method using toluene was also reported [102], however Niu's method [48] was the first investigated due to its short reaction time (2 hours).

Allylamine (1.1 equivalents) was added to **44** in anhydrous ethanol and heated under reflux for one hour (Scheme 9). Upon cooling, **45** was found to precipitate as an off-white powder in 94% yield. Analysis by ^{1}H NMR spectroscopy showed the product was consistent with that described for previous syntheses of **45** in this section, with the melting point agreeing well with the literature value [48]. This method was found to be highly reliable with the desired material obtained in both high purity and high yield (>

90%). Niu's [48] single step method was used in preference to the multi-step procedures in all future syntheses of **45**.

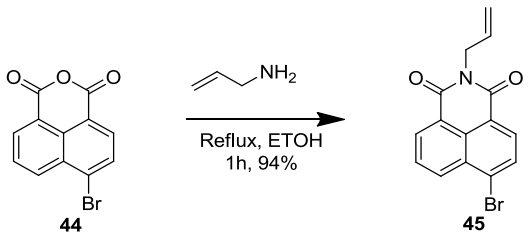

44 45

Scheme 9: Single step synthesis of *N*-allyl-4-bromo-1,8-naphthalimide (45).

3.3 Attachment of the spacer to *N*-allyl-4-bromo-1,8-naphthalimide (45)

Addition of a spacer molecule to the successfully synthesised allyl functionalised fluorophore **45** was necessary in order to covalently link it to the receptor moiety in the final synthesis step. As discussed in Section 1.3.4, a variety of different spacer groups have been employed for this purpose, with the most promising results obtained using the 2- and 4-aminobenzylamines [50, 51, 66]. The following three sections detail the results and observations of experiments directed towards the incorporation of aminobenzylamine at the 4-position of the naphthalimide.

*3.3.1 Synthesis of N-allyl-4-(4-aminobenzylamine)-1,8-naphthalimide (**51**)*

Initial approaches towards the synthesis of **51** (depicted in Scheme 10) were based on previous work by Parkesh, Lee and Gunnlaugsson who synthesised *N*-ethyl-4-(4-aminobenzylamine)-1,8-naphthalmide [66]. The imide **45** was heated to 110^{o}C and stirred for 10 minutes before excess 4-aminobenzylamine was added. The temperature 110^{o}C was used in preference to 130^{o}C (used by Parkesh *et al*.), as **45** had a lower melting point (m.p. 198^{o}C-200^{o}C for *N*-ethyl-4-bromo-1,8-naphthalimide compared to 143^{o}C-145^{o}C for **45**) than the imide used in this study. After 30 minutes, TLC showed a yellow spot (inconsistent with the starting material **45**) suggesting that another compound had been formed in the reaction. Water was added to the reaction, precipitating out the product in 60% yield.

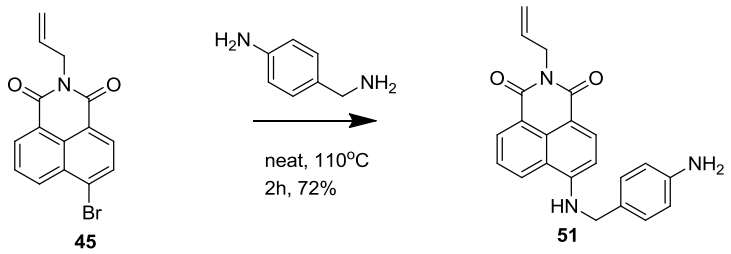

Scheme 10: Synthesis of *N*-allyl-4-(4-aminobenzylamine)-1,8-naphthalimide (51)

The ^{1}H NMR spectrum of the collected material was similar to that reported by Parkesh [66] for *N*-ethyl-4-(4-aminobenzylamine)-1,8-naphthalimide, along with a small impurity from the starting materials (accounting for the change from an ethyl group to an allyl group). The proton of the secondary amine at the 4-position of the naphthalimide unit was observed as a triplet in the ^{1}H NMR spectrum at 8.4 ppm (cf. Parkesh who observed it as a broad signal at 8.4 ppm), with the aromatic protons of the benzylamine observed as doublets each integrating for two protons at 7.1 ppm (cf. 7.1 ppm) and 6.5 ppm (cf. 6.5 ppm). The naphthalimide proton in the 3-position was observed to shift to 6.7 ppm (cf. 6.7 ppm) from 8.5 ppm, due to the replacement of the highly electronegative bromo group with an amino group. The two NH protons from the aniline group were observed as a singlet accounting for two protons at 5.1 ppm (cf. 5.0 ppm). The newly incorporated methylene group was observed as a doublet at 4.5 ppm (cf. 4.5 ppm). FTIR confirmed the addition of the aminobenzylamine group with a sharp signal at 3887 cm^{-1} indicative of the amino group. After recrystallisation from ethanol the recovered yield was only 6%.

During repeat syntheses, reaction temperature was identified as being crucial to ensuring high yield. In one example, the temperature was observed to have gone above 110^{o}C. The reaction was cooled and continued, however upon finishing the reaction only resulted in a 26% crude yield. Conversely if reaction temperature was observed to drop, a solid material was quickly formed. In one instance of this occurring, analysis by ^{1}H NMR spectroscopy showed a pure product had been obtained, reinforcing that only a short reaction time was required. Yield however was poor at only 27%. Contrary to this other attempts were unsuccessful in obtaining a pure product. This highlighted that both temperature control and length of the reaction were critical to ensure successful synthesis. Careful control of both reaction

temperature and reaction time ensured yields of greater than 60% with a highest yield of 73% obtained.

*3.3.2 Synthesis of N-allyl-4-(2-aminobenzylamine)-1,8-naphthalimide (**50**)*

After successful introduction of the *para* substituted benzylamine spacer at the 4-position of the naphthalimide ring, attention was directed towards incorporation of the *ortho* substituted benzylamine spacer (Scheme 11).

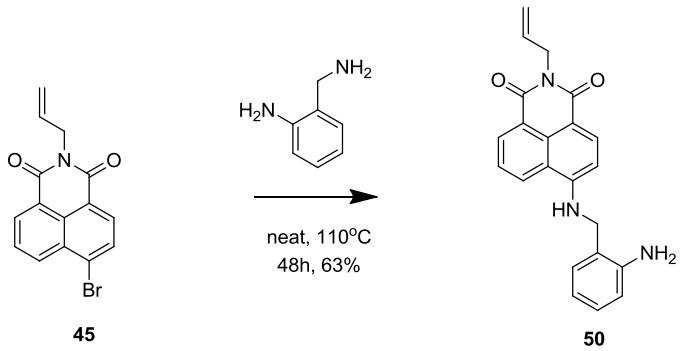

45 **50**

Scheme 11: Synthesis of *N*-allyl-4-(2-aminobenzylamine)-1,8-naphthalimide (50)

Owing to the similarities between *N*-allyl-4-(2-aminobenzylamine)-1,8-naphthalimide (**50**) and **51**, the method developed for the synthesis of **51** was initially trialled. Imide **45** was stirred for 10 minutes at 110°C before addition of excess 2-aminobenzylamine (added as a solid (m.p.=58°C-61°C) [103]). After one hour, water was added to precipitate the product.

Proton NMR spectroscopy analysis of the resulting flaky red crystalline material exhibited signals relating to both the expected product and the starting materials, with integration suggesting approximately 25% purity. The formation of the new material was confirmed by the presence of a new resonance at 8.35 ppm which was assigned as the NH proton from the amine in the 4-position of the naphthalimide ring.

In order to improve yield of the reaction, DMF was investigated as a reaction solvent. The naphthalimide **45** was heated at 110°C for ten minutes prior to the addition of DMF and five equivalents of 2-aminobenzylamine. The reaction was maintained at 110°C (with stirring) for one hour, and water was added to precipitate the product. Analysis of the resulting viscous red material by ^{1}H NMR spectroscopy showed

similarity with the previously described spectrum for **51** (molecule with the 4-aminobenzylamine spacer) however there were some impurities still present. As detailed in Section 1.3.4, overnight heating in a sealed tube had been previously employed to obtain a similar product (*N*-ethyl-4-(2-aminobenzylamine)-1,8-naphthalimide) [50]. Consequently, in an attempt to improve the reaction yield and purity an overnight heating step was investigated (although not using a sealed tube). Analysis of the residue by ^{1}H NMR spectroscopy showed an impure material had formed, which bore little resemblance to the starting material or the expected product suggesting the longer reaction time was not beneficial.

From a purely mechanistic point of view, it would appear that the nucleophillic aromatic substitution reaction should proceed quite readily, as was observed for the reaction involving 4-aminobenzylamine. It would appear unlikely that the use of excess 2-aminobenzylamine inhibited the reaction as no issue was observed with excess 4-aminobenzylamine (Section 3.3.1). It would also be unexpected for 2-aminobenzylamine to attach to multiple parts of the molecule, particularly as 4-aminobenzylamine was observed not to. The only major difference between the two reactions other than the substitution (2 vs. 4) and potential steric issues, was the use of DMF as a solvent in the 2-aminobenzylamine reactions. Therefore further experiments were undertaken in a solvent free environment. Repeating the above experiment without DMF and monitoring by TLC showed a mixture of materials forming. Water was added after 48 hours to precipitate the product, with ^{1}H spectroscopy analysis performed on the recovered material. A much cleaner spectrum (but still impure) was obtained, than that obtained when using DMF as solvent, suggesting DMF was playing a role in the reaction or that too much DMF was being used (i.e a concentration issue).

Further thought was given to the purity of the reactants used in the reaction, as it was known from the literature that it should be possible to obtain the compound in a relatively pure form without the use of column chromatography [50]. Due to ^{1}H NMR spectroscopy data indicating that the previously synthesised imide **45** was pure (Section 3.2), attention was directed towards the purity of 2-aminobenzylamine. Initial analysis by ^{1}H NMR spectroscopy suggested that no organic impurity was present. In

order to further investigate the purity a crude recrystallisation was performed on 2-aminobenzylamine using hexane. Upon recrystallisation the 2-aminobenzylamine material was observed to go from a crystalline brown material, to white-sheet like crystals, suggesting the starting material did contain some impurity not observable using ^{1}H NMR spectroscopy. Initial reactions utilising the recrystallised 2-aminobenzylamine (without DMF) showed that the product **50** was able to be synthesised in pure form.

Crude **50** was recrystallised from ethanol, with the few crystals recovered confirmed by ^{1}H NMR spectroscopy to be consistent with **50**. The five naphthalimide protons were observed at 8.8, 8.5, 8.2, 7.7 and 6.7 ppm, with the last proton being that at the 3-position of the naphthalimide ring and shifted due to the change from a bromo group to an NH group. The 4-amino proton resonance was observed at 8.35 ppm as a triplet, consistent with observations for **51**. The aminobenzylamine protons were observed as triplets at 6.9 ppm and 6.5 ppm and doublets at 7.0 and 6.6 ppm. These were not consistent with **51** due to the four protons being in different chemical environments (there are only 2 chemical environments for the aminobenzylamine protons in **51**). All other proton signals were similar to those observed for **51**. One minor unassignable peak corresponding to an unknown impurity was observed at 4.4 ppm.

As would be expected several new peaks were observed in the ^{13}C spectrum when the product was compared to the starting material, confirming addition of the aminobenzylamine group. The methylene group introduced was evident as a resonance 43.28 ppm and apart from one of the allyl carbons present in the starting material, is the only signal in the spectrum below 100 ppm. Two dimensional HMQC experiments also confirm that this carbon correlates with the methylene protons.

Reproducibility of the reaction was an issue, with subsequent experiments producing impure mixtures, rather than the mostly pure product above. As the purity of 2-aminobenzylamine had been identified as an issue in successfully forming the product, a new bottle of 2-aminobenzylamine was sourced and the material obtained was vastly different in appearance to the original, supporting the theory of some contaminant

being present in the original bottle. Using the new source of 2-aminobenzylamine mixed results were obtained. Some experiments produced **50** in a pure form, however most attempts resulted in impure mixtures.

Finally, the reaction was undertaken as previously with the imide **45** stirred at 110^{o}C for 10 minutes before addition of five equivalents 2-aminobenzylamine, except this time stirring was continued for approximately forty eight hours. Water was added to precipitate out the product, with the collected material recrystallised from ethanol. Analysis by ^{1}H NMR spectroscopy of the recrystallised material showed it was consistent with previously obtained pure **50**, suggesting a longer reaction time was beneficial. Further attempts using the longer reaction time, were found to produce similar results, with the highest yield obtained being 63%.

*3.3.3 Synthesis of N-allyl-4-(3-aminobenzylamine)-1,8-naphthalimide (**52**)*

The molecule 3-aminobenzylamine was also inserted as a spacer. It was envisaged similar chemistry to that observed for the 2-aminobenzylamine and 4-aminobenzylamine would be required for the synthesis and due to its much shorter reaction time, the method for the synthesis of **51** (with the 4-aminobenzylamine spacer) was initially trialled. Imide **45** was stirred at 110^{o}C for 10 minutes before addition of excess 3-aminobenzylamine (depicted in Scheme 12). After three hours, water was added with the product precipitating out as a yellow solid. This solid was recrystallised from ethanol with ^{1}H NMR spectroscopy indicating the product, **52**, was obtained in pure form.

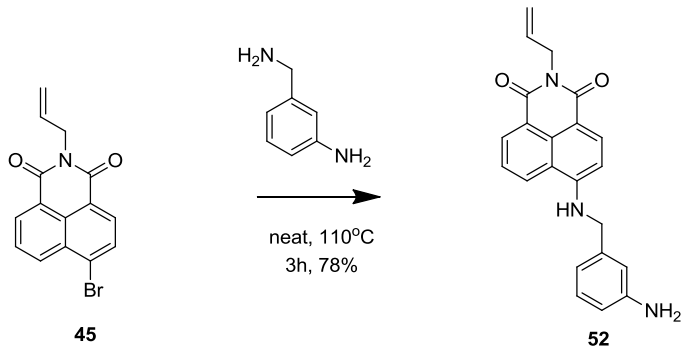

45 **52**

Scheme 12: Synthesis of *N*-allyl-4-(3-aminobenzylamine)-1,8-naphthalimide (52).

Consistent with ^{1}H NMR spectra for similar compounds **50** and **51**, the naphthalimide protons resonances were identified at 8.8, 8.5 (overlaps with 4-amino NH proton), 8.2,

7.7 and 6.6 ppm (with the signal at 6.6 ppm due to the proton at the 3-position of the naphthalimide which was shifted due to the change from a bromo group to the amino group). The 4-amino NH proton was observed at 8.5 ppm, overlapping with one of the naphthalimide protons. The four aminobenzylamine protons were identified as a triplet at 7.0 ppm (the proton in the 5 position), a singlet at 6.6 ppm (the proton in the 2 position), and two doublets accounting for the final two protons at 6.5 ppm and 6.4 ppm. The resonance relating to the newly introduced aniline protons was observed at 4.5 ppm. Further repetition showed that the reaction was both scalable and reproducible with a highest yield of 78%.

3.4 Incorporation of the recognition unit

After successful alkylation of the anhydride (Section 3.2) and addition of the spacer molecules (Section 3.3), attention was directed towards incorporation of the recognition group; the final stage in the preparation of the sensor molecules. The following section details the synthesis of the final sensor molecules, with an isocyanate or isothiocyanate reacted with the amine group on the spacer.

Reactions involving Phenyl Isocyanate

*3.4.1 Synthesis of N-allyl-4-(4-(N-phenylureido)benzylamino)-1,8-naphthalimide (**1**)*

Initial investigations to synthesise *N*-allyl-4-(4-(*N*-phenylureido)benzylamino)-1,8-naphthalimide (**1**) utilised **51** and phenyl isocyanate. The methodology was based on the methods used by Pfeffer *et al.* [49] and Gunnlaugsson *et al.* [51] to synthesise *N*-ethyl-4-(4-(*N*-phenylthioureido)benzylamino)-1,8-naphthalimide where phenyl isothiocyanate was employed to form the recognition unit, as described in Section 1.5. It was hypothesised that as phenyl isocyanate was a structurally similar molecule it would react using a similar method. **51** was dissolved in anhydrous chloroform and stirred at room temperature. Phenyl isocyanate (one equivalent) was added and the reaction was stirred at room temperature overnight. Subsequent TLC analysis showed little difference between the starting material and the material produced in terms of their retention factors. However it was noted that the two compounds were different colours, indicating the possible presence of a new compound. Water was added to the

reaction flask to precipitate out the product. Analysis by ^{1}H NMR spectroscopy of the recovered material showed a high degree of similarity with the starting material **51** with all signals accounted for but also some signals which could be attributed to the desired product, including the aromatic protons of the receptor between 7.5 and 7.2 ppm. Column chromatography was carried out (100% chloroform, alumina). Solubility in this solvent was poor (with the compound being relatively insoluble in most common solvents), with the solute appearing to come out of solution when it was added to the top of the column, in turn affecting the successful separation of the components.

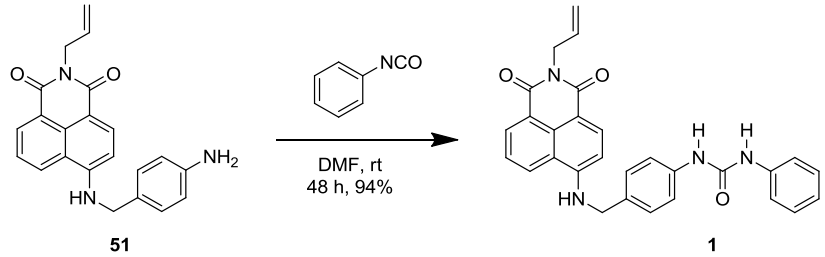

Scheme 13: Synthesis of *N*-allyl-4-(4-(*N*-phenylureido)benzylamino)-1,8-naphthalimide (1).

The above reaction was repeated using anhydrous DMF as solvent, along with the addition of triethylamine (TEA) (depicted in Scheme 13). Triethylamine was added as personal communication with Pfeffer indicated it would have a beneficial effect on the reaction [104]. After stirring for sixty hours at room temperature, TLC showed a mixture of starting material and a material which was thought to be the product. Stirring was continued and after a further twenty-four hours, with no change in the reaction detected by TLC, an additional 0.2 equivalents of phenyl isocyanate (1.2 equivalents total) and one drop of TEA were added. Stirring was continued for a further 15 hours whereupon TLC indicated there was no starting material present. Addition of water to the flask was found to precipitate out the suspected product as yellow crystals. After recrystallisation from methanol, the ^{1}H NMR spectrum obtained was consistent with what would be expected for **1** (comparing to similar compounds) [49-51]). The newly introduced urea protons were apparent as two singlets right next to each other at 8.6 ppm. The *ortho* protons on the newly introduced aromatic ring appear as part of a multiplet where they overlap with two of the aminobenzylamine protons at 7.4 ppm. The aromatic protons in the *meta* positions appear as a multiplet

at 7.2 ppm, and the final aromatic proton (*para* position) was observed at 6.9 ppm. The naphthalimide protons are present at 8.8, 8.5, 8.2, 7.8 and 6.7 ppm. The remaining two aminobenzylamine protons were present as a doublet at 7.3 ppm. The 4-amino NH proton is present as a triplet at 8.5 ppm. Resonances for the allyl protons were present as previously described, whilst the methylene group in the spacer was at 4.6 ppm, overlapping with proton signals from the allyl moiety.

As the reaction was observed to proceed using an excess of phenyl isocyanate, the reaction from above was repeated, with an excess from the outset. Phenyl isocyanate (1.5 equivalents) and three drops of TEA were added to **51** in DMF. After 48 hours, TLC analysis showed the evolution of a new pure compound. Water was added to precipitate out the product, which was obtained as a bright yellow powder in 94% yield. The recovered material was confirmed using ^{1}H NMR spectroscopy as **1**, with spectra consistent with the assignment described above. The reaction was found to be reproducible and scalable.

As further batches of **1** were synthesised it was noted using ^{1}H NMR spectroscopy that the chemical shift of the two NH protons between batches shifted, suggesting a possible change in the product (as depicted in Figure 18 (original) and Figure 19 (changed)). The order of urea protons and one of the naphthalimide protons was reversed.

Considering all of the starting materials appeared to be pure (using ^{1}H NMR spectroscopy) it would make sense that the same material was being obtained. It was known that NH proton shifts are susceptible to a range of influences such as sample concentration [105] and the water content of the NMR spectroscopy solvent. Therefore it was possible that the same material was obtained with the differences in the resonances simply due to the analysis by ^{1}H NMR spectroscopy under slightly different environmental/chemical conditions. A concentration study showed that an increase in sample concentration was not a likely cause, with no shift in the protons observed with increasing concentration (Figure 20).

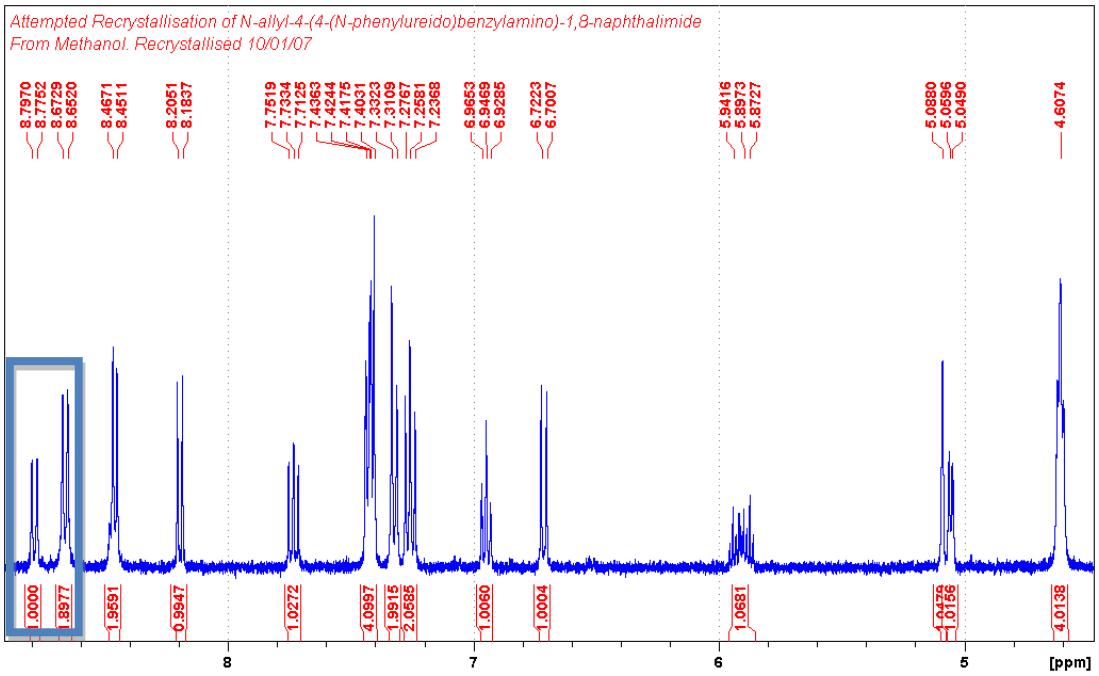

Figure 18: **^{1}H NMR spectrum of *N*-allyl-4-(4-(*N*-phenylureido)benzylamino)-1,8-naphthalimide (1) (Original Spectrum, protons of interest highlighted).**

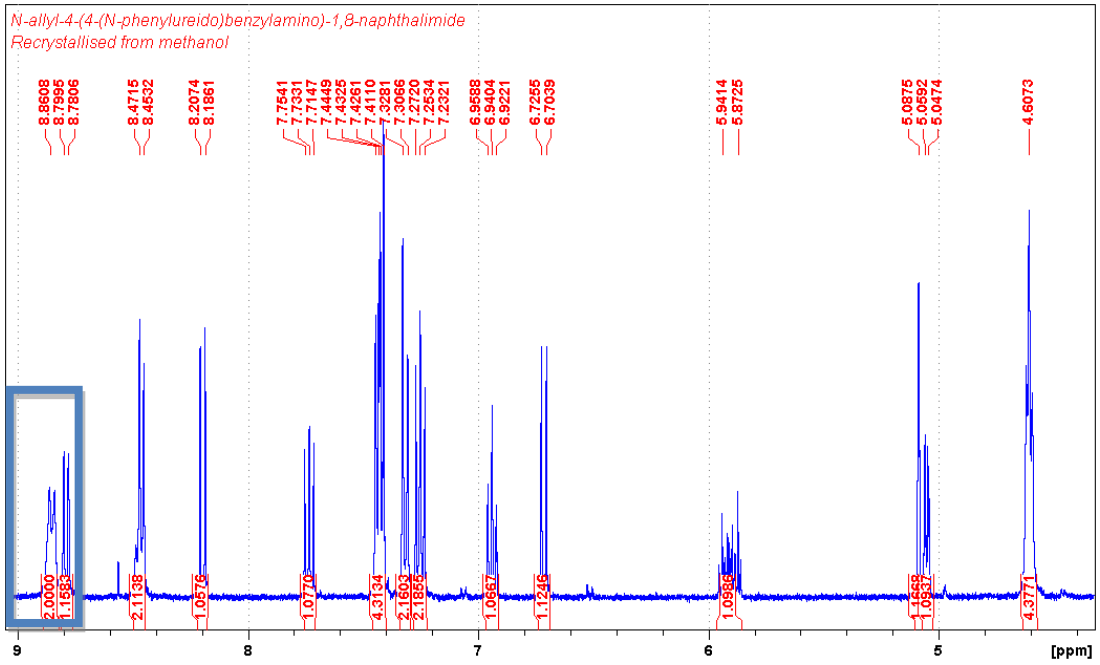

Figure 19: ^{1}H NMR spectrum of *N*-allyl-4-(4-(*N*-phenylureido)benzylamino)-1,8-naphthalimide (1) (Changed Spectrum, protons of interest highlighted).

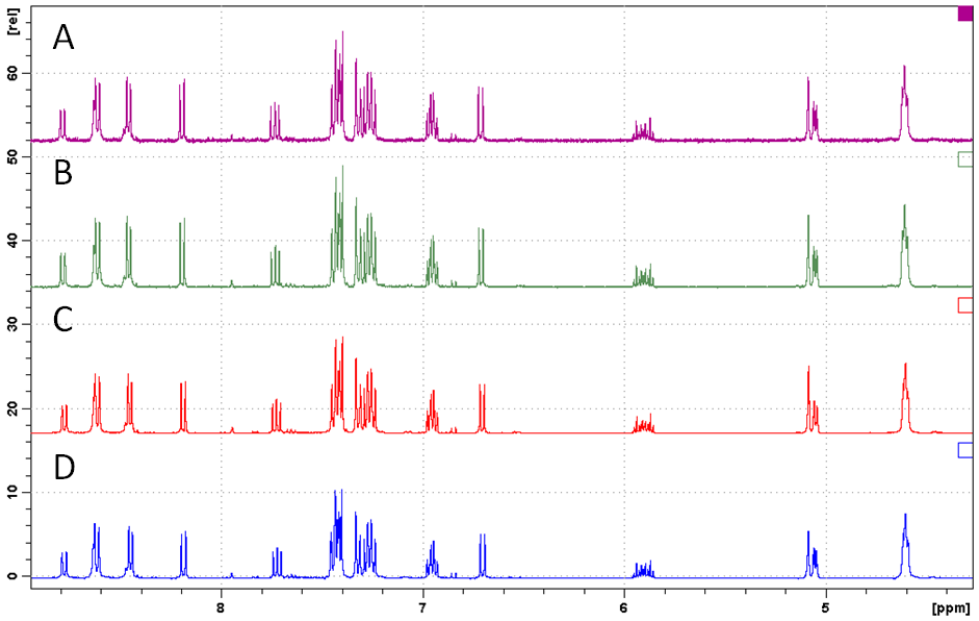

Figure 20: ^{1}H NMR spectrum of *N*-allyl-4-(4-(*N*-phenylureido)benzylamino)-1,8-naphthalimide (1) at different concentrations. A=1 mg/mL, B=2.5 mg/mL, C=10 mg/mL, D=15 mg/mL.

The purity of phenyl isocyanate was also considered as a possible source of contamination in the final product. Analysis by ^{1}H NMR spectroscopy of the different sources of phenyl isocyanate used in the various syntheses suggested little organic impurity was present. Purification was undertaken using Kugelrohr distillation to remove water. Freshly distilled phenyl isocyanate and triethylamine were added to a stirred solution of 51 in DMF at room temperature. Subsequent TLC after 16 hours, showed the reaction to be complete. Water was added in an attempt to precipitate the product. Whilst the reaction mixture was observed to go to the bright yellow colour associated with product formation, no precipitate was collected using a Hirsch funnel. Consequently the filtrate was extracted in ethyl acetate, with resultant 1H NMR spectroscopy on the obtained material consistent with the original spectra obtained for 1, suggesting that the use of a purified isocyanate was beneficial to the successful synthesis of 1. When this reaction was repeated, 1H NMR spectroscopy showed the protons again shifting, suggesting conditions other than water affecting the stability of the isocyanate were the cause.

In order to confirm the successful synthesis of N-allyl-4-(4-(N-phenylureido)benzylamino)-1,8-naphthalimide (**1**), given the shifting NH proton signals, ESI-MS was undertaken on a number of samples. Samples were prepared

initially as 1mg/mL samples in DMF and then diluted to 10 μg/mL in acetonitrile. All six samples were shown to contain **1**, however, purity was found to be an issue when the samples were run through a liquid chromatograph (multiple small peaks were present in the chromatograph, as well as the large expected product peak). The positive ion was identified as 477.2 m/z $[M+H]^+$ and the negative ion was identified as 475.2 m/z $[M-H]^-$. The m/z of the dominant ion of the contaminants was 117.9 and 213.2 in positive ion mode and 211.2 in the negative ion mode. These were inconsistent with the starting materials and final products.

3.4.2 Synthesis of N-allyl-4-(2-(N-phenylureido)benzylamino)-1,8-naphthalimide (4)

The initial approach towards the synthesis of *N*-allyl-4-(2-(*N*-phenylureido)benzylamino)-1,8-naphthalimide (**4**) (depicted in Scheme 14) used the same method as used to synthesise **1** (Section 3.4.1). *N*-allyl-4-(2-aminobenzylamine)-1,8-naphthalimide (**50**), was dissolved in anhydrous DMF and stirred at room temperature. Phenyl isocyanate (1.4 equivalents) and three drops of TEA were added. TLC analysis after 16 hours (100% chloroform, alumina) indicated an incomplete reaction. Regular TLC monitoring over the course of one week still indicated the reaction was not heading towards completion. The role of temperature in the rate of the reaction was investigated with the temperature increased to 40°C. After 24 hours at this elevated temperature, TLC analysis (100% chloroform, alumina) still showed the reaction to be incomplete. Increasing the temperature to 60°C also failed. Finally the temperature was increased to 100°C for a period of 4 hours, after which TLC showed no change in the reaction progress. At this point water was added to precipitate the product out for further analysis.

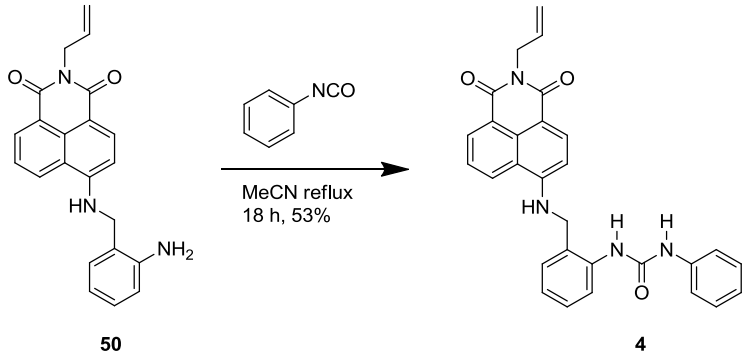

Scheme 14: Synthesis of *N*-allyl-4-(2-(*N*-phenylureido)benzylamino)-1,8-naphthalimide (4).

Analysis by ^{1}H NMR spectroscopy showed the product was forming, with a spectrum similar to that obtained for **1**, with some starting material impurities present. The similarity of the ^{1}H NMR spectrum obtained to the spectrum of **1** was expected as the only difference between **4** and **1** is the position of the urea group with regards to the spacer. Column chromatography (50:50, ethyl acetate: chloroform, alumina) was carried out on the material. Solubility of the mixture in the mobile phase was poor; however, three components were eventually separated on the column. Analysis by ^{1}H NMR spectroscopy of the purified material gave results that were consistent with the expected spectrum for **4**. The two newly introduced urea proton resonances were observed as broad singlets at 9.2 ppm and 8.3 ppm. The naphthalimide proton resonances were observed as doublets at 8.8, 8.5, 8.2 and 6.6 ppm, with a multiplet at 7.7 ppm (overlayed with an aromatic proton signal). The 4-amino NH proton resonance was present at 8.4 ppm. The aromatic protons from both the aminobenzyl group and the phenyl ring from the addition of the isocyanate group are exhibited as a number of signals in the region 7.7 - 6.9 ppm. Two-dimensional COSY experiments on the sample failed to provide conclusive evidence as to which signals were from each group. The allyl protons exhibited the resonances discussed previously, whilst the methylene protons were observed at 4.6 ppm, partially resolved from a signal relating to the allyl protons at 4.6 ppm as a doublet. Similar results were obtained when using chloroform, a solvent used by other researchers for similar reactions [49, 51] and also trialled for the synthesis of **1**.

Acetonitrile was also investigated as a reaction solvent. **50** was heated at reflux in anhydrous acetonitrile. Phenyl isocyanate (1.5 equivalents) was added and stirring continued over approximately 18 hours. Subsequent TLC showed only one material present, which differed from the starting material. As a result, the reaction was removed from the heat, with the suspected product settling out upon cooling. The product was collected using a Hirsch funnel and washed with cold acetonitrile. Analysis by ^{1}H NMR spectroscopy confirmed the material as **4** in a yield of 51%. The reaction was found to be reproducible with the best yield obtained being 53%, suggesting acetonitrile was the solvent of choice.

3.4.3 Synthesis of N-allyl-4-(3-(N-phenylureido)benzylamino)-1,8-naphthalimide (5)

Initial approaches towards the synthesis of *N*-allyl-4-(3-(*N*-phenylureido)benzylamino)-1,8-naphthalimide (**5**) from *N*-allyl-4-(3-aminobenzylamine)-1,8-naphthalimide **52** were inspired by previous experiments reacting **50** (with the 2-aminobenzyl spacer, Section 3.3.2) and **51** (with the 4-aminobenzyl spacer, Section 3.3.1) with phenyl isocyanate. **52** was suspended in anhydrous acetonitrile (dissolving upon heating) and heated under reflux in the presence of 1.5 equivalents phenyl isocyanate (as depicted in Scheme 15). It was noted that as the reaction progressed an orange material was observed to form. After 3 hours, TLC monitoring indicated the reaction was complete. The reaction was removed from the heat with the product precipitating out upon cooling. The solid material was recovered *via* Hirsch funnel filtration and recrystallised from methanol, with ^{1}H NMR spectrum showing the required product **5** was obtained in a yield of 73%.

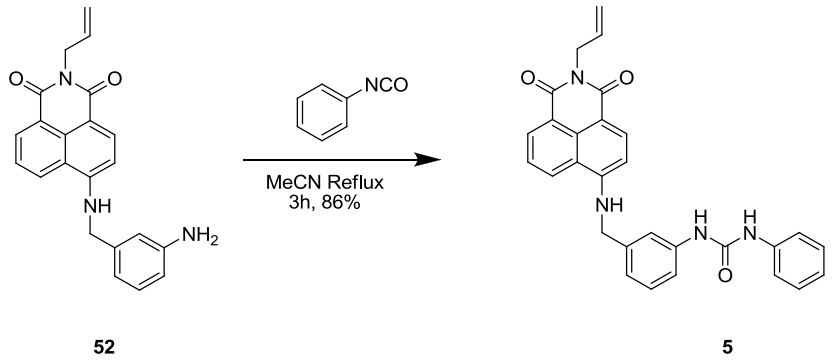

52 **5**

Scheme 15: Synthesis of *N*-allyl-4-(3-(*N*-phenylureido)benzylamino)-1,8-naphthalimide (5).

The two newly introduced urea protons were observed at 8.7 and 8.6 ppm as broad singlets. The naphthalimide protons were observed as doublets at 8.8, 8.5, 8.2 and 6.7 ppm and a multiplet at 7.7 ppm. The 4-amino NH proton was observed as a triplet at 8.6 ppm. The aminobenzyl proton in the 2-position (between where the aromatic ring is joined to the spacer (the 1-position) and the recognition unit (the 3-position) was present at 7.4 ppm as a broad singlet. The other aromatic protons were represented as a multiplet at 7.4 ppm (integrating for 3 protons, slightly resolved from the single aminobenzylamine proton described above), a multiplet at 7.3 ppm (3 protons), a doublet at 7.0 ppm (1 proton) and a triplet at 6.9 ppm (1 proton). Resonances for the

allyl protons were present as previously described, with the methylene protons slightly resolved from two of the allyl protons at 4.6 ppm. The reaction was shown to be scalable and able to be repeated (maximum yield - 86%).

Reactions involving Phenyl Isothiocyanate

*3.4.4 Synthesis of N-allyl-4-(4-(N-phenylthioureido)benzylamino)-1,8-naphthalimide (**2**)*

Initial approaches towards the synthesis of *N*-allyl-4-(4-(*N*-phenylthioureido)benzylamino)-1,8-naphthalimide (**2**) (depicted in Scheme 16) were based on previous work by both Pfeffer *et al.* [49] and Gunnlaugsson *et al.* [51] described in Section 1.5. **51** was stirred in dry chloroform at room temperature and one equivalent of phenyl isothiocyanate was added. After eighteen hours TLC analysis showed little difference between the starting material and any product formed. Stirring was continued at room temperature for a further forty-eight hours however no progress was observed using TLC. Water was added to precipitate the product, with ^{1}H NMR spectroscopy on the recovered material indicating it was **51**, the starting material.

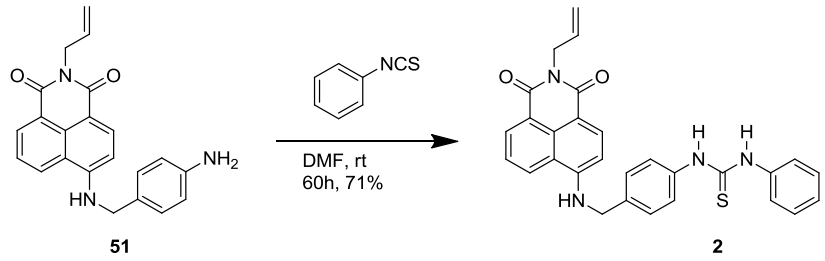

Scheme 16: Synthesis of *N*-allyl-4-(4-(*N*-phenylthioureido)benzylamino)-1,8-naphthalimide (2).

In the next attempt at the synthesis of **2** the reaction was repeated as above with the addition of three drops of triethylamine to the solution of **51** (As detailed for the synthesis of **1** (Section 3.4.1)). Monitoring by TLC over several days showed the reaction to be incomplete, with the stirring turned off after one week and the product allowed to precipitate upon standing. Proton NMR spectroscopy showed a mixture of product and staring material was obtained. A resonance was observed at 9.7 ppm which would be expected for the thiourea protons. This indicated there was some progress in obtaining the desired product.

As anhydrous DMF had been used successfully for the synthesis of **1** (Section 3.4.1) it was trialled as a solvent in an attempt to improve the purity of the reaction products. **51** was dissolved in DMF and stirred at room temperature. One equivalent of phenyl isothiocyanate and one drop of triethylamine were added to the stirred solution. After sixteen hours it was observed that the reaction had changed from orange in colour to red in colour. TLC analysis conducted on a sample from the reaction flask indicated a mixture of suspected product and starting material. After stirring for a further 24 hours, TLC analysis showed only the suspected product present. Water was added and the mixture was left to stand overnight to allow the product to precipitate. After no precipitate was observed, the product was extracted into ethyl acetate, where a small amount of solid product was obtained after the solvent was removed *in vacuo*. Comparison of the ^{1}H NMR spectrum of the obtained material with the reported ^{1}H NMR spectrum of *N*-ethyl-4(-4-(*N*-phenylthioureido)benzylamino)-1,8-naphthalimide [51] showed the two were similar although the synthesised material appeared to contain some impurities.

In order to push the reaction to completion, the addition of excess phenyl isothiocyanate was investigated, as addition of excess phenyl isocyanate had been beneficial in the synthesis of **1** (section 3.4.1). **51** was dissolved in DMF and stirred at room temperature. An excess of phenyl isothiocyanate (1.5 equivalents) and one drop of triethylamine were added, with stirring continued at room temperature for 48 hours. TLC analysis showed only one spot on the TLC plate, differing to that of the starting material and of a 'brighter' shade of yellow. Water was added to precipitate out the product, which caused the previously transparent orange coloured solution to change into a bright yellow solution. The product was not observed to crystallise out, so the product was extracted into ethyl acetate, which after the solvent was removed *in vacuo* resulted in a viscous oil. Analysis by ^{1}H NMR spectroscopy showed the oil was similar to the expected product *N*-allyl-4-(4-(*N*-phenylthioureido)benzylamino)-1,8-naphthalimide (**2**), however there still remained some impurities. It was thought that the impurities were from phenyl isothiocyanate starting material as the similar reaction detailed in section 3.4.1 (same solvent, use of TEA) involving phenyl isocyanate with the same source of the naphthalimide **51** was successful.

An experiment was undertaken using a different bottle of phenyl isothiocyanate, to investigate if impurities from the isothiocyanate could be inhibiting successful reaction progress. The reaction was stirred for sixty hours under nitrogen at room temperature. After this time, TLC (100% chloroform/alumina) indicated the reaction was complete. Water was added with the product precipitating out upon standing. Analysis by ^{1}H NMR spectroscopy of the recovered yellow material was consistent with that observed for the literature compound *N*-ethyl-4-(4-(*N*-phenylthioureido)benzylamino)-1,8-naphthalimide [51], accounting for the difference between an allyl group and an ethyl group. The newly introduced thiourea proton resonances were evident as a broad singlet at 9.8 ppm. The five naphthalimide proton resonances were located as doublets at 8.8, 8.5, 8.2 and 6.7 ppm and as a multiplet at 7.7 ppm. The 4-amino proton resonance was identified as a triplet at 8.5 ppm (only slightly resolved from the naphthalimide doublet). The majority of the aromatic protons from both the aminobenzylamine ring and the phenyl isocyanate occur as a series of multiplets between 7.5 ppm and 7.0 ppm. The allyl proton resonances were again present as described previously, with the methylene protons overlapping with part of the allyl signal at 4.6 ppm. This result suggested that the source of the phenyl isothiocyanate did have an impact on reaction success. Repetition of this result was difficult, with an upscaled experiment producing an orange coloured material as opposed to a bright yellow powder. A direct repetition (i.e. same amounts of reactants) was also observed not to go to completion. The use of further phenyl isothiocyanate after the initial amount was added, to push the reaction to completion was also met with no success. As the purity of phenyl isothiocyanate had been identified as a possible source of contamination, a third bottle of isothiocyanate was examined. Repeating the successful experiment using the third bottle, showed the reaction to be complete (by TLC) within 24 hours. Water was added to precipitate out the product and a bright yellow fluorescent powder was collected. However, repetition and up-scaling again proved difficult.

The use of Kugelrohr distillation to purify phenyl isothiocyanate was also investigated. Despite TLC results indicating the product had formed using the above method, ^{1}H NMR spectroscopy showed the viscous substance obtained was an impure version of **2**.

Many attempts at a successful reaction obtained this viscous substance rather than the pure crystalline solid.

Previous experiments detailed for the synthesis of **1** (section 3.4.1) and **4** (section 3.4.2) indicated that increasing the amount of equivalents, and adding extra equivalents after the reaction had started, allowed these similar reactions to go to completion and a more pure product to be formed. Therefore the number of equivalents of phenyl isothiocyanate added was further increased to two, in an effort to force the synthesis of **2** to completion. The reaction was again stirred at room temperature for approximately sixty hours. Subsequent TLC showed that the reaction was complete. Water was added to precipitate out the product. Analysis by ^{1}H NMR spectroscopy of the product showed that the material obtained was as expected for **2** with a slight DMF impurity (71% yield).

Due to the inability of the developed method to reliably reproduce pure **2**, new methodologies were required to ensure successful synthesis of the product. The method developed by Ali *et al.* [52], which was used successfully for the synthesis of **4**, was investigated for the synthesis of **2**. Under a nitrogen atmosphere, **51** was dissolved in anhydrous acetonitrile and heated under reflux. Phenyl isothiocyanate (1.5 equivalents) was added with heating continued under reflux conditions. Regular monitoring *via* TLC indicated a new material was forming as a result of the reaction and therefore the reaction was continued under reflux. After seventeen hours, TLC showed that the starting materials had been consumed and a new material had been made. The reaction was removed from the heat, with the product precipitating out upon cooling. The solid material was collected using a Hirsch funnel and washed with acetonitrile. The ^{1}H NMR spectrum of the recovered material was consistent with what had been observed in the successful DMF reactions to produce **2**. A repetition of the above reaction was found to yield 54% of yellow crystals. Further attempts at synthesis using this method however proved unsuccessful with focus turned towards the synthesis of other sensor molecules and the immobilisation of these sensors.

*3.4.5 Attempted synthesis of N-allyl-4-(2-(N-phenylthioureido)benzylamino)-1,8-naphthalimide (**62**)*

The synthesis of *N*-allyl-4-(2-(*N*-phenylthioureido)benzylamino)-1,8-naphthalimide (**62**), was attempted as depicted in Scheme 17 using the acetonitrile method utilised for the synthesis of **2**. Under a nitrogen atmosphere **50** was heated under reflux in acetonitrile. Phenyl isothiocyanate (1.5 equivalents) was added, with stirring and heating continued overnight. Subsequent TLC analysis of the reaction mixture showed the reaction had not gone to completion, with the starting material still present as well as a material which was potentially the desired product. To investigate the reaction, the flask was removed from the heat. Upon cooling, no precipitate was observed to form, so water was added to aid precipitation. The solution was filtered using a Hirsch funnel to collect any crystals which may have precipitated however only a viscous substance was obtained. This viscous substance and the filtrate were extracted in ethyl acetate, producing a viscous substance, as well as a few small reddish brown crystals in the viscous material.

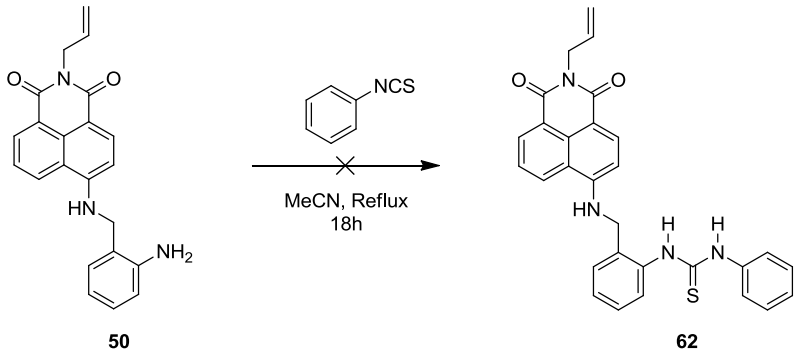

Scheme 17: Attempted synthesis of *N*-allyl-4-(2-(*N*-phenylthioureido)-benzylamino)-1,8-naphthalimide (62) from 50.

Analysis by ^{1}H NMR spectroscopy on the recovered material showed that the product was highly impure, with lots of small peaks occurring around potential peaks of interest These were most likely due to starting materials. The thiourea proton resonances are clearly evident in the spectrum as broad singlets at 9.9 ppm and 9.5 ppm. Whilst the unsuccessful synthesis was not entirely unexpected as there had been many issues with the synthesis of **2**, it still seemed unusual that the synthesis didn't proceed, especially given how similar the other two molecules (**1** and **4**) synthesised using this method are (urea vs. thiourea recognition group). A second attempt using a

different batch of the starting material **50** produced similar results as above and therefore further investigations were abandoned in order to focus on successful synthesis of the other sensing compounds.

Reactions involving 4-chloro phenyl isocyanate.

*3.4.6 Synthesis of N-allyl-4-(4-(N-4-chlorophenylureido)benzylamino)-1,8-naphthalimide (**3**)*

As detailed in Section 1.3.4 there are a number of examples where substituted isocyanates and isothiocyanates have been added to an amine, including amines attached to naphthalimide sensors [49-53]. It was observed that generally these isocyanates/isothiocyanates are added using the same experimental procedures used for the unsubstituted analogues. Therefore, 4-chlorophenyl isocyanate was targeted as an isocyanate for reaction with **51**, using the successful methodology developed for the synthesis of **1** (depicted in Scheme 18). It would be expected that the addition of the electron withdrawing chlorine group would have a marked effect on the sensing properties of the molecule; as evidenced where groups such as the electron withdrawing fluoride have been added [50].

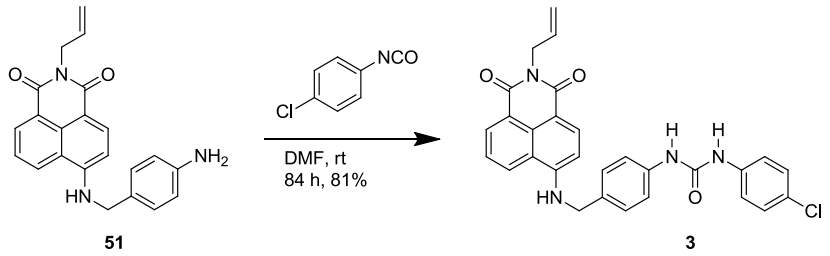

51 **3**

Scheme 18: Synthesis of *N*-allyl-4-(4-(*N*-4-chloro-phenylureido)-benzylamino)-1,8-naphthalimide (3) from 51.

51 was dissolved in DMF and allowed to stir at room temperature. An excess of 4-chlorophenyl isocyanate (1.5 equivalents) and 3 drops of triethylamine were added to the stirred solution and stirring continued for eighty-four hours. Subsequent TLC showed the reaction was complete. Water was added to precipitate out the product. Analysis by ^{1}H NMR spectroscopy of the recovered material (81% yield) showed it was consistent with what would be expected for *N*-allyl-4-(4-(*N*-4-chlorophenylureido)benzylamino)-1,8-naphthalimide (**3**). The reaction was undertaken again to confirm the repeatability of the method, particularly in light of problems

encountered during the synthesis of **1** and **2**. The reaction was stirred overnight, where subsequent TLC (100% chloroform/ alumina) showed the reaction was complete confirming repeatability.

Attempts were made at the synthesis of a molecular similar to **3**, with **50** reacted with 4-chlorophenyl isocyanate instead of **51** *via* the same method, however this was found to be unsuccessful.

Reactions involving 3-(triethoxysilyl)propyl isocyanate

The final isocyanate used to create a urea recognition group was 3-(triethoxysilyl)propyl isocyanate. This isocyanate had the advantage of also containing triethoxysilyl groups which could later be used in the immobilisation of the sensors onto silica. Previously Seo and co-workers reacted 1,8-diaminonaphthalene with 3-(triethoxysilyl)propyl isocyanate in THF to form a receptor containing naphthalene as the fluorophore, urea binding sites and a silanol group bonded to ethoxy groups which could then be used to enable surface immobilisation [77]. The three sensors (**6**, **7** and **8**) depicted in Figure 10 were synthesised using a similar method to Seo [77].

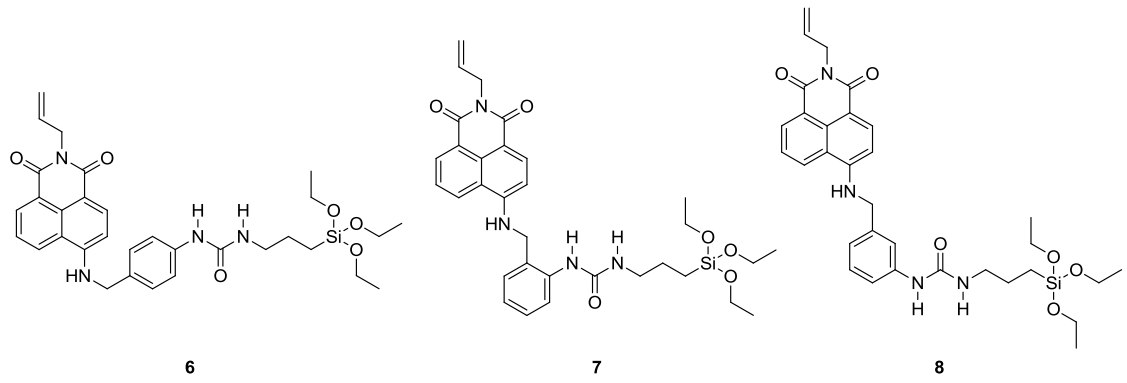

Figure 21: Chemical structures of the triethoxysilyl naphthalimide sensors with the receptor in the *para* (6), *ortho* (7) and *meta* (8) positions.

*3.4.7 Synthesis of N-allyl-4-(4-(N-3-(triethoxysilyl)propylureido)benzylamino)-1,8-naphthalimide (**6**)*

The approach towards the synthesis of *N*-allyl-4-(4-(*N*-3-(triethoxysilyl)propylureido)benzylamino)-1,8-naphthalimide (**6**) (depicted in Scheme 19) focussed on the work of Seo and co-workers [77]. **51** was dissolved in freshly distilled THF and heated under reflux in a nitrogen atmosphere. To the stirred solution, two equivalents of 3-(triethoxysilyl)propyl isocyanate in freshly distilled THF was added, with the stirred solution allowed to reflux for eighteen hours. After 18 hours TLC (100% chloroform/alumina) showed that a new material had formed, yet there was still starting material so heating was continued. After a further 18 hours TLC showed no evidence of starting material. The reaction flask was removed from the heat and allowed to cool to room temperature. THF was removed by rotary evaporation and the resultant solid was dried under reduced pressure to remove residual THF, and recrystallised from methanol (Yield -21%).

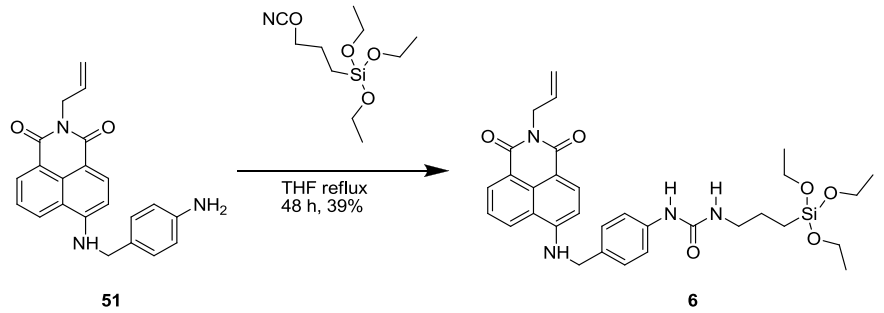

Scheme 19: Reaction between 51 and 3-(triethoxysilyl)propyl isocyanate to form 6.

The newly introduced urea protons were assigned to resonances at 8.37 ppm and 6.12 ppm, with the former being a singlet and the latter appearing as a triplet. The change in the resonances of the proton is due to the removal of the phenyl group previously attached to the receptor group, shifting one of the urea proton resonances upfield. The addition of the triethoxysilyl groups also made it clear the reaction had taken place, as previously no sensor had been observed with resonances below 4 ppm. The triethoxysilyl groups were present, with resonances at 3.72 ppm and 1.13 ppm, whilst the propyl group between the urea receptor and the triethoxysiyl group was represented by three resonances at 3.01 ppm, 1.45 ppm and 0.55 ppm. Carbon NMR

spectroscopy also showed a number of new signals below 60 ppm, which were all assigned to the propyl-triethoxysilyl moiety indicating successful synthesis.

As the initial reaction was found to be successful, the reaction was repeated and scaled up. The reaction time was slightly longer than the first attempt with refluxing for over 48 hours before TLC (chloroform/alumina) showed that the reaction was complete. The solid material was collected using a Hirsch funnel and recrystallised from methanol, yielding 39% of **6** as yellow powder.

*3.4.8 Synthesis of N-allyl-4-(2-(N-3-(triethoxysilyl)propylureido)benzylamino)-1,8-naphthalimide (**7**)*

After the successful synthesis of **6**, it was decided to investigate whether the same reaction pathway was suitable for the synthesis of **7**. As for synthesis of **6**, *N*-allyl-4-(2-aminobenzylamine)-1,8-naphthalimide (**50**) was dissolved in freshly distilled THF and heated under reflux in a nitrogen atmosphere (Scheme 20). 3-(triethoxysilyl)propylisocyanate in freshly distilled THF was then added to the stirred naphthalimide and heating continued overnight. TLC (chloroform/alumina) showed the reaction was incomplete, so heating was continued for a further ninety-six hours with regular monitoring by TLC. It was known from Seo's research [77] that the reaction can take up to 4 days even though it was observed to occur for **6** (see section 3.4.7) in a quicker time frame. After ninety-six hours the reaction was removed from the heat and cooled to room temperature. The THF was removed *in vacuo* to produce a yellow solid. Proton NMR spectroscopy indicated that whilst the material was highly impure, the spectrum contained many of the same peaks observed in the spectrum of the 4-amino derivative suggesting the correct product was being formed. TLC results indicated the material contained the starting material as well as potentially the product **7**. Recrystallisation from methanol was only partially successful in removing by-product impurities.

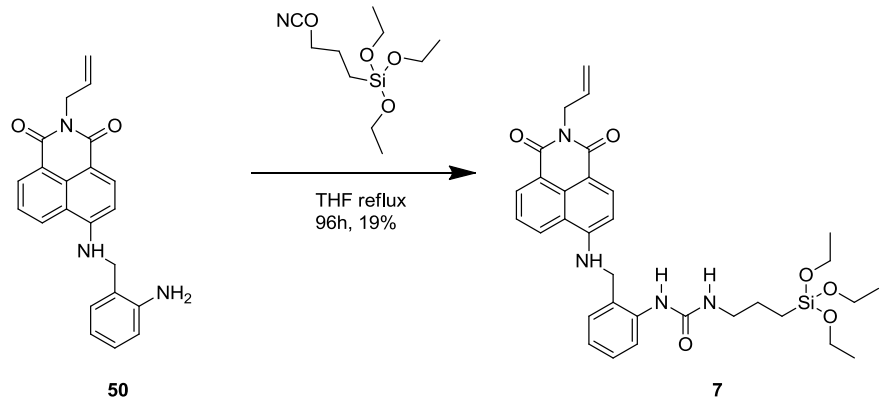

Scheme 20: Reaction between 50 and 3-(triethoxysilyl)propyl isocyanate to form 7.

A second attempt was made at the synthesis of **7** this time using extra isocyanate to try and push the reaction to completion). The reaction was carried out the same way as above and left for 84 hours after which time TLC monitoring (chloroform/alumina) showed that the reaction was complete The THF was removed *in vacuo*, with the resultant material recrystallised from methanol. Proton NMR spectroscopy revealed that the material was consistent with what would be expected for **7**. Resonances relating to the newly introduced urea protons were observed as a singlet at 7.96 ppm and a triplet at 6.51 ppm, consistent with the trend observed in **6** with the urea proton resonances appearing in a more upfield position than observed for the non-triethoxysilyl sensors. Again the propyl-triethoxysilyl group resonances were all observed to be below 4 ppm, with assignment similar to that observed for **6**.

The yield however was found to be only 11.5% with much lost during the recrystallisation process, particularly in the washing step with ice cold methanol. It was also difficult to get the sensor to precipitate out of the recrystallisation solution most likely leading to this low yield. Several attempts yielded the same product however the yields were always below 20%, with a highest yield of 19%.

*3.4.9 Synthesis of N-allyl-4-(3-(N-3-(triethoxysilyl)propylureido)benzylamino)-1,8-naphthalimide (**8**)*

After the successful synthesis of **6** and **7** it was decided to investigate whether the same reaction pathway was suitable to produce **8** (Scheme 21). *N*-allyl-4-(3-aminobenzylamine)-1,8-naphthalimide (**52**) was reacted with 3-(triethoxysilyl)propylisocyanate in a similar manner to the synthesis of **7**. After twenty-

four hours TLC showed the reaction was incomplete, so refluxing was continued. After approximately fourty-eight hours the reaction was removed from the heat and cooled to room temperature and THF was removed *in vacuo,* producing a yellow solid. Proton NMR spectroscopy indicated that the crude material was slightly impure. Recrystallisation from methanol was used to remove these impurities with a yield of 22%.

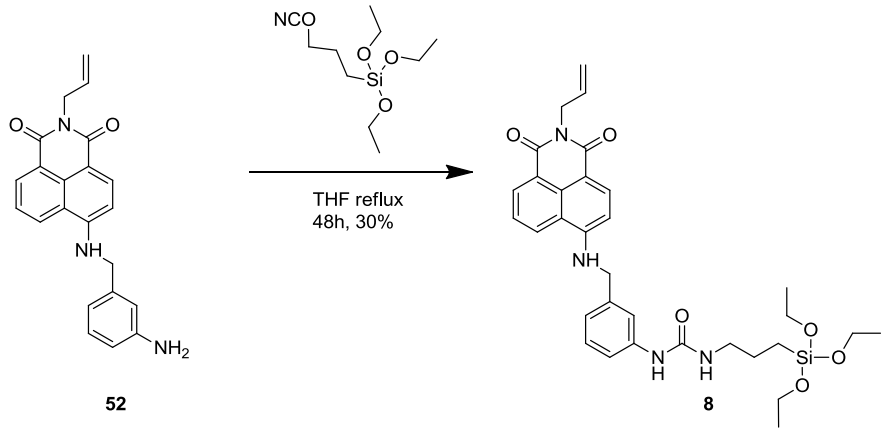

Scheme 21: Reaction between 52 and 3-(triethoxysilyl)propyl isocyanate to form 8.

Proton NMR spectroscopy found that the material was consistent with what would be expected for **8**. Consistent with the urea protons resonances in **6** and **7**, the urea protons were observed upfield in comparison to the non-triethoxysilyl sensors as a singlet at 8.38 ppm and a triplet at 6.08ppm. Again the propyl-triethoxysilyl group resonances were all observed to be below 4 ppm, with assignment similar to that observed for **6** and **7**. Again the reaction was found to be reproducible with a highest yield of 30%.

3.5 Conclusions

The synthesis of several compounds leading to the formation of the final 4-amino-1,8-naphthalimide based anion sensors has been detailed. The initial two step method to form the fluorophore *N*-allyl-4-bromo-1,8-naphthalimide (**45**) with a terminal double bond to enable future surface immobilisation successfully saw the repetition of work by Karishin and Kustol [84] heating 4-bromo-1,8-naphthalic anhydride (**44**) under reflux in aqueous ammonia to form 4-bromo-1,8-naphthalimide (**49**) in 81% yield. Various approaches used to alkylate the imide with allyl bromide did meet with some success

to produce **45**, but reproducibility was an issue. An alternative method based on the work of Niu and co-workers however was found to be successful for the synthesis of **45**. The anhydride **44** was reacted with allylamine in ethanol under reflux, forming the imide **45** in yields that regularly exceeded 90%. Purity as determined using proton NMR spectroscopy was found to be excellent.

After successful synthesis of the fluorophore attention was drawn to the nucleophillic aromatic substitution reaction required to add the spacer to join the fluorophore and the recognition unit. These molecules, whilst similar to molecules prepared by other researchers, had not previously been synthesised and presented in the scientific literature. *N*-Allyl-4-(2-aminobenzylamine)-1,8-naphthalimide (**50**) was synthesised by heating at 110^{o}C with the imide **45** for forty-eight hours, followed by recrystallisation from ethanol in a yield of 63%. *N*-Allyl-4-(4-aminobenzylamine)-1,8-naphthalimide (**51**) was synthesised by heating at 110^{o}C with the imide for two hours, followed by recrystallisation from ethanol, in a yield of 72%. Finally *N*-allyl-4-(3-aminobenzylamine)-1,8-naphthalimide- (**52**) was synthesised by heating at 110^{o}C with the imide **45** for three hours, in a yield of 78% after recrystallisation from ethanol.

Finally the recognition unit was added to form the final sensor molecule. Using **50**, *N*-allyl-4-(2-(*N*-phenylureido)benzylamino)-1,8-naphthalimide (**4**) was synthesised by overnight reflux in acetonitrile in the presence of phenyl isocyanate (1.5 equivalents), with a maximum yield of 53%. Using **51**, *N*-allyl-4-(4-(*N*-phenylureido)benzylamino)-1,8-naphthalimide (**1**) was synthesised by stirring overnight at room temperature in DMF, in the presence of phenyl isocyanate and triethylamine. Also from **51**, *N*-allyl-4-(4-(*N*-phenylthioureido)benzylamino)-1,8-naphthalimide (**2**) was synthesised in a similar way to **1**, however reproducibility of the reaction was an issue, with most reactions producing a viscous solid material instead of the expected yellow solid. Finally from **51**, *N*-allyl-4-(4-(*N*-4-chlorophenylureido)benzylamino)-1,8-naphthalimide (**3**) was synthesised by stirring in DMF overnight in the presence of 4-chlorophenyl isocycante and triethylamine, in a yield of 79%. *N*-Allyl-4-(3-(*N*-phenylureido)benzylamino)-1,8-naphthalimide (**5**) was synthesised from **52** by refluxing in acetonitrile for three hours and recrystallisation from methanol in a yield of 86%**.**

Three sensors **6**, **7** and **8** were synthesised containing a triethoxysilyl group to enable later immobilisation onto a silica surface. *N*-Allyl-4-(4-(*N*-3-(triethoxysilyl)propylureido)benzylamino)-1,8-naphthalimide (**6**) was synthesised by reaction of **51** with 3-(triethoxysiyl)propyl isocyanate in refluxing THF for fourty-eight hours in 39% yield. *N*-Allyl-4-(2-(*N*-3-(triethoxysilyl)propylureido)benzylamino)-1,8-naphthalimide (**7**) was synthesised by reaction of **50** with 3-(triethoxysiyl)propyl isocyanate in refluxing THF for ninety-six hours in 19% yield. Finally *N*-allyl-4-(3-(*N*-3-(triethoxysilyl)propylureido)benzylamino)-1,8-naphthalimide (**8**) was synthesised by reaction of **52** with 3-(triethoxysiyl)propyl isocyanate in refluxing THF for fourty-eight hours in 30% yield. All triethoxysilyl sensors were obtained pure after recrystallisation from methanol.

This chapter described the synthesis of the sensors using conventional heating techniques. The following chapter describes experiments again relating to the synthesis of the sensors and their components but this time involving microwave irradiation techniques. Microwave irradiation has the ability to decrease reaction times and hence was investigated to provide greater ease in the synthesis of the sensors.

Chapter 4

SYNTHESIS – MICROWAVE IRRADIATION

4.1 Microwave Chemistry

Any molecule which has a dipole moment has the ability to turn microwave irradiation into heat [106]. This use of 'microwave' technology is well known for the rapid heating of foods and has been common place in the kitchens of the world for well over 30 years. Microwave technology was first applied to organic synthesis in 1986, [107, 108] however the uptake was initially slow due to issues with controllability and reproducibility [106]. Improved instrumentation facilitating greater control over the irradiation process has resulted in increased use of microwaves in synthetic chemistry over the last two decades. It has been shown that many synthetic reactions can be carried out using microwave assisted procedures, often within significantly shorter timeframes and with greater yields than traditional approaches [93, 94]. Furthermore, the use of microwave assisted synthetic methods has enabled the development of rapid multicomponent synthesis techniques [109]. As such, microwave technology is ideally placed to improve synthetic processes that are laborious and time consuming.

It was established in Chapter 3 that the synthesis of sensors based on the 4-amino-1,8-naphthalimide fluorophore with a terminal double bond was possible, utilising conventional heating techniques. In this Chapter, the synthesis (depicted in Scheme 22) will again be investigated, this time using the techniques of microwave irradiation with aims to decrease the reaction time and increase the yield of the developed sensor molecules.

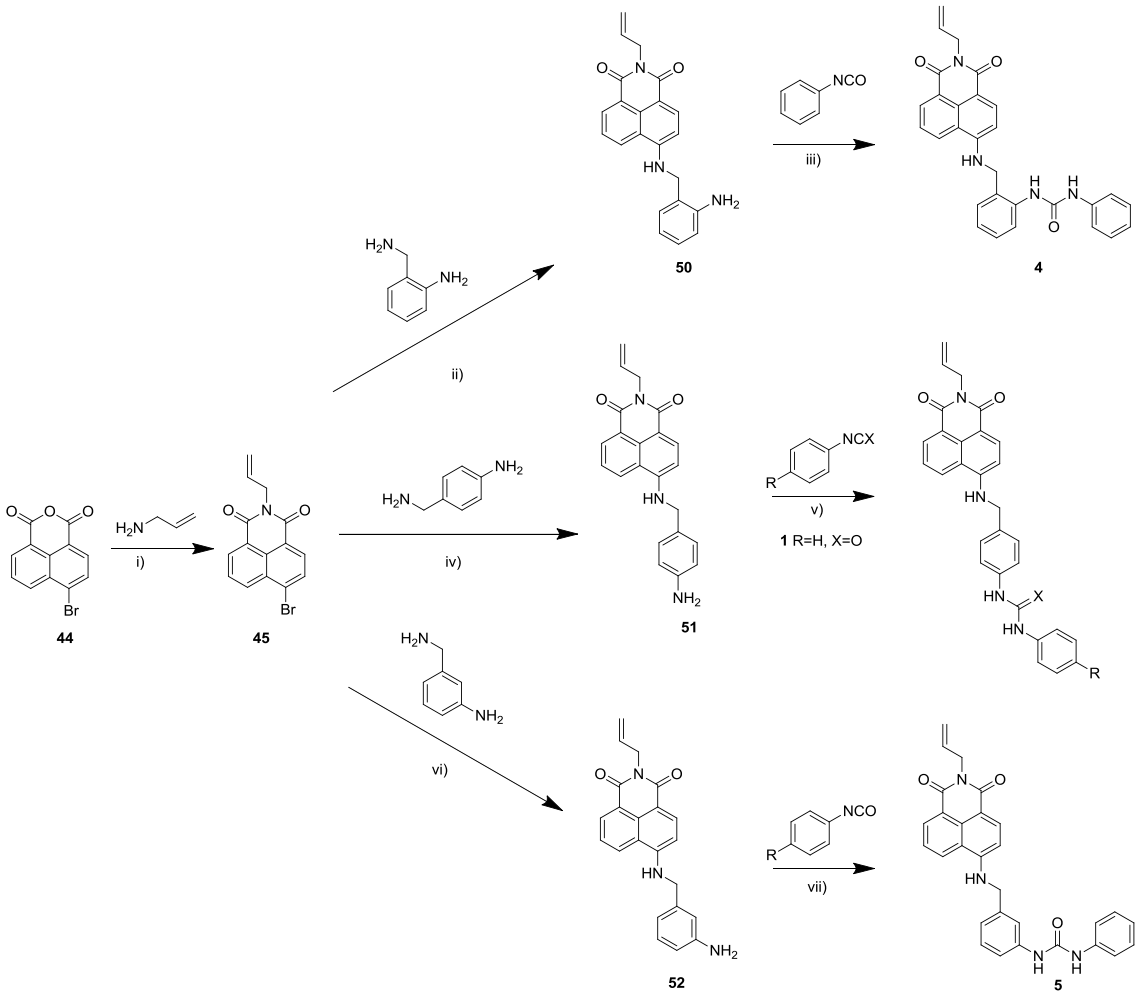

Scheme 22: Synthetic pathway for the synthesis of sensors based on the 4-bromo-1,8-naphthalimide fluorophore, using microwave irradiation techniques.

i) EtOH, 70°C, 8 min, 87% ii) neat, 105°C, 60 min, 44% iii) MeCN, 70°C, 6 min, 75% iv) neat, 105°C, 4 min, 68% v) DMF, 40°C 2 min, 54% vi) neat, 110°C, 8 min, 71% vii) MeCN, 70°C, 6 min, 69%.

Whilst the exact reactions depicted in Scheme 22, to our knowledge have not been reported using the assistance of microwave energy before, there are examples of similar transformations to those required being obtained by other researchers. In the first step the anhydride moiety of the starting material 4-bromo-1,8-naphthalic anhydride (**44**) is transformed into an imide moiety, with many examples in the literature showing various anhydrides transformed into their corresponding different imides [110-113]. The literature shows examples where maleic (**63**) and phthalic anhydrides (**64**) have been reacted with various alkylamines and amino acids (**65** where R^2 = H, Me or Ph and R^3 = CO_2H or CO_2Me or Ph) to synthesise *N*-carboxyalkyl maleimides **66**-**70** and *N*-substituted phthalimides **71**-**72** (Scheme 23) [111]. Equimolar amounts of the reactants were placed together in a conical flask and heated for either

two or three minutes (depending on the reactants) in a 2450 MHz domestic microwave oven (operating at 70% power) with yields of between 82 and 96% obtained [111].

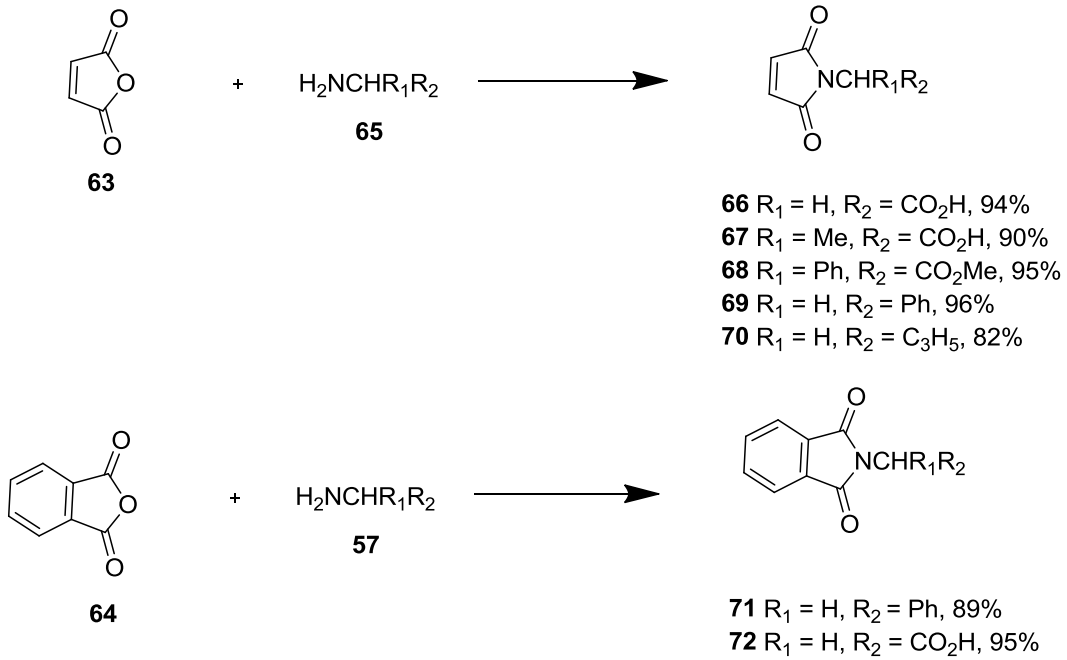

Scheme 23: *N*-carboxyalkyl maleimides (66-70) and *N*-substituted phthalimides (71-72) synthesised by Borah *et al.* [111]

Using a five to seven minute irradiation time in a 448 watt microwave oven, Chandrasekhar and co-workers [112] synthesised a number of imide derivatives from anhydrides using a $TaCl_5$-silica gel catalysed microwave synthesis (selected examples **73-75** made from **64** with a five minute irradiation depicted in Scheme 24). The compounds were obtained in 74-92% yield after column chromatography.

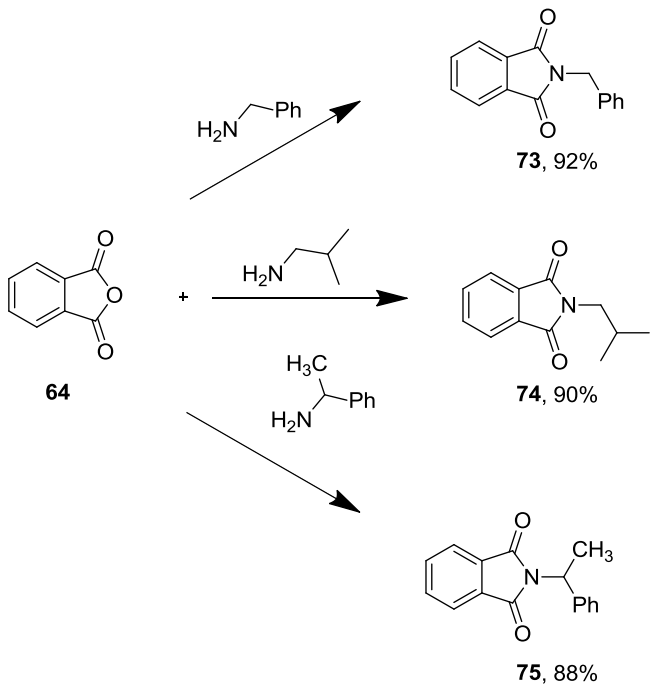

Scheme 24: *N*-substituted phthalimides (73-75) synthesised by Chandrasekhar and co-workers [112].

In the second step in Scheme 22, the bromo group of **45** was displaced with an aminobenzylamine in a nucleophillic aromatic substitution reaction. Elder and Holtz were able to react dinitrochlorobenzene (**77**) with aniline (**76**) in tetraethyleneglycol in a domestic microwave oven (900W) for one minute at 50% power to produce *N*-phenyl-2,4-dinitroaniline (**78**) in 70-85% yield. This indicated that nucleophillic aryl substitution reactions, with a halide leaving group and an amine nucleophile do proceed when using microwave irradiation (Scheme 25) [114].

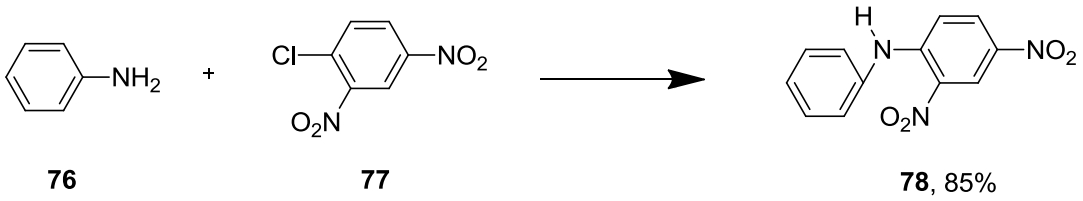

Scheme 25: *N*-phenyl-2,4,-dinitroaniline synthesised by Elder and Holtz [114].

Finally in the last step depicted in Scheme 22, an amine is reacted with an isocyante, introducing the urea recognition moiety. Yu and co-workers[115] performed a reaction between an amine **79** and a isocyanate on a resin embedded with the specified amine in dichloromethane (generalised in Scheme 26). The reaction was found to be complete in four to twelve minutes depending on the amine and the isocyanate

selected. Three to six equivalents of isocyanate were required for successful reaction. Previously the reaction had been undertaken at room temperature with typical reaction times of two to three and a half hours. The use of microwave irradiation therefore greatly decreased reaction time.

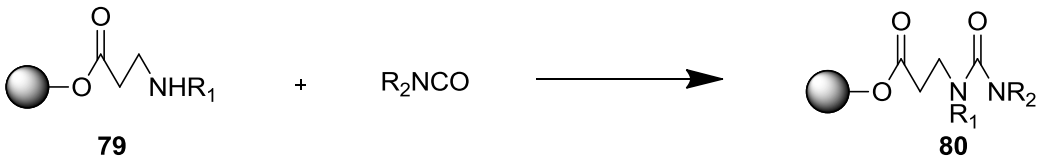

79 **80**

Scheme 26: Generalised reaction between a resin embedded amine and an isocyanate by Yu and co—workers [115].

Armed with the knowledge that similar transformations had been obtained by other researchers, investigations were carried out in order to synthesise the compounds detailed in Scheme 22.

4.2 Synthesis of the fluorophore (45)

In the first step, attention was directed to the synthesis of the fluorophore unit **45**. As detailed in Section 3.2, the synthesis of *N*-allyl-4-bromo-1,8-naphthalimide (**45**) was successfully achieved using traditional bench chemistry by taking 4-bromo-1,8-naphthalic anhydride (**44**) and heating in ethanol under reflux in the presence of allylamine for approximately one hour. The product was obtained as a pale beige powder in 94% yield.

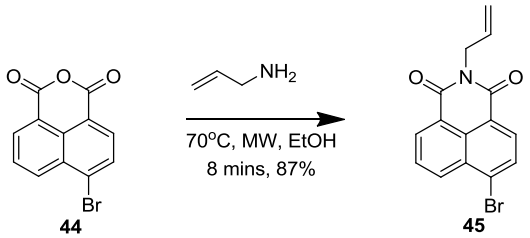

44 **45**

Scheme 27: Microwave synthesis of *N*-allyl-4-bromo-1,8-naphthalimide (45)

Initial approaches using microwave irradiation used the anhydride **44** and allylamine in anhydrous ethanol and were undertaken at 70^{o}C, with an irradiation time of two minutes. Upon standing a milky white solid was observed suspended in solution and another solid material was observed at the bottom of the tube. The milky white solid was collected using a Hirsch funnel. Analysis by ^{1}H NMR spectroscopy of the recovered

material from the suspension showed that the material was consistent with what was observed for *N*-allyl-4-bromo-1,8-naphthalimide (**45**) prepared by conventional heating methods (spectra are compared in Figure 22, with similar comparisons observed for each successfully synthesised molecule).

Analysis by ^{1}H NMR spectroscopy of the solid material from the bottom of the tube showed that it was highly impure. In order to ensure all starting material was consumed by the reaction, the synthesis was repeated with a stirrer bar. The addition of a stirrer bar however was found to be detrimental to product purity (no pure product was obtained) and therefore all further reactions were conducted unstirred.

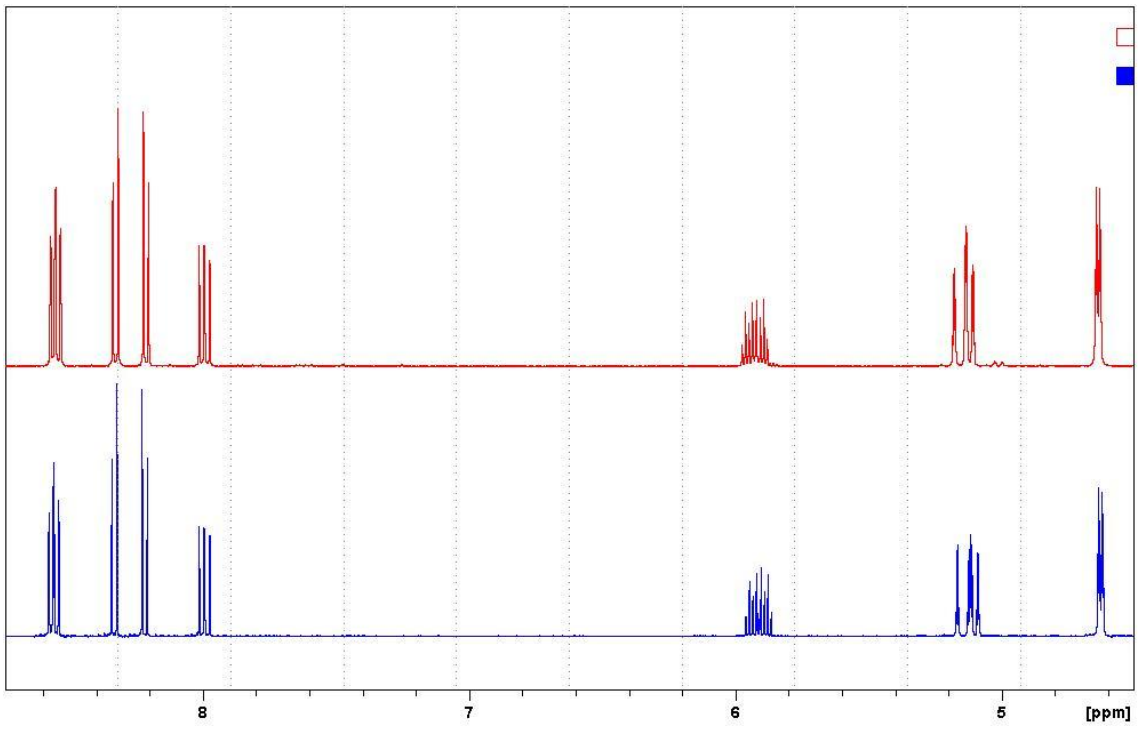

Figure 22: Stacked ^{1}H NMR (400 MHz) spectra of *N*-allyl-4-bromo-1,8-naphthalimide (45) synthesised by microwave heating methods (top) or conventional heating methods (bottom).

In an attempt to improve yield and purity, the reaction was repeated using the same conditions as above (50 mg, 70°C) with the inclusion of a sequence of four two minute microwave irradiation steps in place of a single two minute irradiation. The reaction was allowed to cool to 50^{o}C between each irradiation. By conducting the synthesis in discrete steps we were able to monitor the course of the reaction. The reaction was continued until only a small amount of the second solid material talked of above was observed in the bottom of the tube. This approach proved to be successful and

resulted in the imide, **45**, in 56% yield as an off-white powder. This yield was able to be increased by doubling the amount of allylamine added to the reaction (2.2 equivalents), with a yield of 87% obtained. Further investigation using the 70°C method with four sets of microwave irradiation for two minutes showed that the reaction could easily be scaled up. Increasing the ratio of reactants by four, still afforded pure imide **45** using the same four by two minute irradiation at 70°C method (84% yield).

When compared with the conventional heating method, the purity was the same; however the yield was slightly decreased (87% microwave, 94% conventional heating). In order to achieve the 87% yield of **45** using the microwave approach the ratio of allylamine to anhydride was increased from 1.1:1 (conventional heating method) to 2.2:1. Increasing the temperature to 90°C, in lieu of an increase in the equivalents of allylamine was investigated; however the overall yield of this reaction was lower (70% yield). The major improvement when using the microwave synthesis was the decrease in reaction time, from one hour down to eight minutes, a 7.5 fold decrease.

4.3 Addition of the spacer

*4.3.1 Synthesis of N-allyl-4-(4-aminobenzylamine)-1,8-naphthalimide (**51**)*

As detailed in Section 3.3.1, using conventional heating techniques *N*-allyl-4-(4-aminobenzylamine)-1,8-naphthalimide (**51**), was prepared by reaction of 4-aminobenzylamine (5 equivalents) with the imide **45** at 110°C for two hours. Recrystallisation from ethanol gave a pure bright yellow solid (72% yield).

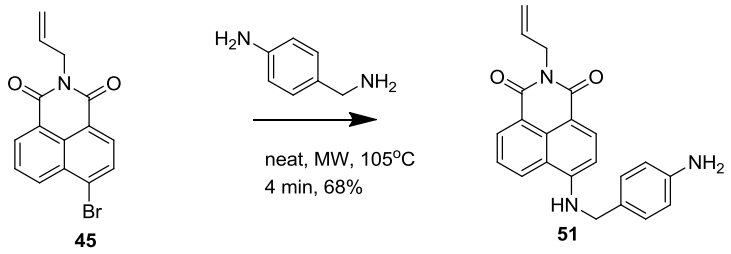

Scheme 28: Microwave synthesis of *N*-allyl-4-(4-aminobenzylamine)-1,8-naphthalimide (51)

Initial investigations utilising microwave irradiation used an amount of the liquid 4-aminobenzylamine that was just enough to cover the surface of the naphthalimide,

with the sample irradiated at 105^{o}C (Scheme 28). After two minutes (and subsequent cooling to 50^{o}C) water was added to the irradiation tube in order to precipitate out the product. The precipitated material was collected using a Hirsch funnel, as a yellow solid. After recrystallisation from ethanol, the solid obtained retained only a slight yellow colour, compared to the very bright yellow solid obtained using bench techniques. Analysis by ^{1}H NMR spectroscopy of the pale yellow solid found the solid was an impure version of the imide starting material **45**.

In the next attempt more attention was given to the exact amount of 4-aminobenzylamine added to the reaction tube. Using conventional heating (Section 3.3.1) the optimal amount to ensure the reaction was able to stir was found to be five equivalents. Therefore five equivalents of 4-aminobenzylamine were added to the imide **45**, along with a stirrer bar in an effort to ensure adequate mixing, as it was thought the reaction may have only been occurring at the solid-liquid interface. The reaction was irradiated at 105^{o}C for 2 minutes. Upon cooling to 50^{o}C, water was added to precipitate out the product, with the solid material collected using a Hirsch funnel. After recrystallisation from ethanol the resultant pale yellow powder was analysed using ^{1}H NMR spectroscopy and the spectrum obtained was found to be identical to that of the imide starting material **45**. In further investigations the amount of 4-aminobenzylamine was doubled (10 equivalents) to fully ensure enough 4-aminobenzylamine was available for reaction. Again proton NMR spectroscopy analysis of the recovered material, found the spectrum obtained was consistent with that of imide starting material **45**.

In further experiments the stirrer bar was removed, as this had been a hindrance in the synthesis of the imide **45** when using microwave irradiation (Section 4.2) Again using ten equivalents of 4-aminobenzylamine, the irradiation was carried out as previously. Upon analysis of the recrystallised material using ^{1}H NMR spectroscopy, several signals were deemed to be from the expected product **51**, with the newly introduced aminobenzylamine protons present and observed as doublets at 7.1 ppm and 6.5 ppm. However the spectrum was dominated by the presence of signals relating to the starting material.

Following on from the promising results above, the irradiation time was doubled to four minutes. The imide **45** and ten equivalents of 4-aminobenzylamine were irradiated at 105^{o}C. Water was added to afford a solid precipitate which was recrystallised from ethanol (Yield – 68%). Analysis by ^{1}H NMR spectroscopy afforded a spectrum consistent with the product *N*-allyl-4-(4-aminobenzylamine)-1,8-naphthalimide (**51**). Reducing the equivalents of 4-aminobenzylamine required for successful synthesis was investigated, however this led to impure products, suggesting ten equivalents was required for successful reaction.

The final reaction time of just four minutes (excluding cooling) compared very favourably with the reaction time using conventional heating of approximately an hour, although considering conventional heating reactions could be undertaken on a larger scale the conventional heating reaction would likely be preferable. The reaction yields were similar for the two synthesis methods (72% conventional versus 68% microwave), with the slightly greater yield for the conventional heating synthesis achieved using a smaller amount of 4-aminobenzylamine.

*4.3.2 Synthesis of N-allyl-4-(2-aminobenzylamine)-1,8-naphthalimide (**50**)*

Section 3.3.2 detailed the successful synthesis using conventional heating methods of *N*-allyl-4-(2-aminobenzylamine)-1,8-naphthalimide (**50**). The product was synthesised by reacting the imide **45** with five equivalents of 2-aminobenzylamine for 48 hours at 110^{o}C. Recrystallisation from ethanol saw the product obtained in high purity as an orange coloured solid (63% yield).

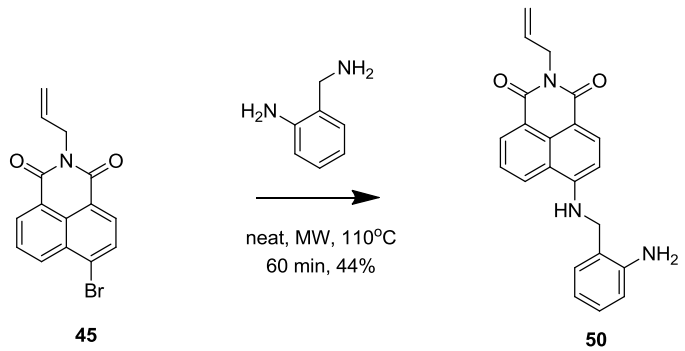

45 **50**

Scheme 29: Microwave synthesis of *N*-allyl-4-(2-aminobenzylamine)-1,8-naphthalimide (50)

Initial approaches at the synthesis of *N*-allyl-4-(2-aminobenzylamine)-1,8-naphthalimide (**50**) using microwave irradiation techniques mimicked the approaches trialled for the synthesis of *N*-allyl-4-(4-aminobenzylamine)-1,8-naphthalimide (**51**) (Scheme 29). As such ten equivalents of 2-aminobenzylamine (double the amount used in the conventional heating synthesis) was added to the imide **45** as a solid and irradiated at 110^{o}C for four minutes. Upon cooling to 50^{o}C a dark viscous solid was found at the bottom of the tube. Water was added to the tube to aid precipitation of the product. The solid material was collected using a Hirsch funnel and washed with ethanol. Upon washing most of the colour from the solid material was lost leaving the recovered material as a very pale yellow powder as opposed to the orange powder expected. Proton NMR spectroscopy showed that material had a spectrum consistent with that of the imide starting material **45**.

Bearing in mind the results from the initial experiments utilising microwave irradiation to synthesise **51**, it seemed evident that a longer reaction time was necessary. It was also noted that using conventional heating (see Section 3.3.2 and Section 3.3.1) it had been observed that the reaction involving 2-aminobenzylamine took forty-eight hours, whereas the 4-aminobenzylamine reaction took approximately an hour and therefore a much greater reaction time for the synthesis of **50** vs **51** would be expected. The reaction was repeated as previously with a ten minute irradiation. Upon cooling to 50^{o}C the viscous material in the tube was stirred and placed back in the microwave reactor for a further ten minute irradiation at 105^{o}C. After the twenty minutes of irradiation, water was added to precipitate out the product. The precipitated material was collected using a Hirsch funnel, with ^{1}H NMR spectroscopy on the crude yellow solid showing a mixture of products and starting material, indicating that the reaction was progressing.

The irradiation time was increased to sixty minutes, with ^{1}H NMR spectroscopy on the obtained product again showing continued improvement towards obtaining the final pure product. The crude material was recrystallised from ethanol, however only very few crystals were obtained. Proton NMR spectroscopy on these crystals however found they were consistent with pure *N*-allyl-4-(2-aminobenzylamine)-1,8-

naphthalimide (**50**) The experiment was repeated and was found to be reproducible with a highest yield of 44% obtained.

Whilst yields were lower (63% using conventional heating vs 44% using microwave irradiation), and a greater amount of the 2-aminobenzylamine starting material was required for a pure synthesis, the great benefit of the microwave irradiation technique was its ability to decrease the time of reaction from forty-eight hours, to just one hour.

*4.3.3 Synthesis of N-allyl-4-(3-aminobenzylamine)-1,8-naphthalimide (**52**)*

As detailed in Section 3.3.3, the synthesis of *N*-allyl-4-(3-aminobenzylamine)-1,8-naphthalimide (**52**) was successfully achieved by conventionally heating excess 3-aminobenzylamine with *N*-allyl-4-bromo-1,8-naphthalimide (**45**) at 110^{o}C for three hours (yield of 78%).

Initial approaches involving microwave irradiation were undertaken using a method modified from the microwave irradiation synthesis of *N*-allyl-4-(4-aminobenzylamine)-1,8-naphthalimide (**51**) detailed in Section 4.3.1. The imide **45** was added to the reaction vessel and its surface covered in 3-aminobenzylamine (ten equivalents) (depicted in Scheme 30). The sample was irradiated at 110^{o}C for four minutes, followed by a second four minute irradiation. The product precipitated upon addition of water and after recrystallisation from ethanol, was obtained in 71% yield.

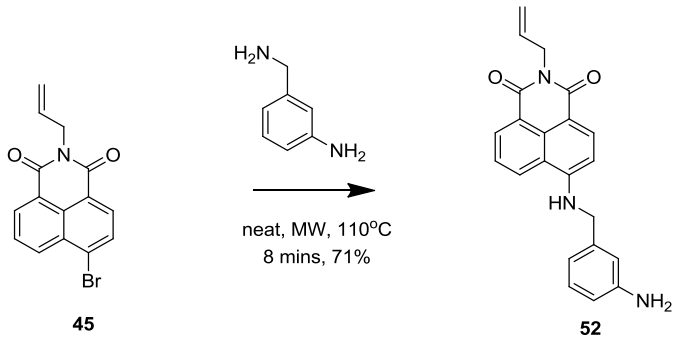

45 **52**

Scheme 30: Microwave synthesis of *N*-allyl-4-(3-aminobenzylamine)-1,8-naphthalimide (52)

Again as observed for other reactions involving aminobenzylamines, the reaction time involved was shorter (Table 8), with a microwave irradiation of eight minutes for **52** versus a reaction time using conventional heating of three hours. Yields for all of the

reactions involving aminobenzylamine were lower when using microwave irradiation (Table 8), considerably so for **50**, highlighting the need to strike a balance between reaction time and product yield.

Table 8: Comparison of reaction time and yield using conventional and microwave heating methods for the addition of the 4-amino group to the fluorophore.

	Conventional Heating		Microwave Heating	
Compound	Reaction Time	Yield (%)	Reaction Time	Yield (%)
50	48 hours	63	60 mins	44
51	1 hour	72	4 mins	68
52	3 hours	78	8 mins	71

4.4 Incorporation of the recognition unit

4.4.1 Synthesis of N-allyl-4-(4-(N-phenylureido)benzylamino)-1,8-naphthalimide (1)

As with the sensors synthesised using conventional heating methods (Chapter 3), the final step in the synthesis was the addition of an isocyanate or isothiocyanate to the aminobenzylnaphthalimide. The sensor **1** was successfully synthesised using conventional heating as detailed in Section 3.4.1. This involved stirring **51** in DMF, in the presence of phenyl isocyanate and TEA for 24 hours at room temperature. The product precipitated upon addition of water and was obtained in 70% yield.

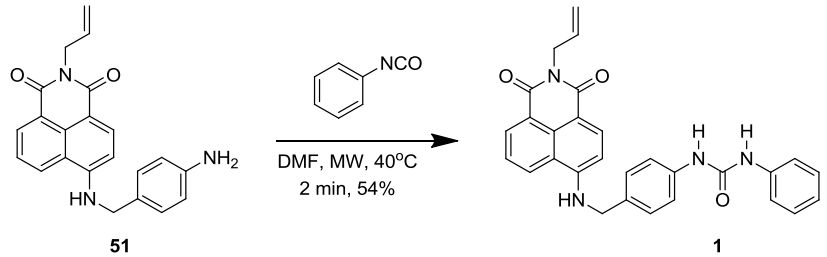

Scheme 31: Microwave synthesis of *N*-allyl-4-(4-(*N*-phenylureido)benzylamino)-1,8-naphthalimide (1)

Using microwave irradiation (see Scheme 31) **51** was dissolved in DMF, excess phenyl isocyanate was added and the sample was irradiated at 40°C. After two minutes water was added to the tube to precipitate out the product. When the solid product was

analysed using proton NMR spectroscopy, it was found to be consistent with the previously obtained spectrum for **1** in a 54% yield.

The main improvement using microwave irradiation techniques was the decrease in the reaction time, with a reaction time upwards of twenty-four hours, being reduced to two minutes. Yields and purity however were lower, offsetting this decreased reaction time benefit. Taking into account potential purification *via* column chromatography, it is possible the bench reaction with increased yield may be a better alternative in this case.

*4.4.2 Synthesis of N-allyl-4-(2-(N-phenylureido)benzylamino)-1,8-naphthalimide (**4**)*

Section 3.4.1.2 details the synthesis using conventional heating of *N*-allyl-4-(2-(*N*-phenylureido)benzylamino)-1,8-naphthalimide (**4**), successfully synthesised in 53% yield by overnight reflux of **50** in acetonitrile in the presence of the phenyl isocyanate.

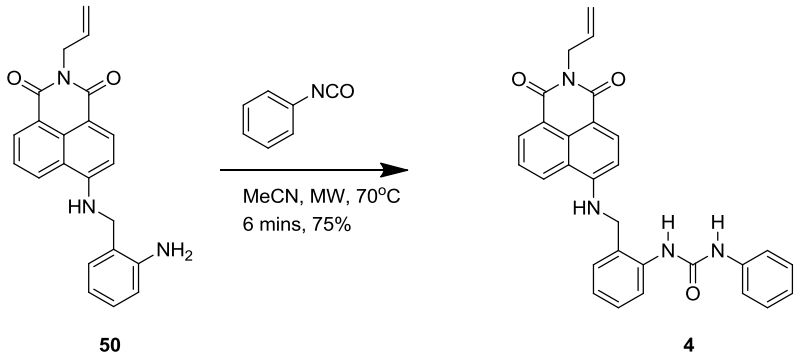

50 **4**

Scheme 32: Microwave synthesis of *N*-allyl-4-(2-(*N*-phenylureido)benzylamino)-1,8-naphthalimide (4).

Initial approaches using microwave irradiation involved the suspension of **50** in acetonitrile (Scheme 32). Phenyl isocyanate was added and the tube irradiated at 70°C. After two minutes, the sample was cooled to 50°C and was stirred, following which the sample was irradiated (at 70°C) for a further two minutes. After three lots of the two minute irradiations and subsequent cooling cycles, water was added to the microwave tube to assist with precipitation of the product. The recovered material was recrystallised from methanol yielding a pure sample of **4.**

After the successful synthesis using 50 mg of starting material, the reaction was scaled up four times (200 mg). Following the same irradiation procedure and subsequent recrystallisation of the crude product using methanol, **4** was produced in 75% yield.

The irradiation time was further investigated, to see if it was possible to cut down the reaction time. Visual observation indicated that there was not much difference when the tube was removed after the first two minute irradiation and what it looked like after the third two minute irradiation. However isolation and analysis of the material after two minutes revealed that there were a few impurities still present, even after recrystallisation of the crude material and thus the longer irradiation was preferable as it produced a more pure product.

A reaction involving one six minute irradiation as opposed to three lots of two minute irradiations was also investigated to see if this would lead to a pure product in a shorter time. Again on a 50 mg scale, the reaction was conducted for six minutes at 70^{o}C. After recrystallisation from methanol, ^{1}H NMR spectroscopy showed that the material obtained was similar to pure **4**, however even after recrystallisation there were some impurities present. These impurities were not evident when using the three lots of two minute irradiations method, which had been used on numerous occasions to produce a pure product **4** after recrystallisation.

There were several advantages to the microwave synthesis of **4**. Purity was easily achieved using the microwave technique by employing the three times two minute irradiation procedure and a simple methanol recrystallisation step. Using conventional heating purity was found to be variable, with time consuming column chromatography required. The yield of material was also found to be increased in the microwave synthesis with a maximum yield of 75%, compared to 53% on the bench. Finally an overnight reflux was required for synthesis using conventional heating methods (this meant including column chromatography, synthesis time was close to twenty-four hours), whereas the total synthesis using microwave irradiation including recrystallisation could be performed in approximately three hours.

*4.4.3 Synthesis of N-allyl-4-(3-(N-phenylureido)benzylamino)-1,8-naphthalimide (**5**)*

N-Allyl-4-(3-(*N*-phenyureido)benzylamino)-1,8-naphthalimide (**5**) was synthesised under conventional heating reflux conditions using acetonitrile as solvent for three hours (detailed in Section 3.4.1.3). Recrystallisation from methanol was required to obtain the pure compound in 86% yield.

In initial microwave irradiation experiments, **52** was suspended in acetonitrile and excess phenyl isocyanate was added (depicted in Scheme 33). The tube was irradiated at 70^{o}C, for three lots of two minute irradiations. After the first irradiation it was evident that a new material was forming with a material observed to precipitate in the tube upon standing. After the final irradiation a small amount of water was added to further aid precipitation. The solid product was collected using a Hirsch funnel and recrystallised from methanol. Analysis by ^{1}H NMR spectroscopy of the material, found it to be consistent with that of **5** produced using conventional heating methods with high purity. Repetition of the experiment yielded the same results with a maximum yield of 69%.

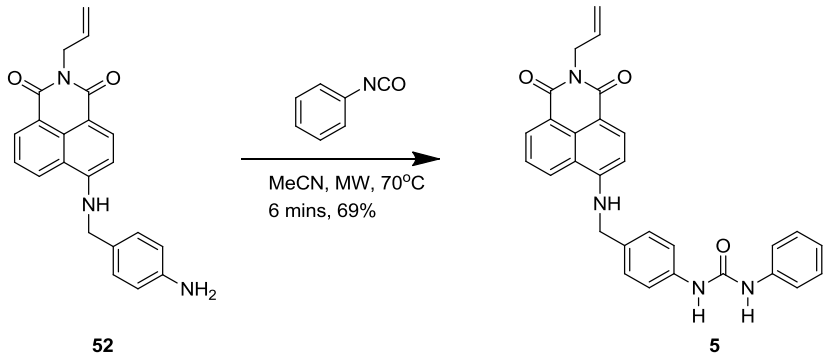

52 **5**

Scheme 33: Microwave synthesis of *N*-allyl-4-(3-(*N*-phenylureido)benzylamino)1-,8-naphthalimide (5)

Using microwave irradiation the overall reaction time was quicker, with an irradiation time of six minutes (not including cooling) comparing to a reaction time of approximately three hours using conventional heating methods. A pure sample was easily achieved in both reactions using a recrystallisation process from methanol. The yield was higher when the conventional heating method was used (86% versus 69%).

4.5 Conclusion

In this chapter it has been shown that use of microwave irradiation is suitable for the synthesis of sensors based on the 4-amino-1,8-naphthalimide fluorophore (Results comparing synthesis by microwave and conventional heating are presented in Table 9). The fluorophore *N*-allyl-4-bromo-1,8-naphthalimide (**45**) was able to be formed from 4-bromo-1,8-naphthalic anhydride (**44**) and allylamine in ethanol using a four by two minute irradiation method at 70^{o}C. Purity as determined by NMR spectroscopy was found to be good, with the yield only slightly lower than achieved using conventional heating (87% versus 94%). The overall synthesis time was lower, however consumption of reagents was slightly increased.

Table 9: Summary of products synthesised using microwave irradiation, and details comparing to the synthesis *via* conventional heating.

	Conventional Heating		**Microwave Heating**	
Compound	Reaction Time	Yield (%)	Irradiation Time	Yield (%)
45	3 hours	94	8 mins	87
51	1 hour	72	4 mins	68
50	48 hours	63	60 mins	44
52	3 hours	78	8 mins	71
1	15 hours	70	2 mins	54
4	15 hours	54	6 mins	75
5	3 hours	86	6 mins	69

After successful synthesis of the fluorophore attention was drawn to the nucleophillic aromatic substitution reaction required to add the spacer to join the fluorophore to the recognition unit. *N*-Allyl-4-(2-aminobenzylamine)-1,8-naphthalimide (**50**) was synthesised by using one microwave irradiation of sixty minutes at 105^{o}C. After recrystallisation from ethanol, yield was 44%, lower than when using conventional heating (63%). The reduction in reaction time from greater than forty-eight hours to one hour, highlighted the time saving capabilities of the microwave irradiation method as opposed to conventional heating. *N*-Allyl-4-(4-aminobenzylamine)-1,8-naphthalimide (**51**) was synthesised with one irradiation at 105^{o}C for four minutes. Finally the sensor with the 3-aminobenzylamine spacer (**52**) was synthesised requiring two lots of four minute irradiations at 105^{o}C. Purity for both **51** and **52** purity was

obtained after recrystallisation from ethanol, with yields of both being similar no matter the heating method used.

Finally the recognition unit was added to form the final sensor molecule. Using **50**, *N*-allyl-4-(2-(*N*-phenylureido)benzylamino)-1,8-naphthalimide (**4**) was synthesised by the use of three, two minute irradiations at 70^{o}C in acetonitrile, with a maximum yield of 75%, 21% higher than that obtained when using conventional heating. It should also be noted that purity was taken care of using a simple methanol recrystallisation, whereas using conventional heating, time consuming column chromatography had usually been required. Using **51**, *N*-allyl-4-(4-(*N*-phenylureido)benzylamino)-1,8-naphthalimide (**1**) was synthesised by microwave irradiation at 40^{o}C for 2 minutes in DMF, although purity was not as good as when using conventional heating techniques. Finally *N*-allyl-4-(3-(*N*-phenylureido)benzylamino)-1,8-naphthalimide (**5**) was synthesised from **52** using the same method for the synthesis of **4**.

Despite many of the microwave irradiation methods showing a decrease in reaction time compared to conventional heating, this has to be balanced with the yield obtained and possible purity considerations. The ability to scale up reactions and reduced reagent use are key factors which conventional heating has over the microwave irradiation methods developed, although it is possible to obtain microwave reactors able to deal with larger reaction vessels, which would enable scale up.

Chapter 5

SENSOR EVALUATION

5.1 General

After synthesising the sensors as demonstrated in Chapters 3 and 4, attention was turned towards the evaluation of the hosts, for various anionic guests, using ^{1}H NMR spectroscopy and fluorescence spectrophotometry, although UV-Visible spectrometry, calorimetry and other techniques can be used [35, 116]. The tetrabutylammonium salts of dihydrogen phosphate, acetate, fluoride and bromide were chosen as the anionic guests for evaluation. These guests were chosen based on their different geometries (spherical – fluoride and bromide, trigonal planar – acetate, tetrahedral – dihydrogen phosphate) and sizes (even though both are spherical, bromide is much larger than fluoride). These salts have been consistently used by other researchers in the evaluation of similar anion sensors as the tetrabutylammonium ion has been shown to not interfere with binding analysis [3, 7, 39, 49-51, 53, 57, 60, 117-120].

The calculation of a binding constant gives a measure of the strength of a host-guest interaction in a given solvent [8]. The equations which allow the calculation of the binding constant are those reported by Thordarson [35] and Schalley [116], with details of the equation derivation included in Appendix B. Equation 7 is the formula which has been used in this work to calculate binding constants assuming the binding stoichiometry is 1:1. Binding stoichiometry was determined using a Job plot, which was constructed from data collected using UV-Visible spectrometry. Fluorescence spectrophotometry and ^{1}H NMR spectroscopy can also be used to obtain data to construct the Job plot [35, 116].

$$\Delta Y = Y_{\Delta HG}\left(\frac{1}{2}\left\{\left([G]_0 + [H]_0 + \frac{1}{K}\right) - \sqrt{\left([G]_0 + [H]_0 + \frac{1}{K}\right)2 - 4[H]_0[G]_0}\right\}\right) \qquad (7)$$

(Where ΔY=Change in physical property (in the case of ^{1}H NMR spectroscopy, the change in the chemical shift of the monitored resonance and in the case of fluorescence spectrophotometry the change in emission intensity), $Y_{\Delta HG}$ is the observed value of the physical property, K is the binding constant, $[G]_0$ is the initial guest concentration and $[H]_0$ is the final guest concentration).

5.1.1 Job plot determined by UV-Visible spectrophotometry

The determination of binding constants described in the rest of this Chapter relies on the fact that the host-guest interaction forms a 1:1 complex. Binding stoichiometry in solution is unequivocally determined using Job's method of continuous variations [121, 122]. Solutions were made up varying the concentration of host and guest in each, such that the sum of their concentration was kept constant [123]. Each mixture was then analysed using UV-Visible spectrophotometry (it is also possible to do this with fluorescence spectrophotometry, NMR spectroscopy and various other methods, however UV-Visible spectrophotometry was favoured due to instrument availability) [123]. A plot can then be obtained graphing the measured absorbance (corrected for the contribution of any coloured components) against the mole fraction of the host or guest added [123]. The binding stoichiometry can be determined from the maximum of this plot, which if it occurs at a mole fraction of 0.5 is 1:1 [116].

5.1.2 Binding constant determination by ^{1}H NMR Spectroscopy

Proton NMR spectroscopy has been widely used in supramolecular chemistry for the investigation of host-guest interactions [35, 116]. Binding constants are generally determined by following changes in NMR proton resonances upon titration of the host with successive aliquots of guest. Two different phenomena can be observed using proton NMR spectroscopy when host-guest complexes are analysed; slow exchange or fast exchange. If the exchange between guest, host and complex is slow on the NMR spectroscopy time scale, then resonances for both the complexed and uncomplexed species will be observed, however if exchange is fast, the chemical shift will be a weighted average of the resonances. In the following discussion, all of the host-guest complexes exhibit fast exchange on the NMR spectroscopy timescale. In order to calculate binding constants a titration curve, like that depicted in Figure 23 was constructed showing the concentration of guest to host versus the change in chemical shift observed for the target proton [8, 35, 116]. The binding constant can then be determined by fitting the data to equation 7 using non-linear regression analysis [8, 35, 116]. A spread sheet was set up in Microsoft Excel and the SOLVER command was used to calculate the binding constant from the chemical shift and concentration data entered.

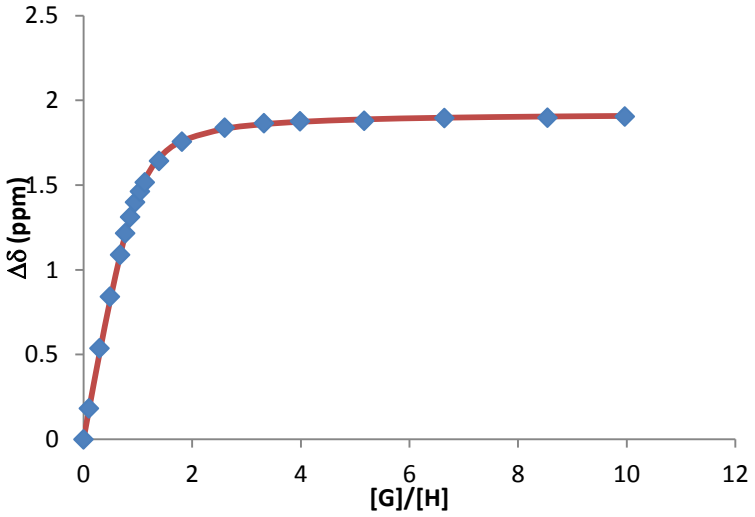

Figure 23: Example titration curve for the determination of a binding constant using ^{1}H NMR spectroscopy.

The change in chemical shift of the proton being monitored is graphed versus the concentration of guest. The diamonds represent the observed change in chemical shift versus the added molar equivalents of guest whilst the line is the predicted change in chemical shift versus the added molar equivalents of guest as determined using a non-linear least squares data treatment process.

A detailed experimental procedure for the ^{1}H NMR spectroscopy titrations of the synthesised sensor (host) molecules with anions (guest) is described in Chapter 2, Section 2.4. Unless otherwise specified, the titration involved the addition of a solution of guest to a solution of host, with the guest solution made up in host so that the concentration of host was kept constant throughout. Solutions were prepared in DMSO-d_6 with 0.5% water as per the method of Gale [98, 99]. The addition of water to the solvent ensures that any water which is being added atmospherically will be minimal and thus reduces any discrepancy in water concentration between aliquots, reducing the error between titrations.

5.1.3 Binding constant determination by fluorescence spectrophotometry

The determination of binding constants by fluorescence spectrophotometry, is another commonly used method, and is considered the most sensitive of all methods for the determination of binding constants [35]. The hosts synthesised in Chapters 3 and 4, all contain the 4-amino-1,8-naphthalimide fluorophore and thus it would be expected that changes would be observed upon the addition of a guest to a solution of the fluorophore. Indeed evaluation of similar molecules by other researchers has shown

there is a decrease in the fluorescent emission of the sensor upon addition of common anions such as acetate, dihydrogen phosphate and fluoride [3, 7, 39, 49-51, 53, 57, 60, 117-120]. By monitoring changes in the intensity of the fluorescence spectrum of the host as greater amounts of guest are added and using equation 7, a binding curve similar to that obtained for ^{1}H NMR spectroscopy can be obtained (Figure 24).

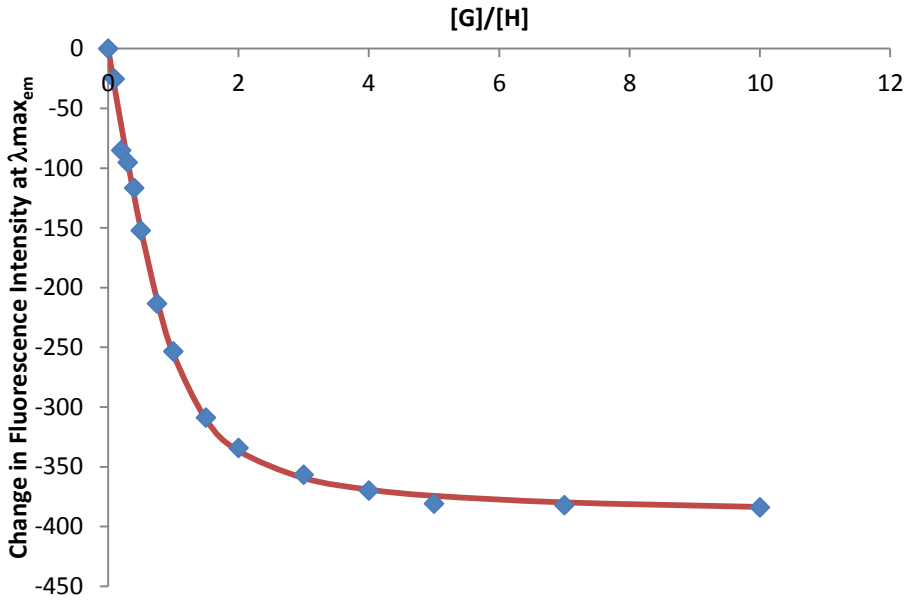

Figure 24: Binding curve obtained using fluorescence spectrophotometry.

Changes in fluorescence intensity are graphed against increasing guest concentration. The diamonds represent the observed change in fluorescence intensity versus the added molar equivalents of guest whilst the line is the predicted change in fluorescence intensity versus the added molar equivalents of guest as determined using a non-linear least squares data treatment process.

5.2 Sensor Evaluation

*5.2.1 N-allyl-4-(4-(N-phenylureido)benzylamino)-1,8-naphthalimide (**1**)*

The ability of *N*-allyl-4-(4-(*N*-phenylureido)benzylamino)-1,8-naphthalimide (**1**) to complex with anions was examined by its titration with the tetrabutylammonium salts of dihydrogen phosphate, bromide, acetate and fluoride. Titrations were performed using both ^{1}H NMR spectroscopy and fluorescence spectrophotometry.

Job Plot experiments for 1

A Job plot was constructed for **1**, using UV-Vis spectrophotometry as detailed in Chapter 2, Section 2.4. Figure 25 shows the Job plot obtained for various mole

fractions of tetrabutylammonium dihydrogen phosphate and **1** in DMSO. As can be seen the maxima occurs when the mole fraction is 0.5, indicating that the binding stoichiometry is 1:1. The slight skewing of the plot (*i.e.* it is not perfectly parabolic) evident in Figure 25, suggests the interaction may not be strictly 1:1, but may be impacted slightly by other factors. Similar plots were obtained for bromide and acetate both exhibiting approximately 1:1 binding stoichiometry with **1**.

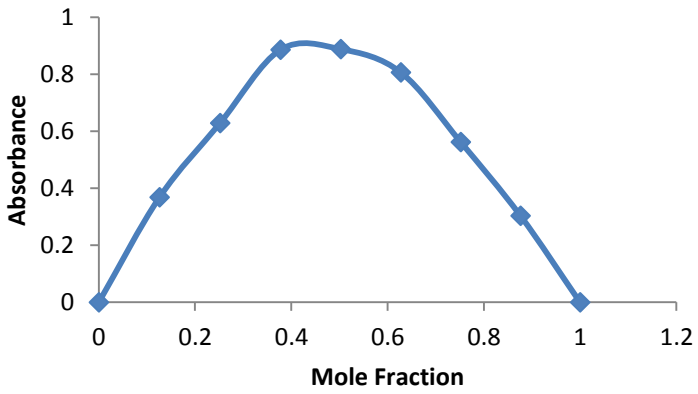

Figure 25: Job plot for 1 and dihydrogen phosphate in DMSO.

The maximum point indicates that the binding is of a 1:1 stoichiometry.

A Job plot was not performed for the fluoride anion as sensor **1** produces a colorimetric response upon addition of the fluoride anion (depicted in Figure 26) which resulted in unusual changes in the UV-Visible spectrum. This colour change could be seen by the naked eye and was reversible upon addition of a hydrogen bonding solvent such as methanol (depicted in Figure 27).

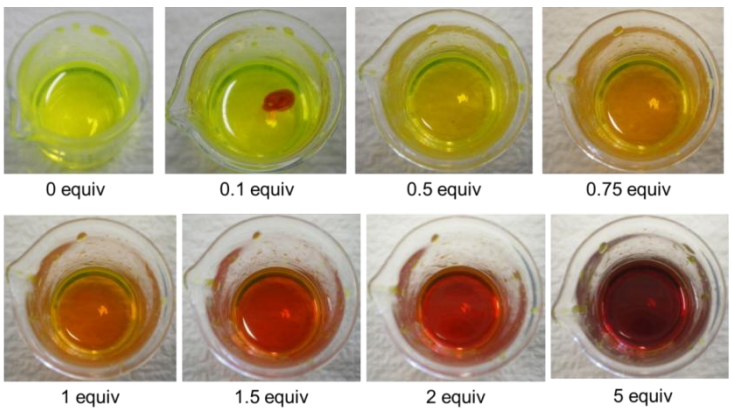

Figure 26: Colorimetric response observed upon addition of fluoride to 1 in DMSO.

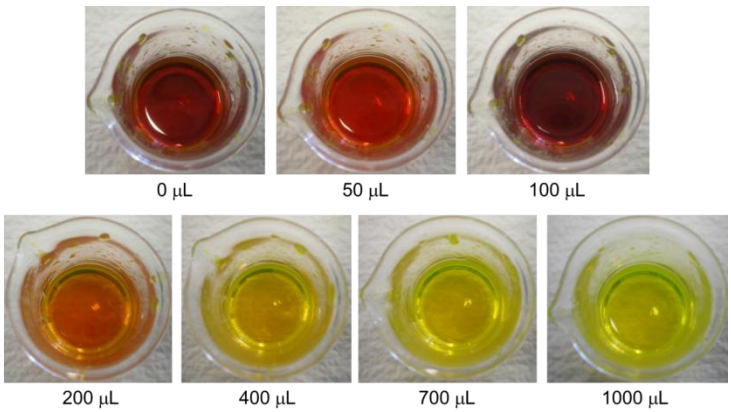

Figure 27: Colorimetric response observed upon addition of methanol to a solution of 1 complexed with fluoride in DMSO.

This colour change has been reported by other researchers for similar molecules and results from deprotonation of the 4-amino NH proton by the highly basic fluoride anion. To confirm this was the case, a series of titrations were performed adding fluoride to **1** (host concentration not kept constant). After the addition of 1.25 equivalents the previously bright yellow titration solution, had quite an obvious orange taint, changing to completely orange after the addition of two equivalents of fluoride. This was followed by a change to a deep red almost purple colour upon addition of 3.5 equivalents of fluoride. These visual colour changes were accompanied by changes in the ^{1}H NMR spectra (Figure 28). Addition of 1.25 equivalents of fluoride saw the two resonances due to the urea protons broadening to an extent they were no longer discernible as two separate signals. The broadened signal was downfield shifted slightly ($\Delta\delta$=0.05 ppm). After addition of two equivalents the resonance for the 4-amino NH proton observed previously as a triplet had broadened and moved downfield ($\Delta\delta$=0.32 ppm). Upon addition of 2.5 equivalents, the urea resonance had downfield shifted further ($\Delta\delta$=1.63 ppm total) and a new resonance was observed as a very broad and weak signal at 16.14 ppm, concurrent with the disappearance of the 4-amino NH proton resonance. This new signal was assigned to the bifluoride anion, formed from the deprotonation of the 4-amino NH moiety. Other resonances were not affected to any great extent. These results and the appearance of the resonance relating to the bifluoride anion, compare well with details reported in the literature for similar molecules [49, 50].

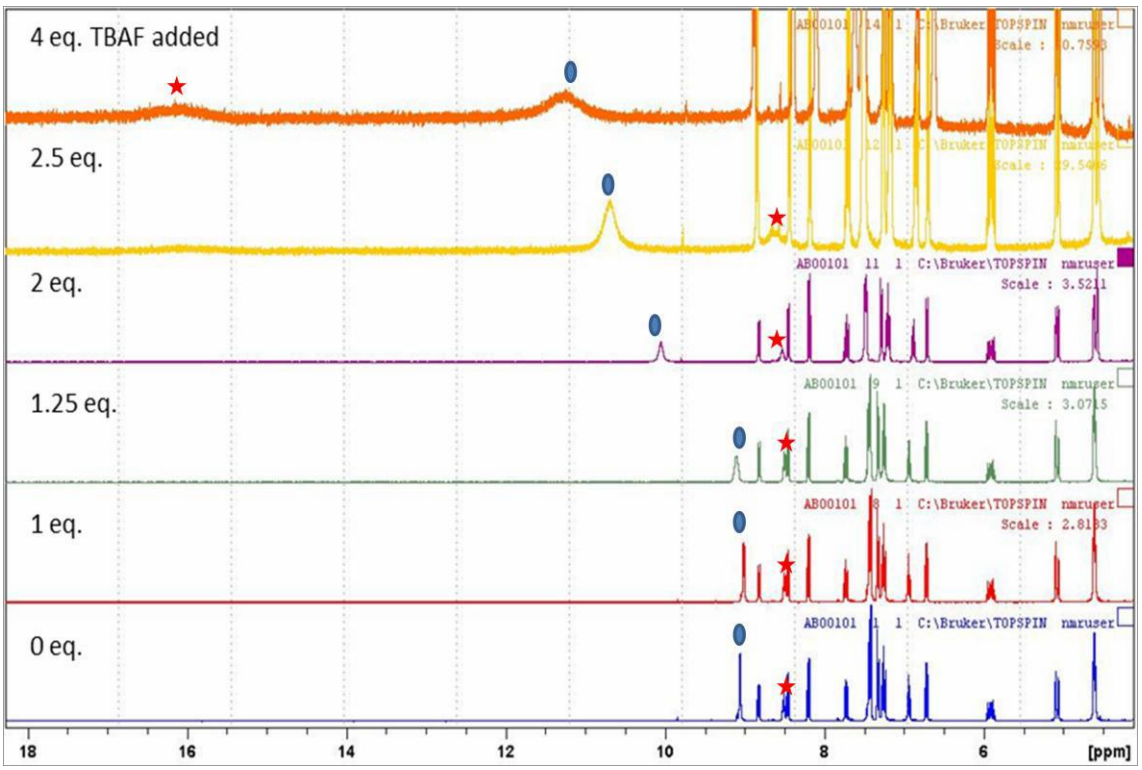

Figure 28: Stacked ^{1}H NMR spectra of the interaction observed between fluoride and 1 in DMSO-d_6.The urea proton resonances are marked with a blue circle, whilst the 4-amino proton resonance is marked by a red star.

Interaction of 1 with anions monitored by ^{1}H NMR Spectroscopy

Several changes were observed in the ^{1}H NMR spectrum when the dihydrogen phosphate anion was added to a solution of sensor **1** in hydrated DMSO-d_6 (the host concentration was kept constant). Figure 29 depicts the ^{1}H NMR spectra obtained with shifts of the key proton resonances given in Table 10. Similar plots were obtained for acetate, bromide and fluoride. The most striking change observed was in the position of the resonance for the two urea protons, originally present (before addition of anion) as two singlets at 8.65 ppm and 8.67 ppm. These resonances were shifted downfield upon successive additions of dihydrogen phosphate, and after addition of four equivalents of the anion the urea resonances had moved to 10.63 ppm. This suggests a strong interaction between the urea protons and the dihydrogen phosphate anion and is consistent with the interaction between an anion and the urea protons of a similar molecule synthesised by Gunnlaugsson and co-workers [51]. Researchers have suggested that the 4-amino NH proton may be involved in the binding process [49], however the 4-amino proton resonance only shifted 0.11 ppm downfield (from 8.49 ppm to 8.60 ppm) suggesting minimal interaction between the guest and this proton (consistent with the results in [51]).

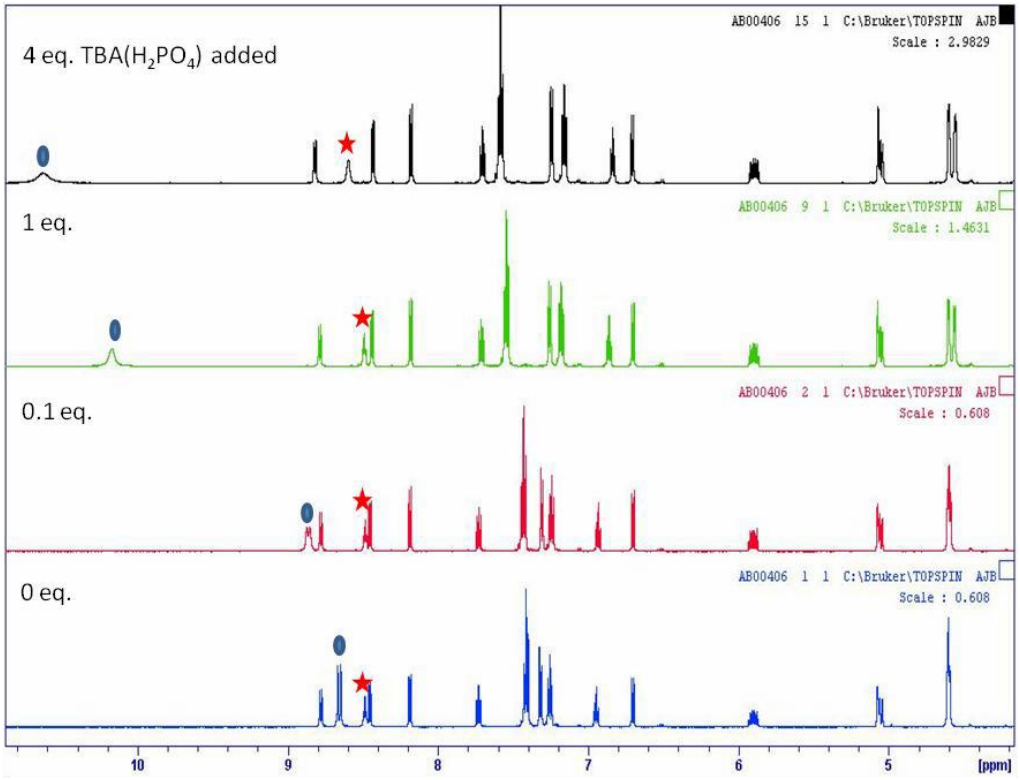

Figure 29: ^{1}H NMR spectra of the interaction observed dihydrogen phosphate and 1 in hydrated DMSO-d6. The urea proton resonances are marked with a blue circle, whilst the 4-amino proton resonance is marked by a red star.

Table 10: Chemical shift (δ) (ppm) observed upon addition of dihydrogen phosphate to 1 in hydrated DMSO-d_6.

Equivalents of Guest Added	Urea Proton 1	Urea Proton 2	4-amino
0.0	8.65	8.67	8.49
0.1	8.86	8.88	8.49
0.5	9.59	9.59	8.49
1.0	10.17	10.17	8.49
2.5	10.56	10.56	8.55
4.0	10.63	10.63	8.60
Change After 4 equivalents	Δδ=1.98	Δδ=1.96	Δδ=0.11

As depicted in Figure 29 changes in chemical shift (both upfield and downfield) were noted for other proton resonances within the host molecule, however the changes were small in comparison to those observed for the urea proton resonances. This

indicates that complexation is occurring at the urea functionality within the molecule. In light of this and as the changes were similar in the different sensors, the focus will be on changes in the urea proton resonances and the 4-amino NH proton resonance only.

Binding constants for the complexation observed between the two urea protons of **1** and dihydrogen phosphate were calculated from the shift data. A typical binding curve for the interaction between one of the urea protons in **1** and dihydrogen phosphate is shown in Figure 30, similar binding curves were obtained for each host-guest pair. The binding constant from the first urea proton was found to be log *K* =3.05±0.09, whilst the second was determined to be log *K* = 3.05±0.08.

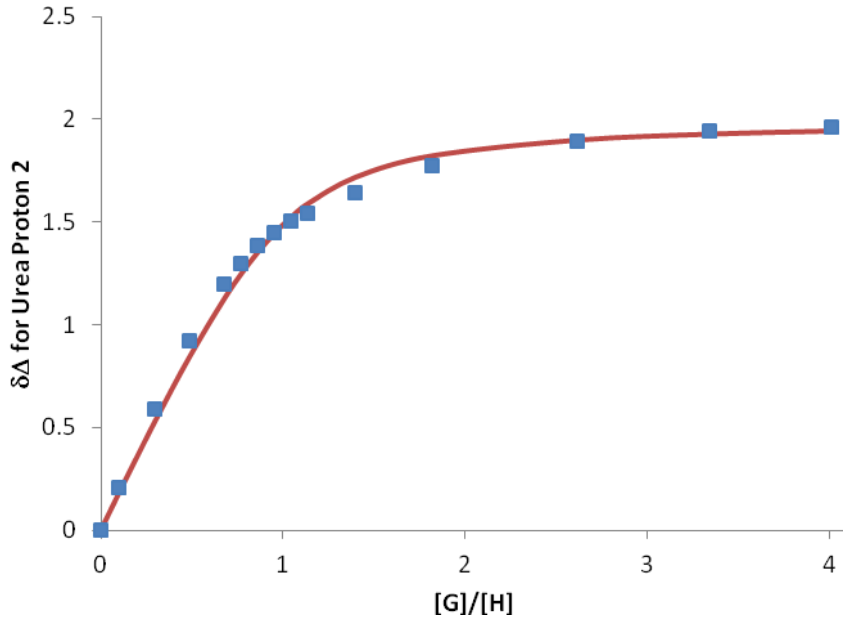

Figure 30: Binding curve for the complexation observed between 1 and dihydrogen phosphate determined by ^{1}H NMR spectroscopy.

The diamonds represent the observed change in chemical shift versus the added molar equivalents of guest whilst the line is the predicted change in chemical shift versus the added molar equivalents of guest as determined using a non-linear least squares data treatment process.

Similar trends were observed for the chemical shifts of **1** upon addition of acetate (tabulated in Table 11). As with the addition of dihydrogen phosphate, the most marked changes were in the resonances observed for the two urea protons; which moved downfield from 8.64 and 8.66 ppm to 11.71 and 11.74 ppm after the addition of ten equivalents of acetate. Only minor changes were observed for the resonance

attributed to the 4-amino NH proton, particularly when larger amounts of acetate were added (from 8.50 to 8.85 ppm after addition of ten equivalents).

Binding constants were calculated for the complex formed between acetate and **1** (Table 12), as log *K* =2.83±0.01 and log *K* = 2.84±0.01. These constants were lower than those calculated for dihydrogen phosphate, suggesting a stronger complex is formed with dihydrogen phosphate.

Table 11: Chemical shift (ppm) observed upon addition of ten equivalents of anion to 1 in hydrated DMSO-d_6.

HOST: *N*-Allyl-4(4-(*N*-phenylureido)benzylamino)-1,8-naphthalimide (1)

	Urea Proton 1			Urea Proton 2			4-amino NH Proton		
Anion	δ Initial	δ After	δΔ	δ Initial	δ After	δΔ	δ Initial	δ After	δΔ
Acetate	8.64	11.71	3.07	8.66	11.74	3.04	8.50	8.85	0.35
Bromide	8.64	8.92	0.28	8.66	8.94	0.28	8.49	8.57	0.08
Fluoride	8.64	11.15	2.51	8.66	11.15	2.49	8.49	9.20	0.71

Table 12: Binding constants (log *K*) for the complexation of 1 with anions as determined by ^{1}H NMR spectroscopy in hydrated DMSO-d_6.

Anion Added	Urea Proton 1	Urea Proton 2	Average
Dihydrogen Phosphate	3.05±0.09	3.05±0.08	3.05±0.12
Acetate	2.83±0.01	2.84±0.01	2.84±0.01

1 exhibited comparatively minor changes in ^{1}H chemical shift values when titrated with bromide (Table 11). The urea proton resonances were present as two singlets next to each other at 8.64 and 8.66 ppm in the absence of guest and were observed to shift downfield to 8.92 and 8.94 ppm after addition of ten equivalents a change of 0.28 ppm for both. The magnitude of these changes is less than that observed when only small amounts of dihydrogen phosphate were added to **1**, showing that bromide induces a much smaller change in the host proton resonance than the dihydrogen phosphate anion. These observations are in accordance with those presented by other researchers who have found that bromide has little interaction with naphthalimide based sensors [3, 7, 39, 49-51, 53, 57, 60, 117-120]. Due to the small changes observed

for the addition of bromide to **1**, a binding constant was not calculated, as the resultant constant could not be reported with any certainty.

Finally **1** was titrated with fluoride, changes in the chemical shift of the urea protons are noted in Table 11. The guest solution was of a dark red colour as opposed to the usual yellow colour of the host due to the deprotonation described earlier in this section. Upon addition of 0.1 equivalents of fluoride to the host solution, the colour maintained its bright yellow appearance, however immediate changes were observed for the urea proton resonances which experienced a downfield shift from 8.64 ppm to 8.71 ppm and 8.66 ppm to 8.73 ppm. Little change was observed in the 4-amino NH proton resonance at this point. After the addition of five equivalents the urea proton resonances (now broadened and appearing as one signal) were present at 11.00 ppm and the 4-amino NH resonance at 8.80 ppm (8.49 ppm initially). With the host concentration kept constant the 4-amino NH proton was not observed to be deprotonated, even when up to ten equivalents of fluoride were added (the proton resonance was observed as a very broad signal at 9.20 ppm). The formation of the bifluoride anion was also not evident (was evident after addition of 2.5 equivalents when the host concentration was not kept constant). Due to the known deprotonation process evident upon addition of fluoride, no binding constant was calculated for the complex formed between **1** and fluoride.

In summary, the major change in the proton NMR spectrum upon addition of an anion to **1** was in the resonances attributed to the two urea protons. The resonance was most changed (moved downfield) upon addition of the acetate anion and least when bromide was added. The 4-amino NH proton was also monitored to see if it would play a role in the sensing of an anion. The most significant change for this resonance was when fluoride was added. This was expected as fluoride is basic enough to remove this proton if present in high enough concentration. A stronger complex was observed to form between **1** and dihydrogen phosphate (log k=3.05±0.12) than **1** and acetate (2.84±0.01).

Interaction of 1 with anions monitored by fluorescence spectrophotometry

Fluorescence spectrophotometry titrations were performed on host solutions made up in hydrated DMSO, so that there was consistency with the solvent used for the ^{1}H NMR spectroscopy titrations. As with ^{1}H NMR spectroscopy, the guest solutions were prepared with host also present, and the guest then added to a separate host solution in specified aliquots.

Hydrated DMSO solutions of **1** were shown to have excitation maxima at 503.9 nm. Emission spectra (Figure 31) were collected from 510-700 nm (λ_{max}=531.9 nm). Fluorescence spectrophotometry titrations with dihydrogen phosphate, acetate, bromide and fluoride were performed with the results tabulated in Table 13 and Table 14 and discussed below.

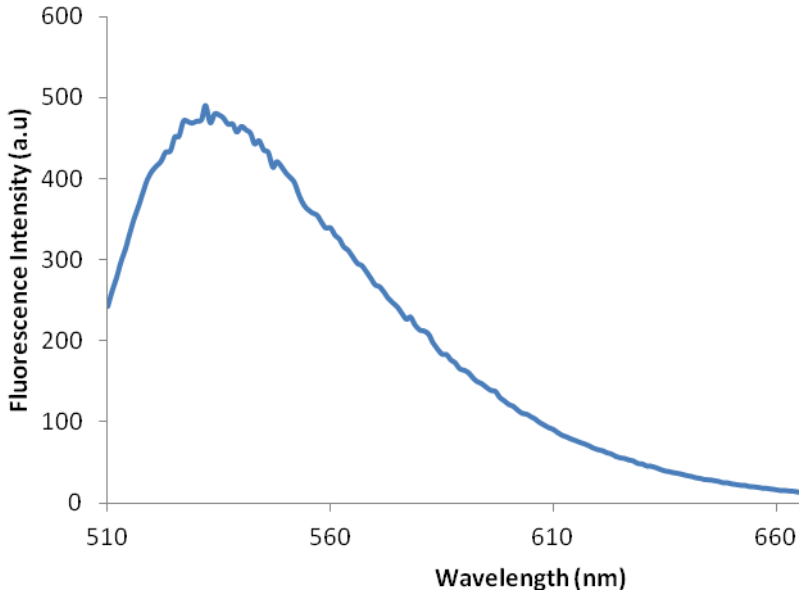

Figure 31: Fluorescence emission spectrum of 1 in hydrated DMSO. λ_{ex} = 503.9 nm.

As shown in Table 13 fluorescence emission was progressively quenched upon titration of **1** with dihydrogen phosphate. The addition of one equivalent of dihydrogen phosphate to the solution of **1** resulted in a 40% decrease in intensity when compared to the initial emission (see Figure 32). The addition of more guest further decreased the emission intensity of **1,** and after three and half equivalents the signal plateaued at around 40% of the initial intensity (60 % reduction in intensity).

Table 13: Percentage fluorescence quenching observed for 1 upon addition of various anions in hydrated DMSO.

	Percentage quenching observed after addition of:			
Anion added	1.0 equiv	6.0 equiv	11.0 equiv	20.0 equiv
Dihydrogen Phosphate	40	65	68	70
Acetate	38	66	71	73
Bromide	0	9	11	15
Fluoride	49	90	98	*

The fluorescence emission of **1 was fully quenched before addition of 20.0 equivalents of fluoride.*

Table 14: Binding constants for the complexation of 1 with anions determined by fluorescence spectrophotometry in hydrated DMSO.

Anion Added	Binding Constant (log *K*)
Dihydrogen Phosphate	3.02±0.03
Acetate	2.94±0.02

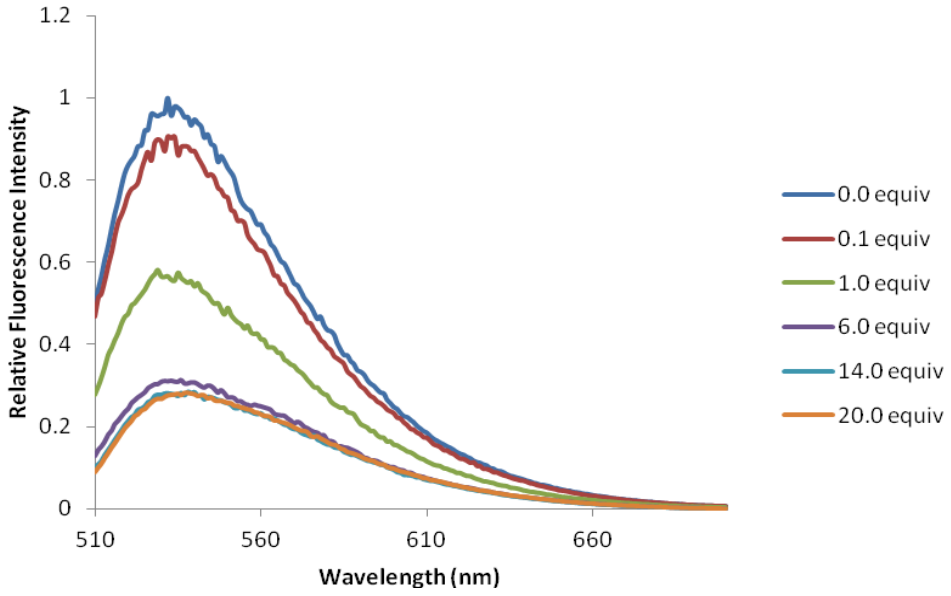

Figure 32: Fluorescence emission spectra observed for the complex formed between 1 and dihydrogen phosphate (λ_{ex}=503.9 nm).

The fluorescence emission signal is quenched because when the anion is bound at the receptor (urea moiety) the reduction potential of the urea is altered. This alteration leads to an enhancement in the free energy of PET quenching. Therefore when the

anion is recognised at the receptor (through hydrogen bonding), the reduction potential of the receptor-anion complex is increased which leads to a greater rate of PET between the HOMO of the receptor and the excited state of the naphthalimide moiety. Thus the fluorescent emission of the naphthalimide moiety is quenched or "switched off".

The binding constant (Table 14) for the complex formed between dihydrogen phosphate and **1** was determined using non-linear regression as log *K*=3.02±0.03. This value, whilst slightly lower, compares well with that obtained via ^{1}H NMR spectroscopy, log *K*=3.05±0.12. The addition of small amounts of methanol to solutions of **1** containing twenty equivalents of dihydrogen phosphate elicited an increase in fluorescence emission. The magnitude of the increase was proportional to the amount of methanol added. The fluorescence emission however was not observed to go back to its original level, with the addition of larger amounts of methanol resulting in a decrease in fluorescence emission (possibly due to dilution effects). This result is consistent with the hypothesis that hydrogen bonding is responsible for the intermolecular interaction between host and guest.

Similarly to dihydrogen phosphate, the addition of acetate to **1** resulted in quenching of the fluorescence emission (Table 13). The emission intensity was quenched by 38% after the addition of one equivalent of acetate, with quenching of the original signal being 73% after addition of twenty equivalents. The binding constant (Table 14) obtained from fluorescence spectrophotometry titration (log *K*=2.94±0.02), was consistent with that calculated by NMR spectroscopy log *K*=2.84±0.01. As with dihydrogen phosphate, the addition of methanol to solutions of **1** containing twenty equivalents of acetate resulted in a reinstatement of the emission.

The addition of bromide to **1** resulted in minimal quenching of fluorescence intensity (9% after six equivalents, 15% after twenty equivalents) in comparison to acetate and dihydrogen phosphate (Table 13). This is consistent with reports for a similar molecule, as the large size and low charge density of the anion was likely to prevent successful binding [51]. Due to the comparatively small changes observed in the fluorescence

spectrum of **1** when bromide was added, a binding constant was not calculated for the formation of **1**-bromide complex.

From (Table 13) it can be seen that as with acetate and dihydrogen phosphate, the addition of greater amounts of fluoride to a solution of **1**, causes a decrease in the fluorescence intensity observed (50% decrease after the addition of one equivalent and 83% after four and a half equivalents). The addition of more equivalents of fluoride saw the emission effectively quenched. It would appear that in the initial stages, there is indeed binding between **1** and the fluoride anion, however as the titration progresses, it is the deprotonation (consistent with the colour change observed from yellow to red) process which is likely to be having a greater effect on the fluorescence spectrum obtained. Addition of methanol to the titration solution saw a reversal of the colour change and an increase in the fluorescence signal observed. This is consistent with previous reports and provides further evidence for the deprotonation process and binding *via* hydrogen bonding. As with ^{1}H NMR spectroscopy, due to the deprotonation process no binding constant was calculated for the complex formed between **1** and fluoride.

In summary, addition of an anion to a solution of **1** caused a quenching of the fluorescence emission of **1**. The addition of fluoride caused the largest decrease in fluorescence emission, however this was due to both binding and a deprotonation process. Similar quenching was observed for both dihydrogen phosphate and acetate, with addition of bromide having little impact on the emission spectrum of **1**. The binding constants determined by fluorescence spectrophotometry, correlated well with those determined by ^{1}H NMR spectroscopy.

5.2.2 Evaluation of other synthesised sensors

As similar results were obtained for sensors **3**-**8**, results for these will be described in less detail. Experimental data (change in chemical shift, fluorescent quenching) for the other synthesised sensor molecules **3**-**8**, are tabulated in Appendix C, with the binding constants determined tabulated in Table 15. For the same reasons as with sensor **1**, binding constants were only determined for dihydrogen phosphate and acetate.

Similar trends to those of **1** were observed for each of the sensors. That is, when analysed by both ^{1}H NMR spectroscopy and fluorescence spectrophotometry, interaction was observed for both the dihydrogen phosphate and acetate anions, whilst little interaction was observed upon addition of the bromide anion. Similarly to **1**, the addition of excess fluoride to each sensor also resulted in an obvious colour change from yellow to dark red, due to deprotonation of the 4-amino NH proton. These results will now be discussed, first looking at the differences and similarities observed between the interaction of anions and **1**, **4** and **5** (the urea recognition group is in a different orientation with respect to the spacer ring), followed by examination of the addition of an electron withdrawing group on the urea recognition group (**1** vs **3**) and finally observations obtained for the three sensors with a triethoxysilyl group (**6**,**7** and **8**).

Table 15: Binding constants for sensors 1, 3-8 determined by ^{1}H NMR spectroscopy and fluorescence spectrophotometry.

	Dihydrogen Phosphate		**Acetate**	
Sensor	*log K* NMR (average)	*log K* Fluorescence	*log K* NMR (average)	*log K* Fluorescence
1	3.05±0.12	3.02±0.03	2.84±0.01	2.94±0.02
3	3.08±0.07	3.17±0.02	3.17±0.02	3.30±0.02
4	3.21±0.04*	3.39±0.09	3.08±0.03	3.18±0.05
5	2.80±0.06*	2.50±0.02	2.88±0.01	3.09±0.06
6	2.00±0.05	2.61±0.04	2.03±0.06	2.57±0.04
7	2.36±0.10	2.67±0.03	2.38±0.26	3.27±0.10
8	1.90±0.12	2.38±0.12	2.18±0.04	2.13±0.06

*These log *K* values are the average of the log *K* for the two urea protons. In the case of these two values, the log *K* values used to determine the average were quite different and are discussed specifically in text.

Effect of the position of the urea recognition group on the spacer ring

Sensors **1**, **4** and **5** differ only in the position of the urea moiety on the aromatic ring of the spacer (Highlighted in Figure 33). Sensor **1**, discussed previously has the urea moiety in the *para* position, whereas sensor **4** has it connected at the *ortho* position and sensor **5** is bonded at the *meta* position.

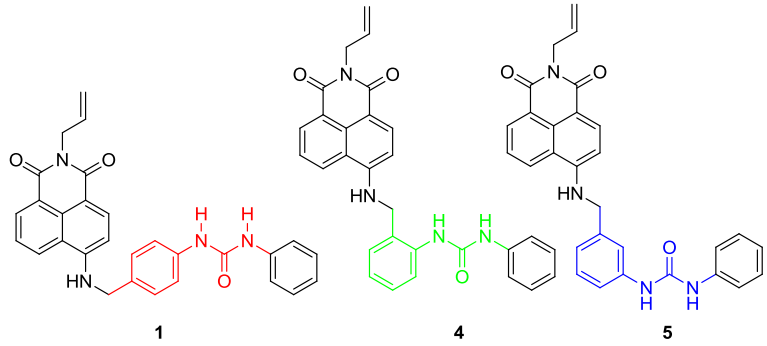

Figure 33: Structures of sensors 1, 4 and 5

Proton NMR spectroscopy titrations were conducted as previously on sensors **4** and **5**. The most marked difference between the two sets of data for **1** and **4** which follow similar trends for the changes observed in the resonance of the urea protons, was the change observed for the resonance of the 4-amino NH proton (Table 16). This was particularly notable upon addition of dihydrogen phosphate where the proton resonance in **4** was observed to move downfield ($\Delta\delta$= 1.56 ppm) after addition of ten equivalents, compared to a downfield change of 0.11 ppm for the same proton in **1**. This suggests that the 4-amino proton is playing a role in the binding of dihydrogen phosphate to **4**, which is not possible in **1** due to the position of the proton in relation to the urea group. This result is consistent with that obtained by Pfeffer and co-workers [50] for a structurally similar compound.

Table 16: Changes in chemical shift (ppm) observed upon addition of ten equivalents of anion to 4 in hydrated DMSO-d_6.

	Urea Proton 1			Urea Proton 2			4-amino NH Proton		
Anion Added	δ Initial	δ After	δΔ	δ Initial	δ After	δΔ	δ Initial	δ After	δΔ
Dihydrogen Phosphate	9.01	10.92	1.91	8.26	9.96	1.70	8.40	9.96	1.56
Acetate	9.01	11.54	2.53	8.26	10.97	2.71	8.40	9.14	0.74
Bromide	9.02	9.43	0.41	8.26	8.52	0.26	8.40	8.56	0.16
Fluoride	9.01	11.38	2.37	8.25	11.17	2.92	8.40	10.72	2.32

There was also an increase in the downfield shift of the 4-amino proton resonance upon addition of acetate, (0.74 ppm for **4**, 0.35 ppm for **1**) however it was not as prominent as the increase for dihydrogen phosphate, a result consistent with Pfeffer

[50]. Again, only a small shift was observed for the 4-amino NH proton resonance upon addition of bromide, whilst a large shift was observed when fluoride was added. This larger shift for fluoride is likely due to the proximity of the 4-amino NH proton to the urea protons, and also is evidence of the deprotonation process. It would be expected further additions of fluoride would show the formation of the bifluoride anion, due to the deprotonation of the 4-amino NH moiety.

Results from the fluorescence spectrophotometry titration of **4** upon addition of anion are detailed in Table 17. In comparison to **1**, there are distinct differences observed in the quenching observed for dihydrogen phosphate and acetate, showing that small changes to the molecule do have an effect on the fluorescence spectrophotometry response. Whilst dihydrogen phosphate and acetate gave similar quenching results for **1**, dihydrogen phosphate clearly quenches the fluorescence emission to a much greater degree when added to **4**. This is due to the change in the position of the urea recognition group and its proximity to the 4-amino NH group and therefore the changes in the interaction the sensor has between different shaped anions. Fluoride appeared to produce less of a quenching effect for **4** than **1**, as a signal was still able to be observed upon addition of twenty equivalents for **4**, whereas the fluorescence emission was effectively switched off after addition of eleven equivalents for **1**, again showing that subtle changes to the molecule can lead to changes in the fluorescence emission behaviour.

Table 17: Fluorescent quenching observed of 4 upon addition of anion, in hydrated DMSO.

	Percentage quenching observed after addition of:			
Anion added	1.0 equiv	4.5 equiv	11.5 equiv	20.5 equiv
Dihydrogen Phosphate	47	65	69	70
Acetate	29	46	51	54
Bromide	3	6	8	8
Fluoride	29	58	62	64

The binding constants (Table 15) obtained for acetate, calculating from both urea protons in the ^{1}H NMR spectroscopy titration and fluorescence spectrophotometry are in reasonable agreement (log *K*=3.08±0.03 vs log *K*=3.18±0.05 respectively). However, interesting results were obtained when using ^{1}H NMR spectroscopy to calculate

binding constants for the interaction between **4** and dihydrogen phosphate with different binding constants calculated for the two urea protons (log *K*=3.07±0.02 vs log *K*=3.34±0.04), with both curves having a good fit between predicted and observed data. The binding constant determined for this complexation *via* fluorescence spectrophotometry was similar to the latter NMR spectroscopy constant (log *K*=3.39±0.09) which may suggest the latter was closer to the correct value. Attempts were also made to calculate a binding constant for the interaction between dihydrogen phosphate and the 4-amino NH proton in **4.** This was not possible using the method used above, as a poor isotherm was obtained. A better isotherm was produced when fitting to a 2:1 model, using a method published by Thordarson [124] with log K_1 = 2.99±0.010 and log K_2 = 2.05±0.01, indicating the 4-amino NH proton is playing a significant role in the binding.

The binding constants for the urea protons were calculated using a "local" analysis method, in that only one isotherm was used to calculate the binding constant. In an effort to gain more insight into the binding constant the data was also submitted to a "global" method as detailed by Lowe *et al.* [125] and with the software provided by Thordarson [124]. In the global method more than one isotherm can be analysed at a time. Using this method to analyse both NMR spectroscopy isotherms produced for the interaction between the urea protons of **4** and dihydrogen phosphate simultaneously returned log *K*=3.17+0.02, close to the average of the two values determined using the "local" analysis. Adding the 4-amino NH proton into the global analysis saw the returned binding constant drop to log *K*=3.01±0.04 (although it should be noted the fit for the 4-amino NH proton is poor as this global method is still fitting the data to a 1:1 model), which is lower than the other constants obtained.

As with **4**, when **5**, (urea recognition group attached in a *meta* position), was analysed, different binding constants were observed for the complex formed between **5** and dihydrogen phosphate, depending on which urea proton resonance was used. Here the difference between the two binding constants was larger than observed for **4** with log *K*=2.50±0.01 and log *K*=3.10±0.06. The binding constant determined by fluorescence spectrophotometry was log *K*=2.50±0.02 consistent with one of the constants determined by ^{1}H NMR spectroscopy. Again the use of a global method to

determine log *K* from the NMR spectroscopy data was investigated with log *K*=2.73±0.08 obtained again close to the average determined using the local method, and within ten percent of the fluorescence spectrophotometry value. Adding in the 4-amino NH proton to the global analysis for the interaction between dihydrogen phosphate and **5** does bring the binding constant even closer to the fluorescence spectrophotometry value with log *K*=2.56±0.18 (although it should be noted that the fit to a 1:1 isotherm is poor for the 4-amino NH proton). Like for **4**, **5** also experienced a large downfield shift in the resonance of the 4-amino NH proton resonance when dihydrogen phosphate was the anion titrated. This suggests that the *meta* orientation of the urea group in relation to spacer, also allows the anion to interact with the 4-amino NH proton. Attempts were made to calculate binding constants for the 4-amino NH proton for the interaction of dihydrogen phosphate with **5**, however a suitable fit was not able to be obtained for a 1:1 interaction. Applying the 1:2 model, using the same software from above however returned log K_1 = 2.87±0.01 and log K_2 = 2.06±0.01, indicating the 4-amino NH proton does play a strong role in binding analysis. This contribution has likely affected the calculation of the binding constant for the two urea protons as the binding will not be exactly 1:1, despite the Job plot being consistent with a 1:1 interaction. Again, like with **4** only a comparatively small change was observed in the resonance assigned to the 4-amino NH proton in the presence of acetate.

In terms of the extent of fluorescence emission quenching, little difference was observed between the quenching observed for **5** when acetate and dihydrogen phosphate were added. Quenching was slightly higher for addition of acetate after addition of one equivalent (34% vs 24%), however after addition of six equivalents the signal was observed to be quenched 52% on addition of dihydrogen phosphate and 51% on addition of acetate (Tabulated in Appendix C). The fluorescence emission of **5** was found to be effectively quenched after the addition of approximately eight equivalents of fluoride.

Comparing **1**, **4** and **5**, the strongest complex formed by dihydrogen phosphate was with **4** (log *K*=3.39±0.09 as determined by fluorescence spectrophotometry) and the strongest complex formed by acetate was also with **4** (log *K*=3.18±0.05 as determined

by fluorescence spectrophotometry). All binding constants however were of a level which would be considered useful for a fluorescent sensor. In terms of selectivity for dihydrogen phosphate and acetate, sensor **4** also provided the greatest discrimination between the two, with dihydrogen phosphate quenching the fluorescence emission more effectively than acetate (70% after twenty equivalents for dihydrogen phosphate versus 54% after twenty equivalents of acetate). In contrast the two anions were virtually indistinguishable when added to **1** (70 % versus 73% respectively after addition of twenty equivalents). Sensor **5** showed some selectivity for the anions, at low concentration, but quenching results were again similar at higher concentrations. These changes with relation to selectivity show how small changes to the sensor (all three sensors have the same chemical formula, they are only structurally different), can have an impact on how they can be used as a sensor.

Effect of the introduction of an electron withdrawing group (1 versus 3)

Sensor **3** (Figure 34) is a similar sensor molecule to **1**, but with a chloro group on the phenyl ring attached to the urea recognition group. The incorporation of the chloro group will have an inductive electron withdrawing effect on the phenyl ring. This is expected to result in changes to the acidity of the urea group, altering the stability of the complex formed, producing different binding constants and potentially producing a different fluorescence emission response.

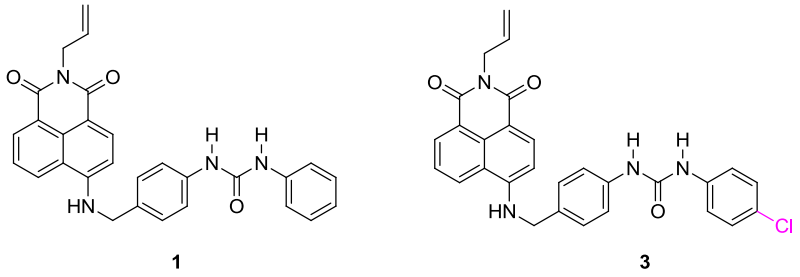

1 3

Figure 34: Structures of sensors 1 and 3, highlighting the position of the electron withdrawing chloro group in 3.

Changes were monitored in the ^{1}H NMR spectrum of **3** upon addition of various anions in a similar fashion to the experiments described above (Tabulated in Appendix C). Broadly similar results were observed with the addition of dihydrogen phosphate and acetate anions resulting in significant downfield shifts to the resonances of the urea

protons, with again acetate producing greater changes than dihydrogen phosphate. The addition of bromide produced little change, whilst significant changes were also observed upon the addition of fluoride. It is important to note that unlike **4** and **5**, only small changes were observed for the resonance of the 4-amino NH proton, supporting the hypothesis that that the changes observed upon addition of dihydrogen phosphate to **4** and **5** were due to the changed position of the urea group with regards to the spacer. Sensors **3** and **1** have the same *para* positioning of the urea group in relation to the spacer.

The binding constant (Table 15) of the complex formed between **3** and dihydrogen phosphate (fluorescence spectrophotometry log K=3.19±0.02 was higher than the average NMR spectroscopy log K=3.08±0.07) was similar to the binding constant for **1** and dihydrogen phosphate (average NMR spectroscopy log K=3.05±0.12 and fluorescence spectrophotometry log K=3.02±0.03). Interestingly the log K for the complex formed between **3** and acetate was higher (average NMR spectroscopy log K=3.17±0.02, fluorescence spectrophotometry log K=3.30±0.02) than that formed between **1** and acetate (average NMR spectroscopy log K=2.84±0.01, fluorescence spectrophotometry log K=2.94±0.02), meaning acetate is more strongly complexed by **3**.

The fluorescence emission of **3** was quenched upon addition of dihydrogen phosphate and acetate (Appendix C), with the values obtained similar to those of **1** suggesting the addition of a chloro group did not have a great effect on the quenching observed. Higher quenching was observed for **1** than **3** upon addition of fluoride (49% versus 32% after addition of one equivalent respectively).

Sensors containing a triethoxysilyl group

The final three sensors **6**, **7** and **8** (Figure 35), all contain a triethoxysilyl group and like **1**, **4** and **5** differ in the position of the urea group connectivity to the spacer. Sensor **6** has the urea group connected in the *para* position of the aromatic spacer, **7** has the sensor connected in the *ortho* position and **8** in the *meta* position. Proton NMR spectroscopy and fluorescence spectrophotometry titration data for the three sensors

containing the triethoxysilyl group attached to the urea recognition unit are summarised in Appendix C.

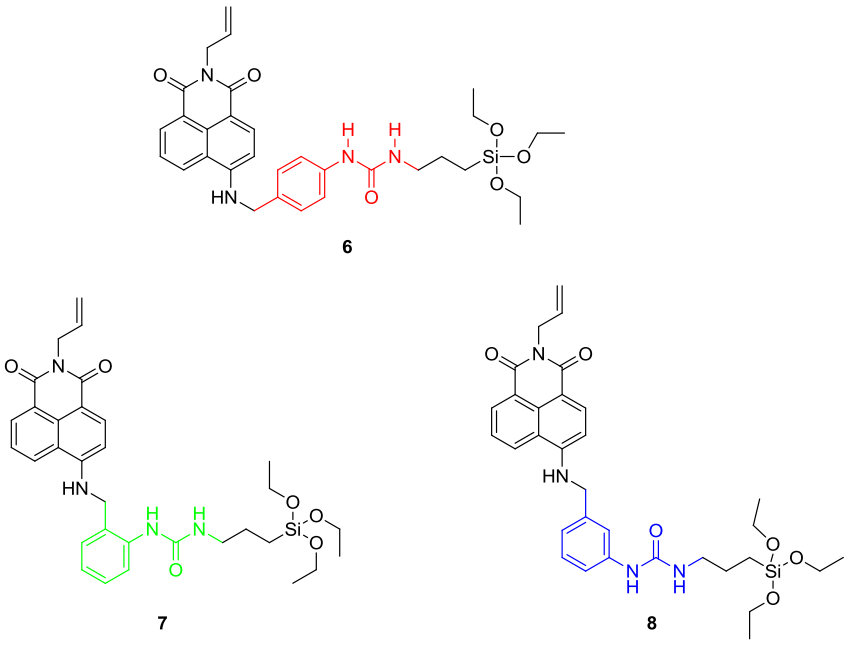

Figure 35: Structures of sensors 6, 7 and 8.

Attempts were made to measure Job plots for **6**-**8** using UV-Visible spectrometry as for sensors **1**, **3**, **4** and **5**. Unlike with the earlier discussed sensors, after repeated attempts the stoichiometry for any complexation was unable to be determined. Essentially for a 1:1 association the plot obtained should be parabolic in nature [122], whereas Job plots for **6**, **7** and **8** with various anions did not display this normal shape. This most likely reason for this unexpected behaviour is the process of hydrolysis [126]. In aqueous solution, silanes are hydrolysed to form silanol groups *via* the following reaction (Reaction 1) [126].

$$(CH_3CH_2O)_3Si\text{-}CH_2CH_2\text{-}Si(OCH_2CH_3)_3 + 6\ H_2O \dashrightarrow (OH)_3Si\text{-}CH_2CH_2\text{-}Si(OH)_3 + 6\ CH_3CH_2OH$$

Reaction 1: Hydrolysis of silanes in solution [126].

Whilst the Job plot experiments are performed in DMSO, due to its hygroscopic nature, DMSO does contain some water content. Indeed all titration experiments involved the addition of 0.5% water to the solvent to reduce the error between titrations due to the atmospheric addition of water. Therefore there is potential for the ethoxy groups that form part of sensors **6**, **7** and **8** to be hydrolysed. The hydrolysis reaction is also catalysed by addition of base [126]. Given dihydrogen phosphate, fluoride and acetate

are basic, this increases the chance of hydrolysis occuring. As there are three ethoxy groups on the sensor molecules, depending on the extent of the hydrolysis there is potentially four different molecules present in the solutions being analysed. Each of these four molecules will interact slightly differently, therefore complicating the result obtained.

Evaluation of the sensors was still undertaken using ^{1}H NMR spectroscopy and fluorescence spectrophotometry as for all other sensors described in this Chapter, despite the binding stoichiometry not being determined.

Figure 36 shows ^{1}H NMR spectra obtained after the addition of various equivalents of dihydrogen phosphate to a solution of **6** in hydrated DMSO-d_6. It can be noted that as further equivalents of dihydrogen phosphate are added, there are several extra peaks which appear in the spectrum in the aromatic region. As stated above, if hydrolysis is occurring (which is highly likely as during the course of the titration we are making the solution more basic), there is potentially four different molecules in the titration solution, each which will have a slightly different ^{1}H NMR spectrum and therefore cause extra resonances to appear in the overall ^{1}H NMR spectrum, thus convoluting the spectra. These extra peaks are not an artefact of the titration process as they have not appeared in the titration experiments performed with **1**, **3**, **4** and **5**. This provides further evidence suggesting that hydrolysis is occurring as the titration proceeds. This hydrolysis process was also observed for **7** and **8** with dihydrogen phosphate as well as **6, 7** and **8** with fluoride (the most basic of the anions titrated). Due to the hydrolysis process occurring, results obtained for the complexation of **6**, **7**, and **8** with dihydrogen phosphate or fluoride are unlikely to be reliable.

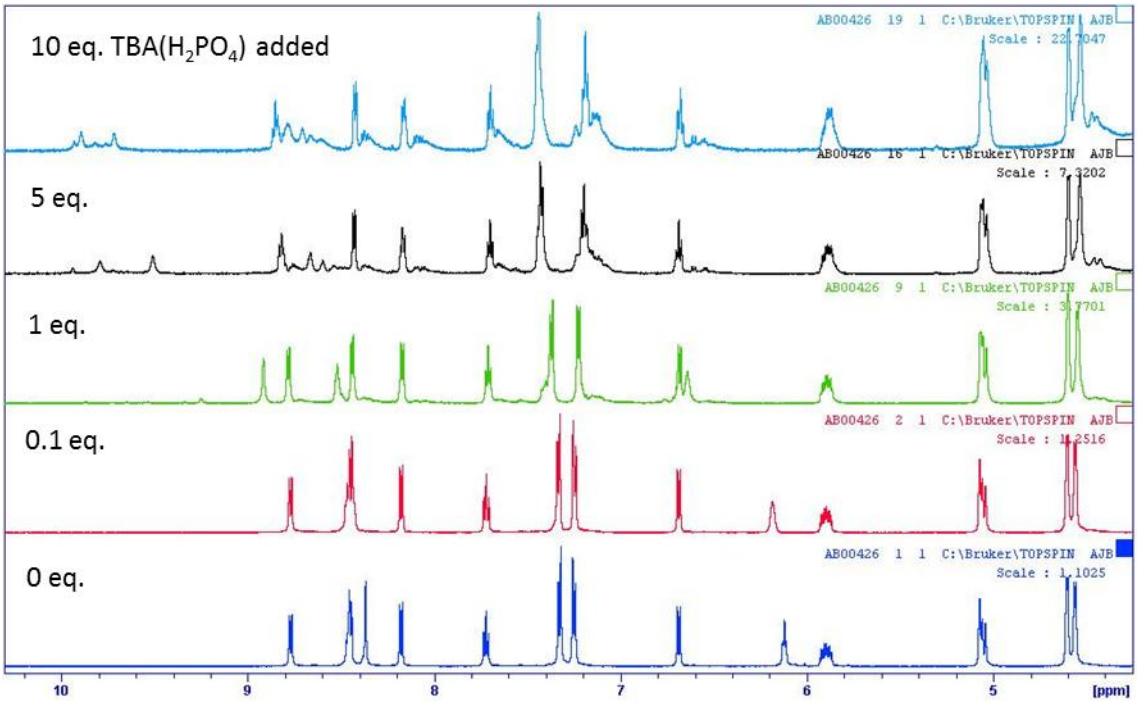

Figure 36: Stacked ^{1}H NMR spectra of the interaction observed between various equivalents (from top to bottom 10, 5, 1, 0.1 and 0 equivalents) of dihydrogen phosphate (TBA salt) and sensor 6 in hydrated DMSO.

The first thing that can be noted from the data collected for **6**, **7** and **8** (tabulated in Table 15 and Appendix C) and comparing that to the data obtained for **1**, **3**, **4** and **5** (Appendix C), is that in general smaller changes in the ^{1}H NMR spectrum are observed and that smaller binding constants are obtained (log *K*=2.03±0.06, 2.38±0.26, 2.18±0.04 for acetate and **6**, **7** and **8** respectively whereas log *K*=2.84±0.01, 3.08±0.03 and 2.88±0.01 for acetate complexed with **1**, **4** and **5** respectively)**.** This suggests that the interaction between the anion and a host containing the triethoxysilyl group is not as strong as that for the sensors without a triethoxysilyl group. This reduction in interaction is due to the removal of the phenyl ring attached to the urea recognition group which is present in sensors **1**,**3**,**4** and **5**. The bis-aryl urea system in **1**,**3**,**4** and **5** increases the rate of PET efficiency compared to the aryl/alkyl system in **6**,**7** and **8**. Complexes formed between **7** and **8** again showed a larger change in the shift of the 4-amino NH proton resonance when compared to the complex formed between **6** and dihydrogen phosphate (changes of 0.75 and 0.74 ppm compared to 0.25 ppm for **6**), however the change in the resonance was nowhere near the magnitude of the change observed for **4** and **5**, the two non-triethoxysilyl sensors with the urea recognition group in a *ortho* and *meta* relationship to the aromatic ring spacer (as in **7** and **8**).

Hydrolysis of the sensor however prevented the accurate assignment of the 4-amino NH resonance as greater amounts of dihydrogen phosphate were added which could be a factor in this change. It is also notable from Table 15 that the binding constants determined by ^{1}H NMR spectroscopy and fluorescence spectrophotometry for molecules with a triethoxysilyl group are not as consistent as those observed for the sensors without this moiety. As with the NMR spectroscopy analysis, this is likely to result from hydrolysis of the sensor upon the addition of the basic anion. The fluorescence spectrophotometry binding curve is based on the quenching effect due to potentially all four molecules in the titration solution. Unlike with NMR spectroscopy, we are unable to directly follow individual protons, rather the signal is a combination of all species in solution.

Fluorescence emission quenching was again observed when dihydrogen phosphate, acetate and fluoride were added to the sensors, with fluoride again showing a colour change from yellow to red, consistent with deprotonation of the 4-amino NH proton. As greater amounts of the anions were added to hosts **6**, **7** and **8**, the percentage quenching of the original signal for both acetate and dihydrogen phosphate tended to be similar, meaning it would be difficult to discriminate between acetate and dihydrogen phosphate using these sensors. The still reasonably sized binding constants (although not as large as for the non-triethoxysilyl sensors) would still make the sensors appropriate for the sensing of anions, even though selectivity would be difficult.

5.3 Conclusions

It has been established that the sensors synthesised in Chapters 3 and 4, do interact with the tetrabutylammonium salts of dihydrogen phosphate, acetate and fluoride. Little interaction was observed with the bromide anion. These interactions were able to be observed using ^{1}H NMR spectroscopy and fluorescence spectrophotometry.

In the ^{1}H NMR spectrum significant downfield shifts were observed for the resonances of the two urea protons in each sensor molecule when dihydrogen phosphate, acetate and fluoride were added. In the case of sensors **4** and **5**, when titrated with dihydrogen

phosphate, significant downfield changes in the resonance of the 4-amino NH proton were also noted.

Using fluorescence spectrophotometry, significant quenching of the emission spectrum of the host, was noted upon addition of dihydrogen phosphate, acetate and fluoride. This quenching was partially reversed when methanol was added to solutions of the host-guest complex. The addition of fluoride to all sensors was found to induce a colour change from yellow to red. This colour change could be reversed by addition of methanol to the complexed solution.

The highest binding constant for a complex with dihydrogen phosphate was observed with sensor **4**, with log *K*=3.39±0.09. Sensor **4** also had the highest binding constant with acetate, with log *K*=3.18±0.05. The triethoxysilyl compounds showed lower binding constants than those compounds without triethoxysilyl groups; due to the change in nature of the urea recognition unit, which has bis-aryl character in **1**, **3**, **4** and **5** and aryl/alkyl character in **6**, **7** and **8**. Hydrolysis which was considered to be an issue in analysis of sensors **6**, **7**, and **8** in the solution phase will not be an issue when the triethoxysilyl sensors are immobilised onto a solid surface, as the ethoxy groups will no longer be able to be hydrolysed.

In terms of selectivity for dihydrogen phosphate and acetate, sensor **4** provided the greatest discrimination between the two, with dihydrogen phosphate quenching the fluorescence emission more effectively than acetate (70% after twenty equivalents for dihydrogen phosphate versus 54% after twenty equivalents of acetate). Sensor **5** showed some selectivity for the anions, at low concentration, but quenching results were again similar at higher concentrations. Sensors **1**, **3**, and **6**-**8** all showed similar quenching results for both anions, suggesting selectivity would be an issue with these sensors if a solution contained both dihydrogen phopshate and acetate. All sensors showed the colour change from yellow to red upon addition of the fluoride anion, which shows that potentially fluoride could be selectively detected over dihydrogen phosphate and acetate in a mixture of the three anions (no tests were undertaken in mixed anion solutions).

Chapter 6

IMMOBILISATION OF NAPHTHALIMIDE SENSORS ONTO A SILICA SURFACE

6.1 Introduction

Over the past few decades there has been a shift to environmentally friendly chemical technologies and an increase in research in "green chemistry" [127]. Paul Anastas and John C. Warner whilst working at the United States Environmental Protection Agency are credited with defining the twelve key concepts of "green chemistry", which include designing processes so that they are atom efficient and that the raw materials are not wasted, using non-toxic and environmentally friendly substances and ensuring processes are energy efficient [127]. With this in mind, efforts were focussed towards how the sensors developed in Chapters 3 and 4 could be used in an environmentally friendly way.

Ideally for environmentally friendly "real world" applications the sensor would be reusable. This reduces waste (same sensor used multiple times) and cost (as you are only outlaying for the sensing molecule once). Using the sensor in the liquid phase however presents difficulties when it comes to the recovery of the sensor. Whilst some solvents are readily removed to yield solid sensor, solvents such as DMSO (used in the previous chapter) are difficult to remove due to their high boiling points and low vapour pressure. Additionally, the anion can remain bound to the sensor molecule and a series of washings is often required to fully regenerate the sensor. Each step results in loss of product, further decreasing the recovery. These difficulties could be overcome by covalently immobilising the sensor onto a solid support. This would enable regeneration of the surface with minimal loss of sensor. Integration of the immobilised sensor into an instrumental device, would allow regeneration to be completed automatically as part of the operating sequence. [48, 71-75].

Silica is one of the most commonly used surfaces for sensor immobilisation. Examples used for this purpose include mesoporous silica [77-79], microscope slides [74], silicon wafers and silicon oxide [72], silica gel [77] and fused silica [80, 81]. Silica is a mechanically stable surface with high thermal resistance [82]. It is resistant to organic solvents and thus can be easily washed using a vast range of organic solvents – ideal for regeneration [82]. In addition, silica can be reacted with a variety of silylation agents which allows the immobilisation of many different types of compounds [82].

Attachment is generally considered easier on a silica surface, than on organic polymeric supports due to simpler surface activation [82]. Silica also has a very high specific surface area and a constant composition, which enables easy analysis of results obtained using a sensor immobilised onto such a surface [82]. Immobilising onto a silica surface as opposed to immobilising onto a polymer surface ensures that the sensor is on the surface and not bound inside the polymer structure. This means all of the immobilised molecules are accessible, which may not be the case if the sensor was immobilised on a polymer surface.

Silanisation is a commonly used technique for the direct immobilisation of organic molecules onto silica and is the preferred method used by manufacturers for the preparation of chemically bonded silica based stationary phases for HPLC [81]. In this process a trifunctional organosilane is reacted with surface silanols which crosslink to form the final bonded phase as shown in Scheme 34 [81].

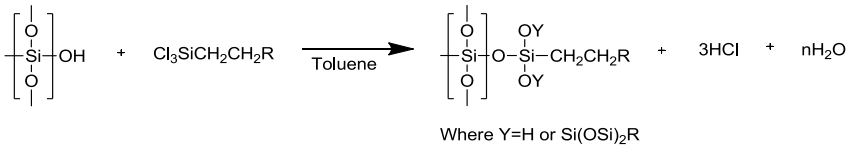

Scheme 34: General scheme for the organosilisation process. Where n=1-3 and Y=H or $Si(OSi)_2R$ depending on the extent that cross linking occurs [13].

Alternatively, a two-step process of silanisation to form a hydride terminated surface (depicted in Scheme 35) followed by reaction of the hydride surface with a compound that contains a terminal double bond using hydrosilation chemistry (depicted in Scheme 36) can be used to immobilise compounds onto silica based stationary phases. These processes have been used previously in particular with capillaries for open tubular capillary electrochromatography [81].

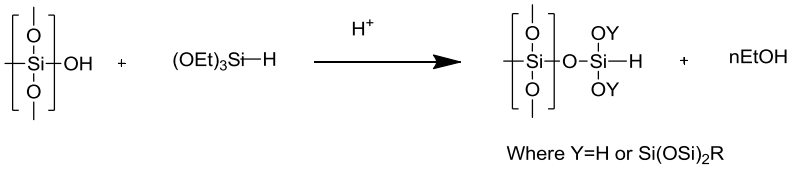

Scheme 35: General scheme for the silanisation process. Where n=1-3 and Y=H or $Si(OSi)_2R$ depending on the extent that cross linking occurs. The typical acid source used is hydrochloric acid [13].

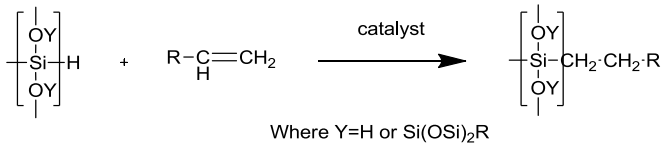

Scheme 36: General scheme for the hydrosilation process. Where Y=H or $Si(OSi)_2R$ depending on the extent that cross linking occurs. The catalysts commonly used include metal complexes such as hexachloroplatinic acid or free radical initiators such as tert-butyl peroxide [12].

Niu and co-workers have previously reported the immobilisation of a naphthalimide based sensor **25** for the detection of nitrofurantoin onto a silanised glass surface via a polymerisation process. Glass plates were initially prepared for silanisation by successive immersion in 3% hydrofluoric acid for 10 minutes and then 10% hydrogen peroxide for a further 10 minutes. After a water wash, the glass plates were immersed in 3-(trimethoxysilyl)propyl methacrylate (TSPM) for two hours. Meanwhile, the sensor molecule was mixed with 2-hydroxypropyl methacrylate (HPMA) and cast onto a PTFE plate. The silanised glass plates were then placed over the casting and irradiated using UV light of 254 nm for four hours to facilitate the polymerisation reaction. After irradiation was complete the plates were washed with water and methanol until no further unreacted sensor molecule could be detected [48].

In this Chapter, preliminary results into the immobilisation of the naphthalimide sensors onto silica are discussed (Figure 37). In the first instance (Figure 37, step i), experiments used the terminal double bond of the sensor molecules to surface immobilise the sensors using the hydrosilation chemistry described above. A further approach (Figure 37, step ii) focussed on the use of a 3-aminopropyl functionalised silica gel and synthesising the sensor step-wise on the surface rather than attaching the final sensor molecule to the gel. Finally (Figure 37, step iii) uses the triethoxysilyl groups which were incorporated into three of the sensors, with the sensors immobilised onto mesoporous silica gel using hydrolysis and condensation reactions.

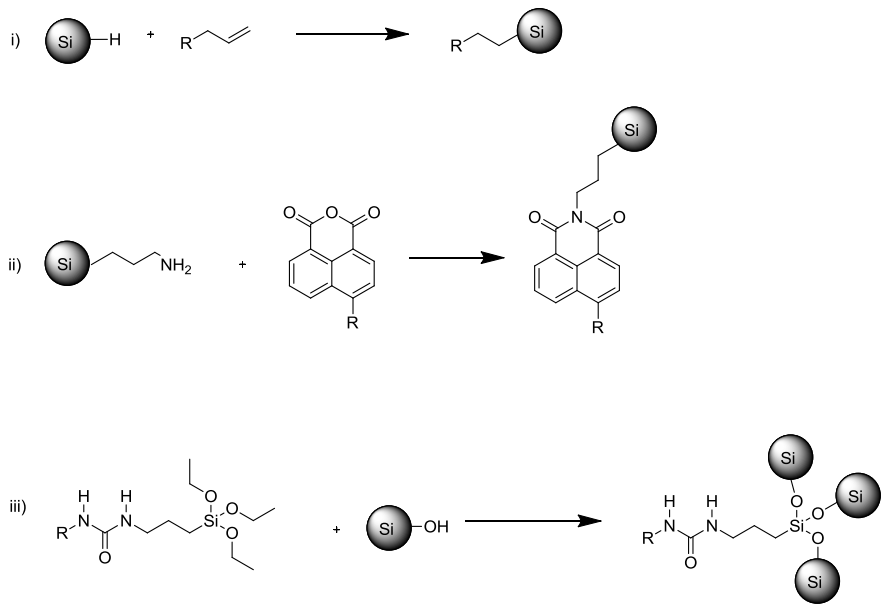

Figure 37: Generalised pathways used for immobilisation of naphthalimide sensors.

i) Hydrosilation. ii) Build the sensor on the surface. iii) Incorporate ethoxy groups into the sensor and then immobilise on silica via hydrolysis.

6.2 Immobilisation through the terminal double bond

Immobilisation utilising the terminal double bond of the sensor molecules was trialled on three different silica surfaces; glass microscope slides, silicon wafer and hydride modified silica gel. Using glass microscope slides, FTIR evidence was obtained to suggest the slides were able to be successfully silanised with terminal hydride groups; however spectroscopic and evidence for immobilisation of the sensor onto the silanised glass was not observed. Similarly when using silicon wafer, AFM showed a change in the surface when the wafer was silanised, but when the surface was reacted with the sensor it was not possible to determine if there was significant changes to the surface of the silicon wafer (comparing the immobilised and silanised wafer versus the silanised only wafer). The most promising results were obtained when immobilising the sensor onto hydride modified silica gel, as discussed below.

6.2.1 Immobilisation onto hydride modified silica gel

Silica gel used for column chromatography was initially modified using a method adapted from Gubbuk and co-workers [95] (Scheme 37). Triethoxysilane was used in place of 3-chloropropyltrimethoxysilane (CPTS) in order to hydride modify the surface as opposed to a surface modified with chloro groups. Triethoxysilane and silica were

allowed to react under reflux in toluene. After three days the reaction was removed from the heat, and the silica left to settle out. The solid silica was collected using a Hirsch funnel, washed with toluene and dried under reduced pressure.

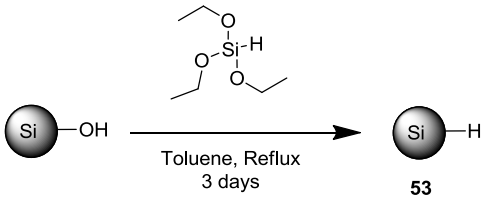

Scheme 37: Reaction between silica gel and triethoxysilane to create hydride modified silica gel (53).

FTIR analysis (KBr) was performed on the hydride modified silica gel **53** (Figure 38). A very small peak was observed at 2262cm^{-1}, representative of the Si-H moiety [105]. This was not observed in the spectra of the unmodified activated silica gel (Figure 39) which had a major peak for the hydroxyl moiety at 3462 cm^{-1}. This hydroxyl peak was only observed in small amounts (comparatively) in the two samples of hydride modified silica analysed. This was expected as it was considered unlikely that 100% of the surface hydroxyl groups would be converted to the hydride.

The sensor *N*-allyl-4-(4-(*N*-phenylureido)benzylamino)-1,8-naphthalimide (**1**) was initially targeted for surface immobilisation *via* hydrosilation chemistry (Scheme 38). The method used was adapted from research by Gubbuk *et al.* [95] and Pesek and Matyska [96]. The hydride modified silica **53** was added to sensor **1**, suspended in anhydrous toluene along with 120 μL of 10 mM Spier's Catalyst solution and heated under reflux for three days. Spier's Catalyst was prepared as a solution of hexachlorplatinic acid in isopropanol (10mM solution as used by Matyska and Pesek [96]). It was noted that as the immobilisation reaction took place, the reaction solution changed from a yellowish colour due to the presence of the sensor and gained a distinct greyish tinge. After approximately seventy-two hours the reaction was removed from the heat and the silica allowed to settle out.

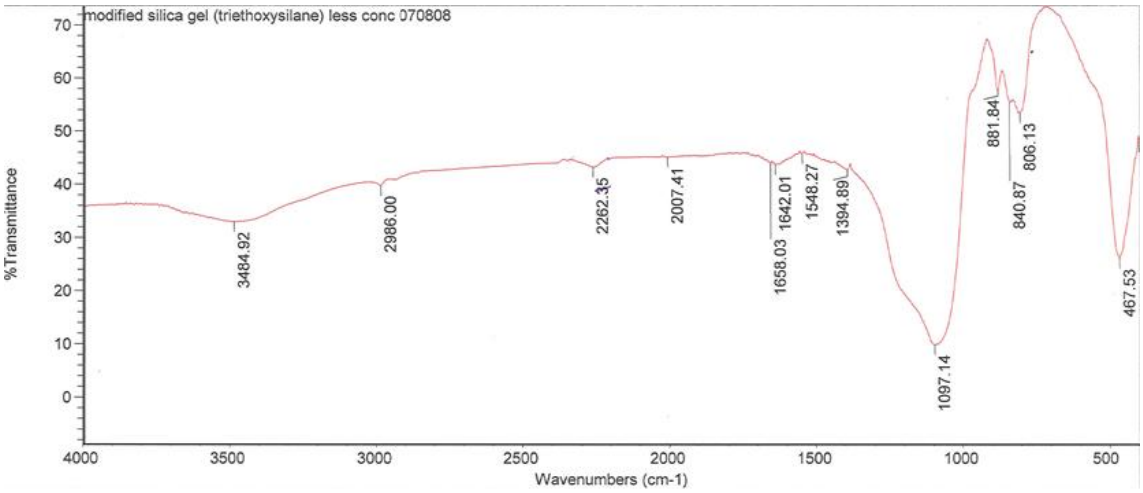

Figure 38: FTIR spectrum of hydride modified silica gel 53.

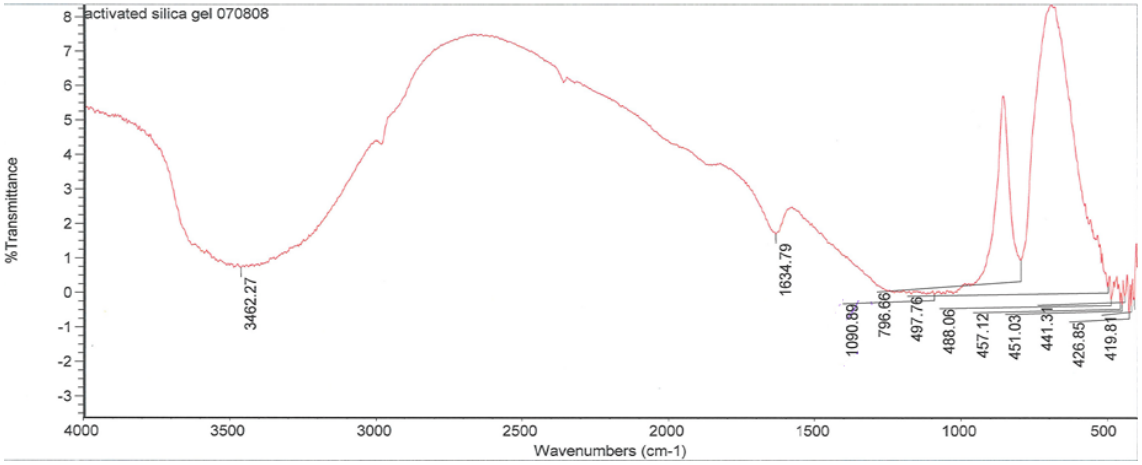

Figure 39: FTIR spectrum of unmodified silica gel.

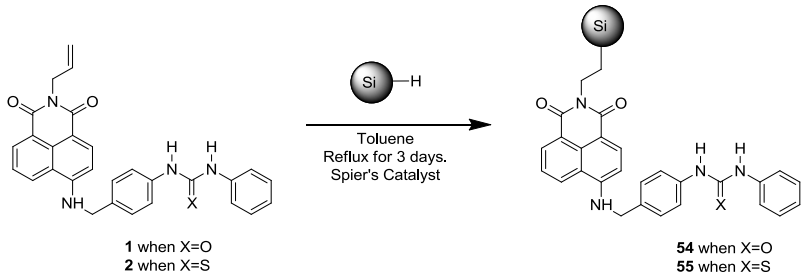

Scheme 38: Reaction between *N*-allyl-4-(4-(*N*-phenylureido)benzylamino)-1,8-naphthalimide (1) where X=O or *N*-allyl-4-(4-(*N*-phenylthioureido)benzylamino)-1,8-naphthalimide (2) where X=S and hydride modified silica.

The solid material was collected using a Hirsch funnel and washed with acetone. A soxhlet extraction technique (using acetone) was used in an effort to remove all unbound sensor. Visually using this technique all unbound sensor had been removed

during a period of less than three hours, however the material was left to extract overnight to fully ensure all unbound sensor was removed. The recovered material was dried *in vacuo*, with the product **54** obtained as a bright golden yellow silica powder.

The sample was analysed using solid state NMR spectroscopy. Solid state NMR spectroscopy produces a greatly different spectrum to that produced using liquid state NMR spectroscopy because of the process of line broadening [22]. Line broadening eliminates or obscures the sharp peaks which are typically observed for the resonances relating to the individual carbons seen in the spectrum acquired using a liquid sample [22]. Line broadening can be due to several factors including static dipolar interactions between ^{13}C and ^{1}H and chemical-shift anisotropy [22]. In the former, characteristic dipolar line splittings can occur because of the heteronuclar dipolar interactions between ^{1}H and ^{13}C [22]. These interactions depend on the angle between the C-H bonds and the externally applied field, meaning that in any one solid there will be several of these interactions which can occur [22]. This in turn means that broad peaks are observed instead of clearly defined peaks for each resonance [22]. The effect can be removed by the process of dipolar decoupling, where the sample is irradiated at proton frequencies whilst the carbon spectrum is obtained [22]. In chemical-shift anisotropy, the broadening is caused by changes in the chemical shift due to the interaction with the external magnetic field [22]. Broadening due to this can be removed using the concept of magic angle spinning, where samples are spun at speeds of greater than 2kHz and maintained at an angle of 54.7^{o} with respect to the applied field, 54.7^{o} being the “magic angle” [22] (Spinning at the magic angle can also remove some of the dipolar coupling as well). Solid spectra also typically take much longer to acquire than liquid spectra, due to the long spin-lattice relaxation time of ^{13}C nuclei in the solid phase [22]. This process can be overcome using a process called cross polarization, which operates a complicated pulse technique giving the proton and carbon nuclei identical Larmor frequencies. This causes the magnetic fields of both to interact, causing the carbon nuclei to relax [22]. Whilst in theory using these techniques should provide spectra where the signals are sharp, in practice broad signals are still observed.

Solid state ^{13}C-^{1}H NMR spectroscopy of the sensor modified silica surface **54** observed under conditions of cross polarisation-magnetic angle spinning (CP-MAS) (Figure 40) showed that some carbon based material was bound on the silica surface; however the signal obtained after scanning the sample for one day was very weak. There was little in the way of aromatic and carbonyl resonances observed, it was thought this was likely due to a small loading on the silica gel itself.

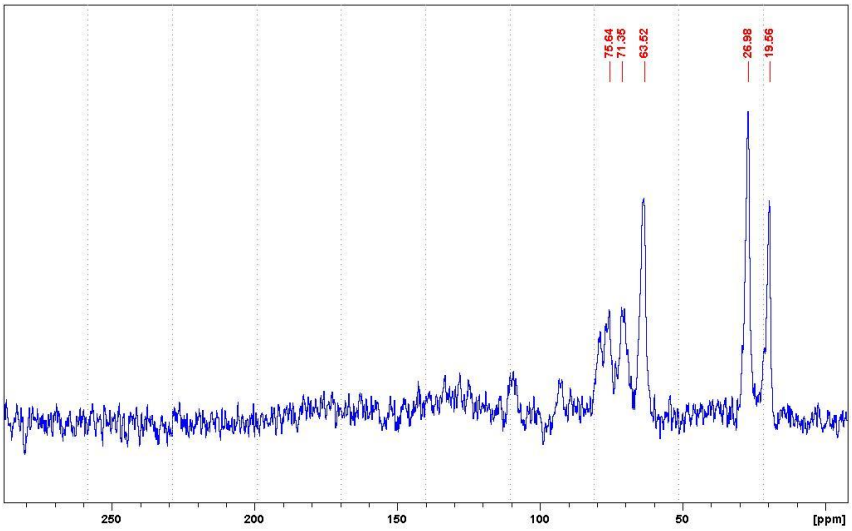

Figure 40: Solid state ^{13}C-^{1}H CP-MAS NMR spectrum of hydride silica modified with *N*-allyl-4-(4-(*N*-phenylureido)benzylamino)-1,8-naphthalimide, 54.

Solid state ^{29}Si-^{1}H CP-MAS NMR spectroscopy was also performed (Figure 42). Silica gel has a number of different resonances in the ^{29}Si NMR spectrum, due to the different condensation states of silica, which can be designated as Q^0,Q^1, Q^2, Q^3 and Q^4 (Figure 41) [128-132]. The resonances for each condensation state are observed at approximately -85 ppm for Q^0, -90 ppm for Q^1, -95 ppm for Q^2, -100 ppm for Q^3 and -110 ppm for Q^4 [128-132]. The resonances in the region -80 ppm to -120 ppm can therefore be assigned as from the silica gel, as we would not expect it to all exist in one state. Indeed the spectrum obtained for the sensor modified silica **54** was similar to that for unmodified silica with the addition of one extra peak at approximately -78 ppm, which is due to a Si-O-C bond. This would suggest a change in the environment of the silicon atom, supporting a successful immobilisation reaction.

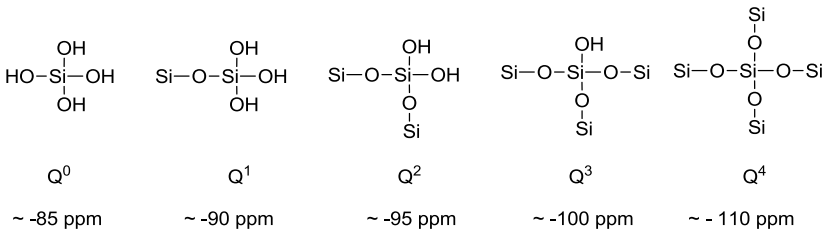

Figure 41: Designation of the different condensation states of silica.

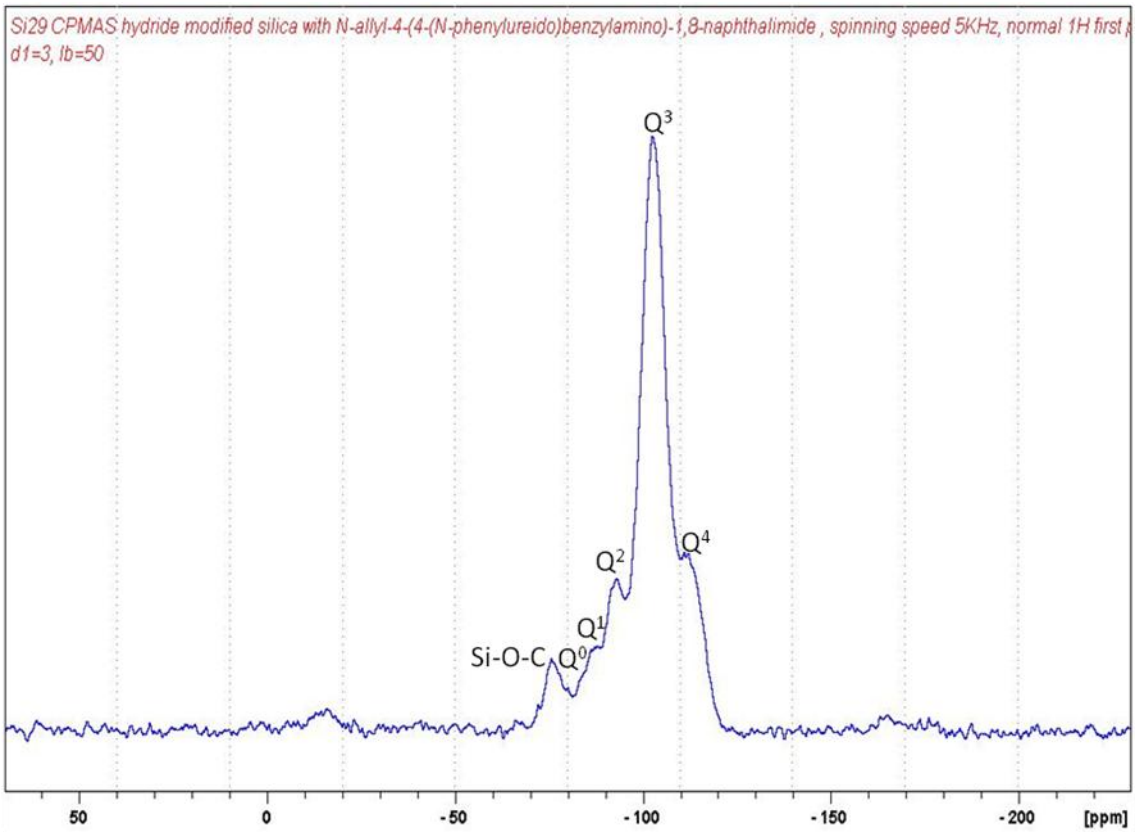

Figure 42: Solid state ^{29}Si NMR spectrum of hydride silica modified with *N*-allyl-4-(4-(*N*-phenylureido)benzylamino)-1,8-napthalimide, 54.

Attenuated Total Reflectance Infrared (ATR-IR) was also investigated as a technique to examine the recovered material. Initial ATR results showed little difference between plain silica gel and the sensor modified sample despite their vastly different visual appearance, meaning ATR was of little use. The unbound sensor has a completely different (Figure 43) spectrum to that of the hydride modified silica (Figure 38), and thus it would be expected there would be significant changes when the sensor is bound to the silica surface. However the spectra for the sensor modified silica **54** (Figure 44) appeared to show little of the characteristics observed in the spectrum of the unbound sensor (Figure 43). A more concentrated sample was prepared of the sensor modified silica, however the signal remained unchanged, which would seem to

indicate there is no difference and therefore nothing is bound. Visually though the silica has changed colour to bright yellow which indicates some material has attached and points to surface loading being an issue. It would appear there needs to be a higher surface loading so that traditional chemical techniques can show the existence of the sensor immobilised onto a silica surface.

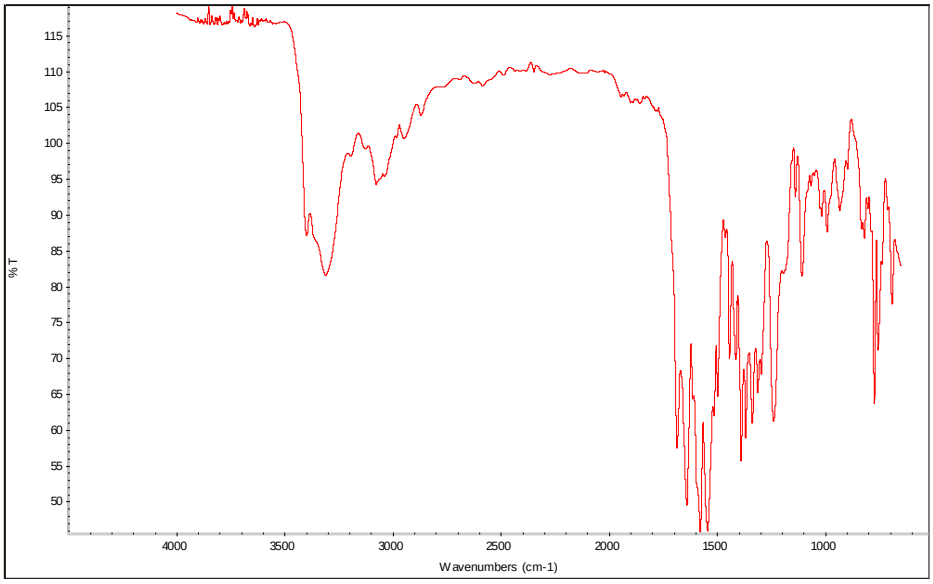

Figure 43: FTIR spectrum of *N*-allyl-4-(4-(*N*-phenylureido)benzylamino)-1,8-naphthalimide (1).

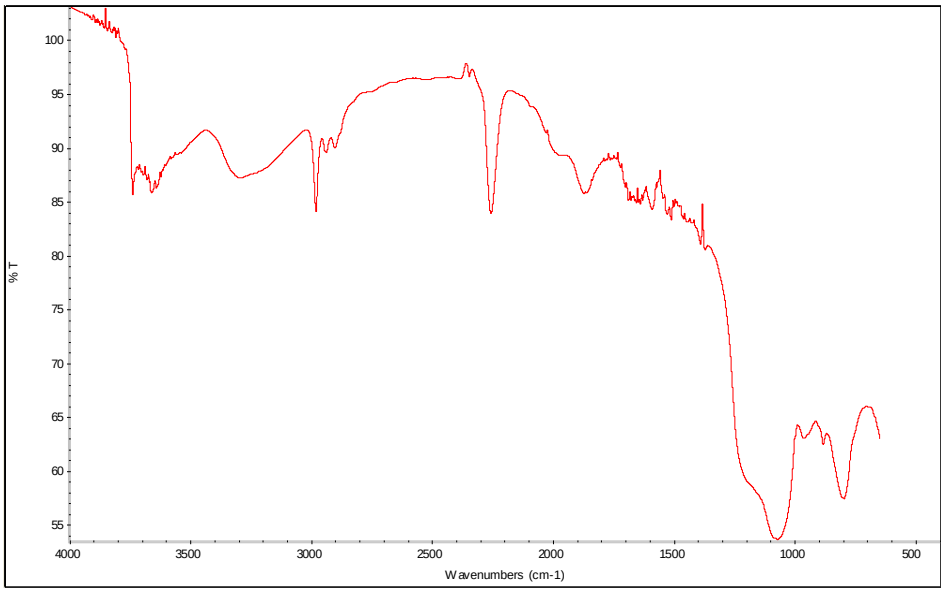

Figure 44: FTIR spectrum of hydride modified silica reacted with *N*-allyl-4-(4-(*N*-phenylureido)benzylamino)-1,8-naphthalimide, 54.

The immobilisation of **2** was also investigated using the method outlined above. As observed for the immobilisation of **1**, as the immobilisation of **2** progressed, the initial yellow colour of the reaction solution gained a distinct greyish tinge, thought to be due to the effect of the catalyst. After three days, the silica collected was using a Hirsch funnel. In order to confirm that the sensor was irreversibly bound, the silica collected was washed with acetone (soxhlet extraction), until the draining acetone was colourless, suggesting no further unbound sensor was present on the silica surface. The silica obtained was again bright yellow in colour, suggesting successful attachment had occurred.

Although results obtained by FTIR and NMR spectroscopies were inconclusive, visually it would appear that the desired transformation had been obtained (the sensor modified silica gel was highly coloured, a colour that could not be washed out despite extensive soxhlet extraction). As further evidence a small sample of the sensor modified silica was taken and exposed to a solution of tetrabutylammonium fluoride in DMSO. As detailed in Chapter 5, the addition of fluoride to a solution of naphthalimide sensor was found to elicit a colour change from yellow to deep red/purple (due to the deprotonation of the 4-amino moiety). As can be observed in Figure 45, addition of the fluoride solution to the derivatised silica gel resulted in the deep red/purple colour forming. Upon addition of a hydrogen bonding solvent (methanol), this colour change was observed to reverse. This would seem to confirm that the sensor was attached to the silica surface (and bound either irreversibly or quite strongly as no remaining sensor was able to be extracted using the soxhlet extraction technique) and that the surface could be used more than once as the colour change due to the interaction with fluoride was able to be reversed. These results would seem to indicate that hydrosilation is a viable method for the immobilisation of the sensors onto a silica surface however surface loading would appear to be an issue preventing full characterisation.

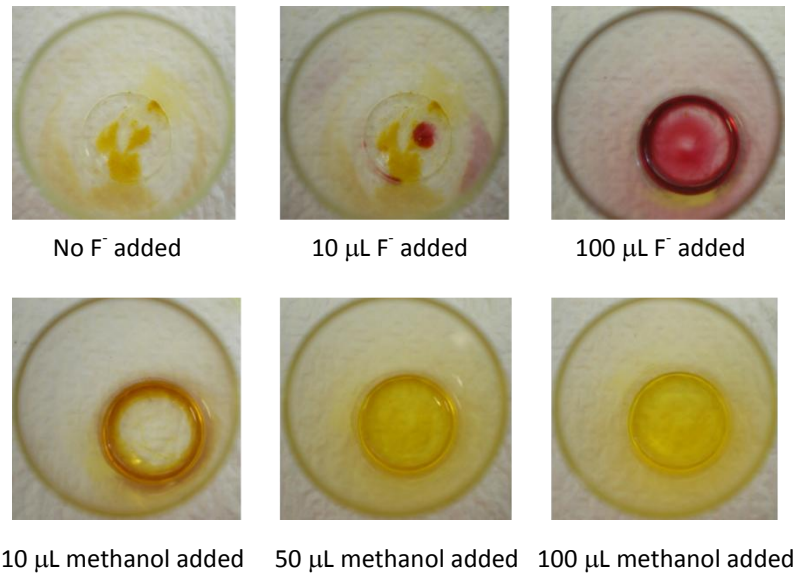

Figure 45: Addition of Fluoride (TBA salt) in DMSO to sensor modified silica, 54 (top) and addition of methanol (bottom).

6.3 Immobilisation onto 3-aminopropyl functionalised silica

In an effort to try and obtain more definitive spectroscopic characterisation of the sensor modified silica surface, an approach was taken to synthesise the sensor on the surface, rather than synthesise the molecule fully and then immobilise it. In this way it was a hoped a higher surface loading would be obtained. To this end, 3-aminopropyl functionalised silica was purchased from Sigma Aldrich, with the silica used in the place of allylamine to react with the anhydride **44** (depicted in Scheme 39) allowing covalent attachment through the imide functionality.

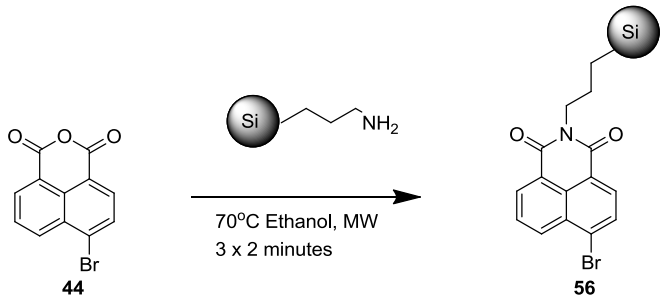

Scheme 39: Reaction between 4-bromo-1,8-naphthalic anhydride (44) and 3-aminopropyl-functionalised silica.

This reaction was initially attempted using conventional heating methods (anhydride **44** was refluxed in anhydrous ethanol with 3-aminopropyl functionalised silica for three hours), however FTIR results showed little difference between the 3-aminopropyl functionalised silica and the product after it was reacted with the anhydride **44**. As the synthesis of naphthalimide based sensors was established to be successful using microwave irradiation in Chapter 4, it was decided to investigate the possibility of using microwave irradiation to react **44** with 3-aminopropyl functionalised silica. The results obtained were much more promising and are discussed below.

*6.3.1 Formation of naphthalimide functionalised silica (**56**)*

Initial immobilisation experiments were trialled on a small scale (50 mg of silica) in relation to the functionalised silica. Taking into account that only nine percent of the silica was functionalised (as detailed on the packaging from Sigma Aldrich), one equivalent of anhydride **44** was added with anhydrous ethanol as reaction solvent (Scheme 39). The reaction was initially irradiated for two minutes at 70^{o}C.

After cooling it was noted that the reaction solution had changed to a dark beige colour, with a small amount of a light beige powder at the bottom of the tube. The reaction tube was placed back in the microwave reactor for a further two lots of two minutes at 70^{o}C (for a total irradiation time of six minutes). No change was observed during the period between the two irradiations or after the second irradiation, with a small amount of the light material being observed at the bottom of the reaction tube. After the tube was cooled a precipitate was observed to form (in a similar manner to the reaction between allylamine and the anhydride **44**). The solid material was washed thoroughly with ethanol and then acetone (until the filtrate was seen to be colourless) to ensure removal of any unreacted material. The recovered silica was then dried under a stream of nitrogen.

ATR-FTIR spectroscopy was used to analyse the recovered solid material (Figure 46 black line). ATR spectra showed that there was some evidence that the anhydride had reacted with the 3-amino propyl silica to form the imide functionalised surface **56**, with new peaks occurring in the region 1900-1300 cm^{-1}. The peak at approximately

1710 cm^{-1} is characteristic of the imide functionality introduced by reaction of the anhydride with the amine on the functionalised silica [105]. Further peaks at *ca*. 1590 cm^{-1} and 1540 cm^{-1} are due to the aromatic rings in the naphthalimide moiety, as is the very weak band in the 3000 cm^{-1} region [105]. This would suggest the anhydride had reacted with the terminal amine group of the 3-aminopropyl functionalised silica gel forming the naphthalimide functionalised silica gel.

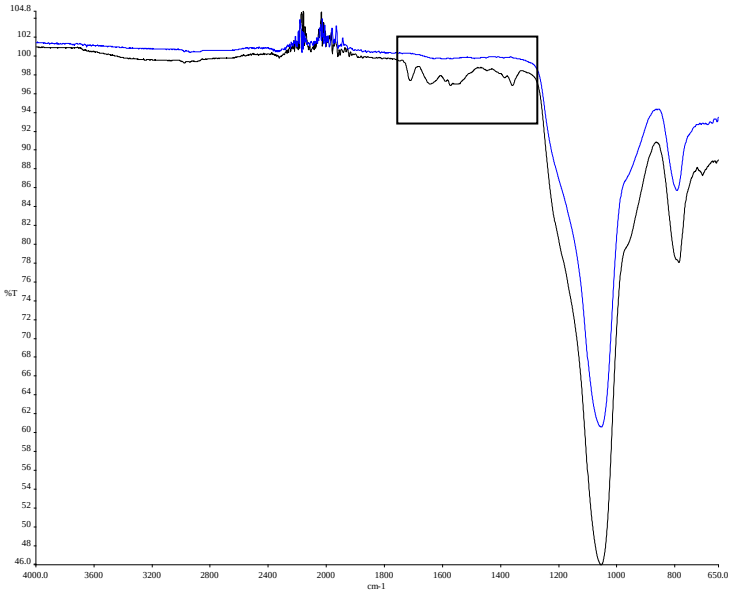

Figure 46: Overlayed FTIR spectra of 3-aminopropyl functionalised silica reacted with 4-bromo-1,8-naphthalic anhydride (56, black) and 3-aminopropyl functionalised silica (blue).

Solid state carbon (^{13}C-^{1}H under CP-MAS conditions) experiments were performed on the 3-aminopropyl functionalised silica gel obtained from Sigma Aldrich, the anhydride starting material **44** and the recovered 3-aminopropyl functionalised silica gel modified with 4-bromo-1,8-naphthalic anhydride **56** (Figure 47). As can be seen the purchased silica gel has five resonances in the solid state ^{13}C spectrum all below 70 ppm. The existence of five resonances was unexpected, as the amino propyl group has only three carbons, which would mean we should see a maximum of three carbon resonances, consistent with the literature which reports them at approximately 43, 25 and 10 ppm [133, 134]. The two extra resonances are due to residual ethoxy groups (at 18 and 60 ppm) still present in the functionalised silica as detailed by Luan [134].

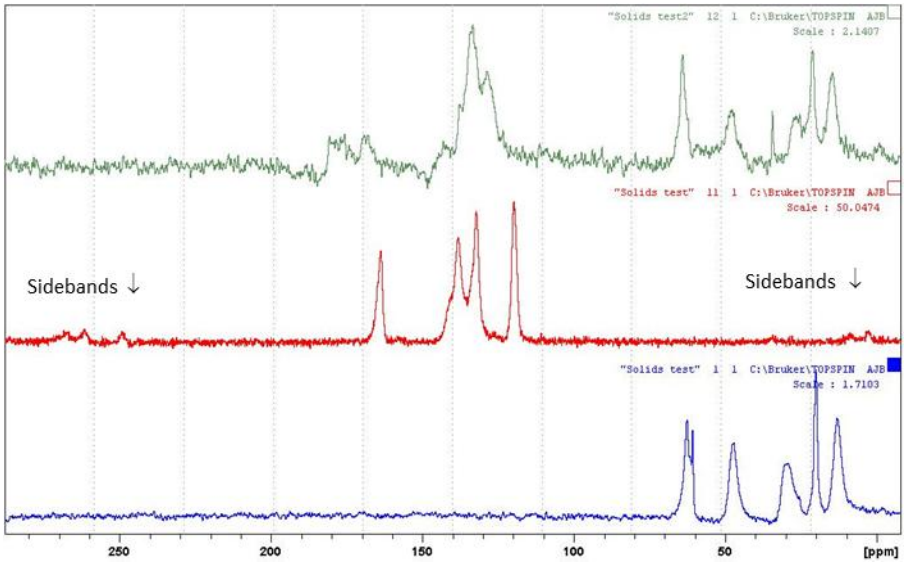

Figure 47: Stackplot solid state ^{13}C NMR spectra of (bottom) 3-aminopropyl functionalised silica gel (obtained from Sigma Aldrich), (middle) 4-bromo-1,8-naphthalic anhydride (44) starting material and (top) 3-aminopropyl functionalised silica modified with 4-bromo-1,8-naphthalic anhydride 56.

The anhydride **44** exhibited four main resonances between 120 ppm and 170 ppm. In a solution phase ^{13}C NMR spectrum, we would expect to see twelve resonances, as there are twelve unique carbon environments in the molecule. The reason only four resonances are observed is most likely due to the broader bands observed in solid state NMR spectroscopy, therefore obscuring resonances under one another. Also as the solid state spectrum are obtained under CP-MAS conditions, the signal due to the quaternary carbons will not be enhanced (due to lacking a proton) and hence may not be observed in the acquired spectrum.

In the spectrum of the final product **56** a number of resonances are observed, those below 70 ppm are easily assigned to the 3-aminopropyl functionalised silica whilst it would appear those peaks between 120 ppm and 190 ppm arise from the addition of the naphthalimide moiety. The centre resonances from the starting material are present in the product (although the intensity differs), whilst the resonances at 120 ppm and 165 ppm are no longer present. The two new resonances at 168 ppm and 180 ppm are most likely due to the change from the anhydride to the imide. This is consistent with observations in the unbound sensor where upon conversion of the anhydride to an imide, the carbon resonances assigned to the carbonyl moieties moved further downfield. As the naphthalimide moiety had been successfully attached to the silica surface, further steps were taken to synthesise the sensor on the surface.

*6.3.2 Reaction of **56** with 4-aminobenzylamine to form **57***

In the next step the naphthalimide modified silica **56** was reacted with 4-aminobenzylamine (Scheme 40) using microwave conditions. The reaction temperature was set at 105^{o}C, and excess 4-aminobenzylamine was added to **56** and heated for an initial two minutes. An additional two further two minute irradiations at 105^{o}C (with a cooling cycle to 50^{o}C in-between) were undertaken. The reaction was observed to turn a dark red colour consistent with the conventional heating reaction between *N*-allyl-4-bromo-1,8-naphthalimide (**45**) and 4-aminobenzylamine to form *N*-allyl-4-(4-aminobenzylamine)-1,8-naphthalimide (**51**).

Upon addition of water a bright yellow solid was observed to form. The solid material obtained was collected using a Hirsch funnel and washed with acetone until the acetone was seen to run colourless. The material was then dried under a stream of nitrogen. This left a brightly yellow coloured silica gel, greatly different in colour to the beige silica obtained in the first step, which would seem to indicate that a reaction had occurred and the amino group has displaced bromide on the naphthalimide ring.

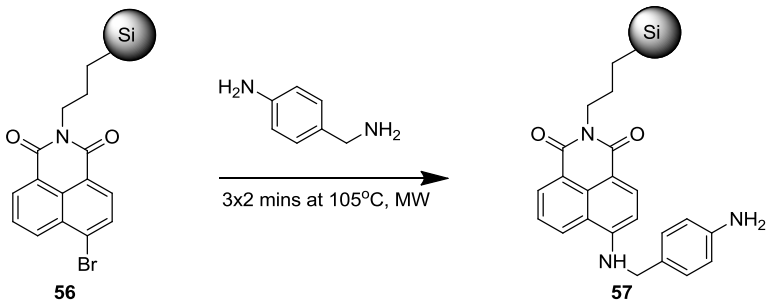

56 **57**

Scheme 40: Reaction between naphthalimide functionalised silica 56 with 4-amionbenzylamine to form 57

FTIR spectroscopy was used to characterise the recovered silica (Figure 48). Little difference however was observed between **56** and the material formed when **56** was reacted with 4-aminobenzylamine to form **57**.

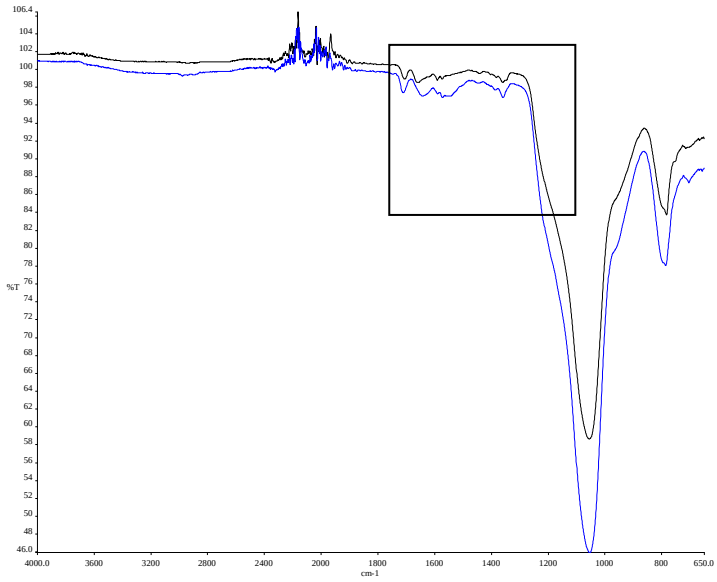

Figure 48: Overlayed FTIR spectra of 3-aminopropyl functionalised silica reacted with 4-bromo-1,8-naphthalic anhydride to form 56 (shown in blue) and 56 reacted with 4-aminobenzylamine to form 57 (shown in black).

Characterisation was also attempted using solid state ^{13}C-^{1}H NMR (CP-MAS) spectroscopy. As depicted in Figure 49 there are some subtle differences between spectra of the starting material **56** and the recovered material **57**. It is particularly evident that there is a reduction in the number of resonances in the region from 80 ppm to 0 ppm assigned to the amino propyl group. The differences in the spectra in the 100 ppm to 200 ppm indicate there are changes in the molecule (addition of the aminobenzyl group) and provide evidence a reaction has occurred.

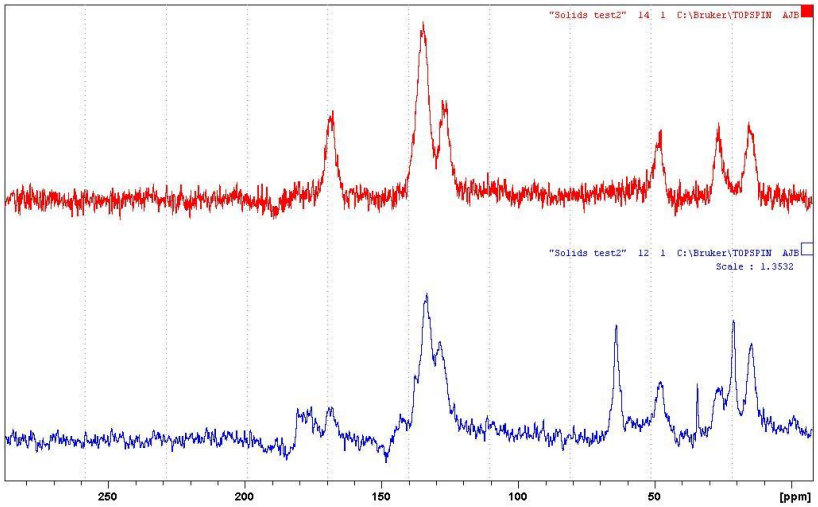

Figure 49: Stackplot solid state ^{13}C-^{1}H (CP-MAS) NMR spectra showing (bottom) naphthalimide functionalised silica 56 and (top) naphthalimide functionalised silica reacted with 4-aminobenzylamine 57.

The changes observed in the solid state ^{13}C NMR spectrum and the colour change from white silica to yellow silica was considered great evidence that the reaction had occurred and it was decided to continue with the next step of urea formation to synthesise the sensor.

*6.3.3 Reaction of **57** with phenyl isocyanate to form **58***

In the final step to produce the surface mounted sensor, the amino naphthalimide modified silica **57** was allowed to react with phenyl isocyanate in acetonitrile (Scheme 41). One of the methods used to create a similar non-immobilised sensor using conventional heating was undertaken in acetonitrile at reflux so a temperature below the boiling point of acetonitrile (81-82^{o}C) of 70^{o}C was selected for the microwave reaction. Again three irradiations of two minutes duration were undertaken.

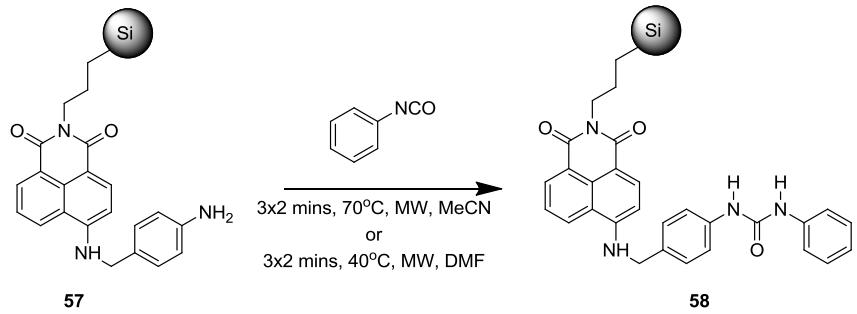

57 **58**

Scheme 41: Reaction between amino naphthalimide modified silica 57 and phenyl isocyanate to form 58.

Impurities were removed by washing with acetone, until the acetone was a colourless solution and then the solid was dried under a stream of nitrogen. The solid material was then soxhlet extracted in acetone to remove any unreacted sensor. The recovered material was similar in colour to that obtained after the reaction between 4-aminobenzylamine and the naphthalimide modified silica. The same reaction was also repeated using DMF as a solvent, with 3 irradiations of 2 minutes each at 40^{o}C, along with 2 drops of triethylamine, mimicking the conventional heating DMF method. As above, the solid recovered was soxhlet extracted using acetone until there were no traces of unreacted sensor. Samples were then analysed *via* solid state ^{13}C NMR spectroscopy.

^{13}C-^{1}H (CPMAS) NMR spectra were obtained for the aminobenzylamine silica reacted with phenyl isocyante **58** produced from both the acetonitrile and DMF methods and found to be the same, indicating both sets of reaction conditions produced as expected the same results. Slight differences were observed between the spectra obtained for **58** and **57** (Figure 50) consistent with another change in the material. The extra resonance clearly observed at 142 ppm is likely due to the additional phenyl ring introduced with the urea recognition group. Unexpectedly there is no new resonance which could be assigned to the urea carbonyl. This could be due to the broadness of the resonance relating to the imide carbonyls, as it would be expected that resonance relating to the urea carbonyl would have a similar shift.

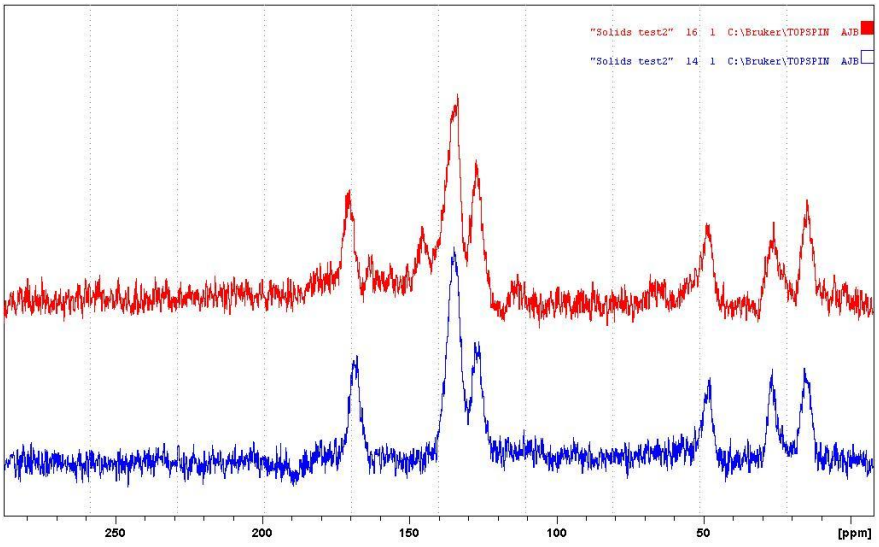

Figure 50: Overlayed ^{13}C-^{1}H (CPMAS) solid state NMR spectra of 57 (blue) and 58 (red).

As with the silica obtained using hydrosilation processes (Section 6.2.1), a solution of tetrabutylammonium fluoride in DMSO (0.2 M) was added to **58**, with a colour change from yellow to light orange observed. Whilst the change observed was not as significant (yellow to deep red) as that observed for the immobilised sensor using hydrosilation (Section 6.2.1, Figure 45), nor is as significant as that observed for the free sensor in Chapter 5, there is a distinct colour change as greater amounts of fluoride are added. This colour change was reversed upon addition of methanol.

In summary there was some evidence that the use of microwave irradiation to build the sensor onto an aminopropyl silica was successful. There was a clear change in the look of the silica, which started out as a white powder, changed to a beige powder

upon addition of the fluorophore and then to yellow upon addition of the spacer. This was consistent with the colours of the materials obtained in the synthesis of the free sensors. Definitive spectral characterisation was again difficult, however solid state NMR spectroscopy showed there were changes in the material at each step. Surface loading was considered a potential issue preventing successful characterisation.

6.4 Incorporation of silyl groups in the sensor molecule

As spectroscopic evidence of successful attachment had been hard to prove definitively potentially due to low surface loadings, further investigations were undertaken into determining successful ways to immobilise the sensor onto a surface with increased efficiency. Seo and co-workers reacted 1,8-diaminonaphthalene with 3-(triethoxysilyl)propyl isocyanate in THF to form a receptor containing naphthalene as the fluorophore, urea binding sites and a silanol group bonded to ethoxy groups for surface immobilisation [77]. They then immobilised the sensor onto both mesoporous silica and silica particles *via* a siloxane linkage. As described in Chapter 3 during this research a series of three naphthalimide based sensors **6**-**8** were synthesised based on the methodology developed by Seo [77]. The following sections describe the immobilisation studies, initially on the sensor **6** with the spacer in the *para* position onto silica gel and mesoporous silica.

*6.4.1 Immobilisation of N-allyl-4-(4-(N-3-(triethoxysilyl)propylureido) benzylamino)-1,8-naphthalimide (**6**) – silica particle*

Silica gel and mesoporous silica were considered for immobilisation of *N*-allyl-4-(4-(*N*-3-(triethoxysilyl)propylureido)benzylamino)-1,8-naphthalimide (**6**). Initial experiments used silica gel and were based on the methodology developed by Seo and co-workers [77]. The sensor, **6** was dissolved in anhydrous DMSO and heated to reflux under a nitrogen atmosphere. An equal quantity of silica gel particles from a 300^{o}C oven were added to the refluxing mixture. The reflux was continued for approximately 24 hours, after which time the reaction was removed from the heat and allowed to cool to room temperature, with the silica settling out as it cooled. The silica was filtered *in vacuo* with the solid washed with copious amounts of DMSO to remove unreacted sensor. The solid was then dried in an oven to remove excess DMSO, leaving a dark orange

coloured silica gel. Washings with DMSO and also acetone suggested visually that no unreacted sensor remained on the silica surface. Despite being strongly coloured, with no more unbound sensor being able to be removed from the surface, ATR-FTIR results show no discernible difference between a sample of unmodified silica gel and a sample of silica gel immobilised with the sensor, indicating again that surface loading was insufficient for spectroscopic characterisation.

6.4.2 Formation of mesoporous silica

The final surface investigated with the triethoxysilyl sensors was mesoporous silica as investigated by Seo and co-workers [77]. Mesoporous silica has a much larger surface area than regular silica gel and therefore it was considered that this could lead to a higher surface coverage. Mesoporous silica was produced by the method proposed by Seo [77], the only change made was replacing the surfactant octadecyltrimethyl ammonium bromide (ODTMA) with cetyl trimethyl ammonium bromide (C-TAB) primarily due to its availability. A mixture of distilled water, hydrochloric acid, tetraethyl orthosilicate and C-TAB was placed in an 80^{o}C oven. The mesoporous silica was removed from the oven after six days, with the contents of the flask collected using a Hirsch funnel and washed with water. The recovered mesoporous silica was then placed in a 100^{o}C oven overnight to remove water, followed by five hours in a 600^{o}C furnace to remove residual C-TAB.

*6.4.3 Immobilisation of N-allyl-4-(4-(N-3-(triethoxysilyl)propylureido) benzylamino)-1,8-naphthalimide (**6**) – mesoporous silica*

Mesoporous silica was functionalised with **6** using the same procedure (DMSO, reflux, twenty-four hours, nitrogen atmosphere) described for the silica gel particle (Section 6.4.1) and as utilised by Seo and co-workers [77]. After twenty-four hours the reaction was removed from the heat and cooled to room temperature. The solid mesoporous silica was collected using a Hirsch funnel and washed with DMSO to remove unreacted sensor. Washing was continued until the DMSO was observed to be colourless. The solid at this point had a brownish red colour, which was unexpected, as it was anticipated it would be the yellow/orange colour of **6**. The collected material was dried under vacuum in an effort to remove excess DMSO, resulting in a granular pale yellow solid. The solid material was then soxhlet extracted in acetone, until no more colour

was observed in the solvent. ATR-IR spectra (Figure 51) showed several differences between the spectra of mesoporous silica (shown in black) and the functionalised mesoporous silica (shown in green) particularly around the carbonyl (ca 1600 cm^{-1}) and C-O bond stretching (ca. 1100 cm^{-1}) regions, suggesting that some material had attached, however the IR spectrum was similar to mesoporous silica refluxed in DMSO (blue) making it difficult to confirm attachment of the sensor *via* IR.

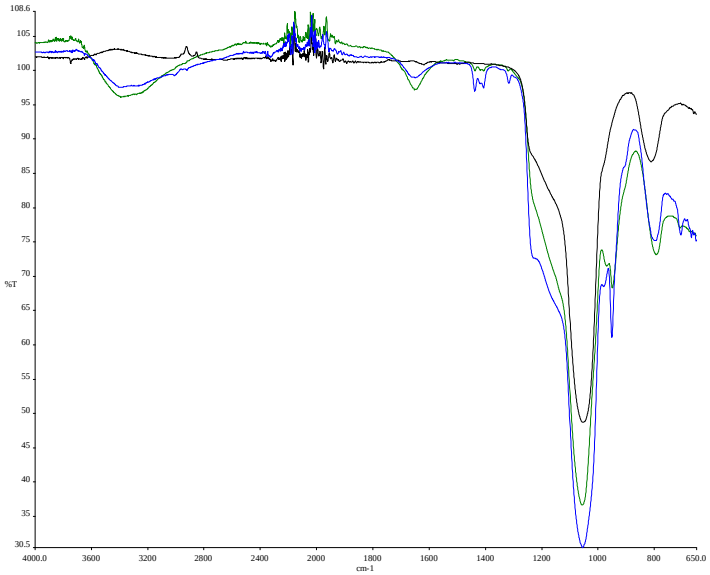

Figure 51: FTIR spectra of meosporous silica (black), mesoporous silica refluxed in DMSO (blue) and mesoporous silica with 6 attached (59) (green).

In an effort to further characterise the solid containing immobilised **6**, solid state silicon (^{29}Si-^{1}H (CP-MAS)) NMR spectroscopy was undertaken on samples of mesoporous silica (red), the unbound 4-triethoxysilyl sensor **6** (blue) and with **6** bound on mesoporous silica **59** (green) (depicted in Figure 52). As can be seen only one resonance is observed for the 4-triethoxysilyl sensor (**6**) at -48.11 ppm due to the triethoxysilyl group within the sensor. The mesoporous silica has the typical ^{29}Si spectrum observed for condensed silica discussed in Section 6.2.1 with the major resonance being Q_3 at -102.86 ppm, with shoulder resonances (-93.50 ppm being Q_2 and -114.30 ppm, Q_4) on both sides. When **6** was attached to mesoporous silica the resulting ^{29}Si spectrum indicated that there was a change in the mesoporous silica with two new overlapping resonances introduced at -58.48 ppm and -67.33 ppm, in addition to the resonances originating from the mesoporous silica itself (slightly shifted with the main resonance at -102.75 ppm and a shoulder resonance at -93.11 ppm).

Whilst the new resonance is not the same as observed for the triethoxysilyl sensor this is due to the different chemical environment it exists in after surface attachment, indicating successful attachment.

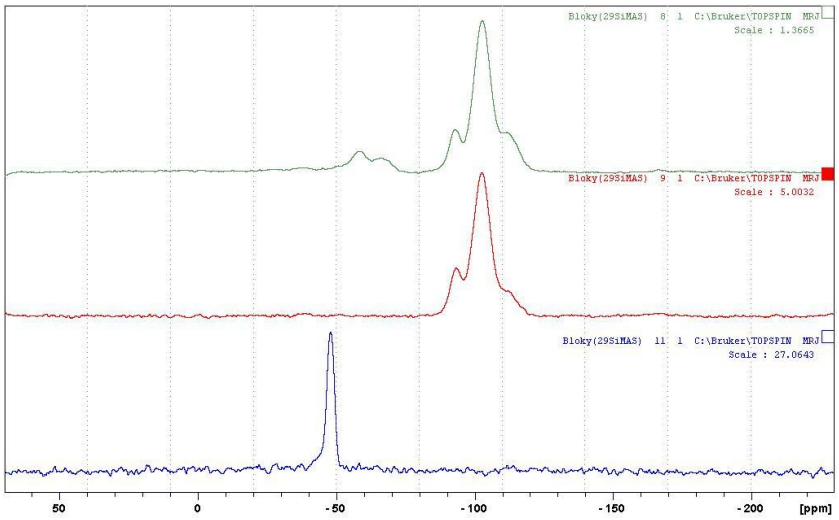

Figure 52: Stacked solid state ^{29}Si (CP-MAS) spectra of, unbound 4-triethoxysilyl sensor 6 (bottom), mesoporous silica (middle) and 6 bound on mesoporous silica 59 (top).

As previously carried out, a solution of tetrabutylammonium fluoride in DMSO (0.2 M) was added to **6** immobilised on mesoporous silica, with a colour change from yellow to light orange. Whilst the change observed is not as significant as that observed from the immobilised sensor using hydrosilation (Section 6.2.1, Figure 45), nor is as significant that that observed for the free sensor in Chapter 5, there is a distinct colour change as greater amounts of fluoride are added. Upon addition of methanol there was a slight reversal of the change in colour, suggesting the deprotonation is reversed. More work would be required to obtain this reversibility for practical applications.

*6.4.4 Immobilisation of N-allyl-4-(2-(N-3-(triethoxysilyl)propylureido) benzylamino)-1,8-naphthalimide (**7**) – mesoporous silica*

After success was observed with the immobilisation of **6** onto mesoporous silica, immobilisation of **7** was carried out using the same method. Solid state silicon (^{29}Si-^{1}H (CP-MAS)) NMR spectroscopy was undertaken on a sample of **7** (Figure 53) and a sample of **7** bound on mesoporous silica (depicted in Figure 53). As observed when **6** was bound on mesoporous silica (Figure 52) the resulting ^{29}Si spectrum indicated that

there was a change in the mesoporous silica with two new overlapping resonances introduced at -55 ppm and -65 ppm (clearly present in the spectrum of the unbound sensor), in addition to the resonance originating from the mesoporous silica itself.

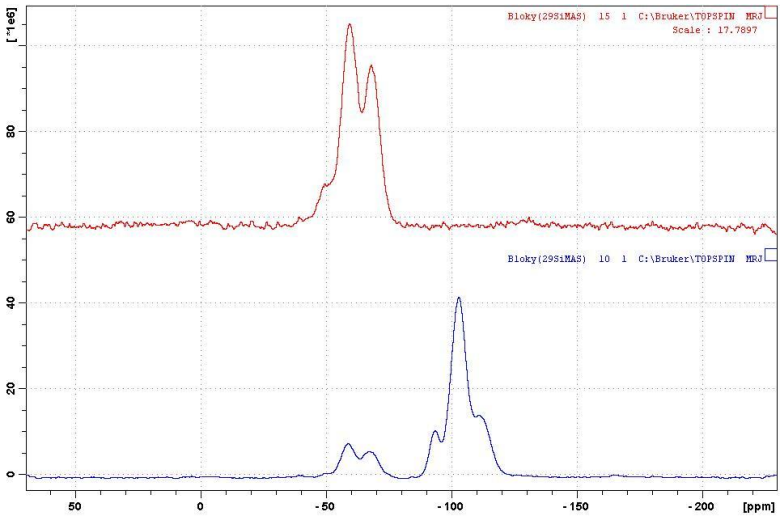

Figure 53: Stacked solid state ^{29}Si (CP-MAS) spectra of, of *N*-allyl-4-(2-(*N*-propylureidotriethoxysilyl)benzylamino-1,8-naphthalimide (7) (top) and *N*-allyl-4-(2-(*N*-propylureidotriethoxysilyl)benzylamino-1,8-naphthalimide (7), immobilised onto mesoporous silica 60 (bottom).

The solid state ^{29}Si spectrum of **7** differs from that of **6**, as there are three Si signals for **7** and only one for **6** which was not expected as the only difference between the two molecules (position of the spacer molecule) would be expected to have minimal impact on the ^{29}Si spectrum. The most likely reason for the difference is the process of hydrolysis, in which the ethoxy groups are converted to hydroxyl groups (discussed briefly in Chapter 5) as the sample ages and is in contact with water (atmospheric from storage) [126]. The chemical shift of the silicon resonance will change dependant on the groups attached to the Si atom and will result in multiple signals if the process of hydrolysis is occurring.

As observed with **59**, ATR-IR characterisation of **60** was complicated by the reaction solvent, with little difference able to be observed between **60** and a sample of mesoporous silica refluxed in DMSO. Again, a solution of tetrabutylammonium fluoride in DMSO (0.2 M) was added to **60.** Whilst the change observed was not as significant as that observed from the immobilised sensor using hydrosilation (Section 6.2.1, Figure 45), nor as significant as that observed for the free sensor in Chapter 5, there is a slight

colour change from yellow to orange as greater amounts of fluoride are added. Upon addition of methanol there is a reversal of this colour change, suggesting that complexation is inhibited and that a reversal of the interaction is possible.

*6.4.5 Immobilisation of N-allyl-4-(3-(N-3-(triethoxysilyl)propylureido) benzylamino)-1,8-naphthalimide (**8**) – mesoporous silica*

As detailed for **6** in Section 6.4.3 and **7** in Section 6.4.4, a similar process was undertaken to immobilise **8**, a similar molecule with the spacer in the *meta* orientation onto mesoporous silica. Solid state silicon (^{29}Si-^{1}H (CP-MAS)) NMR spectroscopy was undertaken on a sample of **8** and a sample of **8** bound on mesoporous silica (**61**) (Figure 54). As observed when **6** was bound on mesoporous silica (Figure 52) the resulting ^{29}Si spectrum indicated that there was a change in the mesoporous silica with two new overlapping resonances introduced at -55 ppm and -65 ppm (also present in the spectrum of the unbound sensor and most likely due to different states of condensation), in addition to the resonances originating from the mesoporous silica itself. As expected this result was near identical to that obtained for **59** and **60**.

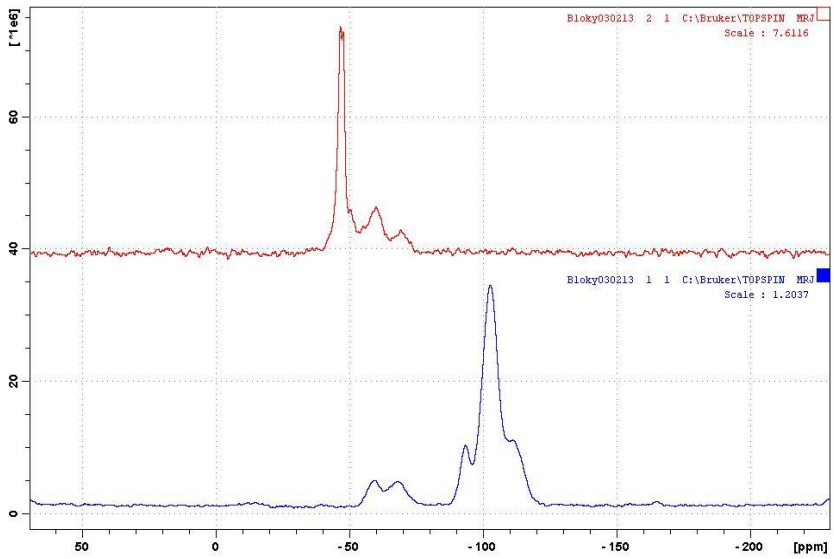

Figure 54: Stacked solid state ^{29}Si (CP-MAS) spectra of, of *N*-allyl-4-(3-(*N*-propylureidotriethoxysilyl)benzylamino-1,8-naphthalimide (8) (top) and *N*-allyl-4-(3-(*N*-propylureidotriethoxysilyl)benzylamino-1,8-naphthalimide (8), immobilised onto mesoporous silica 61 (bottom).

Again characterisation of **61** was hindered by the use of DMSO as reaction solvent, with **61** having a similar spectrum to unmodified mesoporous silica refluxed in DMSO.

Addition of a solution of tetrabutylammonium fluoride in DMSO (0.2 M) was again trialled for **61** with results showing there was a definite colour change (yellow to orange) as greater amounts of fluoride were added. Upon addition of methanol this colour change was reversed, showing that sensors based on **8** have the potential to be reused.

In summary, the use of hydrolysis chemistry to immboilise the sensor onto mesoporous silica would appear to have been successful, with solid state silicon NMR spectroscopy seemingly indicating the sensors are immobilised onto a mesoporous silica surface. Little evidence however was obtained for the immobilisation *via* IR and the colour change observed in Section 6.2.1 was not observed to the same extent.

6.5 Conclusion

In this chapter, results from preliminary investigations into the immobilisation of the naphthalimide sensors onto silica using three different approaches were detailed

In the first approach (Section 6.2), immobilisation was carried out using the terminal double bond already in place from the allyl group, specifically included in the designed sensors for this purpose. Little evidence in terms of data from NMR or IR spectroscopies was able to show that the sensor was successfully immobilised, however visually upon addition of fluoride to the immobilised silica a colour change was observed. This colour change from yellow to red, was due to the removal of the 4-amino proton as established in Chapter 5. As the silica has been extensively extracted in acetone to remove any unbound sensor, it would appear that this would provide evidence that successful attachment occurred.

In Section 6.3, an approach was taken to build the sensor stepwise on the surface starting from a 3-aminopropyl functionalised silica obtained from Sigma Aldrich. It was hoped in this way definitive spectroscopic evidence could be obtained at each step. Several changes could be noted *via* FTIR and NMR spectroscopies throughout the step-wise building process suggesting changes were occurring, although still it was difficult to characterise the final materials obtained. A colour change was observed similar to

that mentioned above, however the result was not as definitive as that obtained in Section 6.2.

Finally in Section 6.4, triethoxysilyl groups were inserted into the molecule at the synthesis stage so as to allow direct immobilisation of the sensor onto mesoporous silica gel *via* condensation reactions. This method had the benefit of there being only one step to attach the sensor to the surface, hence any change to the silica must be due to sensor being immobilised onto the surface. Again results suggested immobilisation had occurred, with solid state silicon NMR spectroscopy results indicating successful surface attachment. The solvent used for the reaction however hindered definitive characterisation by IR. Similar colour changes to Section 6.3 were observed, again lacking the absolute certainty of the colour change observed in Section 6.2.

Overall, a variety of approaches were trialled to immobilise a 4-amino-1,8-naphthalimide based sensor onto a solid silica support surface. In all methods trialled there was indications that the methods were successful to a certain extent. It is likely that small loadings of the sensor onto the surface made definitive characterisation difficult. Despite the lack of “hard” characterisation data, surface chemistry was successful (particularly those in Section 6.2). It was also established that it was possible to reverse the observed chemical interactions – hence sensors produced using these methods could be used repeatedly. Further work is required in this area and these ideas will be presented in Chapter 7, Future Work and Conclusions.

Chapter 7

CONCLUSIONS AND FUTURE WORK

7.1 Conclusions

In this thesis, research has been presented into the synthesis and evaluation of anion sensors based on the 4-amino-1,8-naphthalimide fluorophore. After establishing that the sensors were able to bind with anions in the solution phase, preliminary investigations into the immobilisation of the sensors onto silica was undertaken.

7.1.1 Synthesis of 4-amino-1,8-naphthalimide based anion sensors

4-Amino-1,8-naphthalimide based sensors were synthesised using conventional heating techniques with three steps. In the first step the starting material 4-bromo-1,8-naphthalic anhydride (**44**) was reacted with allylamine in refluxing ethanol to form *N*-allyl-4-bromo-1,8-naphthalimide (**45**) in yields that regularly exceeded 90%.

In the second step a nucleophillic aromatic substitution reaction was performed to add the 4-amino group and spacer to the fluorophore. These molecules, whilst similar to molecules prepared previously, have not been previously reported in the scientific literature. *N*-Allyl-4-(2-aminobenzylamine)-1,8-naphthalimide (**50**) was synthesised by heating at 110^{o}C with the imide **45** for forty-eight hours (Yield – 63%). *N*-Allyl-4-(4-aminobenzylamine)-1,8-naphthalimide (**51**) was synthesised by heating at 110^{o}C with the imide for two hours. Yields were higher than that of the 2-amino compound at 72%. Finally the sensor with the 3-aminobenzylamine spacer (**52**) was synthesised by heating at 110^{o}C with the imide (**45**) for three hours in a yield of 78%.

In the third step, the recognition unit was added to form the final sensor molecule. Using **50**, *N*-allyl-4-(2-(*N*-phenylureido)benzylamino)-1,8-naphthalimide (**4**) was synthesised by heating under reflux overnight in acetonitrile in the presence of phenyl isocyanate (1.5 equivalents), with a maximum yield of 53%. Using **51**, *N*-allyl-4-(4-(*N*-phenylureido)benzylamino)-1,8-naphthalimide (**1**) was synthesised by stirring overnight at room temperature in DMF, in the presence of phenyl isocyanate and triethylamine. Also from **51**, *N*-allyl-4-(4-(*N*-phenylthioureido)benzylamino)-1,8-naphthalimide (**2**) was synthesised in a similar way to **1**, however reproducibility of the reaction was an issue. Finally from **51**, *N*-allyl-4-(4-(*N*-4-

chlorophenylureido)benzylamino)-1,8-naphthalimide (**3**) was formed by stirring in DMF overnight in the presence of 4-chlorophenyl isocyante and triethylamine (Yield – 79%). From **52**, *N*-allyl-4-(3-(*N*-phenylureido)benzylamino)-1,8-naphthalimide (**5**) was synthesised by heating under reflux in a yield of 86%**.**

Sensors **6**, **7** and **8** were synthesised containing a triethoxysilyl group to enable later immobilisation through condensation reactions onto a silica surface. *N*-Allyl-4-(4-(*N*-3-(triethoxysilyl)propylureido)benzylamino)-1,8-naphthalimide (**6**) was synthesised by reaction of **51** with 3-(triethoxysiyl)propyl iscoayante under reflux in THF for fourty-eight hours (39%). *N*-Allyl-4-(2-(*N*-3-(triethoxysilyl)propylureido)benzylamino)-1,8-naphthalimide (**7**) was synthesised by reaction of **50** with 3-(triethoxysiyl)propyl iscoayante under reflux in THF for ninety-six hours (19%). Finally *N*-Allyl-4-(3-(*N*-3-(triethoxysilyl)propylureido)benzylamino)-1,8-naphthalimide (**8**) was synthesised by reaction of **52** with 3-(triethoxysiyl)propyl iscoayante under reflux in THF for fourty-eight hours (30% yield). All triethoxysilyl sensors were obtained pure after recrystallisation from methanol.

Microwave irradiation was also trialled as a synthetic technique in order to reduce reaction times. As can been seen in Table 18 reaction time was greatly decreased for all of the examined reactions, although in most cases yields were slightly decreased. This was particularly evident for the synthesis of **50** where the reaction time was decreased from 48 hours down to 60 minutes. This benefit in decreased reaction time was however tempered by a greater use of starting materials (double the amount of 2-aminobenzylamine was required for the microwave irradiation method) and a lower yield (63% using conventional heating versus 44% using microwave irradiation). The synthesis of sensor **4** by microwave irradiation was also pleasing with a higher yield obtained versus using conventional heating in shorter time. Particularly important with this method was the need for only a recrystallisation step to purify the sensor. Using conventional heating time-consuming column chromatography was involved.

Table 18: Summary of products synthesised using microwave irradiation, and details comparing the synthesis *via* conventional heating.

	Conventional Heating		Microwave Heating	
Compound	Reaction Time	Yield (%)	Irradiation Time	Yield (%)
45	3 hours	94	8 mins	87
51	1 hour	72	4 mins	68
50	48 hours	63	60 mins	44
52	3 hours	78	8 mins	71
1	15 hours	70	2 mins	54
4	15 hours	54	6 mins	75
5	3 hours	86	6 mins	69

7.1.2 Evaluation of 4-amino-1,8-naphthalimide based anion sensors

Sensors **1**, **3**-**8** were evaluated using ^{1}H NMR spectroscopy and fluorescence spectrophotometry, for their ability to sense the tetrabutylammonium salts of dihydrogen phosphate, acetate fluoride and bromide. Binding constants for the complexes formed between the sensors and dihydrogen phosphate and acetate are tabulated in Table 19. Little interaction was observed for all sensors when the bromide anion was added.

Table 19: Binding constants for sensors 1, 3-8 determined by ^{1}H NMR spectroscopy and fluorescence spectrophotometry.

	Dihydrogen Phosphate		Acetate	
Sensor	*log K* NMR (average)	*log K* Fluorescence	*log K* NMR (average)	*log K* Fluorescence
1	3.05±0.12	3.02±0.03	2.84±0.01	2.94±0.02
3	3.08±0.07	3.19±0.02	3.17±0.02	3.30±0.02
4	3.21±0.04	3.39±0.09	3.08±0.04	3.18±0.05
5	2.80±0.06	2.50±0.02	2.88±0.01	3.09±0.06
6	2.00±0.05	2.61±0.03	2.03±0.06	2.57±0.04
7	2.36±0.10	2.67±0.03	2.38±0.26	3.27±0.10
8	1.90±0.12	2.38±0.12	2.18±0.04	2.13±0.06

Using ^{1}H NMR spectroscopy significant downfield shifts were observed in the resonance of the two urea protons in each sensor molecule when dihydrogen phosphate, acetate and fluoride were added. In the case of sensors **4** and **5**, when titrated with dihydrogen phosphate, significant downfield changes in the resonance of the 4-amino NH proton were also noted.

Using fluorescence spectrophotometry, significant quenching of the emission spectrum of the host, was noted upon addition of dihydrogen phosphate, acetate and fluoride. Reinstatement of the signal was observed when methanol was added to solutions of the host-guest complex. The addition of fluoride to all sensors was found to induce a colour change from yellow to red. This colour change could be reversed by addition of methanol to the complexed solution.

The highest binding constant when dihydrogen phosphate was the bound anion was observed with **4**, with log *K*=3.39±0.09 (determined by fluorescence spectrophotometry), whilst the highest bonding constant when acetate was the bound anion was log *K*=3.30±0.02 with sensor **3**. The triethoxysilyl compounds **6**-**8** showed lower binding constants than those compounds without triethoxysilyl groups, this is due to greater aromatic character of the urea recognition group in sensors **1**, **3**-**5**.

7.1.3 Immobilisation of 4-amino-1,8-naphthalimide based sensors onto silica

Immobilisation of 4-amino-1,8-naphthalimide based anion sensors onto silica was trialled using three methods. In the first approach immobilisation was carried out *via* a hydrosilation reaction between the terminal double bond of the sensor molecule and hydride terminated silica surface (**53**). Some immobilisation of the sensor onto the surface (**54**-**55**) was indicated by a colour change from yellow to red upon addition of fluoride. Addition of methanol was able to reverse this colour change. However, spectroscopic characterisation of the surface using CP-MAS NMR or IR spectroscopies was unable to show that the sensor was successfully immobilised most likely due to low surface loadings.

In the second approach the sensor was incorporated stepwise onto a 3-aminopropyl functionalised silica obtained from Sigma Aldrich. Several changes were noted *via* FTIR and CP-MAS NMR spectroscopies throughout the step-wise building process suggesting changes were occurring on the surface in each step, although still it was difficult to characterise the final surfaces obtained. A colour change was observed similar to that mentioned for the first approach when fluoride was added, however the colour change wasn't as definitive.

In the third approach the sensors with triethoxy groups **6**-**8** were immobilised onto mesoporous silica **59**-**61**. This method had the benefit of there being only one process (in approach one the surface has to be silanised then reacted and in approach two the sensor is synthesised in three steps) to attach the sensor to the surface, hence any change to the surface must be due to sensor being immobilised onto the surface. Again results suggested immobilisation had occurred. Addition of fluoride to the surface resulted in minor colour changes which suggested there was some interaction at the surface (the colour change was not as marked as that observed for approach one and two).

In conclusion a variety of sensors based on the 4-amino-1,8-naphthalimide fluorophore were synthesised and shown to interact with the anions dihydrogen phosphate, fluoride and acetate in solution (hydrated DMSO). Positive first steps were shown to immobilise these sensors onto a silica surface although surface loading appeared to be an issue making spectroscopic characterisation different. A colour change due to deprotonation of the sensor was able to be shown on the surface, suggesting that the sensors are suitable to be immobilised onto the surface.

7.2 Future Work

There are three main avenues for future work in this project:

(i) Synthesis of new sensors

(ii) Evaluation of sensors

(iii) Further immobilisation studies

7.2.1 Synthesis

As was shown in Chapter 5, by making small changes to the molecular structure we are able to influence the binding strength displayed by the sensor molecules to different anions. Methodology to synthesise isothiocyanates is widely available and when isothiocyanates are reacted with an amine, they rapidly form the thiourea signalling subunit, which as detailed in Chapter 1 is a strong and commonly used anion recognition unit. It follows that being able to synthesise novel isothiocyantes would mean that new sensors could be formed and could be evaluated for their selectivity towards different anions.

In the past isothiocyanates have been synthesised using thiocarbonyl insertion reagents such as thiophosgene and dipyridiyl thionocarbonate. Whilst both of these reagents are highly reactive they are also highly toxic and display low chemoselectivity and thus the synthesis of isothiocyanates has been problematic [135]. Boas and collaborators however have developed methodology that allows for the synthesis of isothiocyanates and also the subsequent formation of the thiourea sub-signalling unit without the use of thiophosgene and dipyridiyl thionocarbonate. The basic methodology involves the reaction of a primary amine with carbon disulfide and common peptide coupling reagents in a suitable reaction solvent [135-137].

The initial method developed to produce isothiocyanates using this procedure was discovered when Boas and Jakobsen attempted the synthesis of *N*-(3-isothiocyananto-propyl)-2-anthraquinone carboxamide. The developed method was then used to produce a range of isothiocyanates with the reaction proceeding smoothly at room temperature in a variety of different solvents including dichloromethane, DMF and DMSO and with several different protecting groups [136]. Boas and collaborators have also looked at other variations of the synthesis [137].

Pfeffer *et al.* [49] have applied the principles outlined above to the synthesis of isothiocyanates for use with the naphthalimide based sensors. The example presented uses alternative reagents to those of Boas and Jakobsen with benzyl amine converted

to benzyl isothiocyanate in the presence of carbon disulfide, DIPEA and *N*-ethyl-(3-dimethylaminopropyl)-N”carbodiimide hydrochloride (EDCl) [49].

7.2.2 Evaluation

All of the evaluation of the synthesised sensors detailed in Chapter 5, has been undertaken using the tetrabutylammonium salts of the required anion. Whilst the tetrabutylammonium salt of an anion is commonly used in the literature to conduct binding studies, the salt is of little interest to real-world applications. Further evaluation of the sensors would need to be undertaken using sodium, potassium or other relevant salts, to ensure the anion sensing function of the synthesised molecules is not affected by the cation.

7.2.3 Immobilisation

Chapter 6 presented preliminary investigations into the immobilisation of naphthalimide based sensors onto a solid silica surface. Further work is necessary to definitively characterise these surfaces and to evaluate them for use as a sensing media. One of the major issues effecting characterisation was presumed to be the low surface loading of the sensor onto the silica surface, therefore resulting in difficulties in characterising the surface. This difficultly was partially overcome by using mesoporous silica as a surface instead of silica gel. Seo and co-workers, reported that mesoporous silica was a better surface due to its greater surface area (therefore enabling more molecules to be immobilised) [77]. Despite being able to observe more characterisation details using solid state NMR and ATR-FTIR spectroscopies when immobilising onto mesoporous silica, further characterisation would be beneficial and is obviously an area where greater attention is required. Elemental microanalysis would be of particular use in determining if the sensor is on the surface. Potential improvements to the current methods which could be explored including adding more sensor into the immobilisation reaction or increasing the reactivity of the surface (i.e. activation of the silica gel, level of silanisation). Use of other immobilisation techniques could also be beneficial.

One interesting immobilisation technique that was considered briefly in the course of this research was using copper (I) catalysed alkyne-azide click chemistry to immobilise the sensor onto a surface. There were several examples where molecules have been immobilised onto a surface using click chemistry [138-142]. In order to exploit this reaction there is need for the synthesised sensor molecules to contain either an alkyne or azide group. Research was undertaken to form **81** reacting propargylamine with 4-bromo-1,8-naphthalic anhydride (**44**), to introduce a terminal triple bond at the imide position, in a similar fashion to the synthesis of **45**. Attempts were made at the synthesis of **82** in a similar fashion to the synthesis of **51**. All attempts led to an impure product. The fact that **81** is able to be synthesised in a pure fashion and that the synthesis of **82** could be achieved employing chromatography (and potential further optimisation of the method to yield a pure product) would indicate that there is potential to form sensors **1**-**5** with a terminal triple bond which would enable their immobilisation onto an azide functionalised silica surface (Lummerstorfer and Hoffmann detail the formation of azide functionalised surfaces and their subsequent reaction with substituted acetylenes [139].

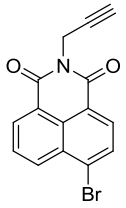

81

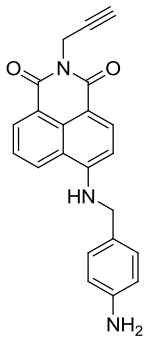

82

Once there has been sufficient characterisation of the surface immobilised anion sensors, attention would then need to turn toward evaluation of the surface for use in anion sensing. Binding studies to allow the determination of log *K* values to give an indication of binding strength, and also investigations to determine the selectivity of the surfaces for various anions. Further studies into regeneration of the surface after use also would need to be investigated. Finally, after vigorous evaluation, potential real-world applications for the surface immobilised sensors could be investigated.

Appendix A

LIST OF CHEMICALS

Chemical Name	Grade	Supplier
2-aminobenzylamine	98%	Sigma-Aldrich
3-(Triethoxysilyl)propyl isocyanate	95%	Sigma-Aldrich
3-aminobenzylamine	99%	Sigma-Aldrich
4-aminobenzylamine	99%	Sigma-Aldrich
4-bromo-1,8-naphthalic anhydride	95%	Sigma-Aldrich
4-chlorophenyl isocyanate	98%	Sigma-Aldrich
Acetamide	AR grade, 98% min	Ajax Fine Chemicals (UNIVAR)
Acetone	GR for analysis	Merck
Acetonitrile	Gradient Grade for Liquid Chromatography	Merck
Acetonitrile	HPLC Grade	Lab-Scan Analytical Services
Allyl Bromide	97%	Aldrich
Allylamine	98%	Sigma-Aldrich
Ammonia Solution	28-30% GR for analysis	Merck
Ammonium Formate	AR grade	Ajax Fine Chemicals (UNIVAR)
Chloroform	GR for analysis	Merck
Diethyl ether	Absolute for analysis	Merck
Dimethyl sulfoxide	99.9+%, anhydrous	Sigma-Aldrich
Ethanol	Absolute, AR grade	Merck Pty. Ltd
Hexadecyltrimethylammonium bromide	AR grade	Sigma-Aldrich
Hydrochloric Acid	37%	BDH Laboratory Supplies
Methanol	GR for analysis	Merck
N,N-Dimethylformamide	99.8% anhydrous	Sigma-Aldrich
n-heptane	99% anhydrous	Aldrich, Millwauke

Phenyl Isocyanate	**98%**	**Simga-Aldrich**
Phenyl Isothiocyanate	Puriss	Koch-Light Laboratories
Phenyl Isothiocyanate	98%	Acros Organics, Belgium
Platinic Chloride Hexahydrate	ACS Reagent	Sigma-Aldrich
Potassium Carbonate	Anhydrous >99.9%	Sigma-Aldrich
Propargylamine	98%	Sigma-Aldrich
Sodium hydride	60% dispersion in mineral oil	Sigma-Aldrich
Tetrabutylammonium Acetate	98%	Sigma-Aldrich
Tetrabutylammonium Bromide	ACS Reagent > 98.0%	Sigma-Aldrich
Tetrabutylammonium Fluoride Hydrate	98%	Sigma-Aldrich
Tetrabutylammonium Phosphate Monobasic	97%	Sigma-Aldrich
Tetraethoxysilane	97%	Sigma-Aldrich
Tetrahydrofuran	Analytical Reagent	Chem Supply
Toluene	Anhydrous 99.8%	Sigma- Aldrich
Triethoxysilane	Unknown	Advanced Molecular Technologies, Pty. Ltd (Clayton, Victoria)
Triethylamine	Min 99%	Sigma-Aldrich

Appendix B

DETERMINATION OF BINDING CONSTANTS

The calculation of a binding constant gives a measure of the stability of a host-guest complex in a given solvent [8]. For the generalised reaction depicted in Scheme 42 the binding constant is the same as the equilibrium constant for the reaction (equation 1).

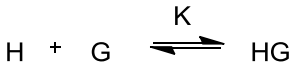

Scheme 42: Generalised Host Guest Reaction

$$K = \frac{[HG]}{[H][G]} \quad (1)$$

If more than one guest can be bound to a host the equation to calculate the constant becomes much more complicated. A larger binding constant indicates a more stable complex [8]. Values are typically reported as a log *K* value [8]. A binding constant can be calculated using data from any experimental technique where it is possible to monitor a change as the host-guest complex forms [8].

A 1:1 equilibrium is the most commonly encountered system in supramolecular chemistry [35, 116]. As the complexation takes place it is however not common to know what [HG], [H] and [G] are and therefore it isn't as simple as it initially looks to calculate the binding constant *K*. However we do know the initial concentration of host ($[H]_0$) and the initial concentration of guest ($[G]_0$). These two terms can be related to [H] and [G] using equations (2) and (3) [35, 116].

$$[H]_0 = [H] + [HG] \quad (2)$$

$$[G]_0 = [G] + [HG] \quad (3)$$

Substituting equations (2) and (3) into (1) and rearranging gives (4)

$$K = \frac{[HG]}{[H]_0[G]_0 - [HG]([H]_0 + [G]_0) + [HG]^2} \quad (4)$$

Putting equation (4) into terms of [HG] and rearranging gives (5)

$$[HG]^2 - [HG]\left([G]_0 + [H]_0 + \frac{1}{K}\right) + [H]_0[G]_0 = 0 \quad (5)$$

The real solution of (5) can then be expressed as (6)

$$[HG] = \frac{1}{2}\{\left([G]_0 + [H]_0 + \frac{1}{K}\right) - \sqrt{\left([G]_0 + [H]_0 + \frac{1}{K}\right)2 - 4[H]_0[G]_0\} \quad (6)$$

In equation six, all properties are known except for *K*, as [HG] can be measured indirectly through titration methods. After some further manipulation, the equation can be expressed in the form shown below as (7), where ΔY is the change observed through experiment.

$$\Delta Y = \mathrm{Y}_{\Delta HG}(\frac{1}{2}\{\left([G]_0 + [H]_0 + \frac{1}{K}\right) - \sqrt{\left([G]_0 + [H]_0 + \frac{1}{K}\right)2 - 4[H]_0[G]_0\}) \quad (7)$$

$Y_{\Delta HG}$ and K can then be determined from a binding curve using a non-linear regression analysis tool. More detail can be found regarding these calculations and a step by step process to deriving (7) in a book chapter prepared by Thordarson [35] and a book chapter by Hirose [116].

Appendix C

SENSOR EVALUATION SUMMARY

The following pages tabulate data relating to the titration experiments conducted in Chapter 5.

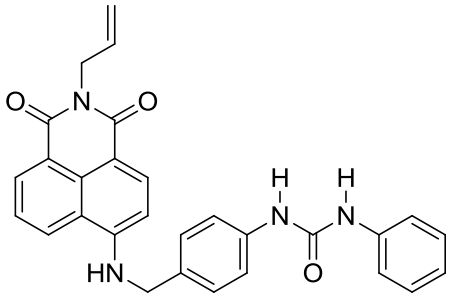

Table 20: Changes in chemical shift (ppm) observed upon addition of ten equivalents of anion to 1 in DMSO-d6 with 0.5% water.

	Urea Proton 1			Urea Proton 2			4-amino NH Proton		
Anion Added	Initial	Final	Change	Initial	Final	Change	Initial	Final	Change
Dihydrogen Phosphate*	8.65	10.63	1.98	8.67	10.63	1.96	8.49	8.60	0.11
Acetate	8.64	11.71	3.07	8.66	11.74	3.04	8.50	8.85	0.35
Bromide	8.64	8.92	0.28	8.66	8.94	0.27	8.49	8.57	0.08
Fluoride	8.64	11.15	2.50	8.66	11.15	2.49	8.49	9.20	0.71

**Dihydrogen Phosphate only to four equivalents.*

Table 21: Fluorescent quenching observed (as a % of the original signal before addition of guest) of 1 upon addition of anion, in DMSO with 0.5% water

	% Quenching observed after addition of			
Anion added	1.0 equiv	5.0 equiv	10.0 equiv	20.0 equiv
Dihydrogen Phosphate	40	65	68	70
Acetate	38	66	71	73
Bromide	0	9	11	15
Fluoride	49	90	98	*

Fluoride was found to fully quench the emission of **1 before addition of twenty equivalents.*

Table 22: Binding constants (log *K*) for the complexation of 1 with various dihydrogen phosphate and acetate as determined by ^{1}H NMR and fluorescence.

Anion Added	^{1}H NMR Proton 1	^{1}H NMR Proton 2	Average ^{1}H NMR	Fluorescence
Dihydrogen Phosphate	3.05±0.09	3.05±0.08	3.05±0.12	3.02±0.03
Acetate	2.83±0.01	2.84±0.01	2.84±0.01	2.94±0.02

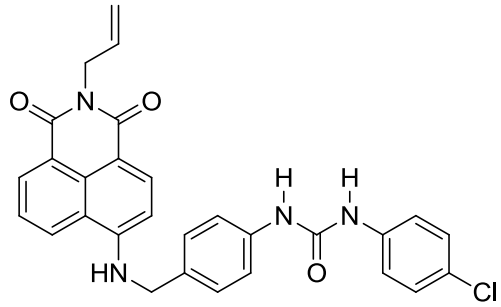

Table 23: Changes in chemical shift (ppm) observed upon addition of ten equivalents of anion to 3 in hydrated DMSO-d_6.

	Urea Proton 1			Urea Proton 2			4-amino NH Proton		
Anion Added	Initial	Final	Change	Initial	Final	Change	Initial	Final	Change
Dihydrogen Phosphate	8.79	10.97	2.18	8.70	10.75	2.01	8.49	8.72	0.24
Acetate	8.80	11.96	3.17	8.71	11.78	3.07	8.49	8.76	0.28
Bromide	8.80	9.09	0.29	8.71	8.96	0.26	8.49	8.57	0.08
Fluoride	8.79	11.48	2.62	8.70	11.07	2.37	8.49	9.08	0.59

Table 24: Fluorescent quenching observed (as a % of the original signal before addition of guest) of 3 upon addition of anion, in hydrated DMSO.

	% Quenching observed after addition of			
Anion added	1.0 equiv	6.0 equiv	11.4 equiv	20.0 equiv
Dihydrogen Phosphate	37	60	62	64
Acetate	44	64	69	71
Bromide	2	4	6	9
Fluoride	32	77	89	95

Table 25: Binding constants (log *K*) for the complexation of 3 with various dihydrogen phosphate and acetate as determined by ^{1}H NMR and fluorescence.

Anion Added	^{1}H NMR Proton 1	^{1}H NMR Proton 2	Average ^{1}H NMR	Fluorescence
Dihydrogen Phosphate	3.06±0.05	3.09±0.05	3.08±0.07	3.19±0.02
Acetate	3.17±0.01	3.17±0.02	3.17±0.02	3.30±0.02

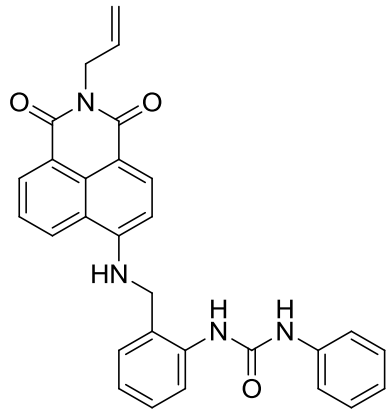

Table 26: Changes in chemical shift (ppm) observed upon addition of ten equivalents of anion to 4 in DMSO-d_6 with 0.5% water.

	Urea Proton 1			Urea Proton 2			4-amino NH Proton		
Anion Added	Initial	Final	Change	Initial	Final	Change	Initial	Final	Change
Dihydrogen Phosphate	9.01	10.92	1.91	8.26	9.96	1.70	8.40	9.96	1.56
Acetate	9.01	11.54	2.53	8.26	10.97	2.72	8.40	9.14	0.74
Bromide	9.02	9.43	0.41	8.26	8.52	0.26	8.40	8.56	0.16
Fluoride	9.01	11.38	2.37	8.25	11.17	2.91	8.40	10.72	2.32

Table 27: Fluorescent quenching observed (as a % of the original signal before addition of guest) of 4 upon addition of anion, in DMSO with 0.5% water

	% Quenching observed after addition of			
Anion added	1.0 equiv	4.5 equiv	11.5 equiv	20.5 equiv
Dihydrogen Phosphate	47	65	69	70
Acetate	29	46	51	54
Bromide	3	6	8	8
Fluoride	29	58	62	64

Table 28: Binding constants (log *K*) for the complexation of 4 with various dihydrogen phosphate and acetate as determined by ^{1}H NMR and fluorescence.

Anion Added	^{1}H NMR Proton 1	^{1}H NMR Proton 2	Average ^{1}H NMR	Fluorescence
Dihydrogen Phosphate	3.07±0.02	3.34±0.04	3.21±0.04	3.39±0.09
Acetate	3.09±0.02	3.07±0.02	3.08±0.03	3.18±0.05

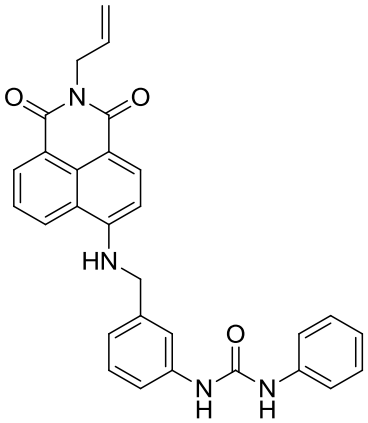

Table 29: Changes in chemical shift (ppm) observed upon addition of ten equivalents of anion to 5 in hydrated DMSO-d_6.

	Urea Proton 1			Urea Proton 2			4-amino NH Proton		
Anion Added	Initial	Final	Change	Initial	Final	Change	Initial	Final	Change
Dihydrogen Phosphate	8.68	10.86	2.19	8.58	10.34	1.76	8.55	2.75	1.19
Acetate	8.68	11.69	3.01	8.59	11.66	3.08	8.55	8.79	0.20
Bromide	8.68	8.68	0.00	8.59	8.59	0.00	8.55	8.62	0.07
Fluoride	8.68	11.14	2.46	8.59	11.14	2.57	8.55	9.34	0.79

Table 30: Fluorescent quenching observed (as a % of the original signal before addition of guest) of 5 upon addition of anion, in hydrated DMSO.

	% Quenching observed after addition of:			
Anion added	1.0 equiv	6.0 equiv	14.0 equiv	20.0 equiv
Dihydrogen Phosphate	24	52	62	65
Acetate	34	51	56	58
Bromide	1	12	20	23
Fluoride	60	100	100 (8.3 equiv)	*

The fluorescence emission of **5 was effectively quenched upon addition of 8.3 equivalents of fluoride.*

Table 31: Binding constants (log *K*) for the complexation of 5 with various dihydrogen phosphate and acetate as determined by ^{1}H NMR and fluorescence.

Anion Added	^{1}H NMR Proton 1	^{1}H NMR Proton 2	Average ^{1}H NMR	Fluorescence
Dihydrogen Phosphate	2.50±0.01	3.10±0.06	2.80±0.06	2.50±0.02
Acetate	2.88±0.01	2.88±0.01	2.88±0.01	3.09±0.06

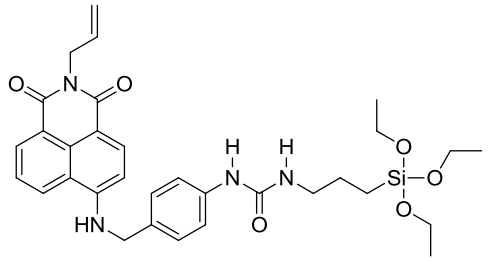

Table 32: Changes in chemical shift (ppm) observed upon addition of ten equivalents of anion to 6 in hydrated DMSO-d_6.

	Urea Proton 1			Urea Proton 2			4-amino NH Proton		
Anion Added	Initial	Final	Change	Initial	Final	Change	Initial	Final	Change
Dihydrogen Phosphate	8.40	9.66	1.26	6.12	7.18	1.06	8.46	8.71	0.25
Acetate	8.37	10.58	2.21	6.11	8.53	2.41	8.46	8.79	0.33
Bromide	8.37	8.55	0.19	6.12	6.26	0.14	8.45	8.55	0.11
Fluoride	8.37	N/A	N/A	6.12	N/A	N/A	8.45	N/A	N/A

Table 33: Fluorescent quenching observed (as a % of the original signal before addition of guest) of 6 upon addition of anion, in hydrated DMSO.

	% Quenching observed after addition of			
Anion added	1.0 equiv	6.0 equiv	11.0 equiv	20.0 equiv
Dihydrogen Phosphate	23	52	61	67
Acetate	24	48	59	68
Bromide	7	9	12	18
Fluoride	11	67	81	*

Fluoride was found to fully quench the emission of **6 before addition of twenty equivalents.*

Table 34: Binding constants (log *K*) for the complexation of 6 with various dihydrogen phosphate and acetate as determined by ^{1}H NMR and fluorescence.

Anion Added	^{1}H NMR Proton 1	^{1}H NMR Proton 2	Average ^{1}H NMR	Fluorescence
Dihydrogen Phosphate	1.94±0.03	2.06±0.04	2.00±0.05	2.61±0.03
Acetate	2.02±0.05	2.04±0.03	2.03±0.06	2.57±0.04

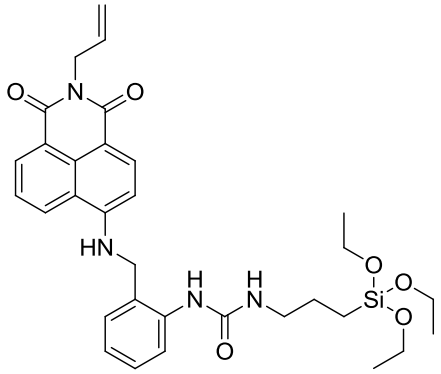

Table 35: Changes in chemical shift (ppm) observed upon addition of ten equivalents of anion to 7 in hydrated DMSO-d_6.

	Urea Proton 1			Urea Proton 2			4-amino NH Proton		
Anion Added	Initial	Final	Change	Initial	Final	Change	Initial	Final	Change
Dihydrogen Phosphate	7.96	8.70	0.74	6.51	7.26	0.75	8.37	9.11	0.75
Acetate	7.95	9.340	1.39	6.53	8.02	1.49	8.38	9.15	0.77
Bromide	7.96	8.05	0.09	6.51	6.62	0.11	8.37	8.43	0.06
Fluoride	7.96	8.12	0.16	6.51	6.63	0.12	8.37	8.54	0.18

Table 36: Fluorescent quenching observed (as a % of the original signal before addition of guest) of 7 upon addition of anion, in hydrated DMSO.

	% Quenching observed after addition of			
Anion added	1.0 equiv	6.0 equiv	11.0 equiv	20.0 equiv
Dihydrogen Phosphate	26	54	63	70
Acetate	43	49	53	56
Bromide	3	8	9	14
Fluoride	64	97	98 (*7.8 equiv)	*

The fluorescence emission of **7 was effectively quenched upon addition of 7.8 equivalents of fluoride.*

Table 37: Binding constants (log *K*) for the complexation of 7 with various dihydrogen phosphate and acetate as determined by ^{1}H NMR and fluorescence.

Anion Added	^{1}H NMR Proton 1	^{1}H NMR Proton 2	Average ^{1}H NMR	Fluorescence
Dihydrogen Phosphate	2.36±0.10	2.36±0.03	2.36±0.10	2.67±0.03
Acetate	2.38±0.17	2.37±0.19	2.38±0.26	3.27±0.10

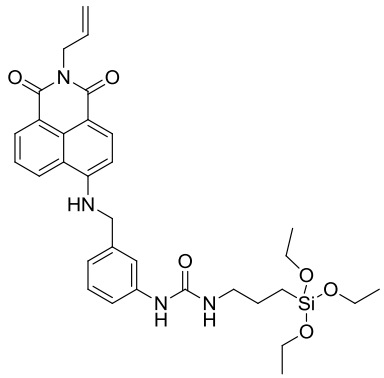

Table 38: Changes in chemical shift (ppm) observed upon addition of ten equivalents of anion to 8 in hydrated DMSO-d_6.

	Urea Proton 1			Urea Proton 2			4-amino NH Proton		
Anion Added	Initial	Final	Change	Initial	Final	Change	Initial	Final	Change
Dihydrogen Phosphate	8.38	9.45	1.07	6.08	7.47	1.39	8.53	9.26	0.74
Acetate	8.38	10.7	2.33	6.08	8.69	2.60	8.53	8.88	0.35
Bromide	8.38	8.55	0.17	6.09	6.23	0.15	8.53	8.60	0.07
Fluoride	8.38	8.68	0.29	6.08	6.40	0.32	8.53	8.68	0.15

Table 39: Fluorescent quenching observed (as a % of the original signal before addition of guest) of 8 upon addition of anion, in hydrated DMSO.

	% Quenching observed after addition of			
Anion added	1.0 equiv	6.0 equiv	14.0 equiv	20.0 equiv
Dihydrogen Phosphate	16	33	46	50
Acetate	11	35	49	54
Bromide	3	5	5	6
Fluoride	51	99	100* (8 equiv)	*

The fluorescence emission of **8 was effectively quenched upon addition of 8 equivalents of fluoride.*

Table 40: Binding constants (log *K*) for the complexation of 8 with various dihydrogen phosphate and acetate as determined by ^{1}H NMR and fluorescence.

Anion Added	^{1}H NMR Proton 1	^{1}H NMR Proton 2	Average ^{1}H NMR	Fluorescence
Dihydrogen Phosphate	1.93±0.09	1.87±0.08	1.90±0.12	2.38±0.12
Acetate	2.19±0.03	2.17±0.03	2.18±0.04	2.13±0.06

Reference List

1. Kotz, J.C. and P. Treichel Jr., *Chemistry and Chemical Reactivity Fourth Edition*. Fourth ed. 1999, Orlando: Saunders College Publishing.
2. Bianchi, A., K. Bowman-James, and E. Garcia-Espana, eds. *Supramolecular Chemistry of Anions*. 1997, John Wiley and Sons Inc: New York, USA.
3. Gunnlaugsson, T., et al., *Design, synthesis and photophysical studies of simple fluorescent anion PET sensors using charge neutral thiourea receptors.* Organic and Biomolecular Chemistry, 2004. **2**: p. 1856-1863.
4. Beer, P.D. and P.A. Gale, *Anion Recognition and Sensing: The State of the Art and Future Perspectives.* Angewandte Chemie International Edition, 2001. **40**: p. 486-516.
5. Liu, B. and H. Tian, *A ratiometric fluorescent chemosensor for fluoride anions based on a proton transfer signalling mechanism.* Journal of Materials Chemistry, 2005. **15**: p. 2681-2686.
6. Hopper, K.G., H. LeClair, and B.R. McCord, *A novel method for analysis of explosives residue by simultaneous detection of anions and cations via capillary zone electrophoresis.* Talanta, 2005. **67**: p. 304-312.
7. Gunnlaugsson, T., et al., *Synthesis and photophysical evaluation for charge neutral thiourea or urea based fluorescent PET sensors of bis-carboxylates and pyrophosphate.* Organic and Biomolecular Chemistry, 2005. **3**: p. 48-56.
8. Steed, J.W. and J.L. Atwood, eds. *Supramolecular Chemistry*. 2000, John Wiley and Sons Inc: Chichester, England.
9. Basabe-Desmonts, L., D.N. Reinhoudt, and M. Crego-Calama, *Design of fluorescent materials for chemical sensing.* Chemical Society Reviews, 2007. **36**(6): p. 993-1017.
10. Hutchinson, J.P., et al., *Identification of inorganic ions in post-blast explosive residues using portable CE instrumentation and capacitively coupled contactless conductivity detection.* Electrophoresis, 2008. **29**(22): p. 4593-4602.
11. Altria, K., *Analysis of Inorganic Anions by Capillary Electrophoresis.* LC GC North America, 2011: p. 58-61.
12. Timerbaev, A.R., *Inorganic analysis of biological fluids using capillary electrophoresis.* Journal of Separation Science, 2008. **31**(11): p. 2012-2021.
13. Johns, C., M. Macka, and P.R. Haddad, *Enhancement of detection sensitivity for indirect photometric detection of anions and cations in capillary electrophoresis.* Electrophoresis, 2003. **24**(12-13): p. 2150-2167.
14. Hughes, R.R. and G.S. Walker, *Rapid Screening for the Detection and Differentiation of Gamma-Hydroxybutyrate using Ion Chromatography.* Journal of Forensic Sciences, 2011. **56**(5): p. 1256-1260.
15. Johns, C., et al., *Identification of homemade inorganic explosives by ion chromatographic analysis of post-blast residues.* Journal of Chromatography A, 2008. **1182**(2): p. 205-214.
16. Nakatani, N., et al., *Recent Progress and Applications of Ion-exclusion/Ion-exchange Chromatography for Simultaneous Determination of Inorganic Anions and Cations.* Analytical Sciences, 2012. **28**(9): p. 845-852.

17. Michalski, R., *Ion Chromatography as a Reference Method for Determination of Inorganic Ions in Water and Wastewater.* Critical Reviews in Analytical Chemistry, 2006. **36**(2): p. 107-127.
18. Zhang, J., et al., *Voltammetric Ion-Selective Electrodes for the Selective Determination of Cations and Anions.* Analytical Chemistry, 2010. **82**(5): p. 1624-1633.
19. Nafady, A., *Voltammetric behaviour of microparticles and thin films of neo-pentyl-ferrocence based polyester (PmFB): Manipulation of anion uptake at the ionic liquid/aqueous electrolyte interface.* Electrochemistry Communications, 2009. **11**(838-1841).
20. Thakur, A., D. Mandal, and S. Ghosh, *A triazole based triferrocene derivative as a multiresponsive chemosensor for Hg(II) ion and a redox chemosensor for H2PO4− ion.* Journal of Organometallic Chemistry, 2013. **726**(0): p. 71-78.
21. Sasso, S.V., et al., *Electropolymerized 1,2-diaminobenzene as a means to prevent interferences and fouling and to stabilize immobilized enzyme in electrochemical biosensors.* Analytical Chemistry, 1990. **62**(11): p. 1111-1117.
22. Skoog, D.A., F.J. Holler, and S.R. Crouch, *Principles of Instrumental Analysis Sixth Edition*. 2007, Belmont, Califronia: Thomson Higher Education.
23. Johns, C., M. Macka, and P. Haddard, R, *Enhancement of detection sensitivity for indirect photometric detection of anions and cations in capillary electrophoresis.* Electrophoresis, 2003. **24**: p. 2150-2167.
24. Liu, Y.M. and J.K. Cheng, *Elemental speciation analysis in capillary electrophoresis.* Electrophoresis, 2003. **24**: p. 1993-2012.
25. Pacakova, V., et al., *The importance of capillary electrophoresis, capillary electrochromatography, and ion chromatography in separations of inorganic ions.* Electrophoresis, 2003. **24**: p. 1883-1891.
26. Paull, B. and M. King, *Quantitative capillary zone electrophoresis of inorganic anions.* Electrophoresis, 2003. **24**: p. 1892-1934.
27. Skoog, D.A., et al., *Fundamentals of Analytical Chemistry Eighth Edition*. 2004, Belmont, California: Thomson Brooks/Cole.
28. Park, C.H. and H.E. Simmons, *Macrobicyclic amines. III. Encapsulation of halide ions by in,in-1,(k + 2)-diazabicyclo[k.l.m.]alkane ammonium ions.* Journal of the American Chemical Society, 1968. **90**(9): p. 2431-2432.
29. Pedersen, C.J., *Cyclic polyethers and their complexes with metal salts.* Journal of the American Chemical Society, 1967. **89**(26): p. 7017-7036.
30. Li, A.-F., et al., *Anion complexation and sensing using modified urea and thiourea-based receptors.* Chemical Society Reviews, 2010. **39**(10): p. 3729-3745.
31. Kang, S.A., et al., *Phosphate uptake by TiO2: Batch studies and NMR spectroscopic evidence for multisite adsorption.* Journal of Colloid and Interface Science, 2011. **364**(2): p. 455-461.
32. Amendola, V., L. Fabbrizzi, and L. Mosca, *Anion recognition by hydrogen bonding: urea-based receptors.* Chemical Society Reviews, 2010. **39**(10): p. 3889-3915.
33. Pascal Jr, R.A., J. Spergel, and D. Van Engen, *Synthesis and X-ray crystallographic characterization of a (1,3,5)cyclophane with three amide N-H groups surrounding a central cavity. A neutral host for anion complexation.* Tetrahedron Letters, 1986. **27**(35): p. 4099-4102.

34. Duke, R.M., et al., *Colorimetric and fluorescent anion sensors: an overview of recent developments in the use of 1,8-naphthalimide-based chemosensors.* Chemical Society Reviews, 2010. **39**: p. 3936-3953.
35. Thordarson, P., *Binding Constants and Their Measurement*, in *Supramolecular Chemistry: From Molecules to Nanomaterials*, P.A. Gale and J.W. Steed, Editors. 2012, John Wiley & Sons Ltd.
36. Beer, P.D. and E.J. Hayes, *Transition metal and organometallic anion complexation agents.* Coordination Chemistry Reviews, 2003. **240**(1–2): p. 167-189.
37. Fabbrizzi, L., et al., *The design of luminescent sensors for anions and ionisable analytes.* Coordination Chemistry Reviews, 2000. **205**(1): p. 85-108.
38. Martinez-Manez, R. and F. Sancenon, *New Advances in Fluorogenic Anion Chemosensors.* Journal of Fluorescence, 2005. **15**(3): p. 267-285.
39. Gunnlaugsson, T., et al., *Anion recognition and sensing in organic and aqueous media using luminescent and colorimetric sensors.* Coordination Chemistry Reviews, 2006. **250**: p. 3094-3117.
40. Ward, M.D., *Photo-induced electron and energy transfer in non-covalently bonded supramolecular assemblies.* Chemical Society Reviews, 1997. **26**(5): p. 365-375.
41. Gale, P.A., *Anion receptor chemistry: highlights from 2008 and 2009.* Chemical Society Reviews, 2010. **39**(10): p. 3746-3771.
42. Bates, G.W. and P.A. Gale, *An introduction to anion receptors based on organic frameworks.* Structure and Bonding, 2008. **129**: p. 1-44.
43. Cranwell, P.B., et al., *Anion recognition and transport properties of sulfamide-, phosphoric triamide- and thiophosphoric triamide-based receptors.* Chemical Communications, 2013. **49**(9): p. 874-876.
44. Bordwell, F.G., *Equilibrium acidities in dimethyl sulfoxide solution.* Accounts of Chemical Research, 1988. **21**(12): p. 456-463.
45. Smith, P.J., M.V. Reddington, and C.S. Wilcox, *Ion pair binding by a urea in chloroform solution.* Tetrahedron Letters, 1992. **33**(41): p. 6085-6088.
46. Qian, X. and F. Liu, *Promoting effects of the hydroxymethyl group on the fluorescent signaling recognition of anions by thioureas.* Tetrahedron Letters, 2003. **44**: p. 795-799.
47. Kanekiyo, Y., R. Naganawa, and H. Tao, *Fluorescence detection of ATP based on the ATP-mediated aggregation of pyrene-appended boronic acid on a polycation.* Chemical Communcations, 2004: p. 1006-1007.
48. Niu, C.-G., et al., *N-Allyl-4-(N-2'-hydroxyethyl)amino-1,8-naphthalimide as a fluorophore for optical chemosensing of nitrofurantoin.* The Analyst, 2002. **127**: p. 512-517.
49. Pfeffer, F.M., et al., *4-Amino-1,8-napthalimide-based anion receptors: employing the napthalimide N-H moiety in the cooperative binding of dihydrogenphosphate.* Tetraherdron Letters, 2005. **46**: p. 6579-6584.
50. Pfeffer, F.M., et al., *Fluorescent Anion Sensors based on 4-amino-1,8-napthalimide that emply the 4-amino N-H.* Tetraherdron Letters, 2006. **47**: p. 5241-5245.
51. Gunnlaugsson, T., et al., *Dual responsive chemosensors for anions: the combination of fluorescent PET (Photoinduced Electron Transfer) and*

colorimetric chemosensors in a single molecule. Tetrahedron letters, 2003. **44**(35): p. 6575-6578.

52. Ali, H.D.P., P.E. Kruger, and T. Gunnlaugsson, *Colorimetric 'naked-eye' and fluorescent sensors for anions based on amidourea functionalised 1,8-naphthalimide structures: anion recognition via either deprotonation or hydrogen bonding in DMSO.* New Journal of Chemistry, 2008. **32** (1153-1161).
53. Gunnalugsson, T., et al., *Colorimetric "Naked Eye" Sensing of Anions in Aqueous Solution.* Journal of Organic Chemistry, 2005. **70**(26): p. 10875-10878.
54. Duke, R.M. and T. Gunnlaugsson, *Selective fluorescent PET sensing of fluoride (F–) using naphthalimide–thiourea and –urea conjugates.* Tetrahedron Letters, 2007. **48**(45): p. 8043-8047.
55. Bao, X.-P., et al., *A Simple Colorimetric and Fluorescent Anion Sensor Based on 4-Amino-1,8-naphthalimide: Synthesis and its Recognition Properties.* Supramolecular Chemistry, 2008. **20**(5): p. 467-472.
56. Esteban-Gómez, D., L. Fabbrizzi, and M. Licchelli, *Why, on Interaction of Urea-Based Receptors with Fluoride, Beautiful Colors Develop.* The Journal of Organic Chemistry, 2005. **70**(14): p. 5717-5720.
57. Veale, E.B., et al., *Demonstration of bidirectional photoinduced electron transfer (PET) sensing in 4-amino-1,8-naphthalimide based thiourea anion sensors.* Organic and Biomolecular Chemistry, 2009. **7**: p. 3447-3454.
58. de Silva, A.P., et al., *New Fluorescent Model Compounds for the Study of Photoinduced Electron Transfer: The Influence of a Molecular Electric Field in the Excited State.* Angewandte Chemie International Edition in English, 1995. **34**(16): p. 1728-1731.
59. He, H., et al., *A Fluorescent Sensor with High Selectivity and Sensitivity for Potassium in Water.* Journal of the American Chemical Society, 2003. **125**(6): p. 1468-1469.
60. Gunnlaugsson, T., T.C. Lee, and R. Parkesh, *A highly selective and sensitive fluorescent PET (photoinduced electron transfer) chemosensor for Zn(ii).* Organic & Biomolecular Chemistry, 2003. **1**(19): p. 3265-3267.
61. Tamanini, E., et al., *Cyclam-Based "Clickates": Homogeneous and Heterogeneous Fluorescent Sensors for Zn(II).* Inorganic Chemistry, 2010. **49**(8): p. 3789-3800.
62. Xu, Z., X. Qian, and J. Cui, *Colorimetric and Ratiometric Fluorescent Chemosensor with a Large Red-Shift in Emission: Cu(II)-Only Sensing by Deprotonation of Secondary Amines as Receptor Conjugated to Naphthalimide Fluorophore.* Organic Letters, 2005. **7**(14): p. 3029-3032.
63. Xu, Z., J. Yoon, and D.R. Spring, *A selective and ratiometric Cu2+ fluorescent probe based on naphthalimide excimer-monomer switching.* Chemical Communications, 2010. **46**(15): p. 2563-2565.
64. Xu, Z., et al., *Zn2+-Triggered Amide Tautomerization Produces a Highly Zn2+-Selective, Cell-Permeable, and Ratiometric Fluorescent Sensor.* Journal of the American Chemical Society, 2009. **132**(2): p. 601-610.
65. Tamanini, E., et al., *A Synthetically Simple, Click-Generated Cyclam-Based Zinc(II) Sensor.* Inorganic Chemistry, 2008. **48**(1): p. 319-324.
66. Parkesh, R., Lee. T.C., and Gunnlaugsson. T., *HIghly Selective 4-amino-1,8-naphthalimide based fluorescent photo induced electron transfer (PET)*

chemosensors for Zn(II) under physiological pH conditions. Organic and Biomolecular Chemistry, 2007. **5**: p. 310-317.

67. Parkesh, R., T. Clive Lee, and T. Gunnlaugsson, *Fluorescence imaging of bone cracks (microdamage) using visibly emitting 1,8-naphthalimide-based PET sensors.* Tetrahedron Letters, 2009. **50**(28): p. 4114-4116.
68. Duke, R.M. and T. Gunnlaugsson, *3-Urea-1,8-naphthalimides are good chemosensors: a highly selective dual colorimetric and fluorescent ICT based anion sensor for fluoride.* Tetrahedron Letters, 2011. **52**(13): p. 1503-1505.
69. Banerjee, S., et al., *Recent advances in the development of 1,8-naphthalimide based DNA targeting binders, anticancer and fluorescent cellular imaging agents.* Chemical Society Reviews, 2013. **42**(4): p. 1601-1618.
70. Britton, H.T.S. and R.A. Robinson, *CXCVIII - Univeral Buffer Solutions and the Dissociation Constant of Veronal.* Journal of The Chemical Society, 1931: p. 1456-1462.
71. Pavlovic, E., et al., *Microfluidic Device Architecture for Electrochemical Patterning and Detection of Multiple DNA Sequences.* Langmuir, 2008. **24**(3): p. 1102-1107.
72. Sans, V., et al., *SE(R)RS devices fabricated by a laser electrodispersion method.* Analyst, 2011. **136**(16): p. 3295-3302.
73. Zhang, K., et al., *A microfluidic system with surface modified piezoelectric sensor for trapping and detection of cancer cells.* Biosensors and Bioelectronics, 2010. **26**(2): p. 935-939.
74. Herranz, S., M.D. Marazuela, and M.C. Moreno-Bondi, *Automated portable array biosensor for multisample microcystin analysis in freshwater samples.* Biosensors and Bioelectronics, 2012. **33**(1): p. 50-55.
75. Mattos, A.B., et al., *A dual quartz crystal microbalance for human cardiac troponin T in real time detection.* Sensors and Actuators B: Chemical, 2012. **161**(1): p. 439-446.
76. Ayadim, M., et al., *Photosensing by a fluorescing probe covalently attached to the silica.* Tetrahedron Letters, 1996. **37**(39): p. 7039-7042.
77. Seo, S.M., et al., *A mesoporous silica functionalized by a covalently bound naphthalene-based receptor for selective optical detection of fluoride ion in water.* Microporous and Mesoporous Materials, 2008. **114**(1-3): p. 448-454.
78. Liu, T., et al., *An inorganic–organic hybrid optical sensor for heavy metal ion detection based on immobilizing 4-(2-pyridylazo)-resorcinol on functionalized HMS.* Journal of Hazardous Materials, 2012. **201–202**(0): p. 155-161.
79. Ismail, A.A., *A selective optical sensor for antimony based on hexagonal mesoporous structures.* Journal of Colloid and Interface Science, 2008. **317**(1): p. 288-297.
80. Minnoor, E., Y. Liu, and D.J. Pietrzyk, *Applications of a sulfonated-polymer wall modified open-tubular fused-silica capillary in capillary zone electrophoretic separations.* Journal of Chromatography A, 2000. **884**: p. 297-309.
81. Matyska, M.T. and J.J. Pesek, *Comparison of silanization/hydrosilation and organosilanization modification procedures on etched capillaries for electrokinetic chromatography.* Journal of Chromatograhy A, 2005. **1079**: p. 366-371.

82. Jal, P.K., S. Patel, and B.K. Mishra, *Chemical modification of silica surface by immobilization of functional groups for extractive concentration of metal ions.* Talanta, 2004. **62**(5): p. 1005-1028.
83. Plakidin, V.L. and V.N. Vostrova, *Reaction of Napthalic Anhydride and its Substituted Derviatives.* Zhurnal Organicheskoi Khimii 1982. **18**(9): p. 1997-1998.
84. Karishin, A.P. and D.M. Kustol, *Synthesis of Naphthalimide and Its Derivatives.* Poltava State Pedagogical Institute, 1957: p. 673-675.
85. Peng, Y., G. Song, and X. Qian, *Imidation of cyclic carboyxlic anhydrides under microwave irradiation.* Synthetic Communications, 2001. **31**(12): p. 1927-1931.
86. Anwar, U., et al., *Palladium catalysed queuing processess. Part 2:Termolecular cyclization-anion capture empolying carbon monoxide as a relay switch with in situ generated vinylstannanes.* Tetrahedron, 2001. **57**: p. 1361-1367.
87. Marson, C.M., A. Khan, and R.A. Porter, *Stereocontrolled Formation of Epoxy Peroxide Functionally Appended to a Lactam Ring.* Journal of Organic Chemistry, 2001. **66**: p. 4771-4775.
88. Tarling, C.A., et al., *B-, y- and d-lactams as conformational constraints in ring-closing metathesis.* Perkin Transactions 1, 1999: p. 1695-1701.
89. McElhinney, A.D. and S.P. Marsden, *A concise synthesis of tashiromine.* Synlett, 2005. **16**: p. 2528-2530.
90. Notari, M., F. Mizia, and F. Rivetti, *Procedure for Alkylation of Imides*. 1998, Enichem S.p.A., Milan Italy: Italy. p. 3.
91. Kumaraswamy, G., et al., *Di-u-hydroxy-bis(N,N,N',N'-tetramethylenediamine)-copper(II) chloride [Cu(OH).TMEDA]2Cl2: an efficient, partical catalyst for benzylation and allylation of amides.* Tetrahedron Letters, 2006. **47**: p. 2013-2015.
92. Khan, A., C.M. Marson, and R.A. Porter, *Synthesis of exocyclic enamides via stereocontrolled allylic isomerization and 1,3-transposition.* Synthetic Communications, 2001. **31**(11): p. 1753-1764.
93. Wathey, B., et al., *The impact of microwave-assisted organic chemistry on drug discovery.* Drug Discovery Today, 2002. **7**(6): p. 373-380.
94. Kappe, C.O. and D. Dallinger, *Controlled microwave heating in modern organic synthesis:highlights from the 2004–2008 literature.* Molecular Diversity, 2009. **13**: p. 71-193.
95. Gübbük, I.H., R. Güp, and M. Ersöz, *Synthesis, characterization, and sorption properties of silica gel-immobilized Schiff base derivative.* Journal of Colloid and Interface Science, 2008. **320**(2): p. 376-382.
96. Pesek, J.J. and M.T. Matyska, *Electrochromatography in chemically modified etched fused-silica capillaries.* Journal of Chromatography A, 1996. **736**(1-2): p. 255-264.
97. Perrin, D.D., W.L.F. Armarego, and D.R. Perrin, *Purification of Laboratory Chemicals.* 1966.
98. Caltagirone, C., et al., *1,3-Diindolylureas: high affinity dihydrogen phosphate receptors.* Chemical Communications, 2008. **0**(26): p. 3007-3009.
99. Haynes, C., *Questions about your work from Australia*, A. Blok, Editor. 2012.
100. Billo, E.J., *Excel for Chemists A Comprehensive Guide (Second Edition)*. Second Edition ed. 2001, New York: John Wiley and Sons Inc.

101. Bojinov, V., G. Ivanova, and D. Simeonov, *Synthesis and Photophysical Investigations of Novel Polymerizable Blue Emitting Fluorophores – Combination of a Hindered Amine with a Benzo[de]isoquinoline-1,3-dione.* Macromolecular Chemistry, 2004. **205**(9): p. 1259-1268.
102. Duda-Johner, S., et al., *Synthesis and pharmacological characterization of new silicon-basedW84-type allosteric modulators for ligand binding to muscarinic M2receptors.* Journal of Organometallic Chemistry, 2003. **686**(1-2): p. 75-83.
103. *Aldrich Catalogue 2005-2006 Australia/New Zealand*. 2005: Sigma Aldrich.
104. Pfeffer, F.M., *Re: Project Update*, A.J. Blok, Editor. 2007.
105. Williams, D.H. and I. Fleming, *Spectroscopic Methods in Organic Chemistry*. 5th ed. 1995, Great Britain: McGraw-Hill.
106. Lidstrom, P., et al., *Microwave assisted organic syntheiss - a review.* Tetrahedron, 2001. **57**: p. 9225-9283.
107. Gedye, R., et al., *The use of microwave ovens for rapid organic synthesis* Tetrahedron Letters, 1986. **13**(3): p. 279-282.
108. Giguere, R.J., et al., *Application of commercial microwave ovens to organic synthesis.* Tetrahedron Letters, 1986. **27**(41): p. 4945-4948.
109. Hugel, H.M., *Microwave Multicomponent Synthesis.* Molecules, 2009. **14**: p. 4936-4972.
110. Vidal, T., et al., *Re-examination of Microwave-Induced Synthesis of Phthalimides.* Tetrahedron, 2000. **56**(30): p. 5473-5478.
111. Borah, H.N., R.C. Boruah, and J.S. Sandhu, *Microwave-induced One-pot Synthesis of N-carboxyalkyl Maleimides and Phthalimides†.* Journal of Chemical Research, 1998(5): p. 272-273.
112. Chandrasekhar, S., M. Takhi, and G. Uma, *Solvent Free N-Alkyl and N-Arylimides Preparation from Anhydrides Catalyzed by TaCl5-Silica gel.* Tetrahedron Letters, 1997. **38**(46): p. 8089-8092.
113. Bose, A.K., et al., *Microwave-assisted rapid synthesis of α-amino-β-lactams.* Tetrahedron Letters, 1996. **37**(39): p. 6989-6992.
114. Elder, J.W. and K.M. Holtz, *Microwave Microscale Organic Experiments.* Journal of Chemical Education, 1996. **73**: p. A104-A105.
115. Yu, A.-M., et al., *Wang Resin Bound Addition Reactions Under Microwave Irradiation.* Synthetic Communications, 1999. **29**(9): p. 1595-1599.
116. Schalley, C.A., ed. *Analytical Methods in Supramolecular Chemistry*. 2007, Wiley-VCH: Weinheim.
117. Gunnlaugsson, T., et al., *Fluorescent Photoinduced Electron Transfer (PET) Sensors for Anions; From Designed to Potential Application.* Journal of Fluorescence, 2005. **15**(3): p. 287-299.
118. Gunnlaugsson, T., et al., *Towards the development of controllable and reversible "on-off" luminescence switching in soft-matter; synthesis and spectroscopic investigation of 1,8-naphthalimide-based PET (photoinduced electron transfer) chemosensors for pH in water-permeable hydrogels.* Arkivoc, 2003. **7**: p. 216-228.
119. Gunnlaugsson, T., et al., *Simple naphthalimide based anion sensors: deprotonation induced colour changes and CO2 fixation.* Tetraherdron Letters, 2003. **44**: p. 8909-8913.

120. Gunnlaugsson, T., A.P. Davis, and M. Glynn, *Fluorescent photoinduced electron transfer (PET) sensing of anions using charge neutral chemosensors.* Chemical Communcations, 2001: p. 2556-2557.
121. Job, P., *Recherches Sur La Formation De Complexs Mineraux En Solution Et Sur Leur Stabilite.* Annali di Chimica, 1928. **9**: p. 113-203.
122. Olson, E.J. and P. Bühlmann, *Getting More out of a Job Plot: Determination of Reactant to Product Stoichiometry in Cases of Displacement Reactions and n:n Complex Formation.* The Journal of Organic Chemistry, 2011. **76**(20): p. 8406-8412.
123. Carmody, W.R., *Demonstrating Job's method with colorimeter or spectrophotometer.* Journal of Chemical Education, 1964. **41**(11): p. 615.
124. Thordarson, P., *Determining association constants from titration experiments in supramolecular chemistry.* Chemical Society Reviews, 2011. **40**(3): p. 1305-1323.
125. Lowe, A.J., F.M. Pfeffer, and P. Thordarson, *Determining binding constants from 1H NMR titration data using global and local methods: a case study using [n]polynorbornane-based anion hosts.* Supramolecular Chemistry, 2012. **24**(8): p. 585-594.
126. van Ooij, W.J., et al., *Corrosion Protection Properties of Organofunctional Silanes—An Overview.* Tsinghua Science & Technology, 2005. **10**(6): p. 639-664.
127. Sanderson, K., *It's Not Easy Being Green.* Nature, 2011. **469**: p. 18-20.
128. Thomas, J.M., *Solid state NMR and the characterization of zeolites: Its genesis, some early errors and final triumph.* Microporous and Mesoporous Materials, 2007. **104**(1–3): p. 5-9.
129. Soares, C.M.F., et al., *NMR characterization of the role of silane precursors on the catalytic activity of sol–gel encapsulated lipase.* Journal of Non-Crystalline Solids, 2006. **352**(32–35): p. 3469-3477.
130. Gröger, C., M. Sumper, and E. Brunner, *Silicon uptake and metabolism of the marine diatom Thalassiosira pseudonana: Solid-state 29Si NMR and fluorescence microscopic studies.* Journal of Structural Biology, 2008. **161**(1): p. 55-63.
131. Vars, S., et al., *29Si{1H} CP-MAS NMR comparison and ATR-FTIR spectroscopic analysis of the diatoms Chaetoceros muelleri and Thalassiosira pseudonana grown at different salinities.* Analytical and Bioanalytical Chemistry, 2013. **405**(10): p. 3359-3365.
132. Brunner, E., et al., *Analytical studies of silica biomineralization: towards an understanding of silica processing by diatoms.* Applied Microbiology and Biotechnology, 2009. **84**(4): p. 607-616.
133. Buaki-Sogo, M., et al., *Host–guest complexes between cucurbit[n]urils and acetanilides having aminopropyl units.* Journal of Colloid and Interface Science, 2013. **399**(0): p. 54-61.
134. Luan, Z., et al., *Preparation and characterization of (3-aminopropyl)triethoxysilane-modified mesoporous SBA-15 silica molecular sieves.* Microporous and Mesoporous Materials, 2005. **83**(1–3): p. 150-158.
135. Boas, U., et al., *Facile synthesis of aliphatic isothiocyanates and thioureas on solid phase using peptide coupling reagents.* Tetrahedron Letters, 2004. **45**: p. 269-272.

136. Boas, U. and M.H. Jakobsen, *A New Synthesis of Aliphatic Isothiocyanates from Primary Amines, Convenient for In Situ Use.* Chemical Communcations, 1995: p. 1995-1996.
137. Boas, U., B. Pedersen, and J.B. Christensen, *Tetramethyl Fluoro Formamidinium Hexafluorophosphate-An Improved Synthesis and Some New Uses.* Synthetic Communications, 1998. **28**(7): p. 1223-1231.
138. Schlossbauer, A., et al., *Click Chemistry for High-Density Biofunctionalization of Mesoporous Silica.* Journal of the American Chemical Society, 2008. **130**(38): p. 12558-12559.
139. Lummerstorfer, T. and H. Hoffmann, *Click Chemistry on Surfaces: 1,3-Dipolar Cycloaddition Reactions of Azide-Terminated Monolayers on Silica.* The Journal of Physical Chemistry B, 2004. **108**(13): p. 3963-3966.
140. Gallant, N.D., et al., *Universal Gradient Substrates for "Click" Biofunctionalization.* Advanced Materials, 2007. **19**(7): p. 965-969.
141. Kacprzak, K.M., N.M. Maier, and W. Lindner, *Highly efficient immobilization of Cinchona alkaloid derivatives to silica gel via click chemistry.* Tetrahedron Letters, 2006. **47**(49): p. 8721-8726.
142. Prakash, S., et al., *"Click" Modification of Silica Surfaces and Glass Microfluidic Channels.* Analytical Chemistry, 2006. **79**(4): p. 1661-1667.